# INTERDISCIPLINARY APPROACHES IN AGRICULTURE, BIOTECHNOLOGY AND ENGINEERING

# INTERDISCIPLINARY APPROACHES IN AGRICULTURE, BIOTECHNOLOGY AND ENGINEERING

**Editors:**

**Prof. Dr. Gülcan DEMİROĞLU TOPÇU**

**Prof. Dr. Abdullah Engin ÖZÇELİK**

# PREFACE

The accelerating convergence of agriculture, biotechnology, and engineering has reshaped the way complex global challenges are understood and addressed. This book, Interdisciplinary Approaches in Agriculture, Biotechnology and Engineering, brings together diverse perspectives to illuminate how integrative frameworks and cross-disciplinary methodologies can drive sustainable innovation across food systems, biological production, and technological development.

Contemporary agricultural systems face unprecedented pressures arising from climate change, resource scarcity, population growth, and evolving societal expectations. Biotechnology offers powerful tools to enhance productivity, resilience, and quality, while engineering provides scalable solutions for precision, efficiency, and system optimization. Yet, meaningful progress increasingly depends on the synthesis of these domains rather than their isolated advancement. This volume emphasizes the conceptual, methodological, and applied intersections that enable such synthesis.

The contributions collected herein present theoretical insights, experimental studies, and case-based applications that reflect the state of the art in interdisciplinary research. By integrating biological principles with engineering design and agricultural practice, the chapters demonstrate how collaborative approaches can translate scientific knowledge into practical outcomes. Particular attention is given to sustainability, innovation pathways, and the transfer of research into real-world contexts.

This book is intended for researchers, graduate students, and professionals seeking a comprehensive and forward-looking perspective on interdisciplinary collaboration. It aims to foster dialogue across disciplines and to serve as a reference that supports the development of resilient, efficient, and sustainable agro-biotechnological systems for the future.

Prof. Dr. Gülcan DEMİROĞLU TOPÇU
Prof. Dr. Abdullah Engin ÖZÇELİK

# CONTENTS

# CHAPTER 1

# DETERMINATION OF APPARENT DENSITIES OF SOME POWDER MATERIALS

Ahmet Furkan MAMIK[1], Asst. Prof. Dr. Mahmut ÜNALDI[2]

[1]Selçuk University Cihanbeyli Vocational School, Department of Motor Vehicles and Transportation Technology, Konya, Türkiye. E-mail: ahmetfurkanmamik@gmail.com
[2]Selçuk University Cihanbeyli Vocational School, Department of Motor Vehicles and Transportation Technology, Konya, Türkiye. ORCID: 0000-0003-2144-8085. E-mail: munaldi@selcuk.edu.tr

# 1. INTRODUCTION

Compared to liquids and gases, density plays a more critical role in the manufacturing of solid materials especially powders due to its influence on porosity and flowability. In powder-based processes, density is a key factor during ore preparation, material storage, beneficiation, mixing, and production stages. In the literature, powder density is defined and measured in various ways, including apparent density, tapped density, Archimedes density, theoretical density, relative density, bulk density, and true density (typically measured using a pycnometer). Each definition corresponds to a specific measurement method and application context (Arslanhan et al., 2023; German, 2007).

The density of powder materials is a critical parameter in the field of powder metallurgy, a key manufacturing technology. Powder metallurgy involves mixing metal powders in specific ratios, compacting them at room temperature in precision molds under pressures that meet technical requirements, and subsequently sintering them under controlled atmospheric conditions to produce finished parts. This method consists of several stages: powder production, mixing, compaction, sintering, and optional post-processing steps such as infiltration, oil impregnation, and deburring. Compared to conventional manufacturing techniques, powder metallurgy offers significant advantages in terms of production speed, energy efficiency, material utilization, cost-effectiveness, and ease of fabrication (Gökçe et al., 2017; Öztürk & İcin, 2015; Augustyn, 2024; Helmenstine, 2024).

Measuring the density of powder materials is more challenging due to the irregular shapes of the particles (Figure 1). These shape variations affect how particles interact with each other, influencing the overall density, flowability, and porosity of the material (Arslanhan et al., 2023).
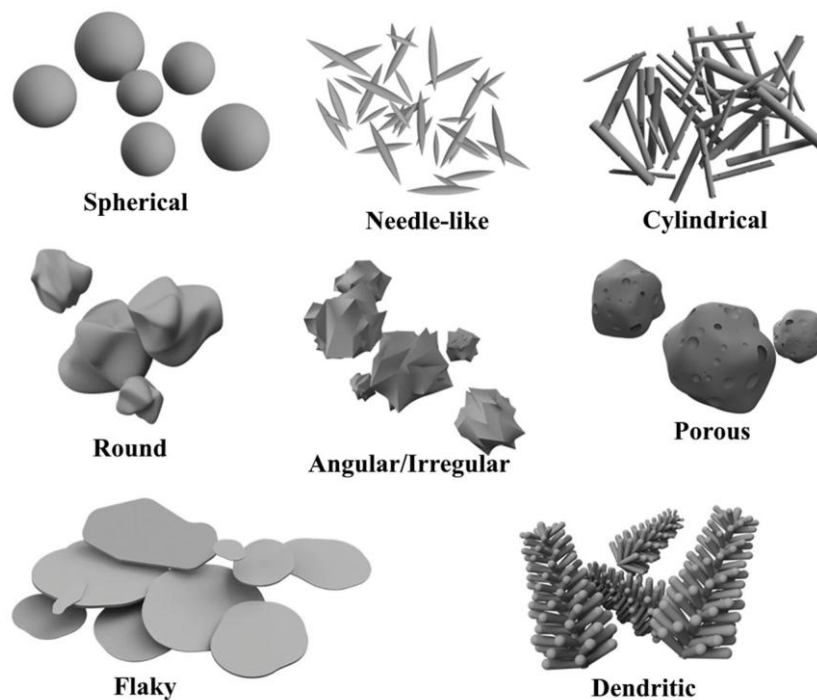


**Figure 1.** Possible shapes of powder materials (German, 2007; Nouri, Sola, 2018)

According to ASTM B329 (2006), the apparent density of powder materials is defined as their density under normal conditions without the influence of pressure, temperature, or liquid. In powder metallurgy studies, determining the apparent density prior to any processing is of critical importance (Öztürk & İcin, 2015). Apparent density plays a key role during the compaction stage, particularly in how effectively the powder fills the mold. It is influenced by particle shape, size, and distribution, and directly affects both flowability and post-compaction properties such as porosity.

Apparent density is determined through a standardized test in which powder material flows freely through a device composed of a funnel, deflector, and Scott volumeter—each dimensioned and shaped according to relevant standards. The test measures the loose, uncompacted density of the powder. A specific amount of powder is gently poured into the funnel at the top of the device. Under the influence of gravity, the powder strikes the deflector plates and fills the Scott volumeter located at the bottom.

Once filled, the 25 cm³ Scott volumeter is weighed using a precision balance, and the apparent density is calculated using the formula:

$$d = m / V, \tag{1}$$

where d is the apparent density of the powder (g/cm³), m is the mass of the powder (g), and V is the volume of the Scott volumeter (fixed at 25 cm³) (ASTM B329, 2006; Berek, 2010).

## 2. MATERIALS AND METHODS

In accordance with ASTM B329, the device used to determine the apparent density of powder materials was designed and dimensioned using a CAD program. This approach enabled the identification of the required part dimensions and quantities for cost-effective manufacturing.
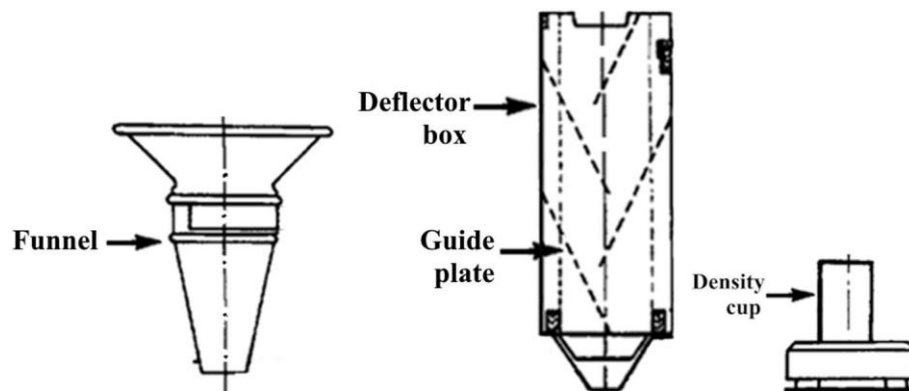


**Figure 2.** Apparent density meter (ASTM B329)

As specified in the standard, the apparent density measurement device consists of four main components: a funnel with a 16-mesh screen at the top to prevent powder dispersion and guide flow; a deflector box in the middle containing four glass guide plates; and a cylindrical density cup (Scott volumeter) at the bottom, with an internal diameter of 28 mm, a volume of 25 cm³, and positioned 19 mm below the deflector box outlet (Figure 2).

Following the design and fabrication of the test apparatus, the powder materials selected for experimentation were barite, calcite, phenolic resin, and cashew powder, commonly used in automotive brake pad formulations. The powder, regardless of exact quantity, was poured into the device through a funnel. As it passed through the deflector, the particles were redirected downward by guide plates, with some filling the density cup and others dispersing around the apparatus. Once the density cup was completely filled and overflowing, the experiment was terminated. Excess powder on the rim was gently removed using a spatula, and the net weight of the filled cup previously tared on a precision balance was recorded. To minimize experimental error, the procedure was repeated five times.

Prior to determining the apparent densities of the powder materials, a sieve analysis was conducted using a sieve shaker (Figure 3) to evaluate particle size distribution and calculate average particle sizes. The technical specifications of the sieve shaker are provided in Table 1. The experiment was carried out at Selçuk University Advanced Technology Research and Application Center, where a suitable set of sieves was selected from the available inventory. To ensure arithmetic progression, sieves with mesh openings of pan, 45 µm, 75 µm, 150 µm, 250 µm, and 500 µm were used. For ease of calculation, 100 grams of powder were placed on the top sieve and shaken for 10 minutes. At the end of the process, the amount of material retained on each sieve was measured using a precision balance, completing the experiment.

**Table 1.** Retsch AS200 Features of sieve shaking device

| Feature | Value |
|---|---|
| Measuring range, (mm) | 0.02-25 |
| Elimination movement | Angular momentum shaking |
| Max. feeding capacity, (kg) | 3 |
| Max. number of fractions, (unit) | 9/17 |
| Max. sieve stack mass, (kg) | 4 |
| Amplitude, (mm) | 0-3 (Analogue) |
| Time indicator, (dk) | 1-60 (Analogue) |
| Suitable for dry/wet sieving | Yes / Yes |
| Suitable sieve diameter, (mm) | 100 / 150 / 200 / 203 |
| Protection code | IP 54 / IP 20 |

**Figure 3.** Sieve shaking device and sieve set

## 3. EXPERIMENTAL RESULTS

After the powder materials were procured, sieve analysis was conducted in accordance with ASTM B214. Subsequently, apparent density measurements were performed using a custom-built device. The collected data were compiled using Microsoft Office tools, and particle size distributions along with average particle sizes were calculated. The average results from individual sieve analyses for each component are presented in Figures 4 and 5.

Fig.4 displays the collective sieve analysis results of the powder materials. The pan represents the section where the finest particles accumulate. According to the graph, alumina exhibits the finest particle structure, while cashew powder contains fewer particles smaller than 45 μm. Due to its organic nature, cashew powder has a coarser structure compared to the others, with 70.78% of its particles larger than 150 μm. In contrast, the other materials show more uniform distributions, with the majority of their particles measuring below 150 μm.
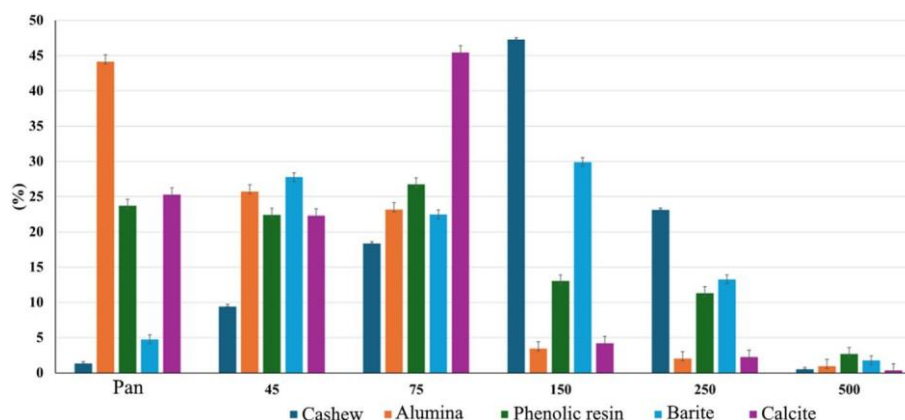


**Figure 4.** Sieve analysis results

While bar charts indicate the amount of material retained on each sieve, cumulative curves reveal the overall particle size distribution. The graphs show that alumina and calcite

have finer particles, as evidenced by their higher accumulation in sieves with smaller mesh openings. In contrast, cashew powder displays a coarser structure, with more than 50% of its mass retained beyond the 75 µm sieve. Cumulative distribution graphs are commonly used to estimate average particle size. In literature, this is often expressed using D-values, where D50 (median) refers to the sieve size at which 50% of the powder is retained. Alternatively, the arithmetic mean of D10, D50, and D90 values may be used (Anonim-D, 2025; Anonim-E, 2025). In this study, since D10 values were unavailable for alumina, phenolic resin, and calcite, the D50 values were estimated using interpolation in Microsoft Excel. The calculated average particle sizes for alumina, calcite, phenolic resin, barite, and cashew were determined as 10, 47, 49, 68, and 108 µm, respectively.
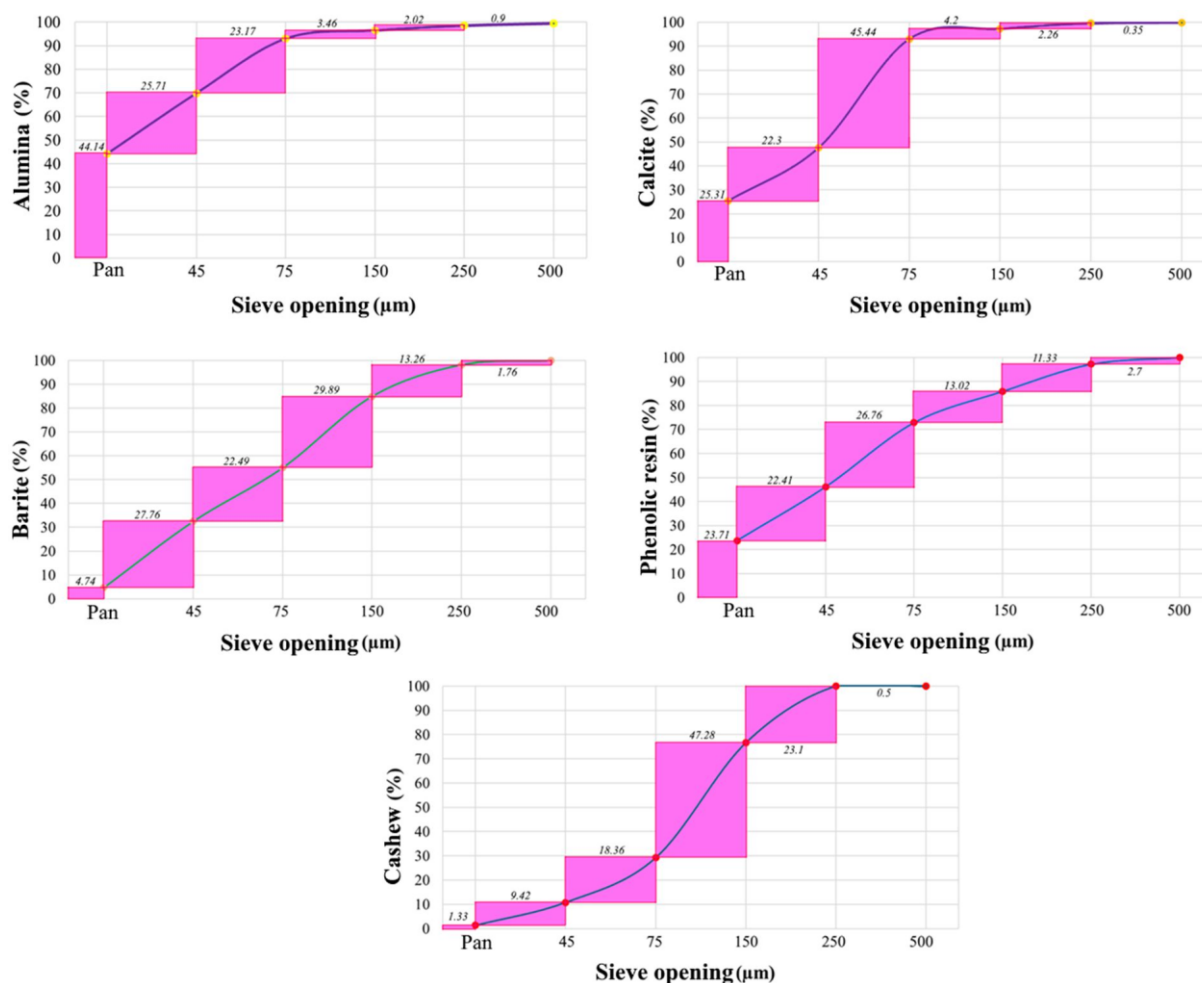


**Figure 5.** Cumulative particle size distribution graphs from sieve analysis

Calcite and alumina, due to their finer particle sizes, exceeded 90% retention at the 75 µm sieve. Despite their fine structure, both materials exhibited low apparent density. Phenolic resin and barite showed a more balanced particle size distribution, with similar accumulation across most sieve ranges except at 500 µm. Cashew powder, being the only organic material, displayed

a coarser structure, as indicated by its curve surpassing 50% beyond the 75 μm sieve, contributing to its lower apparent density due to agglomeration.

Apparent density is a critical parameter that influences product characteristics, particularly in pressing operations. The use of powders with high apparent density enables savings in both material and time during mold construction, while also extending mold life and reducing the risk of fracture (Berek, 2010). The apparent densities of the samples were measured in accordance with ASTM B329, and the results are presented in Figure 6.

It was observed that alumina, calcite, and barite materials with smaller average particle sizes exhibited higher apparent density values. This indicates that such powders can be more tightly packed, offering improved pressability and enhanced sintering performance. Despite its fine particle size, phenolic resin showed a low apparent density, suggesting poor flowability and a tendency to agglomerate. Cashew powder, derived from plant shell material, has relatively coarse particles and also demonstrated low apparent density due to agglomeration.
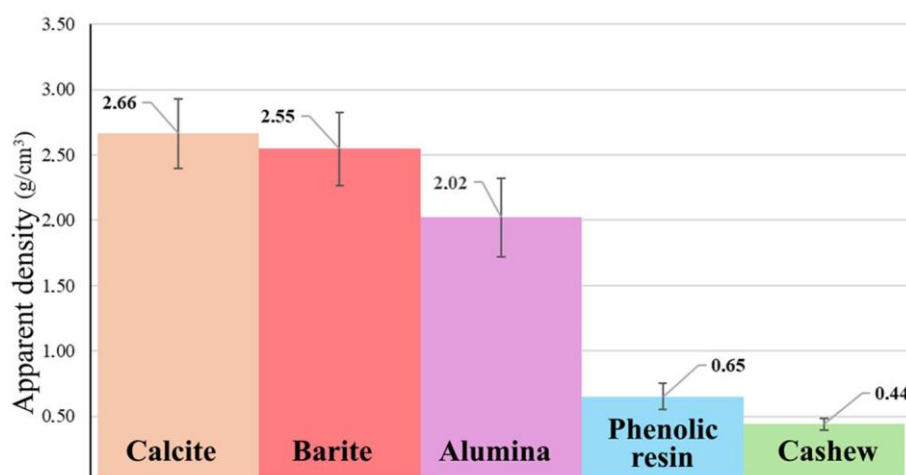


**Figure 6.** Results of apparent density measurements

## 4. CONCLUSIONS AND RECOMMENDATIONS

A study was conducted using a device designed and manufactured in accordance with ASTM B214 and B329 standards to measure the apparent density of calcite, barite, alumina, phenolic resin, and cashew powder materials. Although the metallic and organic powders met the average particle size values stated on their commercial labels, their apparent density values were found to differ significantly. This variation in apparent density is a critical physical property, especially in applications where powder flowability is essential. Therefore, it is a parameter that must be considered in powder-based applications.

According to sieve analysis results, alumina and calcite exhibited finer particle structures, approximately 45 μm smaller on average and their apparent density values were measured as 2.02 and 2.66 g/cm³, respectively. The phenolic resin, which showed nearly equal mass distribution across all sieves, and the relatively coarser cashew powder had apparent density

values of 0.65 and 0.44 g/cm³, respectively. Due to the organic nature of cashew powder, its particles tend to agglomerate, resulting in lower apparent density values. A similar observation can be made for phenolic resin, which also exhibits a tendency to retain air between particles.

If pressing operations are to be applied to powder materials, interpretations can be made based on sieve analysis results. Powders with uniform particle size distribution (such as phenolic resin and barite) tend to exhibit relatively low compressibility. In contrast, a varied particle size distribution can reduce the porosity of composite materials. Pressing powders with uniform particle sizes may lead to increased voids in the final product, resulting in a porous structure. To reduce porosity, powders with diverse particle sizes and higher compaction pressures can be utilized. Evaluating sieve analysis results alongside apparent density data may offer a more comprehensive approach to material characterization and contribute to the reliability of future studies.

Due to economic constraints, metallic and organic powder materials were used in this study. In future research, the apparent density of metals, ceramics, plastics, organic powders, and their mixtures can be tested to evaluate the performance and versatility of the manufactured device. This would allow for a broader assessment of the device's functionality and applicability.

Due to time limitations in the project, powder materials that were readily available on the market were selected. By conducting experiments with powders whose particle sizes are more precisely known, the accuracy and deviation values of the device can be determined. This would enable comparisons with existing literature data.

The device manufactured within the scope of the project can be calibrated by testing powders with standardized particle sizes and moisture content, thereby improving measurement precision.

**REFERENCES**

Anonim-A. (2011). Yoğunluk ve Viskozite. Kimya Teknolojisi, T.C. Milli Eğitim Bakanlığı, Ankara, https://megep.meb.gov.tr/mte_program_modul/moduller_pdf/Yo%C4%9Funluk%20Ve%20Viskozite.pdf, Access date: 01.10.2024.

Anonim-B. (2014). Toz Hazırlama ve Elek Analizi. Bartın Üniversitesi Mühendislik, Mimarlık ve Tasarım Fakültesi Metalurji ve Malzeme Mühendisliği Bölümü, Erişim adresi, https://cdn.bartin.edu.tr/metalurji/d7ee7cd9-f063-4669-8e1c-393503ed6ffb/toz-hazirlama-ve-elek-analizi.pdf#page=9.00, Access date: 10.10.2022.

Anonim-C. (2024). What is Density?.
    https://www.acs.org/middleschoolchemistry/lessonplans/chapter3/lesson1.html, Access
    date: 05.10.2024.

Anonim-D. (2025). Analysis of Particle Size Distribution.
    https://www.microtrac.com/knowledge/particle-size-distribution/, Access
    date:10.06.2025.

Anonim-E (2025). Sieve Analysis.
    https://www.mt.com/us/en/home/applications/Laboratory_weighing/sieve-analysis,
    Access date: 05.06.2025.

ASTM (2006). Standard Test Method for Apparent Density of Metal Powders and
    Compounds Using the Scott Volumeter. New York, USA. B329.

ASTM (2007). Standard Test Method for Sieve Analysis of Metal Powders. New York, USA.
    B214: 1-4.

Arslanhan, M., Kaykılarlı, C. & Duman, Ş. (2023). *Yoğunluk Ölçümü Deneyi*. Bursa Teknik
    Üniversitesi Doğa Bilimleri, Mimarlık ve Mühendislik Fakültesi Metalurji ve Malzeme
    Mühendisliği Bölümü, Unpublished lecture notes.

Augustyn, A. (2024). Density. https://www.britannica.com/science/density, Access date:
    05.10.2024.

Berek S. (2010). *Kuvars ve Diatomit Katkılarının Bronz Esaslı Balataların Aşınma
    Özelliklerine Etkis*i. Yüksek Lisans Tezi, Fen Bilimleri Enstitüsü Metal Eğitimi A.B.D.,
    Sakarya Üniversitesi, Sakarya.

Edizer E. (2006). *Sayısal Görüntü İşleme Yöntemi ile Tane Boyut Dağılımı*. Yüksek Lisans Tezi,
    Fen Bilimleri Enstitüsü, Maden Mühendisliği Anabilim Dalı, Çukurova Üniversitesi,
    Adana, Türkiye.

German, R. M. (2007). Toz Metalurjisi ve Parçacıklı Malzeme İşlemleri. Çeviri, *Türk Toz
    Metalurjisi Derneği Yayınları*, Ankara.

Gökçe, A., Fındık, F. & Kurt, A.O. (2017). Alüminyum ve Alaşımlarının Toz Metalurjisi
    İşlemleri. *Mühendis ve Makina*, 58(686), 21-47.

Helmenstine, A.M. (2024). How to Calculate Density of a Gas.
    https://www.thoughtco.com/how-to-calculate-density-of-a-gas-607847, Access date:
    05.10.2024.

Öztürk, S. & İcin, K. (2015). *Toz Metalurjisi Deneyi*. Karadeniz Teknik Üniversitesi
    Mühendislik Fakültesi Metalurji ve Malzeme Mühendisliği Bölümü Laboratuar Föyü,
    Trabzon, Türkiye.

Moon, J. R. (2007). *Introduction to PM, A Residential Training Course for Young Materials
    Engineer*s. Course Booklet, European Powder Metallurgy Association, London.

Nouri, A. & Sola, A. (2018). *Metal particle shape: A practical perspective*. Metal powder
    report, 73(5), 276-282.

# CHAPTER 2

# BREEDING POTENTIALS OF LOCAL BREAD AND DURUM WHEAT VARIETIES

Agr. Eng.Ahmet Serdar KOKU[1], Assoc. Prof. Dr. R. Refika AKÇALI
GIACHINO[2],
Asst. Prof. Dr. Deniz İŞTİPLİLER[3]

[1]Doktar Technologies, Agricultural Engineer, Senior Sales&Aftersales Support Specialist, İzmir, Türkiye
Orcid: 0009-0003-9100-6394, kokuahmetserdar@gmail.com
[2]Ege University, Faculty of Agriculture, Field Crops Department, İzmir, Türkiye
Orcid: 0000-0002-6473-7250, refika.giachino@ege.edu.tr
[3]Ege University, Faculty of Agriculture, Field Crops Department, İzmir, Türkiye
Orcid: 0000-0002-0887-1121, deniz.istipliler@ege.edu.tr

# 1. INTRODUCTION

Bread wheat (Triticum aestivum L.), according to data obtained from archaeological excavations, began to be cultivated in the Neolithic Period, approximately 8,000 to 10,000 years ago, in the Fertile Crescent region. Wheat, as one of the first agricultural plants of that period, was domesticated and gradually spread to Anatolia, then to Europe and Asia, forming local landraces in various regions of the world. These local landraces adapted to the environmental conditions in which they were found and provided an important genetic resource for plant breeders, especially in new breeding programs developed over the last two centuries. During the hybridization studies on wheat following the Green Revolution, which began after World War II, the development of varieties carrying dwarfing genes led to significant changes in global genetic diversity. Today, wheat, cultivated on approximately 220 million hectares annually, is one of the most widely produced and consumed food products worldwide, providing about 15% of the calories consumed daily. Bread wheat, repeatedly shaped through selection to respond to human needs and adapt to different environmental conditions, became a strategic product for the development of civilizations after the transition from hunting-gathering to agriculture (Balfourier et al., 2019; Broushaki et al., 2016). In addition to its strong adaptability, high genetic diversity, and ease of storage, wheat stands out as one of the important raw materials of the food sector due to its rich and balanced nutritional content. The wide genome structure it possesses also plays an important role in wheat's agricultural significance. With a genome approximately five times the size of the human genome, wheat continues to be one of the indispensable plants of world agriculture with its species at different ploidy levels (Li et al., 2004; Luo et al., 2009; Zimin et al., 2017).



**Figure 1.** İvriz Rock Monument, Late Hittite Period 727–742 BCE (T.C. Konya Valiliği, 2025)

Commercially, the main cultivated wheats are divided into two primary groups: bread wheat (Triticum aestivum L.) and durum wheat (Triticum durum L.). Wheat grains are a staple food containing many compounds important for nutrition and health, such as proteins, carbohydrates, and carotenoids (Kimball et al., 2001). Globally, durum wheat is grown on 8–10% of the wheat-growing areas, while the remaining areas are cultivated with bread wheat

(Hanson et al., 1982). On a global scale, wheat cultivation area increased from 215.12 million hectares in 2000 to 219.15 million hectares in 2022. In terms of production, world wheat production rose from 587.64 million tons in 2000 to 808.44 million tons in 2022. In Türkiye, wheat was cultivated on 9.15 million hectares in 2000, which decreased to 6.60 million hectares by 2022, and production fell from 21.00 million tons in 2000 to 19.75 million tons in 2022. Alongside the growing population, changes in production levels have caused annual fluctuations in import and export levels, in parallel with the quality of the produced crops. As of 2022, Türkiye's wheat exports reached 395.33 thousand tons, while imports were 8.90 million tons (FAO, 2022). As indicated by these results, due to the reduction in wheat cultivation areas, increasing yield per unit area and improving product quality remain equally important. In this context, using the genetic heritage of our own soils in breeding studies, developing varieties suitable for the ecological conditions of the country, and ensuring local genetic resources are diverse and accessible are particularly significant factors. Although currently registered varieties offer high yield potential, local varieties possess unique traits in adaptation to low-input conditions, disease/drought tolerance, and certain quality parameters. This study aims to systematically present the potential contributions that local durum and bread wheat varieties can offer to breeding processes, based on literature and field samples.

## 2. COLLECTION AND PRESERVATION OF LOCAL WHEAT VARIETIES

The most comprehensive studies on the systematic collection and characterization of local wheat varieties in our country were conducted by Mirza Gökgöl. Starting from 1926, approximately 18,000 local village wheat varieties collected from all regions of Türkiye were sown in quantities of 3,000 each year for examination; botanical varieties were determined based on morphological traits, and economically important characteristics were identified through eco-morphological evaluations. The data obtained were compiled in the books Turkish Wheats I and II, and as a result of these studies, 236 new botanical varieties were defined (Salantur, 2017).

Thanks to these comprehensive studies, it was revealed that while there are 270 and 109 botanical varieties of bread and durum wheat worldwide, respectively, in Türkiye these numbers are 223 and 102, respectively (Eser, 2015). Mirza Gökgöl and his colleague K.A. Flaksberger persuaded Vavilov, the founder of the Gene Resources Theory, to include Türkiye among the primary centers of wheat, thereby reshaping the Vavilov Centers of Origin Theory (Gökgöl and Taşan, 1978). In addition, Turkish village wheat varieties were systematically collected and the data published by Zhukovsky (1925–1927), Harlan (1948–1949), Damania et al. (1984), and Zanatta et al. (1993–1994) (Zhukovsky, 1951; Harlan, 1950; Damania et al., 1996; Zanatta et al., 1996, 1998).
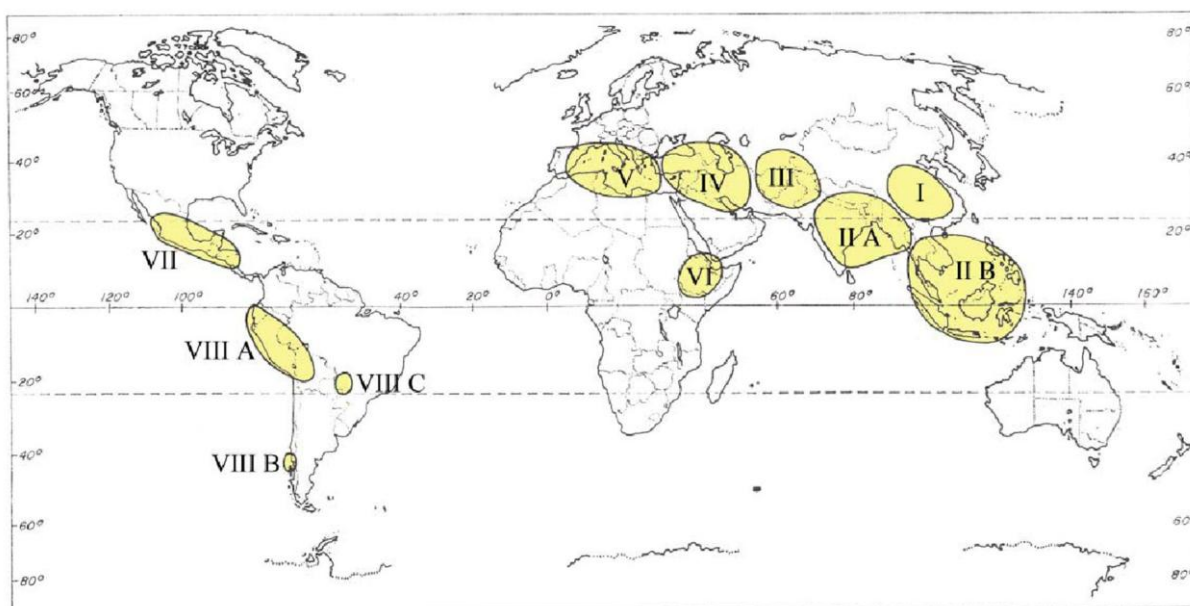
**Figure 2.** Vavilov Gene Centers (OER Commons, 2021)

Among the most comprehensive recent studies is the "National Survey, Collection, and Preservation of Turkish Local Wheat Varieties" project, supported by FAO and IWWIP between 2009 and 2014. Within the scope of this project, 1,587 village wheat varieties were collected, and surveys were conducted with a total of 1,873 farmers. The study identified 162 local variety names, with the varieties having the largest cultivation areas determined, in order, as zerun, white wheat, red wheat, yellow wheat, karakılçık, kırik, emmer (siyez), koca wheat, topbaş, şahman, and üveyik wheat (Kan et al., 2015).

However, it has been emphasized that although local varieties are still cultivated in rural areas, their numbers decrease every year. In one of the most recent studies, it was estimated that the proportion of local wheat varieties within the total wheat varieties is less than 1% (Mazid et al., 2009). Nevertheless, Turkish village wheat varieties are preserved both in our country and in global gene banks (ex-situ) and can be made available upon request by researchers. As reported by Eser (2015), a total of 4,493 local wheat varieties are stored in the National Gene Bank of the Aegean Agricultural Research Institute, comprising 2,729 bread wheat, 1,577 durum wheat, and 187 hulled wheat varieties, while the Central Field Crops Research Institute Türkiye Seed Gene Bank preserves a total of 21,966 local wheat varieties, including 19,292 bread wheat, 2,580 durum wheat, and 94 hulled wheat varieties.

**Figure 3.** National Gene Bank of the Aegean Agricultural Research Institute (Ulusal Tohum Gen Bankası, 2025)

## 3. MAIN FACTORS CAUSING YIELD AND QUALITY LOSS IN WHEAT PRODUCTION

Factors causing yield loss in wheat production not only affect the quantity of production but also directly impact the quality of the product. Reducing the adverse effects of these factors is critically important for ensuring continuity in production and maintaining food security. At this point, breeding efforts will allow the development of varieties with high tolerance to stress conditions and superior quality parameters. By utilizing local genetic resources and developing new varieties adapted to the ecological conditions of our country, it is possible to both reduce yield losses and support sustainable production. The main biotic and abiotic factors that cause yield and quality loss in wheat, but whose impact can be mitigated through breeding, can be listed as follows:

3.1 Biotic Factors: These are living agents that affect the growth and yield of plants. They include disease-causing organisms such as fungi, bacteria, and viruses, as well as insects, mites, and other pests. These agents cause direct or indirect damage to plants, resulting in losses in both yield and quality.

### 3.1.1 Major Fungal Diseases (Adana Directorate of Provincial Agriculture and Forestry, 2014)

1. Powdery Mildew (*Erysiphe graminis*)
2. Septoria Leaf Blotch (*Septoria tritici*)
3. Rust Diseases (*Puccinia graminis*)
4. Loose Smut (*Ustilago nuda tritici*)
5. Common Bunt (*Tilletia caries*)
6. Take-All Disease (*Gaeumannomyces graminis*)
7. Root and Crown Rot (*Fusarium* spp., *Bipolaris* sp., *Rhizoctonia* spp., *Pseudocercosporella herpotrichoides*)

| Name of Disease Agent | Caused Yield Loss (%) |
|---|---|
| Common Bunt (Tilletia spp.) | 15-20 |
| Dwarf Bunt (Tilletia controversa) | 15 |
| Loose Smut (Ustilago nuda tritici) | 5-15 |
| Yellow Rust (Puccinia striiformis) | 10-75 |
| Brown Rust (Puccinia recondita) | 20-60 |
| Stem Rust (Puccinia graminis tritici) | 10-90 |

Table 1. Yield Losses Caused by Major Cereal Diseases (Akan et al., 2006)

### 3.1.2 Major Bacterial Diseases (CIMMYT, 1987)

1. Black Chaff and Bacterial Stripe (*Clavibacter michiganensis* subsp. *sepedonicus*)
2. Basal Glume Rot and Bacterial Leaf Blight (*Pseudomonas syringae* pv. *syringae*)
3. Bacterial Spike Blight (*Xanthomonas translucens* pv. *undulosa*)
4. Yellow Chaff Rot (*Pseudomonas tritici*)

### 3.1.3 Major Viral Diseases (CIMMYT, 1987)

1. Barley Yellow Dwarf (*Luteovirus hordei*)

### 3.1.4 Major Pests (Ministry of Agriculture and Forestry, 2014)

1. Sunn Pest (*Eurygaster integriceps, E. maura, E. austriaca*)
2. Plant Bug (*Aelia* spp.)
3. European Chafer Beetle (*Anisoplia* spp.)
4. Dung Beetle (*Zabrus* spp.)
5. Cereal Moth (*Syringopais temperatella*)
6. Cereal Weevil (*Pachytychius hordei*)
7. Red-legged Earth Mite (*Penthaleus major*)
8. Cereal Scale Insect (*Porphyrophora tritici*)
9. Stem Sawflies (*Cephus pygmaeus, Trachelus tabidus, T. libanensis*)
10. Wheat Fly (*Phorbia securis*)
11. Cereal Aphids (*Sitobion avenae, Rhopalosiphum maidis, Rhopalosiphum padi, Schizaphis graminum, Diuraphis noxia, Metopolophium dirhodum, Macrosiphum euphorbiae, Myzus persicae, Sipha maydis, Sipha elegans*)
12. Thrips (*Haplothrips tritici, Haplothrips aculeatus, Limothrips cerealium, Aptinothrips rufus*)

3.2 Abiotic Factors (Environmental): These are factors that negatively affect the physiological, biochemical, and metabolic functions of plants due to environmental conditions, leading directly to losses in growth and yield (Tanveer & Ahmed, 2020).

1. **1.** Drought and irregular rainfall

2. **2.** Extreme temperature conditions

3. **3.** Late and early frosts

4. **4.** Soil salinity

5. 5. Nutrient deficiencies (particularly N-P-K-Zn)

6. **6.** Soil erosion and loss of organic matter
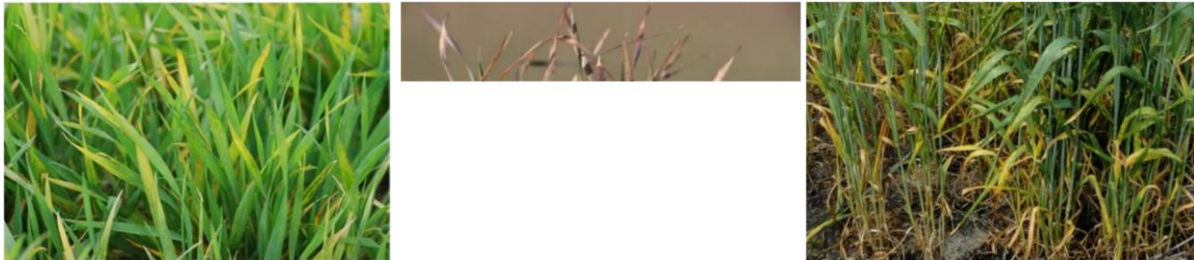


**Figure 4.** Symptoms of Nitrogen, Phosphorus, and Potassium Deficiency in Wheat, Respectively (Agrimeta Tarım, 2024)

## 4. GENETIC POTENTIALS OF LOCAL WHEAT VARIETIES AS BREEDING MATERIAL

Local varieties possess a rich genetic diversity. Having adapted to specific ecosystems over many years, these varieties have naturally acquired resistance to various environmental stress factors. Genetic diversity forms the basis for plants' ability to adapt to changing environmental conditions. In this context, local varieties offer a much broader range of genetic variation compared to commercial varieties (Bellon, 1996; Frankel et al., 1995). For example, local wheat varieties grown in the Southeastern Anatolia Region of Türkiye stand out for their high adaptive capacity to temperature fluctuations and low rainfall conditions (Kaya, 2021). Furthermore, local varieties mostly exhibit a polygenic adaptation structure, meaning that their resilience to stress conditions arises from the combined effect of many genes with small contributions. This trait enhances their survival and productivity under variable climatic conditions (Mercer & Perales, 2010).

As an example, the "Türkiye Red" wheat is also found in the lineage of the Japanese wheat variety Norin-10, the ancestor of the "Green Revolution" varieties that increased lodging resistance by shortening plant height, thereby allowing more efficient use of fertilizers and irrigation. Japanese breeders developed Norin-10 by incorporating the "Türkiye Red" genotype into the Daruma × Fultz cross in 1924, originally made in 1917. Today, "Türkiye Red" is also present in the pedigree of many varieties registered in Türkiye, including Soyer 02, Nacibey, Karahan 99, İkizce, Sultan 95, and Altay 2000. In particular, "Türkiye Red" appears six times in different crossing combinations within the pedigree of Altay 2000. In short, Turkish local wheat varieties have been used directly in production both domestically and internationally and have provided significant contributions to the genetic structure of modern wheat varieties as indispensable genetic materials for wheat breeding programs (Salantur et al., 2017).

**Figure 5.** "Türkiye Red" Wheat (John Deere, 2024)

4.1 Resistance to Climate Change

Climate change has made it a priority to enhance resilience and adaptive capacity in agricultural systems. In this context, local varieties, shaped through natural selection and farmer practices, play an important role as genetic resources in sustainable agriculture. Thanks to both their genetic diversity and the adaptive traits they have developed against environmental stresses, local varieties provide an effective protective mechanism against the adverse effects of climate change (Ceccarelli et al., 2010; Dwivedi et al., 2016).

4.2 Cold Tolerance

In Dumlu's research on local and registered wheat varieties, the cold tolerance of different wheat genotypes was examined. As a result, it was reported that at -15 °C, most genotypes showed over 50% viability except for the Nenehatun and Kırik varieties. At -17 °C, the Kırik and Nenehatun varieties, along with certain lines, maintained viability above 50%, while at -19 °C, only a limited number of genotypes could retain this threshold. These results indicate that there is significant variation in cold tolerance within the Kırik population. The same study noted that some Kırik lines exhibited superior performance compared to modern breeding varieties in certain yield parameters, cold tolerance rates, and quality criteria, and suggested that these lines could be used as parents in pre-breeding programs. Furthermore, it was emphasized that the genes controlling these traits could be identified using molecular markers. It was also proposed that these genotypes, which are morphologically distinctly different from modern varieties, should be preserved through both ex-situ and in-situ conservation methods (Dumlu, 2023).

**4.3 Richness in Certain Elements**

In their research comparing the nutrient element content of grains in local bread wheat lines with registered varieties, Akçura and colleagues examined nine different element concentrations (Fe, Zn, B, K, Mn, Cu, Mg, Ca, and Mo), comparing local bread wheat lines of Black Sea origin (12 local lines) with 25 registered varieties. According to the results, the Bolu-origin TR 36948/5 line among the local bread wheat lines had the highest levels of Fe, Zn, and Ca. Among the registered varieties, Kırik ranked first in K and Cu content, while Konya 2002 and Kenanbey varieties showed the highest levels of Cu and Ca, respectively. Notably, the Bolu-origin TR 36948/5 line exhibited higher Fe, Zn, and Ca content than all 25 registered varieties. It was concluded that local wheat lines are superior to registered varieties in terms of certain

elements and can serve as valuable genetic resources in breeding programs aimed at increasing element content in bread wheat in Türkiye.

**4.4 Yield Increase**

In Türkiye, the first wheat variety developed through hybridization breeding, Melez-13, was obtained from studies using Kızıldil 706 and Akdil 707 varieties as parents. This multiline variety, created from a mixture of five lines selected from the Mentana × Akdil 707 and Mentana × Kızıldil 706 crosses, was put into production starting in 1940 and provided not only high yield stability but also a 25–30% increase in yield (Altay, 2016).

**4.5 Disease Resistance**

In addition to breeding studies conducted in Türkiye, local village wheat varieties have also been used as valuable genetic materials in international breeding programs. The spring durum wheat variety "Horarek," selected from materials collected from Türkiye by Zhukovsky, outperformed many varieties in Russia in 1951 due to its earliness, high yield, and resistance to fusarium disease (Qualset, 1996). Similarly, 51 lines selected from the Şemdinli-origin local variety PI 178.383, which is resistant to yellow rust and collected by Harlan from Türkiye, were used as parents in the development of new varieties in the USA, making significant contributions to the national economy (Damania et al., 1996).

5. CONCLUSION

Thanks to centuries of natural selection and farmers' experiences, our local wheat varieties have developed unique adaptive capabilities across Türkiye's diverse ecological regions. These varieties offer significant advantages over modern cultivars not only in terms of yield and quality parameters but also in resistance to diseases, drought, and extreme climatic conditions. As seen in the example of "Türkiye Red," the ancestor of Norin-10, the genetic contributions of our local varieties have played a critical role even in international breeding programs.

Today, increasing climate uncertainties, areas cultivated with low inputs, and the growing demand for organic production further enhance the strategic importance of our local varieties. However, the intensive practices of modern agriculture and the narrowing of genetic diversity make it more challenging to preserve these valuable resources. Therefore, the conservation and effective use of local varieties as breeding material should be supported through both in-situ and ex-situ approaches and reinforced with farmer participation, genetic monitoring, and flexible seed policies.

Moreover, the nutrient element richness, cold tolerance, and disease resistance of local varieties can serve as key resources in future sustainable and climate-resilient wheat breeding programs. Reintegrating these varieties into agroecological systems will lay the foundation for a production model that ensures both yield stability and ecological balance.

In conclusion, our local varieties are not merely a genetic heritage; they are a guarantee of sustainable agriculture, food security, and our cultural values. Preserving and utilizing them

properly is the most reliable way to strengthen Türkiye's current and future agricultural and ecological resilience.


# REFERENCES

Adana Directorate of Provincial Agriculture and Forestry, 2014, BUĞDAY HASTALIK VE ZARARLILARI. https://adana.tarimorman.gov.tr/Belgeler/SUBELER/bitkisel_uretim_ve_bitki_sagligi_s ube_mudurlugu/hububat_yetistiriciligi_ve_mucadelesi/2014-Hububatta%20Zirai%20M%C3%BCcadele.pdf Erişim Tarihi 5 Kasım 2025

Agrimeta Tarım, 2024, https://www.agrimeta.com.tr/bugday-hastaliklari-ve-besin-noksanliklari/?srsltid=AfmBOoqf-EGf5-HG59Qe3MUHkufXhkJCURr6PInFFvVx-qeCYlWAXvAy Erişim Tarihi: 9 Aralık 2025

Akan, K., Çetin, L., Albostan, S., Düşünceli, F., & Mert, Z. (2006). İÇ ANADOLU'DA GÖRÜLEN ÖNEMLİ TAHIL VE NOHUT HASTALIKLARI. Tarla Bitkileri Merkez Araştırma Enstitüsü Dergisi, 15(1-2), 29-48.

Akçura, M., Hocaoğlu, O., Kılıç, H., & Kökten, K. (2013). Karadeniz bölgesine ait yerel ekmeklik buğday hatlarının tanedeki besin elementleri içerikleri yönünden tescilli ekmeklik buğday çeşitleri ile karşılaştırılması.

Altay, F. (2016). Türkiye Bitki Islahının Öncülerinden: Emcet Yektay. TÜRKTOB, 20, 4-7.

Balfourier, F., Bouchet, S., Robert, S., De Oliveira, R., Rimbert, H., Kitt, J., ... & Paux, E. (2019). Worldwide phylogeography and history of wheat genetic diversity. Science advances, 5(5), eaav0536

Bellon, M. R. (1996). The dynamics of crop infraspecific diversity: A conceptual framework at the farmer level. Economic botany, 26-39.

Broushaki, F., Thomas, M. G., Link, V., López, S., Van Dorp, L., Kirsanow, K., ... & Burger, J. (2016). Early Neolithic genomes from the eastern Fertile Crescent. Science, 353(6298), 499-503.

Ceccarelli, S., Grando, S., Maatougui, M., Michael, M., Slash, M., Haghparast, R., ... & Nachit, M. (2010). Plant breeding and climate changes. The Journal of Agricultural Science, 148(6), 627-637.

Damania, AB., Pecetti, L., Qualset, CO., and Humeid, BO. (1996). Diversity and Geographic Distribution of Adaptive Traits in Triticum turgidum L. (durum group) Wheat Landraces From Turkey. Genet. Res. Crop Evol., 43, 409-422.

Damania, AB., Pecetti, L., Qualset, CO., and Humeid, BO. (1996). Diversity and Geographic Distribution of Adaptive Traits in Triticum turgidum L. (durum group) Wheat Landraces From Turkey. Genet. Res. Crop Evol., 43, 409-422.

Dumlu, B. (2023). Kirik buğday popülasyonlarının soğuğa dayanıklılık, bazı tarımsal özellikler ve kalite bakımından değerlendirilmesi (Doktora tezi, Atatürk Üniversitesi). Atatürk Üniversitesi.

Dwivedi, S. L., Ceccarelli, S., Blair, M. W., Upadhyaya, H. D., Are, A. K., & Ortiz, R. (2016). Landrace germplasm for improving yield and abiotic stress adaptation. Trends in plant science, 21(1), 31-42.

Eser, V. (2015). Genetic Resources for Plant Breeding. II. International Plant Breeding Congress, 1-5 November 2015, Antalya.

FAO, 2022, http://www.fao.org/faostat/en/#data / Erişim Tarihi: 5 Kasım 2025.

Frankel, O. H., Brown, A. H., & Burdon, J. J. (1995). The conservation of plant biodiversity. Cambridge University Press.

Gökgöl, M., Taşan, R. (1978). Yeşilköy Zirai Araştırma Enstitüsünün (Marmara-Trakya Bölge Zirai Araştırma Enstitüsü) 50 Yılı, 1926-1976. İstanbul.

Hanson, H.; N.E. Borlaug and R.G. Anderson, (1982). Wheat in the third world. westview press. molecular studies on bread wheat (Triticum aestivum L.) for drought stress tolerance, Genetic Engineering and Biotechnology Research Institute.

Harlan, JR. (1950). Collection of Crop Plants in Turkey. Agron. J., 42, 258-259.

John Deere, 2024, https://www.deere.com/en/publications/the-furrow/2024/december-2024/legacy-wheat/ Erişim Tarihi: 9 Aralık 2025

Kan, M., Kucukcongar, M., Keser, M., Morgounov, A., Muminjanov, H., Ozdemir, F. and Qualset, C. (2015). Wheat Landraces in Farmers' Fields in Turkey: National Survey, Collection, and Conservation, 2009–2014. FAO, Ankara, Turkey.

Kaya, Y. (2021). Winter wheat adaptation to climate change in Turkey. Agronomy, 11(4), 689.

Kimball, B. A., Morris, C. F. P., Pinter, J., G. W., Jr., D. J., WallHunsaker, Adamsen, F. J., LaMorte R. L., Leavitt, S. W., Thompson, T. L., Matthias, A. D. and Brooks, T. J., (2001). Elevated CO 2, Drought and soil nitrogen effects on wheat grain quality. The New Phytologist Vol. 150, No. 2, Rising CO 2- Future Ecosystems (May, 2001), pp. 295- 303 (9 pages).

Li, W., Zhang, P., Fellers, J.P., Friebe, B., Gill, B.S. (2004). Sequence composition, organization, and evolution of the core Triticeae genome. The Plant Journal, 40(4), 500-511.

Luo, M.C., Deal, K.R., Akhunov, E.D., Akhunova, A.R., Anderson, O.D., Anderson, J.A., Dvorak, J. (2009). Genome comparisons reveal a dominant mechanism of chromosome number reduction in grasses and accelerated genome evolution in Triticeae. Proceedings of the National Academy of Sciences, 106(37), 15780- 15785.

Mazid, A., Amegbeto, K. N., Keser, M., Morgounov, A. I., Peker, K., Bagci, A., ... & Yaktubay, S. (2009). Adoption and impacts of improved winter and spring wheat varieties in Turkey.

Mercer, K. L., & Perales, H. R. (2010). Evolutionary response of landraces to climate change in centers of crop diversity. Evolutionary applications, 3(5-6), 480-493.

OER Commons, 2021, https://oercommons.org/courseware/lesson/87625/student/?section=2 Erişim Tarihi: 9 Aralık 2025

Prescott, J. M., Burnett, P. A., Saari, E. E., Ransom, J. K., Bowman, J., De Milliano, W. A. J., ... & Bekele, G. T. (1987). Bugday hastalik ve zararlilari: Tarlada tanima kilavuzu.

Qualset, C.U., Zannata, A.C.A., Keser, M., Kılınç, N., Brush, S.B. (1996). Agronomic Performance of Wheat Landraces from Western Turkey. Basis for In-situ Conservation Practices by Farmers. In 5. International Wheat Conference, June 10-14, 1996, Book of Abstracts, Ankara.

Salantur, A., Tekin, A. G. M., Bağcı, S. A., Eser, V., & Akar, T. (2017). Türk buğday yerel çeşitleri ve bitki ıslahı. TURKTOB Dergisi, 24, 18–20.

Republic of Türkiye Ministry of Agriculture and Forestry Directorate of Plant Protection Central Research Institute. (2014). Hububat Zararlıları Rehberi. http://arastirma.tarimorman.gov.tr/zmmae/Belgeler/Sol%20Menu/Zirai%20M%C3%BCcadele%20Rehberi/Hububat/Hububat-Zararl%C4%B1.pdf

Tanveer, M., & Ahmed, H. A. I. (2020). ROS signalling in modulating salinity stress tolerance in plants. In M. Hasanuzzaman & M. Tanveer (Eds.), Salt and drought stress tolerance in plants (pp. 299–314). Springer.

T.C. Konya Valiliği, 2025, https://www.konya.gov.tr/konya-ivriz-kaya-aniti Erişim Tarihi: 9 Aralık 2025

Ulusal Tohum Gen Bankası, 2025, https://arastirma.tarimorman.gov.tr/etae/Menu/49/Ulusal-Tohum-Gen-Bankasi Erişim Tarihi: 9 Aralık 2025

Zanatta, ACA., Keser, M., Kilinc, N., Brush, SB., and Qualset, CO. (1996). Agronomic Performance of wheat Landraces from Western Turkey: Bases for in situ Conservation Practices by Farmers. 5th International Wheat Conference, June 10-14, 1996, Ankara, Turkey.

Zanatta, ACA., Keser, M., Kilinc, N., Brush, SB., and Qualset, CO. (1998). Competitive Performance of wheat Landraces from Western Turkey: Basis for Locally Based Conservation of Genetic Resources, Proceedings of the 9th International Wheat Genetics Symposium, 2-7 August 1998, Saskatoon, Saskatchewan, Canada.

Zhukovsky, PM. (1951). Ecological Types and Economic Importance of Anatolian wheat (Translators: C. Kıpçak, H. Nouruzhan and S. Türkistanlı), pp.158-214. In: Agricultural Structure of Turkey (in Turkish). Turkish Sugar Beet Plants Publications No.: 20.

Zimin, A.V., Puiu, D., Hall, R., Kingan, S., Clavijo, B.J., ve Salzberg, S.L. (2017). The first near-complete assembly of the hexaploid bread wheat genome, Triticum aestivum. Gigascience, 6(11).

# CHAPTER 3

# THE EFFECT OF PLANTING SCHEMES AND MINERAL FERTILIZERS ON TOTAL NITROGEN ACCUMULATION IN SUGAR BEET UNDER GREY-BROWN SOILS

Prof. Dr. Aslanov Hasanali Asad[1], Aslanova  Dilbar Hasanali[2]

[1]Azerbaijan State Agricultural University Ganja, Ataturk pr. 450

ORCID: 0009 0000 9927 2310 e-mail: azhas@rambler.ru

[2] Azerbaijan State Agricultural University Ganja, Ataturk pr. 450
ORCID: 0009-0009-7846-3156,  e-mail: dilbaraslanova@adau.edu.az

## 1. INTRODUCTION

In studies conducted in many countries, various aspects of sugar beet cultivation have been investigated over the years, including its global cultivation area, production volume, economic importance, breeding and selection, varieties and hybrids, as well as the impact of different agrotechnical practices on soil fertility, plant growth and development, nutrient accumulation and translocation within the plant, yield, and product quality. However, in the Ganja–Dashkasan economic region, where our research was carried out, almost no studies have been conducted in recent years on the planting schemes and fertilization of sugar beet hybrids. Therefore, it is important to review the literature sources we have consulted regarding sugar beet cultivation.

Sugar beet is an important industrial crop used both for sugar production and as animal feed. It is the only source of sugar production in Azerbaijan. More than 50 countries around the world produce sugar from sugar beet, while over 70 countries—mainly located in tropical and subtropical regions—obtain sugar from sugarcane, a perennial crop native to those climates.

The root crops of sugar beet contain, on average, 16–20% sugar. During industrial processing at sugar factories, valuable by-products such as beet pulp and molasses are obtained. The dry matter of molasses contains up to 60% sugar, 15% nitrogen-free extractive substances, and 8–9% ash. These by-products are used for the production of alcohol, glycerin, food yeast, lactic and citric acids, and pectin glue.After pressing, beet pulp contains about 15% dry matter, including 10% nitrogen-free extractive substances, 3% cellulose, 0.7% ash, 0.1% fat, and 1.2% crude protein. Beet pulp is considered a valuable feed for cattle; each quintal (100 kg) of pulp is equivalent to 80–85 feed units. When the yield of sugar beet reaches 30 tons per hectare, the amount of pulp obtained is approximately 24 tons per hectare. At the same time, sugar beet processing residues are also used as fertilizers in agricultural production. This fertilizer contains approximately 40–50% lime, 15% organic acids, 0.2–1.7% nitrogen, 0.2–0.8% phosphorus, and 0.5–0.9% potassium. During harvesting, the leaves of sugar beet, as well as the tops and upper parts of the root crops, are utilized as livestock feed in fresh, ensiled, or dried forms. In terms of feed value, sugar beet surpasses fodder beet by approximately two times. The leaves are particularly rich in nutrients, containing 2–3% protein, 0.4% fat, and various vitamins. One quintal (100 kg) of sugar beet is equivalent to 26 feed units or about 1.2 kg of protein. One quintal of sugar beet leaves is equivalent to 20 feed units, while fodder beet corresponds to 12 and 9 feed units, respectively. It should be noted, however, that animals should not be fed excessively with sugar beet leaves. Both in fresh and ensiled forms, these leaves contain a high amount of oxalic acid, which can disrupt calcium metabolism in animals (Mammadov and Ismayilov, 2012).

Sugar beet has a long vegetation period and absorbs significant amounts of nutrients from the soil. Therefore, it has high nutritional requirements for optimal growth and development. The crop grows best on humus-rich loamy and sandy-loam soils. Optimal agrochemical soil characteristics include near-neutral soil reaction (pH 6.0–6.8 in KCl), humus content of at least 1.8%, mobile (available) phosphorus and potassium at 15–30 mg/kg and 150–300 mg/kg, respectively, and boron at a minimum of 0.7 mg/kg.Sugar beet absorbs nutrients throughout its entire vegetation period. In the initial stages of growth, it takes up relatively small amounts of

nitrogen, phosphorus, and potassium. At this time, the root system is still weakly developed, but young plants are highly sensitive to the absence of nutrients in the soil, particularly phosphorus. Later, nutrient uptake sharply increases, reaching a maximum during intensive leaf formation and the early stages of root growth. By the end of the vegetation period, approximately 43% of nitrogen, 18% of phosphorus, and 38% of potassium in sugar beet roots are lost due to leaf senescence, shedding, and nutrient leaching back into the soil.

Sugar beet is a potassium-loving crop. Sugar beet with a yield of 60 t/ha can remove up to 414 kg/ha of potassium from the soil. It tolerates chloride-containing fertilizers well and responds positively to the effect of sodium, which helps in the translocation of carbohydrates to the root crops.

Sugar beet also requires significant amounts of micronutrients. Among these, boron is particularly essential, especially on calcareous soils. Boron deficiency in sugar beet can lead to root rot and a reduction in both sugar content and root yield. The fertilization system for sugar beet primarily involves the application of organic and mineral fertilizers, pre-sowing phosphorus or complex fertilizers (NPK), as well as supplementary foliar feeding with nitrogen and micronutrients.

Sugar beet is a crop that is demanding in terms of soil conditions. The most suitable soils for its cultivation are loamy and sandy-loam soils. The optimal soil reaction (pH) for sugar beet is between 6.5 and 7.5.

At the early stages of growth, sugar beet absorbs relatively small amounts of nitrogen, phosphorus, and potassium; however, it is highly sensitive to phosphorus deficiency during this period. Applying 10–20 kg/ha of $P_2O_5$ in the rows at sowing creates a favorable nutrient regime during the first 15–20 days after emergence. During the period of intensive leaf growth, sugar beet requires large amounts of nitrogen and potassium. For root formation, the plants need moderate nitrogen and strong phosphorus and potassium nutrition. The maximum nutrient demand of sugar beet is observed in July–August.Sugar beet responds well to organic fertilizers. Due to its long vegetation period, it efficiently utilizes nutrients. Organic fertilizers, such as well-composted manure or peat-manure composts stored under pressure for 4–5 months, are most effective when applied in spring and summer. In the autumn, these fertilizers should be applied at a rate of 40–80 t/ha under the plow.

Nitrogen fertilizers are the most effective mineral fertilizers for sugar beet. Each kilogram of nitrogen contributes to an increase in root yield by 50–60 kg. However, to improve the quality of root crops, the maximum rate of nitrogen fertilizers should not exceed 130–150 kg/ha. Excessive nitrogen fertilization leads to the accumulation of alpha-amino nitrogen in the roots and a reduction in the purity of cell sap, which ultimately decreases sugar yield. It is recommended to apply nitrogen fertilizers at a rate of 100–110 kg/ha as the main dose and 35–40 kg/ha as a top-dressing.

Phosphorus and potassium fertilizers are recommended for application before sowing, and on heavy soils, in the autumn. For the main application, all types of nitrogen, phosphorus, and potassium fertilizers available in the country can be used. At the same time, the use of ammonium nitrate is characterized by the lowest economic efficiency. To prevent leaf burn during top-dressing, it is advisable to use solid forms of nitrogen fertilizers.

Modern technologies for sugar beet cultivation include the application of complex fertilizers during soil preparation for sowing. This practice significantly affects plant growth and

development, crop yield, and sugar content. It also reduces the costs of fertilizer application and, compared to the use of simple fertilizers (nitrogen, phosphorus, and potassium), ensures a more uniform distribution of nutrients across the cultivated area.

Recently, the modern chemical industry has developed simple, balanced complex fertilizers for sugar beet, taking into account soil fertility and the biological characteristics of the crop. Currently, the most popular complex fertilizer is $N_{13}P_{12}K_{19}$, which contains all the essential mineral nutrients for plants in balanced proportions and also includes B, S, and Na. The use of complex fertilizers provides significant savings (up to 65%) in the application of mineral fertilizers, and additionally eliminates the need to apply ammonium sulfate with nitrogen fertilizer or 2–3 kg/ha of boric acid. Applying 1,000 kg/ha of this complex fertilizer per hectare ensures optimal doses of nitrogen, phosphorus, and potassium. It has been established that increasing the phosphorus rate above 120 kg/ha and potassium above 190 kg/ha is not economically efficient when applied on the background of 60–80 t/ha of organic fertilizer, as their payback period sharply decreases. According to agrochemical criteria, increased rates of phosphorus and potassium do not adversely affect the plants, and some potassium remains in the soil. Therefore, in a resource-efficient fertilizer application system, the optimal rates are determined based on both agrochemical and economic considerations.

In the absence of complex fertilizers, urea, ammophos, or ammonium superphosphate and potassium chloride should be used for sugar beet. Complex fertilizers can be produced according to established technical specifications, incorporating any set of micronutrients, plant growth regulators, or long-acting components as needed.

The application rates of complex nitrogen-phosphorus-potassium fertilizers for sugar beet are determined based on the planned yield and the content of mobile forms of phosphorus and potassium in the soil. Nitrogen and phosphorus doses (within the complex fertilizer) are calculated accordingly.

For the planned yield, full-rate complex nitrogen-phosphorus-potassium (NPK) fertilizers are applied in early spring using a cultivator. With this method, the fertilizers are mainly incorporated into the 0–12 cm soil layer, with approximately 24% distributed within the 7–12 cm layer.For sugar beet, the single-application rate of complex fertilizers within an organo-mineral fertilization system (with 60–70 t/ha of organic manure) is set so that nitrogen does not exceed 140 kg/ha, and in a mineral fertilization system, the effective nutrient content should not exceed 150 kg/ha.During the sugar beet growing season, foliar application of micronutrient fertilizers is performed at the 10–12 leaf stage and 1–1.5 months after the first fertilization. Boron is applied at a rate of 200–300 g/ha, and manganese at 50–75 g/ha. When the soil content of micronutrients is low, additional fertilization is recommended (Aslanov and Huseynov, 2025).

In the Ganja-Dashkasan economic region, under the conditions of Samukh district, research on the effect of planting schemes and mineral fertilizer rates on sugar beet yield and quality was conducted by D.H. Aslanova under the supervision of Prof. S.Z. Mammadova in gray-brown soils. It was determined that, on average over three years, in the control (unfertilized) variant with a 50×15 cm planting scheme, sugar beet root yield was 358.4 c/ha.Within the same planting scheme, increasing doses of nitrogen fertilizers on the background of $P_{120}K_{90}$ significantly influenced sugar beet productivity. The highest yield was observed in the $P_{120}K_{90} + N_{90}$ variant – 602.3 c/ha, which is 243.9 c/ha (68.1%) higher than the

unfertilized control, and the yield increase per 1 kg of NPK was 81.3 kg.With further increase in nitrogen dose ($P_{120}K_{90} + N_{120}$), yield decreased compared to the $P_{120}K_{90} + N_{90}$ variant: 548.6 c/ha, with a yield increase of 190.2 c/ha (53.0%), and the yield per 1 kg of NPK was 57.6 kg (Mammadova and Aslanova, 2021).

Additionally, based on research conducted by D.H. Aslanova, it was determined that the planting scheme and the application of mineral fertilizers increase the content of total nitrogen, phosphorus, and potassium in sugar beet roots, which significantly affects the removal of nutrients from the soil. The highest nutrient removal from the soil was observed in the 50×15 cm planting scheme with mineral fertilizers applied at the rate of $N_{90}P_{120}K_{90}$. Under these conditions, nitrogen removal ranged from 90.20 to 125.42 kg/ha, phosphorus from 36.00 to 50.20 kg/ha, and potassium from 65.50 to 92.00 kg/ha (Aslanova, 2021).

The economic importance of sugar beet is extremely high, which is why this crop is included among the main industrial crops in most countries. In our republic, after key industrial crops such as cotton and tobacco, particular attention has recently been paid to the development of sugar beet. Sugar beet primarily serves as a raw material for sugar, one of the most valuable food products. Worldwide, 40% of sugar production comes from sugar beet.Research has shown that the application of mineral fertilizers together with manure under sugar beet significantly affects the accumulation of total nitrogen in both leaves and roots at different stages of development. As a result of fertilizer application, at the end of the growing season, total nitrogen in the leaves ranged from 0.26–0.29%, and in the roots from 0.30–0.33%, which represents an increase compared to the control (unfertilized) variant. The highest total nitrogen content during each developmental stage was observed in the variant with manure at 10 t/ha combined with $N_{90}P_{120}K_{90}$ mineral fertilizers. It was also determined that, with the application of manure together with mineral fertilizers under sugar beet, there is a significant correlation between total nitrogen content (%) in leaves and roots and the yield of leaves and roots (s/ha) across variants and developmental stages ( Aliyeva, 2015).

In the studies, the application of micronutrients at the 4–6 leaf stage under sugar beet, in combination with mineral fertilizers (NPK), increased nitrogen content in the leaves by 0.02–0.05% during the early leaf stage, by 0.03–0.07% during leaf thickening, and by 0.07% in the roots. Nitrogen accumulation was more pronounced in actively developing organs, which plays a significant role in nutrient uptake by the plant, sugar accumulation in the roots, photosynthesis, cold and drought resistance, root development, maturation, and overall quality improvement. Yield in the variant with only mineral fertilizers was 65.9 t/ha, whereas with the additional foliar application of micronutrients, it increased to 661.3–709.0 s/ha (Buldikova, 2013).

The application of mineral fertilizers under sugar beet at a rate of 240 kg/ha (NPK) increased nitrogen content in the roots from 0.64% to 1.03% in absolute dry matter. Sugar content and sugar yield were most efficient when harvesting was carried out at plant densities of 94–100 thousand plants per hectare and on September 25 (Gureev, and Agibalov, 2002).

The use of mineral fertilizers under sugar beet ($N_{120}P_{120}K_{120}$ and $N_{240}P_{240}K_{240}$) significantly increased the total NPK content in the root crop. As a result of fertilization, nitrogen content ranged from 1.69% to 1.80% (Gvozdov et al 2004).

Research conducted on irrigated gray-chestnut soils has shown that the application of locally sourced organic fertilizers, both individually and in the form of "Mil" compost, under

sugar beet significantly influenced the accumulation of total nitrogen in the leaves and roots at different growth stages. In the control (unfertilized) variant, total nitrogen at the harvesting stage was 2.30% in the leaves and 0.45% in the roots, whereas in the variants with organic fertilizers, total nitrogen ranged from 2.32% to 2.52% in the leaves and from 0.46% to 0.64% in the roots. The use of organic fertilizers under sugar beet positively affected plant height, leaf blade area, the number of leaves at different growth stages, and both root and leaf biomass. The best results were observed in the variant with 40 t/ha of "Mil" compost combined with $N_{50}P_{25}K_{60}$ fertilizers (Ahmadova, 2018).

Research conducted in the Republic of Bashkortostan, Russian Federation, showed that the highest sugar beet yield (32.7 t/ha) was obtained with the application of a 300 kg/ha organic-mineral fertilizer mixture. In this variant, sugar content in the roots ranged from 16.0% to 16.8%, and nitrogen in the roots increased by 0.2% (Khadiyev, 2012).

Analyzing the chemical composition of plants allows for the determination of the agrochemical properties of soils, thereby enabling the assessment of each crop's nutrient requirements (Tserliny and Zinkevich, 1975).

In the northern part of the Lesser Caucasus, the effect of fertilizers on sugar beet yield and feed value was studied on leached mountain-black soils. Compared to the unfertilized control, an increase in sugar beet yield was observed depending on the type and ratio of fertilizers applied. The highest yield was obtained in the $N_{90}P_{120}K_{90} + B_6$ variant. Over three years, the average root yield in the unfertilized control was 231.5 c/ha, whereas in the $N_{90}P_{120}K_{90} + B_6$ variant it reached 383.2 c/ha, representing an increase of 151.7 c/ha, or 65.5%.Fertilizers not only increased root yield but also enhanced aboveground biomass. The aboveground biomass in the control was 87.1 c/ha, while in the $N_{90}P_{120}K_{90} + B_6$ variant it reached 142.3 c/ha, an increase of 55.2 c/ha or 63.3%.Depending on the fertilizer rates and ratios, the feed value of sugar beet also improved. The amount of feed units and digestible protein per unit area increased. The highest feed units and digestible protein were recorded in the $N_{90}P_{120}K_{90} + B_6$ variant, with feed units of 92.2 c/ha and 27.8 c/ha, and digestible protein of 410.8 kg/ha and 303.6 kg/ha in roots and leaves, respectively. In the unfertilized variant, the corresponding values were 41.3 c/ha and 52.4%, respectively (Baghirov, 2016).

The effect of plant density on sugar beet yield and quality was studied on gray-chestnut soils in the Barda district by H.Ş. Hümbətov and A.R. Baxşəliyeva. At a planting scheme of 70x20 cm (71,000 plants/ha), the root yield was 191.5 c/ha, with 26 feed units per centner, equivalent to 49.79 c/ha of feed units. At a 70x25 cm planting scheme (57,000 plants/ha), the yield increased to 276.3 c/ha and 71.83 c/ha of feed units. In the variant with reduced plant density, i.e., 70x30 cm (47,000 plants/ha), the yield was 267.9 c/ha and 69.65 c/ha of feed units.Yields at plant densities of 71,000 and 47,000 plants/ha were lower compared to 57,000 plants/ha. To obtain high and quality sugar beet yield, farmers are recommended to adopt a 70x25 cm planting scheme, corresponding to a density of 57,000 plants/ha (Humbatov and Bakhshaliyeva, 2017).

Currently, sugar beet is considered the most profitable crop among agricultural plants in our republic. Despite being cultivated on only 10–20% of arable land, sugar beet contributes 30–50% of the total income from crop production. The Ganja-Dashkasan region occupies a decisive position in the republic in terms of agricultural production. From the perspective of food security, under the conditions of the western region, the increase of sugar beet productivity

on nutrient-poor irrigated gray-brown (chestnut) soils is a highly relevant issue today. Considering the importance of this problem, determining the optimal planting scheme and efficient mineral fertilizer rates that affect the yield and quality of sugar beet in the region remains a crucial task in the modern era.

## 2. OBJECT AND METHODOLOGY OF THE STUDY

Considering the significance of sugar beet, the study aimed to identify the main cultivation factors, including the planting scheme and mineral fertilizer rates, that ensure high and quality yields on irrigated gray-brown (chestnut) soils in the Ganja-Dashkasan economic region. The research was conducted at the Ganja Regional Agrarian Science and Innovation Center of the Ministry of Agriculture of the Republic of Azerbaijan, in the Samukh district, using the Caucasus variety of sugar beet under irrigated gray-brown soils.

Field experiments were conducted as a two-factorial trial (2×5) following cotton as a preceding crop, according to the following scheme:

**Factor A – Planting scheme:**
1. 50×10 cm (200,000 plants/ha)
2. 50×15 cm (133,000 plants/ha)
3. 50×20 cm (100,000 plants/ha)

**Factor B – Fertilizer rates:**
1. Control (without fertilizer)
2. $P_{120}K_{90}$ (background)
3. Background + $N_{60}$
4. Background + $N_{90}$
5. Background + $N_{120}$

Each experimental plot had a total area of 50.0 m² (20×2.5 m) and was arranged in a randomized row design with 4 replications. The experimental layout of the field trial is presented in the table.

In the experimental plots, the following mineral fertilizers were used: nitrogen – ammonium nitrate (34.7%), phosphorus – simple superphosphate (18.7%), and potassium – potassium sulfate (46%). Seventy percent of phosphorus and potassium was applied in the fall under the plow layer, while the remaining 30% of phosphorus and potassium, along with 50% of nitrogen, was applied at sowing. The remaining 50% of nitrogen was applied as top-dressing at the 7–8 true leaf stage.Sowing was conducted each year in the third ten-day period of March. The assessment of sugar beet was carried out for all replications and variants. Phenological observations included measuring the leaf and root biomass, root length and diameter, number and length of leaves, and assimilation surface area according to developmental stages. Samples were dried, ground, and analyzed in the laboratory. Agronomic practices were performed according to the accepted regional standards.

In the collected soil samples, the following analyses were performed: pH was determined potentiometrically; total humus content was measured according to I.V. Tyurin; ammonium nitrogen was determined by the D.P. Konev method; nitrate nitrogen by the Grandval-Lyage method; total nitrogen and total phosphorus by K.E. Ginzburg and Q.M.

Sheglov; mobile phosphorus by B.P. Machig; total potassium by Smith; and exchangeable potassium by P.B. Protasov method using a flame photometer.In plant samples, the following were determined: dry matter content at 105°C in a thermostat; total nitrogen, phosphorus, and potassium according to K.E. Ginzburg, Q.M. Sheglov, and E.V. Vulfus.

### 3. DISCUSSION AND ANALYSIS OF RESEARCH RESULTS

The effect of planting schemes and mineral fertilizers on the accumulation of total nitrogen in the leaves and root crops of sugar beet during its developmental stages on irrigated gray-brown (light brown) soils was investigated. The results of the study are presented in the table. Plant samples were collected at the stages of 7–8 true leaves formation, row closure, and technical ripeness for analysis. Depending on the planting scheme and fertilizer rates, the maximum total nitrogen content was observed at the 7–8 true leaves stage, while the minimum was recorded at the stage of technical ripeness.

As shown in the table, at a planting density of 200,000 plants per hectare with a 50×10 cm planting scheme, during the 7–8 true leaf formation stage, the total nitrogen content in the leaves of the control (unfertilized) variant was 2.83% on a dry matter basis, and in the root crops, it was 1.12%. During the row closure stage, total nitrogen in the leaves was 2.39% and in the roots 0.92%, while at the stage of technical ripeness, it was 2.08% in the leaves and 0.42% in the roots. In the $P_{120}K_{90}$ (background) variant, these values increased significantly compared to the control. During the 7–8 true leaf stage, total nitrogen was 2.93% in the leaves and 1.20% in the roots; during row closure, 2.47% in the leaves and 0.99% in the roots; and at technical ripeness, 2.15% in the leaves and 0.49% in the roots.

With increasing rates of nitrogen fertilizer combined with the background ($P_{120}K_{90}$), total nitrogen content in the leaves and root crops of sugar beet was higher in all studied growth stages compared to the control (unfertilized) and background variants. Specifically, in the $N_{60}$+background variant, during the 7–8 true leaf formation stage, total nitrogen was 3.05% in the leaves and 1.34% in the roots; during the row closure stage, 2.57% in the leaves and 1.16% in the roots; and at the stage of technical ripeness, 2.19% in the leaves and 0.54% in the roots. The highest total nitrogen content was observed in the $N_{90}$+background variant: during the 7–8 true leaf stage, 3.18% in the leaves and 1.49% in the roots; during row closure, 2.84% in the leaves and 1.29% in the roots; and at technical ripeness, 2.33% in the leaves and 0.68% in the roots. When nitrogen was applied at a rate of 120 kg/ha with the background, total nitrogen content decreased compared to the $N_{90}$+background variant.

Thus, the planting scheme (50×10 cm) and mineral fertilizers had a significant effect on the accumulation of total nitrogen in the leaves and root crops of sugar beet across different growth stages. The highest values were observed in the $N_{90}$+background variant at each growth stage, with total nitrogen at the end of vegetation during the technical ripeness stage increasing by 0.25% in the leaves and 0.26% in the roots compared to the control (unfertilized) variant. There was a strong positive correlation between sugar beet root yield (t/ha) and total nitrogen content (%) in both roots and leaves under the influence of planting scheme and

mineral fertilizers. During the technical ripeness stage, this relationship over the years ranged from r = +0.980 ± 0.020 to 0.974 ± 0.023.

As shown in the table, at a plant density of 133,000 plants per hectare (50×15 cm), the total nitrogen content was higher compared to the 50×10 cm planting scheme. This can be explained by the fact that plants under the 50×15 cm scheme had better nutrient availability and more efficient absorption of nutrients. Specifically, at the 7–8 true leaf stage, on a dry weight basis, total nitrogen in the leaves and roots of the control (unfertilized) variant was 2.88% and 1.14%, respectively; at the inter-row thickening stage, it was 2.43% in leaves and 0.94% in roots; and at the technical ripeness stage, 2.07% in leaves and 0.43% in roots. In the $P_{120}K_{90}$ (background) variant, these values increased significantly compared to the control, reaching 2.94% in leaves and 1.21% in roots at the 7–8 true leaf stage, 2.49% in leaves and 1.02% in roots at the inter-row thickening stage, and 2.22% in leaves and 0.53% in roots at the technical ripeness stage.

**Effect of Planting Scheme and Mineral Fertilizers on Total Nitrogen Accumulation in Sugar Beet at Different Growth Stages (Average Over 3 Years, %)**

Under increasing rates of nitrogen fertilizer applied together with the background $P_{120}K_{90}$, the total nitrogen content in sugar beet leaves and roots was higher compared to both the control (unfertilized) and background-only variants across all growth stages studied.



**Figure 1.** Active vegetative growth phase of sugar beet (Photo by the outher , 2021)

The influence of planting density and mineral fertilizers on total nitrogen accumulation in sugar beet was evaluated at the following growth stages (average over three years, %):

- **7–8 true leaf stage:** Total nitrogen in leaves and roots showed a significant increase with increasing nitrogen rates combined with $P_{120}K_{90}$ compared to control and $P_{120}K_{90}$ alone.

- **Inter-row thickening stage:** Total nitrogen continued to rise with higher nitrogen application, reflecting improved nutrient uptake.
- **Technical ripeness stage:** Although the total nitrogen content decreased compared to earlier stages, fertilized variants maintained higher nitrogen levels than the control, indicating a sustained effect of the applied fertilizers.

Thus, both planting scheme and mineral fertilizer application significantly influenced the accumulation of total nitrogen in sugar beet leaves and roots, with the highest values observed under the $N_{90}+P_{120}K_{90}$ treatment across all growth stages.

**Table 1.** Effect of Planting Density and Fertilizer Application on Total Nitrogen Content in Sugar Beet at Different Growth Stages (% average over three years)

| s/s | Treatment | 7-8 True Leaf Stage | | İnter-Row Thickening stage | | Technical Ripenese Stage | |
|---|---|---|---|---|---|---|---|
| | | Leaves | Roots | Leaves | Roots | Leaves | Roots |
| | | | | 50x10 sm | | | |
| 1 | Control (no fertilizer) | 2,88 | 1,12 | 2,39 | 0,92 | 2,08 | 0,42 |
| 2 | Background ($P_{120}K_{90}$) | 2,93 | 1,20 | 2,47 | 0,99 | 2,15 | 0,49 |
| 3 | $N_{60}$+Fon | 3,05 | 1,34 | 2,57 | 1,16 | 2,19 | 0,54 |
| 4 | $N_{90}$+Fon | 3,12 | 1,49 | 2,84 | 1,29 | 2,33 | 0,68 |
| 5 | $N_{120}$+Fon | 3,15 | 1,43 | 2,76 | 1,24 | 2,27 | 0,63 |
| | | | | 50x15 sm | | | |
| 1 | Control (no fertilizer) | 2,88 | 1,14 | 2,43 | 0,94 | 2,07 | 0,43 |
| 2 | Background ($P_{120}K_{90}$) | 2,94 | 1,21 | 2,49 | 1,02 | 2,22 | 0,53 |
| 3 | $N_{60}$+Fon | 3,08 | 1,36 | 2,59 | 1,20 | 2,26 | 0,56 |
| 4 | $N_{90}$+Fon | 3,21 | 1,52 | 2,86 | 1,32 | 2,40 | 0,74 |
| 5 | $N_{120}$+Fon | 3,18 | 1,45 | 2,78 | 1,27 | 2,35 | 0,66 |
| | | | | 50x20 sm | | | |
| 1 | Control (no fertilizer) | 2,93 | 1,19 | 2,49 | 0,99 | 2,12 | 0,45 |
| 2 | Background ($P_{120}K_{90}$) | 2,98 | 1,24 | 2,54 | 1,09 | 2,24 | 0,56 |
| 3 | $N_{60}$+Fon | 3,15 | 1,45 | 2,65 | 1,24 | 2,29 | 0,62 |
| 4 | $N_{90}$+Fon | 3,23 | 1,54 | 2,90 | 1,36 | 2.48 | 0.80 |
| 5 | $N_{120}$+Fon | 3,21 | 1,49 | 2,84 | 1,33 | 2,39 | 0.70 |

The accumulation of total nitrogen in sugar beet leaves was highest across all growth stages in the $N_{60}$+Fon treatment. Specifically, at the 7–8 true leaf stage, total nitrogen in the leaves reached 3.08% and in the roots 1.36%; during the inter-row compactness stage, nitrogen content was 2.59% in the leaves and 1.20% in the roots; and at the technical maturity

stage, nitrogen content was 2.26% in the leaves and 0.56% in the roots.The highest total nitrogen content was observed in the N90+Fon treatment, with leaf nitrogen reaching 3.21% and root nitrogen 1.52% at the 7–8 true leaf stage, 2.86% and 1.32% at the inter-row compactness stage, and 2.40% and 0.74% at the technical maturity stage, respectively.

At an increased nitrogen rate of 120 kg/ha combined with the base fertilization (Fon), the total nitrogen content decreased compared to the N90+Fon treatment. Specifically, at the 7–8 true leaf stage, total nitrogen reached 3.18% in the leaves and 1.45% in the roots; during the inter-row compactness stage, it was 2.78% in the leaves and 1.27% in the roots; and at the technical maturity stage, nitrogen content was 2.35% in the leaves and 0.66% in the roots.

Thus, the 50×15 cm planting scheme and mineral fertilization had a significant effect on the accumulation of total nitrogen in the leaves and roots of sugar beet across the growth stages, similar to the 50×10 cm planting scheme. The highest total nitrogen content was observed in the N90+Fon treatment at all growth stages, with total nitrogen at the end of vegetation reaching 0.33% in the leaves and 0.31% in the roots, compared to the unfertilized control. The effect of the planting scheme and mineral fertilization showed a strong positive correlation between root yield (t/ha) and the total nitrogen content in both leaves and roots, with the correlation coefficient during the technical maturity stage ranging from r = +0.984 ± 0.014 to 0.992 ± 0.007 across the years.

As shown in the table, at a planting density of 100,000 plants per hectare (50×20 cm), the total nitrogen content in both leaves and roots was higher compared to the 50×10 cm and 50×15 cm planting schemes. This can be attributed to the greater nutrient availability per plant and improved nutrient absorption under the wider spacing. Specifically, at the 7–8 true leaf stage, the total nitrogen in the leaves and roots of the unfertilized control was 2.93% and 1.19%, respectively. During the inter-row thickening stage, nitrogen content was 2.49% in leaves and 0.99% in roots, while at the technical maturity stage, it reached 2.12% in leaves and 0.45% in roots. In the P120K90 (background fertilization) treatment, these values increased significantly compared to the control, with total nitrogen in leaves and roots at the 7–8 true leaf stage of 2.98% and 1.24%, respectively; during inter-row thickening, 2.54% and 1.09%; and at technical maturity, 2.24% and 0.56%.

Under increasing nitrogen fertilizer rates combined with the background fertilization (P120K90), the total nitrogen content in sugar beet leaves and roots was higher at all studied growth stages compared to the control (unfertilized) and background treatments. In the N60+Background treatment, at the 7–8 true leaf stage, total nitrogen in leaves and roots was 3.15% and 1.45%, respectively; during the inter-row thickening stage, it was 2.65% in leaves and 1.24% in roots; and at the technical maturity stage, 2.29% in leaves and 0.62% in roots. The highest total NPK content was observed in the N90+Background treatment, with leaf and root nitrogen reaching 3.23% and 1.54%, respectively, at the 7–8 true leaf stage; 2.90% and 1.36% during inter-row thickening; and 2.45% and 0.78% at technical maturity. Increasing nitrogen to 120 kg/ha in combination with the background fertilization slightly decreased total nitrogen compared to the N90+Background treatment, with values of 3.21% in leaves and

1.54% in roots at the 7–8 true leaf stage, 2.84% and 1.33% during inter-row thickening, and 2.48% and 0.80% at technical maturity.

Thus, the planting scheme (50×20 cm) and mineral fertilizers had a significant effect on the accumulation of total nitrogen, phosphorus, and potassium in sugar beet leaves and roots across developmental stages, similar to other planting schemes. The highest amounts of nitrogen, phosphorus, and potassium were observed in the N90+Background treatment at all growth stages. At the end of the vegetation period, during the technical maturity stage, total nitrogen in leaves and roots increased by 0.36% and 0.35%, respectively, compared to the control (unfertilized) treatment. The influence of the planting scheme and mineral fertilizers also resulted in a strong correlation between sugar beet root yield (t/ha) and the total nitrogen content (%) in leaves and roots. Over the years, this relationship during the technical maturity stage ranged from r = +0.997 ± 0.003 to 0.998 ± 0.002.



**Figure 2.** Sugar beet at full maturity stage maximum root development and sugar accumulation

## 4. CONCLUSION

The planting scheme (50×15 cm) and mineral fertilizers significantly influenced the accumulation of total nitrogen in sugar beet leaves and roots across developmental stages. The highest total nitrogen content was observed in the N90+Background treatment at all

growth stages, and by the end of the vegetation period, it was significantly higher compared to the control (unfertilized) treatment.

**REFERENCES**

Ahmadova, A. F. (2018). *Agrochemical and economic efficiency of applying new organic fertilizers derived from waste and residues in the Mil plain under sugar beet cultivation* (Abstract of dissertation for the degree of Doctor of Philosophy in Agronomy). Baku.

Aliyeva, G. A. (2015). The effect of fertilizers on the accumulation of total nitrogen, phosphorus and potassium in sugar beet under irrigation conditions. In *Innovative development of agrarian science and education: world experience and modern priorities: Proceedings of the International Scientific-Practical Conference* (pp. 35–40). Ganja: ADAU Publishing. October 23–24).

Aslanov, H. A., & Huseynov, N. V. (2025). *System of fertilizer application*. Baku: Elm.

Aslanova, D. G. (2021). Optimization of technological methods for cultivating sugar beet in the Ganja–Gazakh zone of Azerbaijan. *Agrarnaya Nauka (Agrarian Science)*, (1), 125–128.

Baghirov, H. J. (2016). The effect of fertilizers on the yield and nutritional value of sugar beet on leached mountain black soils in the northern part of the Lesser Caucasus. In *Development of agrarian science, food security and environmental protection through international cooperation: Proceedings of the 8th International Scientific-Practical Conference* (Vol. 2, pp. 11–14). October 3–4). Ganja: ADAU Publishing.

Buldikova, I. A. (2013). Dynamics of nitrogen, phosphorus and potassium content in sugar beet plants under the application of microfertilizers. *Enthusiasts of Agrarian Science: Proceedings of KubSAU*, (15), 78–80.

Gureev, I. I., & Agibalov, A. V. (2002). Sugar beet production without manual labor costs. *Sakharnaia Svekla (Sugar Beet)*, (2), 6–10.

Gvozdov, N. V., Lukin, A. P., Bychkova, V. A., Goryachikh, N. G., & Skachkov, S. I. (2004). Productivity and quality of sugar beet varieties and hybrids. *Sakharnaia Svekla (Sugar Beet)*, (9), 24–25.

Humbatov, H. Sh., & Bakhshaliyeva, A. R. (2017). The effect of plant density on root yield of sugar beet. *Scientific Works of ADAU*, (3), 22–23. Ganja: ADAU Publishing.

Khadiyev, I. R. (2012). *Soil fertility and crop productivity in a sugar beet crop rotation under organic-mineral fertilizer application in the Pre-Ural steppe of Bashkortostan* (Abstract of dissertation for the degree of Candidate of Agricultural Sciences). Orenburg.

Mammadov, G. Y., & Ismayilov, M. M. (2012). *Crop production*. Baku: Sharq-Qarb.

Mammadova, S. Z., & Aslanova, D. H. (2021). The effect of plant density and mineral fertilizer rates on the growth and development of sugar beet. *Scientific News of Azerbaijan Technological University*, 1(34), 103–108. Ganja.

State Statistical Committee of the Republic of Azerbaijan. (n.d.). *Statistical data*. Retrieved from https://www.stat.gov.az

Tserliny, V. V., & Zinkevich, A. S. (1975). Biological removal: its characteristics and variability as a diagnostic indicator of plant nutrition for different crops. *Agrokhimiya (Agrochemistry)*, (8), 127–132.

# CHAPTER 4

# EFFECT OF SOWING METHODS AND SOWING RATE ON YIELD COMPONENTS AND KERNEL QUALITY OF BREAD WHEAT (TRITICUM AESTIVUM L.) VARIETY 'QIYMETLI-2/17' IN AZERBAIJAN

Phd. Associate  Aynur Hasanova[1],  Phd. Assistant Professor Aytan Zeynalova[2],
Phd. Assistant Professor Ramila Qehremanova[3]

[1]Azerbaıjan State Agricultural University, Faculty of Agronomy, Department of General Agriculture, Genetics and Selection, Ganja-Azerbaijan, ORCID No: 0009-0008-1713-0860, aynur.hasanova@adau.edu.az
[2] Azerbaıjan State Agricultural University, Faculty of Agronomy, Department of General Agriculture, Genetics and Selection, Ganja-Azerbaijan, ORCID No: 0000-0001-6672-9142, aytan.zeynalova@adau.edu.az
[3] Azerbaıjan State Agricultural University, Faculty of Agronomy, Department of General Agriculture, Genetics and Selection, Ganja-Azerbaijan, ORCID No: 0000-0002-4455-5847, qehremanova1977@gmail.com

## 1. INTRODUCTION

The sowing of wheat using the bed planting method and row spacing, and its inclusion in crop rotation as a cultivated plant, is of great importance in this matter. Compared to other crops, wheat occupies the largest sowing area across all regions of Azerbaijan and is given special attention as the main bread crop.

Results obtained from scientific research indicate that to achieve high yields from cereal crops, it is essential to study the biological characteristics of the cultivated plants, their requirements for a complex of environmental factors in a justified manner, and optimize these conditions. It has been established that bread contains 210 different substances that affect its quality, taste, and aroma. Almost 20% of the total daily caloric intake required by humans comes from wheat.

According to Jumshudov (2013), wheat, as the first cultivated plant in the early stages of agriculture and one of the most important crops for human nutrition, continues to increase in importance today and will remain a strategic crop globally in the future. Today, hunger is the most significant problem threatening humanity. The rapid population growth in underdeveloped and developing countries makes solving this problem increasingly difficult each year. The two main reasons for the worsening global hunger problem and increasing concerns are droughts caused by global climate change and conflicts arising from regional disputes. Three-quarters of the countries most affected by hunger are nations devastated and plundered by wars. It is no coincidence that most of these countries are underdeveloped or developing. The rapid growth of the world population prevents many human needs, especially nutritional needs, from being fully met. The Executive Director of the World Food Programme, Catherine Bertini, explains: "Around 900 million people worldwide suffer from hunger, and the number of chronically hungry people increases by an average of four million each year."

Scientists emphasize that to address this problem, it is necessary to increase the production of wheat (*Triticum aestivum* L.), rice (*Oryza sativa*), maize (*Zea mays*), and other cereals primarily used for human consumption. Some researchers argue that today's food production is sufficient, and if distributed fairly, the food produced would be enough for all humans. When cereals produced worldwide are equally distributed, it amounts to over 300 kilograms per person per year, which is enough to meet the energy needs of all humans. The problem arises because in developed countries, the high consumption of animal-derived foods leads to the consumption of over 600 kilograms of cereals per person annually.

The productivity and quality of wheat grains are influenced by a combination of genetic factors, sowing methods, and environmental conditions. Key parameters such as thousand kernel weight (TKW), grain vitreousness, and test weight (hectoliter weight) serve as important indicators of both yield and processing quality. Variations in these parameters can be caused by sowing density, methods, and agrotechnical measures, which directly affect plant development and grain filling (Seyidaliyev et al., 2014). Understanding the relationship between sowing practices and these quality traits is essential for breeders and agronomists aiming to optimize wheat yield and quality under different agroecological conditions. This study focuses on evaluating the influence of bed sowing and varying sowing rates on the TKW, grain vitreousness, and test weight of the bread wheat variety "QIYMETLI-2/17."

## 2. MATERIALS AND METHODS

The field experiment was conducted using the bread wheat variety "QIYMETLI-2/17", which is widely cultivated in the region for its high yield potential and baking quality. The study aimed to evaluate the effects of sowing method and sowing rate on yield components, thousand kernel weight (TKW), grain vitreousness, and test weight. The trial was carried out in a randomized complete block design with four replications for each treatment.

Two sowing methods were compared:
- Ordinary row sowing (control), with a conventional seed rate of 4.0 million seeds per hectare.
- Bed planting, with sowing rates of 2.0, 2.5, and 3.0 million seeds per hectare.

Each plot had a size of (specify plot size, e.g., 10 m × 5 m), and standard agricultural practices were applied throughout the growing season. Soil preparation included plowing, harrowing, and leveling, ensuring uniform seedbed conditions across all treatments. Fertilization was applied according to local recommendations, with (specify amounts of N, P, K, if known), and pest and disease management was conducted to maintain optimal crop health. Irrigation and weed control were applied uniformly across all plots.

Measurements and data collection:
- Thousand kernel weight (TKW): Measured in grams from air-dried seeds collected from each plot. TKW reflects the size and density of grains and is influenced by environmental and agronomic factors.
- Grain Vitreousness (%): Determined visually by holding grains against light and assessing transparency and glassy sheen of the endosperm. Mealy grains were noted and expressed as a percentage of total grains.
- Test Weight (g/L): Measured as the mass of a defined volume of grain, reflecting bulk density and overall grain quality.

All measurements were taken following standard procedures, and each parameter was averaged across four replications. Statistical analysis was performed using (specify breadware, e.g., SPSS, R, or Excel) to assess the significance of differences between treatments. Variations in yield components and quality traits were interpreted in relation to sowing method, sowing rate, and the interaction with plant growth conditions, including soil fertility, moisture availability, and meteorological factors.

Additionally, environmental conditions, such as temperature, precipitation, and relative humidity, were monitored during the growing season to account for their potential influence on grain development. The integration of these factors allows for a comprehensive assessment of how agronomic practices affect wheat yield and quality under field conditions.

The main purpose of the field observations and laboratory analyses we conducted was to study the effect of plant density on the growth and productivity of the bread wheat variety "QIYMETLI-2/17" under two sowing methods — conventional row sowing (control) and bed planting. The experiment was carried out in four variants, including one control (Sowing 1), and with four replications.

**Table 1.** Scheme of the experiment (Jumshudov, 2013)

| Sowing methods | Sowing rates | Replications | | | |
|---|---|---|---|---|---|
| | | I | II | III | IV |
| Conventional row sowing (control) | 4.0 million seeds | 1 | 5 | 9 | 13 |
| Bed planting | 2,0 million seeds | 2 | 6 | 10 | 14 |
| Bed planting | 2,5 million seeds | 3 | 7 | 11 | 15 |
| Bed planting | 3,0 million seeds | 4 | 8 | 12 | 16 |

Technological observations included sowing time, germination, tillering, heading, flowering, and ripening periods. A few days before harvest, the number of productive stems per 1 m² and plant height were also determined based on the samples taken. Depending on the varieties and the complex of applied agrotechnical measures, changes in the yield components and physical characteristics of the grain in ridge sowing of wheat were also taken into account.

Soil and Climate Conditions of the Experimental Area. Samukh district is part of the Ganja-Gazakh region and the Central Kura economic zone. The climate is dry-continental. The total area of the district is 1,455 km², of which 1,082 km² are state-owned lands, 82 km² belong to municipalities, and 133 km² are privately owned. The district has 708 km² of agricultural land and includes 23 administrative territorial units and 35 settlements, of which 1 is a city, 5 are settlements, and 29 are villages. There are 23 municipalities operating in the district. Samukh borders the city of Ganja, and the districts of Goygol, Shamkir, Tovuz, Qakh, Yevlakh, Goranboy, as well as the Republic of Georgia.

According to Abbasova G.F. (2021), the relief of the mountainous part is of nival-glacial and erosional-glacial origin, while in the middle mountain zone it is of gravitational-denudation and denudation-erosional origin, composed mainly of Jurassic–Anthropogenic sediments.

The hydrographic network of the district includes the rivers Zayamchay, Aghstafachay, Hasansu, Shamkirchay, Tovuzchay, Goshgarchay, Injasu in the west, and Injachay in the east. The vegetation cover is mainly represented by desert, semi-desert, steppe, sparse forest, floodplain meadows, shrubs, and bushlands. The parent rocks of the soils are composed of proluvial, deluvial, loess-like, and alluvial deposits.

The territory of Samukh district is mostly flat. Part of it falls within the Kura depression, the Jeyranchol physical-geographical area, and the Bozdagh massif, bordered by the Alazani valley to the north. Major rivers crossing the district include the Kura, Qabirri (Iori), Alazani (Ganikh), Ganja, and Goshgar rivers.

In the Ganja–Gazakh plain, dry dark brown (chestnut) soils are widespread. These soils are divided mainly into the following types: dark brown (chestnut), brown (chestnut), light brown (chestnut), initial brown (chestnut), and anciently irrigated brown (chestnut) soils (Abbasova, 2021).

The experimental area (fields of the Plant Protection and Technical Crops Research Institute) belongs to the light brown (chestnut) soil subtype of the Western Zone of the Republic. According to Akimsev et al., (2015) light brown soils have a clayey to heavy clayey texture. Since the amount of physical clay in brown soils is relatively low, they are widely used for agricultural crops.

According to R.H. Mammadov, (2017) the granulometric composition of brown soils is as follows:
- Bulk density in the plow layer – 1.18 g/cm³,
- In the subsoil layer – 1.43 g/cm³,
- Specific gravity – 2.83–2.93.

The total porosity averages 54.8–62.4%, the field moisture capacity is 28.4–32.8%, and the water permeability reaches up to 111 mm per hour. The distribution of coarse silt fractions (0.25–0.01 mm) follows a regular pattern, accumulating mainly in the B horizon. These soils are free from easily soluble salts, both in the past and now.

The soils of the Plant Protection and Technical Crops Research Institute belong to the same type, with a well-cultivated plow layer (0–30 cm). The water permeability of these soils is moderate, and their chemical and physical properties are favorable for obtaining high sunflower yields.

According to Figurovski et al., (2014) the Ganja surroundings belong to the central dry subtropical zone and have a mild continental climate. Summers are hot and dry, while winters are mild. Frosts usually last from late November to the second ten-day period of April. The highest temperatures occur in July–August (35–36°C), with average monthly temperatures remaining high due to drought during these months. The annual precipitation ranges from 149 to 416 mm.

In Ganja, the average annual temperature is 13–14°C, with maximum temperatures reaching 35–37°C. The maximum precipitation occurs in May–June, while the minimum is observed in January–February. The number of rainy days reaches 70–75, and the relative humidity averages 70–80%. The climate is dry to semi-arid, of the moderately warm steppe type. The average annual temperature is 11.8–13.1°C, the sum of active temperatures is 4000–5000°C, the average air temperature in winter is 1–2°C, the mean temperature in July is 24–25°C, and in January it is 1.1°C. Annual precipitation ranges between 252 and 294 mm (Abbasova, 2021).

Agrochemical analyses of irrigated brown (chestnut) soils in the Samukh district under Ganja–Gazakh conditions show that, according to the national classification, these soils are poorly supplied with nutrients. Therefore, for the development of grape plants, obtaining high-quality, ecologically clean products, and maintaining soil fertility, the combined application of organic and mineral fertilizers is of great importance (Abbasova, 2021).

**Figure 1.** Samukh distircit in Azerbaijan

### 3. RESULTS

One of the important issues considered in the research plan and methodology was the study of the effect of sowing rate under row sowing on the yield components of wheat, depending on the variety.

The yield components of the wheat spike include: spike length, spike weight, number of spikelets per spike, number of grains, and grain weight. The variation of yield components in all plants depending on the variety, growing conditions, and the complex of agrotechnical measures has been extensively studied in numerous research works.

It has been proven in most cases that the variation of the main yield components of the wheat plant depends on the sowing rate and the method of sowing.

The results regarding the changes in the productivity elements of the ear depending on the sowing rate under bed planting conditions are presented in the relevant tables.

The data presented in the table 2 show that depending on the sowing method and rate, the weight of 1000 grains of the 'Qiymetli-2/17' bread wheat variety studied in the experiment varied between 46.1 and 48.3 grams.

Another parameter of interest in this study, depending on the sowing method and sowing rate, was the natural mass of the ear. In the control variant, the natural ear mass was 790 g, while in other variants it ranged between 791–795 g. The highest indicator was obtained under bed planting with a rate of 2.0 million seeds per hectare – 795 g. In this variant, the natural ear mass was 5 g higher compared to the control.

Another yield component of the wheat ear is grain vitreousness. In the 'Qiymetli-2/17' bread wheat variety, this indicator was 85.0% in the control variant, and 85.4%, 85.7%, and 85.2% in the other variants, respectively. When comparing sowing rates under bed planting, grain vitreousness was slightly higher at 86.6% with a sowing rate of 2.0 million seeds per hectare.

Like many important traits, ear mass is regulated depending on the plant's sufficient provision with a complex of life factors during the vegetation period. Proper supply of plants with water, nutrients, air, heat, and finally light, depending on sowing time, rate, variety, and sowing method, is considered highly important.

Numerous literature sources indicate that the weight of 1000 grains mainly depends on the growing conditions and the variety. The weight of 1000 grains of the same variety also depends on the sowing method, sowing rate, and soil–climatic conditions. The reasons mentioned above have also been confirmed in our findings regarding the variation in the 1000-grain weight.

The 1000-kernel weight is an indicator expressed in grams, reflecting the size and density of air-dried seeds. It is influenced by meteorological factors, agricultural practices, and other external conditions. During periods of drought and lack of soil moisture, seeds in plants are small and light. They are also affected by root placement, plant diseases, and pest damage. Agrotechnical measures applied to seed crops should help increase the 1000-kernel weight. It is crucial to provide plants with sufficient moisture and nutrients. This parameter varies among different plant species and varieties within the same species. It is also an important determinant for the proper calculation of sowing rates. Breeders aim to obtain higher absolute weights from different crops.

The increase in 1000-kernel weight with lower sowing rates can be attributed to reduced competition among plants, allowing for better resource allocation per plant. Chauhdary et al. (2016) also noted that bed planting improved kernel filling, leading to higher 1000-kernel weight. However, it is essential to balance sowing rates to avoid compromising plant density and overall yield. Further studies are needed to explore the long-term effects of sowing rates on other yield components and kernel quality.

The 1000-kernel weight is a significant indicator of kernel quality and yield potential in wheat cultivation. Previous studies have shown that sowing methods and rates can influence this trait. For instance, Chauhdary et al. (2016) observed that bed planting resulted in a higher 1000-kernel weight compared to other sowing methods. Similarly, Iqbal et al. (2010) reported that varying seed rates affected the 1000-kernel weight in wheat. This study aims to further explore the effect of sowing rates under bed planting conditions on the 1000-kernel weight of the 'QIYMETLİ-2/17' bread wheat variety.

**Table 2.** Effect of sowing rate in bed planting on the 1000-kernel weight of the 'QIYMETLİ-2/17' bread wheat variety (g)

| Sowing Method | Plant Density, ha-mln seeds | Replication | | | | Average |
|---|---|---|---|---|---|---|
| | | I | II | III | IV | |
| **Ordinary row (control)** | 4.0 mln seeds | 46.2 | 46.1 | 46.0 | 46.1 | 46.1 |
| **Bed planting** | 2.0 mln seeds | 47.7 | 47.3 | 47.4 | 47.6 | 47.5 |
| | 2.5 mln seeds | 48.2 | 48.1 | 48.0 | 48.1 | 48.1 |
| | 3.0 mln seeds | 48.5 | 48.1 | 48.4 | 48.2 | 48.3 |

Vitreousness is an important characteristic of the endosperm. When a vitreous kernel is held up to the light, it appears transparent and weakly refracts light rays. If such a kernel is cut, the cut surface has a glassy sheen. The opposite of vitreousness is mealiness. When held up to the light, mealy kernels appear dark, and when cut, they look white. The vitreousness (or mealiness) of a kernel is used to determine the structure and consistency of the endosperm, which in turn depends on the bonding of protein substances with starch granules. Vitreousness depends on the content and density of "packing" of protein granules in the endosperm. In vitreous endosperm, a significant portion of the protein is tightly bound to starch granules and forms thick protein layers that are not removed during intensive processing. If the protein substances are located between starch granules and separate during milling, they are called interstitial proteins. Mealy kernels contain more interstitial protein (Seyidaliyev et al., 2014).

It should be emphasized that even in the highest-quality kernels, not all proteins are bound. Vitreous wheat kernels contain more protein than starchy ones. Vitreous kernels are larger and heavier than starchy kernels and are characterized by greater mechanical strength. Sometimes a high degree of vitreousness can coincide with a low protein content (but not vice versa — starchy kernels always have a low protein content). This is because the vitreousness index depends on a greater number of external factors than the kernel's protein content. The analysis of vitreousness is simple, requires no complex equipment, and can be carried out in a short time; therefore, vitreousness analysis is widely used to determine kernel quality.

**Table 3.** Effect of sowing rate in bed planting on grain vitreousness  of the "QIYMETLI-2/17"  bred wheat variety (%).

| Sowing Method | Plant Density, ha-mln seeds | Replication | | | | Average |
|---|---|---|---|---|---|---|
| | | I | II | III | IV | |
| **Ordinary row (control)** | 4,0 mln seeds | 85.1 | 84.9 | 84.0 | 86.0 | 85.0 |
| **Bed planting** | 2,0 mln seeds | 85.2 | 85.3 | 85.5 | 85.6 | 85.4 |
| | 2,5 mln seeds | 85.5 | 85.6 | 85.9 | 85.8 | 85.7 |
| | 3,0 mln seeds | 84.9 | 85.4 | 85.3 | 85.2 | 85.2 |

The quality of kernels as a food product is characterized by a combination of their flour yield and baking properties; therefore, it is necessary to take into account an indicator that reflects the kernel's characteristics and the mass of a defined volume of the product. The test weight (hectoliter weight) is influenced by various factors.

The presence of impurities — mixed kernels are usually lighter, which leads to a decrease in test weight. However, if the kernel contains foreign matter, the test weight increases, while the overall quality of the kernel decreases.

High moisture content — moist kernels have a lower test weight because swelling increases the volume of the kernels and reduces their density. In addition, highly moist kernels have lower flowability, resulting in looser filling, which also decreases test weight.
The presence of broken and damaged kernels — such kernels increase the overall density of the bulk, thereby raising the test weight.

Kernel shape and uniformity — round kernels pack more tightly, increasing test weight accordingly. Non-uniform kernels tend to have higher test weight because smaller kernels fill the spaces between larger ones (Seyidaliyev et al., 2014).

In a number of scientific studies, it is emphasized that the formation of high-yielding and quality kernel in wheat is a key condition for meeting the demand for cereal crops. (Dubovnik, 2013; Zezin et al., 2010; Krivova et al., 2008).

**Table 4.** Effect of sowing rate in bed planting on test weight of the "QIYMETLI-2/17" bread wheat variety (g).

| Sowing Method | Plant Density, ha-mln seeds | Replication | | | | Average |
|---|---|---|---|---|---|---|
| | | I | II | III | IV | |
| Ordinary row (control) | 4,0 mln seeds | 791 | 789 | 788 | 792 | 790 |
| Bed planting | 2,0 mln seeds | 797 | 793 | 794 | 796 | 795 |
| | 2,5 mln seeds | 796 | 794 | 790 | 792 | 793 |
| | 3,0 mln seeds | 793 | 790 | 789 | 792 | 791 |

The data presented in the table 2 show that the thousand kernel weight (TKW) of the studied wheat variety was highest in the variants with a sowing rate of 2.5–3.0 million seeds per hectare. Under ordinary row sowing, the thousand kernel weight was 46.1 g, while under the drill sowing method, depending on the sowing rate, it was 47.5 g, 48.1 g, and 48.3 g, respectively. Compared to the control variant, the thousand kernel weight in these treatments was 1.4–2.2 g higher. The highest TKW value was obtained in the variant with a sowing rate of 3.0 million seeds per hectare.

In this study, along with the thousand kernel weight, the vitreousness of the wheat kernels was also determined. It is well established that the vitreousness of wheat kernels varies significantly depending on the variety and species. The variation in vitreousness largely depends on the growing conditions and the set of applied agrotechnical measures.

Data on the test weight depending on the sowing method and rate are presented in Table 4. Based on the obtained results, it can be concluded that the test weight of the kernel generally depends on its size and vitreousness. For the studied bread wheat variety, this important trait reached its highest value — 795 g/L — in the variant with 2.0 million seeds per hectare under the drill sowing method.

Test weight is especially important for several food kernel crops, particularly for those on which this trait is compulsory measured. The test weight is the first measurable/weighable qualitative trait of cereal kernel mentioned in history, from the 19th century. Since then a great attention has been paid to it. Although it was introduced into regulations during the 20th century, it is hardly mentioned in the seed legislation. The test weight is a weight of one hectolitre of wheat expressed in kilograms. As it is a volume measure, its value depends on a large number of factors, which depend on studied material and methods, and have positive or adverse effects. However, in spite of all this, the test weight has been accepted in the trade as a measure of quality in wheat and other cereals, due to simple and expeditious measurements. Hence, a variety characterized with a higher test weight, other traits being similar to oter varieties, can be better utilized for flour production and therefore this trait can be used orientatively for the evaluation of milling quality. The test weight varies from 60 to 84 kg hl$^{-1}$ . In wheat of hight quality it is above 76 kg hl$^{-1}$ , while a value of below this limit implies wheat of low quality. Šaric et al. (1996) mention that, according to the evaluation of processing quality of the *Triticum aestivum* varieties intended for whole kernel processing, the minimum required test weight is 800 kg m$^{-3}$ . Jevtic (1981, 1992) defines the seed test weight using its dependence on the seed density, shape and size, with the emphasis on the fact that the test weight is an important parameter of quality and that it can be used to estimate the amount of kernel in a warehouse. Miric et al. (2006) state that both, the test weight and, 1,000-kernel weight, have increased in time as a contribution of plant breeding.

The TKW of "QIYMETLI-2/17" ranged from 46.1 g under ordinary row sowing to 48.3 g in bed planting at 3.0 million seeds per hectare. Kernel vitreousness was slightly higher under bed planting, reaching 86.6% at 2.0 million seeds per hectare. Test weight was highest (795 g/L) in the bed planting variant with a sowing rate of 2.0 million seeds per hectare. These results demonstrate that sowing method and rate significantly influence wheat kernel quality parameters. The findings are consistent with previous studies indicating that TKW and test weight depend on environmental conditions, kernel uniformity, and vitreousness (Seyidaliyev et al., 2014).

### 4. CONCLUSION

The study demonstrates that sowing method and sowing rate are crucial determinants of both yield components and kernel quality traits in the bread wheat variety "QIYMETLI-2/17." Bed planting with sowing rates of 2.0–3.0 million seeds per hectare was shown to significantly improve the thousand kernel weight (TKW), kernel vitreousness, and test weight (hectoliter weight), compared to ordinary row sowing. The highest TKW (48.3 g) was recorded at 3.0 million seeds per hectare, while the maximum vitreousness (86.6%) and test weight (795 g/L) were observed at 2.0 million seeds per hectare under bed planting conditions.

These findings indicate that proper determination of sowing rate, tailored to the variety and planting method, is essential for maximizing wheat productivity and improving kernel quality. The results also confirm that kernel characteristics such as size, density, and vitreousness are strongly influenced by agrotechnical factors, including sowing method, seed density, soil–climatic conditions, and plant nutrient and water supply during the vegetation period.

The study highlights that adopting optimized sowing practices can lead to enhanced kernel uniformity, higher flour yield, and better baking properties, which are critical for both food industry applications and commercial seed production. Moreover, the positive effects of bed planting and optimal sowing rates on kernel quality can contribute to more efficient use of agricultural inputs, higher economic returns for farmers, and improved sustainability of wheat production.

In conclusion, the findings provide valuable guidance for wheat growers, agronomists, and breeders aiming to improve bread wheat yield and quality under varying agroecological conditions. Future research should focus on long-term field trials, interaction with soil fertility management, and the impact of climatic variability on these key quality and yield traits.

## REFERENCES

Abbasova, G. F. (2021). Agroecological characteristics and fertility management of grape-growing gray-brown soils of the Samukh district. Baku: *Elm Publishing House*, 156 p.

Chauhdary, J. N., (2016). Effect of sowing methods and seed rates on wheat yield and water productivity. *Quality Assurance and Safety of Crops & Foods, 8*(2), 201–207. https://doi.org/10.3920/QAS2015.0720

Jumshudov, I. M. (2013). Effect of different sowing and fertilizer rates on the productivity of winter wheat. *Scientific Works of the Research Institute of Agriculture, 24*, 259–263.

Iqbal, J., et al. (2010). Effect of seed rate on yield components and grain quality of wheat. Wallingford, UK: CAB International. https://doi.org/10.5555/20210076344

Jevtic, S. (1981). *Biology and seed production of field crops*. Belgrade, Serbia: Nolit, 334 p.

Jevtic, S. (1992). *Biology and seed production of field crops*. Belgrade, Serbia: Naucna Knjiga.

Miric, M., Protic, R., & Jovin, P. (2006). Research on test weight of wheat seed. *Seed Science Research Journal*, Manuscript in print.

Seyidaliyev, N. Y., Gurbanov, F. H., & Mammadova, M. Z. (2014). *Seed science*. Baku, Azerbaijan: Elm Publishing House, 312 p.

Dubovnik, D. V. (2013). Relationship between grain and flour quality indicators. *Bread Products Journal, 10*, 64–65.

Zezin, N. N., & Vorobyev, V. A. (2010). Baking wheat of Ural breeding. *Achievements of Science and Technology of AIC, 11*, 40–42.

Krivova, L. P., & Sukhorukov, A. A. (2008). Influence of genetic and meteorological factors on winter wheat grain quality formation. *Proceedings of the Samara Scientific Center of the Russian Academy of Sciences*, 94–101.

**CHAPTER 5**

**THE EFFECT OF SOIL TILLAGE METHODS AND THE RATES OF MINERAL FERTILIZERS ON BRANCHING OF SOYBEAN GROWN AS A COVER CROP IN THE SOIL-CLIMATIC CONDITION OF GANJA-DASHKESEN ECONOMIC REGION**

Asst. Prof. Dr. Aysel HÜSEYNOVA[1]

[1]Azerbaijan State Agricultural Universitety, Azerbaijan
Orcid: 0000-0003-4935-0127, E-mail: aysel- h91@mail.ru

## 1. INTRODUCTION .

Soybean is a valuable predecessor crop. Compared to other plants, legumes deplete the soil less. In crop rotation, soybean can be grown after cereals, corn, and cotton. The best and most common predecessor crop is winter wheat. It is not recommended to plant soy after legumes and sunflowers. This is because fungal diseases specific to these plants can also infect soybean. In terms of cultivated area, soybean ranks first among cereal-legume crops. In advanced farms under irrigation conditions, grain yield reaches 25-30 quintals, and green biomass yield reaches 250-300 quintals. One of the main biological characteristics of soybean is its ability to absorb atmospheric biological nitrogen through the participation of Rhizobium bacteria. Under normal conditions, a soybean plant develops 25-50 or more root nodules. Soybean is a short-day plant; its vegetation period lengthens as you move north. It has high soil requirements. Soybean grows better in neutral soils with a pH of 6.5-7.0. Except for saline soils, other soils are suitable for soybeans. Due to its strong and deep root system, soybean tolerates short-term soil drought better than other legumes. For good growth and yield, soybean requires up to 300 mm of rainfall during the summer months (June, July, August). Soybean is very sensitive to soil fertility and the application of fertilizers. When 40 kg per hectare of each mineral fertilizer (NPK) is applied, it gives good results. At the same time, applying 10-20 tons of manure along with superphosphate per hectare improves the growth and development of the soybean plant. Deep autumn plowing (28-30 cm) is beneficial for soybean cultivation, but before plowing (if the predecessor crop was a cereal), loosening the soil to a depth of 10-15 cm in the field is necessary (Mammadov et al., 2012)

Based on numerous studies, it has been determined that, given the soil and climatic conditions of our Republic, it is possible to harvest two crops from a single area in one year. The average annual values of the useful temperature content, which is a key factor of the climate conditions in the regions, are sufficient for obtaining two crops per year from one area. It is known that corn is planted for fodder, and sometimes for grain, especially after barley instead of cereals. After harvesting barley, cotton has also been planted experimentally in certain regions at different times (Kazımov et al., 2006).

The studies conducted by Ahmedov, et al., (2016) that under the conditions of the Absheron region investigated the effect of irrigation methods and fertilizer rates on the yield of soybeans cultivated on stubble land. There are extensive opportunities for cultivating soybean in Azerbaijani conditions to obtain high grain and green biomass yields. Soybean is a heat-loving plant, and the total temperature required for its development and maturation ranges from 1700 to 3200 °C. The optimal temperature for seed germination is 20-22 °C." Soybean is a heat-loving plant, and the total temperature required for its development and maturation is 1700-3200 °C. The optimal temperature for seed germination is 20-22 °C. Soybean has a high demand for heat during flowering and pod formation stages. In addition to spring sowing, cultivating soybean on loosened soil after barley harvest is also economically very beneficial. Sowing on loosened soil in irrigated lands allows for additional grain and fodder yields from the same area and enables efficient use of reclamation facilities. This enriches the soil with organic matter, prevents soil salinization, and fully addresses issues related to wind erosion and weed control.

Cultivating crops on loosened soil in large farming enterprises increases the efficient use of labor, irrigation water, irrigation networks, agricultural machinery, and equipment

Soybean production is steadily increasing worldwide. The global cultivation area of soybean is 90 million hectares, and the total production amounts to 200 million tons. The Russian government has developed measures to stabilize soybean production and increase it to 2.7 million tons. Currently, early-maturing northern ecotype soybean varieties have been developed in the northern, southern, and central black soil zones of the Russian Federation (Kobazayeva, 2007).

According to the State Statistics Committee, in 2024, legumes were planted on 17,203.3 hectares in our Republic, producing 1,661.3 tons of crops, with an average yield of 15.6 centners per hectare (Anonymous, 2024)

Due to its biological characteristics, the soybean plant has great potential. Under normal conditions, it produces more than 3.5 tons of grain and 1.5 tons of protein rich in amino acids. Agricultural enterprises harvest far below this potential. The main reasons are the lack of seed supply, machinery, fertilizers, and herbicides. Soybean is cultivated on 53 million hectares in 60 countries worldwide, with an average yield of approximately 1.6 tons per hectare." In Russia, the cultivation area is 0.5 million hectares, and the average yield is 0.7-0.8 t/ha. Therefore, developing new cultivation technologies to increase soybean grain yield is of great national economic importance. Research conducted on soybean in the North Caucasus has shown that it is possible to obtain 2.5-3.0 t/ha grain yield in areas with natural moisture. For late-maturing varieties, the optimal plant density is 270,000 plants/ha; for medium-maturing varieties, 320,000 plants/ha; and for early-maturing varieties, 370,000 plants/ha to achieve high yields." To obtain high-quality soybean grain yield, the Lakta, Astra, and Lira varieties produce 3 t/ha in areas without consistent moisture supply. Therefore, phase-wise irrigation should be carried out by ensuring the plant with optimal moisture. It is recommended to apply the main portion of phosphorus fertilizer to the soil at a rate of 90 kg/ha before sowing, treat the seeds to be sown per hectare with 50 grams of molybdenum before sowing, and apply 2 kg/ha of boron micronutrient to the soil. These technological processes increase soybean grain yield by 20-25% and profitability by 1.5-2 times. Nitrogen enters soybean grain from soil and air by 65-68%, from leaves by 18-20%, from stems by 10-11%, and from root nodules by 2-3% (Kalmykov, 2009).

In Russia, the soybean cultivation area does not exceed 720,000 hectares annually, and the total grain production is 690,000 tons. In 2017, it was planned to increase grain production to 3.0 million tons and the cultivation area to 2.7 million hectares. The expansion of the cultivation area is intended in the European part of Russia, in the northern, southern, and central non-black soil zones of the black soil region (Medvedev, 2006).

Protein is the most valuable part of the human diet. Soybean, being the most promising crop in Russia, holds the first place in the biological intensification of agriculture. Its seeds contain 35-45% protein, 17-26% oil, and up to 2% vitamins. In global agriculture, soybean is the main and leading crop for solving food and feed protein needs. In many countries, soybean is used as food and feed, containing 32-50% protein, whereas these figures are 9-12% in corn, 10-14% in wheat, 16-20% in sunflower, and 22-28% in peas. According to FAO data, an

increase in soybean yield has been observed in many countries. The highest yield is recorded in Switzerland at 4 t/ha (Shchuchka, 2006).

Currently, in the cotton-growing regions of our republic, cotton and other agricultural crops are planted and cultivated on hectares of land after barley harvesting. The main purpose of the research is to study the combined effect of soil cultivation practices and mineral fertilizers on the yield and quality of soybean planted after barley harvest, as well as on the soil's water-physical properties and fertility in the irrigated gray-brown (chestnut) soils of the Ganja-Dashkesen region.

At the same time, based on the scientific research conducted by PhD in Agrarian Sciences, Associate Professor Fariz Alakbarov at the Teaching Experimental Farm of the Agrarian University titled 'The Effect of Modern and Traditional Sowing and Irrigation Methods on the Productivity Elements and Grain Yield of Organic Soybean,' a comparative study was carried out on the effects of modern (ridge planting + drip irrigation) and traditional sowing and irrigation methods, including effective microorganisms (bacterial preparations), on the growth and development of organic soybean, productivity elements (number of grains per pod, grain yield per pod, number of pods per plant, 1000-grain weight, etc.) and grain yield. According to the experimental scheme, the following works were performed and measurements taken for the variants: On May 9, 2024, organic soybean was planted both under ridge planting + drip irrigation conditions and in the control variant (traditional planting). In both ridge planting + drip irrigation and control (traditional planting) variants, soybean seeds were treated with a biopreparation mixture (Esbioful + Esbioful mix + Esbioful oil). During the vegetation period, the organic soybean field was fertilized twice foliar and once via fertigation to the roots with the biopreparation mixture (Esbioful + Esbioful mix + Esbioful oil). Thus, both ridge planting + drip irrigation and control (traditional planting) variants included treatments with and without biopreparation (control). Since soybean plants are demanding regarding soil microbiological activity, moisture, and organic matter, compost was applied at a rate of 500 kg/ha to the sowing rows during planting. Irrigation, weed control, and other agrotechnical measures were carried out timely. The growth and development of soybean plants were studied under modern (ridge planting + drip irrigation) and traditional sowing and irrigation methods, including the application of effective microorganisms (bacterial preparations). The productivity elements of soybean plants (number of grains per 100 pods, grain yield per pod, number of pods per plant, 1000-grain weight, etc.) and grain yield were examined in variants with modern and traditional sowing and irrigation methods, as well as with the application of effective microorganisms. The study revealed that in organic soybean fields grown under ridge planting + drip irrigation, the grain yield per 100 pods was 201.0 grains weighing 29.3 grams in the first variant, 195 grains weighing 28.96 grams in the second variant, and 168 grains weighing 26.1 grams in the third variant. The number of pods per plant and grain yield were 95.05 pods and 27.86 grams in the first variant, 27.26 pods and 7.89 grams in the second variant, and 43.45 pods and 11.35 grams in the third variant. Looking at the figures, it is clear that treating soybean seeds with biopreparations, including foliar and root feeding with the biopreparation mixture (Esbioful + Esbioful mix + Esbioful oil), had a positive effect on the productivity elements of soybean and increased grain yield. Among the variants studied under ridge planting + drip irrigation, the highest grain yield of organic soybean was obtained in the first variant (single-

row ridge planting + drip irrigation + seed treatment with biopreparations) at 34.83 c/ha, which is 15.10 c/ha or 43.3% higher compared to the second variant (double-row ridge planting + drip irrigation + seed treatment with biopreparations) and 20.64 c/ha or 59.3% higher than the control variant. (Alakbarov, et al., 2025).

By Nasirov (2019) the effect of sowing time, planting scheme, and nutrition conditions on the branching of soybean plants was investigated. When sown in the second decade of April, the number of branches per plant in the control (without fertilizer) variant, depending on plant density, was determined to be 2.3-2.4 branches per plant; in the $N_{60}P_{40}$ + 15 tons of manure variant, 5.0-6.2 branches; and in the $N_{90}P_{60}K_{40}$ variant, 4.7-5.8 branches. In the control variant, when sowing was done in the third decade of April, there were 2.6-4.8 branches per plant; in the $N_{60}P_{40}$ + 15 tons of manure variant, 6.5-8.3 branches per plant; and in the $N_{90}P_{60}K_{40}$ variant, 6.3-7.6 branches per plant

The soil-climatic conditions of the studied region. The Ganja-Gazakh physical-geographical district covers the northeastern slope of the Lesser Caucasus. It is bordered to the north by the Ganja-Gazakh plain, to the south by the watershed of the Shahdag and Murovdag mountain ranges. The area is bordered to the west by Armenia and to the east by the Incechay valley. The district extends from an absolute altitude of 200-500 meters in the northeast to 3700 meters over a distance of 60 km. The soils of the northwestern slope of the Lesser Caucasus have been studied in various years (Mammadov, 1991) and others. According to soil formation conditions, the soils of the northwestern slope of the Lesser Caucasus are divided into the following groups: mountain-steppe, brown mountain-forest, brown mountain-forest, mountain-black, mountain gray-brown, gray-brown, steppe-chestnut, alluvial-steppe, gray soils, brown semi-desert, and floodplain steppe-forest soils. In the gently sloping plains belt where our research was conducted, mainly the following soil types are widespread: Chestnut soils cover an area of 2,200.6 thousand hectares (25.5%) in Azerbaijan. They are spread in a fairly wide strip along the foothills and in the low mountain zone up to an altitude of 200 meters. The vegetation of dry steppes is characteristic for this zone. Chestnut soils, according to their properties (humus content, quantity and distribution of carbonates, etc.), are divided into light chestnut, chestnut, and dark chestnut soils. Light chestnut soils are found in the zone of high average annual temperatures (up to 13°C) and insufficient moisture, at the junction of dry steppes and semi-deserts. The annual amount of atmospheric precipitation (250 mm) does not cover water consumption and evaporation . These soils have low humus content (about 2%), exhibit signs of deep salinization, and have an alkaline reaction. Chestnut and dark chestnut soils are distributed in the upper part of the zone. Here, higher moisture is recorded (atmospheric precipitation ranges from 300 to 500 mm), and the average annual temperature is 12.5°C. The humus content ranges between 3-5%, and the reaction is slightly alkaline. The soil-ecological system (SES) of the chestnut soil zone is quite complex: it is characterized by extensive development of microrelief and complexity, which is largely conditioned by the widespread presence of saline, solonetz, and eroded soils. Due to the close proximity of saline rocks, solonetz complexes are involved in the SES of these areas. Complexes containing eroded soils on slopes have developed. Chestnut soils of the republic are highly utilized and used for fruit cultivation, cotton, grapes, cereals, and winter pastures. Dark chestnut soils are used under rainfed conditions, while the other two types are used under irrigation conditions. (Mammadov,

2007)

Babayev et al., (2017) determined that long-term irrigation of chestnut (brown) soils causes sharp changes in their genetic profile, leading to the formation of an anthropogenic agro-irrigation layer (AUair) in the upper (0-30 cm) soil horizon. The authors were the first to identify the genetic layers of these soils (AUalz-AYallve-BCAve-Cca) and provided the modern soil classification of the Republic of Azerbaijan.

Depending on the conditions of soil formation and deposition, as well as the nature of the parent rocks and vegetation cover, brown-gray soils are divided into the following four subtypes: dark brown-gray, ordinary brown-gray, light brown-gray, and "pebble" brown-gray soils.

Physical-chemical, water-physical, and agrochemical properties of the experimental field soils. The pattern of changes in the main components of the soils in the irrigated chestnut (gray-brown) soils somewhat corresponds to the condition found in irrigated dark-chestnut soils. A decreasing trend in humus content is observed both in the arable layer and throughout the soil profile. In the arable layer, this indicator decreased from 2.80% to 2.50%, and in the lowest layer, it decreased from 1.29% to 0.49%. Comparing different years, it is determined that the humus content decreased by 0.30% and 0.80% in the respective layers. There were no significant changes in the percentage content of total nitrogen and phosphorus over the years, but the amount of $CaCO_3$ (calcium carbonate) based on $CO_2$ increased by 6.13%. Over the last 40-50 years, the main components (humus, nitrogen, total agrochemical indicators, etc.) of soils in the northern foothill-steppe subzone of the Lesser Caucasus have undergone significant changes. All these changes can be associated with anthropogenic factors.( Jafarov, Y. A., at al., 2014).

Agrochemical studies conducted by A.O. Hasanov in the Samukh district on gray-brown (chestnut) soils show that these soils are poorly supplied with available forms of nitrogen, phosphorus, and potassium. The pH in the 0-30 cm soil layer in water solution was 7.4, gradually increasing with depth to 7.9 in the 60-100 cm layer. The total humus, nitrogen, phosphorus, and potassium contents in the 0-30 cm layer were 2.11%, 0.13%, 0.12%, and 2.39%, respectively. However, these values significantly decreased with depth, reaching 0.73%, 0.05%, 0.07%, and 1.55% in the 60-100 cm layer, respectively. The absorbed ammonium nitrogen varied between 18.3 and 6.5 mg/kg, nitrate nitrogen between 9.7 and 2.3 mg/kg, mobile phosphorus between 16.3 and 4.9 mg/kg, and exchangeable potassium ranged from 273.5 to 95.3 mg/kg (Hasanova, 2012).

In the research conducted by Alakbarova, (2013) in the Shamkir district within the Ganja-Gazakh region, it was determined that the total humus content in these soils is 2.92%, decreasing to 2.00% in the lower layer. Total nitrogen ranges from 0.17% to 0.07%, absorbed ammonium nitrogen from 26.19 to 18.43 mg/kg, nitrate nitrogen from 13.24 to 9.69 mg/kg, total phosphorus from 0.15% to 0.12%, mobile phosphorus from 19.05 to 12.3 mg/kg, total potassium from 2.41% to 2.05%, and exchangeable potassium from 297.6 to 204.8 mg/kg. The pH level is slightly alkaline. According to the gradation accepted in the republic, these soils are poorly supplied with nutrients (

According to long-term research conducted by Professor H.A. Aslanov in the region, it has been determined that the amount of easily assimilable nutrients by plants in the soils decreases

year by year. The main reason for this is the lack of regular application of organic and mineral fertilizers to the soils.In irrigated gray-brown (chestnut) soils, the total humus, nitrogen, phosphorus, and potassium in the 0-20 cm layer are 2.2%, 0.18%, 0.17%, and 2.53%, respectively, while in the 80-100 cm layer, these values are 0.40%, 0.04%, 0.07%, and 1.4%. The pH in water solution ranges from 7.5 to 7.9. The amounts of easily hydrolyzable nitrogen, absorbed ammonium, water-soluble ammonium, and nitrate nitrogen by soil layers are as follows: 103.0-10.2; 21.0-4.5; 10.1-2.0; and 12.9-2.02 mg/kg, respectively. Mobile phosphorus and exchangeable potassium range from 19.3 to 3.2 mg/kg and 230.0 to 110.2 mg/kg, respectively, while water-soluble phosphorus and potassium are 2.15-0.98 mg/kg and 38.0-9.02 mg/kg .( Aslanov, H.6., 2015).

The agrochemical analysis of studies conducted by T.6. Hasanov at the central experimental base of the Azerbaijan Scientific Research Cotton Institute on long-irrigated gray-brown (chestnut) soils shows that these soils are poorly supplied with available forms of nitrogen, phosphorus, and potassium. The pH in the water solution of the 0-30 cm soil layer was 7.8, increasing with depth to 8.4 in the 60-100 cm layer. The total humus, nitrogen, phosphorus, and potassium contents in the 0-30 cm layer were 2.13%, 0.13%, 0.12%, and 2.28%, respectively. However, these values significantly decreased with depth, reaching 0.81%, 0.05%, 0.06%, and 1.45% in the 60-100 cm layer, respectively. The absorbed ammonium nitrogen ranged from 18.5 to 5.2 mg/kg, nitrate nitrogen from 9.4 to 2.5 mg/kg, mobile phosphorus from 15.3 to 4.0 mg/kg, and exchangeable potassium from 253.0 to 102.4 mg/kg (Hasanova, T.6., 2013).

In other studies conducted by A.6. Aliyeva, the amounts of total and available forms of nutrients in gray-brown (chestnut) soils were determined. Analysis of soil samples shows that gray-brown (chestnut) soils are poorly supplied with available forms of nitrogen, phosphorus, and potassium. The pH in the water solution of the 0-30 cm soil layer was 7.8, increasing to 8.4 in the 60-100 cm layer. The total humus, nitrogen, phosphorus, and potassium contents in the 0-30 cm layer were 2.15%, 0.15%, 0.13%, and 2.39%, respectively. However, these values significantly decreased with depth, reaching 0.85%, 0.06%, 0.07%, and 1.51% in the 60-100 cm layer, respectively. Absorbed ammonium nitrogen ranged from 18.0 to 6.5 mg/kg, nitrate nitrogen from 9.7 to 2.6 mg/kg, mobile phosphorus from 16.8 to 4.5 mg/kg, and exchangeable potassium fluctuated between 263.5 and 105.3 mg/kg (Aliyeva, A.A., 2017).

According to M.M. Alekberova, soils under grapevine in the Ganja-Gazakh region are gray-brown, with the soil reaction being neutral (pH = 7.0–8.2) to slightly acidic. The humus content in the arable layer ranges from 1.3% to 2.5%. The hydrolyzable nitrogen content in the 0-20 cm soil layer is 116.2 mg/kg, and in the 20-40 cm layer, it is 68.0 mg/kg. Total potassium is 1.10%, and total phosphorus ranges from 0.2% to 0.3% (Alakbarova, M.M., 2014).

## 2. MATERIALS AND METHODS

Before the experiment was established, the main physical-chemical, water-physical, and agrochemical properties of the soils were studied following the barley harvest. The main physical-chemical properties of the soil are presented in Table 1. As shown in the table, the total absorbed bases in the 0-30 cm layer amounted to 28.6 meq/100g, decreasing to 20.5 meq/100g

in the 60-100 cm layer. The content of physical clay throughout the profile is 53.1-52.8%, and the silt content ranges from 24.6% to 22.5%. Based on granulometric composition, these soils are classified as light clay soils.

**Table 1. The principal physico-chemical properties of the soils in the experimental field** (Gülyakhmedov et al.,1980)

| Depth cm | The amount of exchangeable bases in 100 grams of soil, mg/ekv | | | Total exchangeable bases mg/ekv | Particle size distribution % | |
|---|---|---|---|---|---|---|
| | Ca | Mg | Na | | <0,001 mm | <0,01 mm |
| 0-30 | 19,8 | 7,4 | 1,4 | 28,6 | 24,6 | 53,1 |
| 30-60 | 18,2 | 6,4 | 0,7 | 25,3 | 25,7 | 56,3 |
| 60-100 | 15,7 | 4,3 | 0,5 | 20,5 | 22,5 | 52,8 |

The main water-physical properties of the experimental field soils are presented in Table 2. As seen from the table, in the 0-30 cm soil layer, moisture content is 16.3%, specific gravity is 2.65 g/cm³, bulk density is 1.23 g/cm³, and total porosity is 53.58%. In the 60-100 cm layer, these values are 22.5%, 2.73 g/cm³, 1.32 g/cm³, and 49.46%, respectively.

**Table 2.** The principal physico-chemical properties of the soils in the experimental field (Gülyakhmedov et al.,1980)

| Depth cm | Soil moisture, % | Bulk density (g/cm³) | Specific gravity (g/cm³) | Total porosity (%) |
|---|---|---|---|---|
| 0-30 | 16,3 | 2,65 | 1,23 | 53,58 |
| 30-60 | 18,3 | 2,67 | 1,27 | 52,43 |
| 60-100 | 22,5 | 2,73 | 1,32 | 51,66 |

The agrochemical properties of the gray-brown (chestnut) soils we studied are presented in Table 3.3.3. As seen from the table, the pH in the water solution was 7.6 in the 0-30 cm layer and 8.2 in the 60-100 cm layer. The total humus, nitrogen, phosphorus, and potassium in the 0-30 cm layer were 2.15%, 0.15%, 0.14%, and 2.43%, respectively. However, these values significantly decreased with depth, reaching 0.80%, 0.05%, 0.06%, and 1.51% in the 60-100 cm layer, respectively. The absorbed ammonium nitrogen ranged from 15.1 to 5.7 mg/kg, nitrate nitrogen from 9.1 to 2.5 mg/kg, mobile phosphorus from 16.5 to 4.3 mg/kg, and exchangeable potassium varied between 261.6 and 105.2 mg/kg.

**Table.3.** Agrochemical properties of subsoil (Gülyakhmedov et al.,1980)

| Depth (cm) | pH (in water solution) | Humus (%) | Nitrogen | | | Phosphorus | | Potassium | |
|---|---|---|---|---|---|---|---|---|---|
| | | | Total (%) | Ammonium nitrogen,, $N/NH_3$ (mg/kq) | Nitrate nitrogen, $N/NO_3$ (mg/kq) | Total, (%) | Mobile, (mg/kq) | Total, (%) | Exchangeable potassium, (mg/kq) |
| 0-30 | 7,6 | 2,15 | 0,15 | 15,1 | 9,1 | 0,14 | 16,5 | 2,43 | 261,6 |
| 30-60 | 8,0 | 1,16 | 0,07 | 11,4 | 4,6 | 0,08 | 10,1 | 1,88 | 161,3 |
| 60-100 | 8,2 | 0,80 | 0,05 | 5,7 | 2,5 | 0,06 | 4,3 | 1,51 | 105,2 |

Thus, the agrochemical analyses conducted on gray-brown (chestnut) soils show that, according to the gradation accepted in our republic (Gülyakhmedov et al.,1980) these soils are poorly supplied with nutrients. Therefore, to obtain a high grain yield froms oybeann planted twice a year on the same area after barley harvest and to maintain soil fertility, the application of mineral fertilizers in these soils is extremely important.

*The Effect of Soil Cultivation and Mineral Fertilizer Rates on the Changes in Soil Water-Physical Properties.* Among the agrotechnical measures aimed at increasing the effective fertility of the soil and improving the yield of cultivated agricultural crops, properly performed mechanical cultivation holds a special place. During soil cultivation, through crushing, loosening, and compacting the soil, the necessary balance between the solid phase of the soil and its capillary and non-capillary pores is created. Depending on the task at hand, soil cultivation can be carried out both in the arable layer and at any desired depth. In arid climatic conditions, the primary goal of cultivation is to create and preserve moisture reserves in the soil. In soils with excessive moisture, cultivation removes the excess water from the soil and establishes a favorable water-air regime in the arable layer. In soils that are properly cultivated, the effectiveness of other agrotechnical measures such as irrigation, fertilization, crop rotation, etc. is increased. Weeding and moisture retention in the soil in cultivated fields are mainly achieved through mechanical cultivation. The effectiveness of soil cultivation can be enhanced by selecting the appropriate methods and carrying them out in a timely manner.

*The following tasks stand before soil cultivation:*

To change the structure and structural condition of the arable layer in order to create favorable water, air, temperature, and nutrient regimes for plants; 1.To use nutrients located in relatively deep soil layers consecutively, improve the nutrient regime by placing fertilizers at various depths, and direct microbiological processes appropriately by enhancing the activity of beneficial microorganisms; 2.To destroy pests, pathogens, and weeds of agricultural crops; 3.To incorporate plant residues and fertilizers into the soil; 4.To protect the soil from water and wind erosion; 5. To eliminate perennial weeds when cultivating raw and fallow soils; 6.To facilitate the optimal depth placement of cultivated plant seeds; 7. To create favorable microrelief through ridge opening, bed and furrow formation, etc. In some cases, solving one problem of soil cultivation contradicts another. For example, intensive cultivation of the soil improves its structural condition but at the same time accelerates the decomposition of humus and negatively affects the efficient use of soil fertility. Similarly, while retaining plant residues on the soil

surface prevents erosion, it also creates favorable conditions for the spread of weeds, diseases, and pests. As a result of multiple passes of machines and tools used in mechanical soil cultivation, the soil becomes more compacted, and its water-physical properties deteriorate. Therefore, it is preferable to combine operations to minimize the number of soil cultivation treatments. Soil cultivation involves the mechanical impact of the working parts of the machines and tools used on the soil. During this process, various technological operations are performed. These operations include turning the soil, crushing, loosening, mixing, compacting, leveling the surface, cutting weeds, forming ridges and beds, retaining plant residues on the soil surface, and so on.

Field experiments were conducted in 2018-2020 in the territory of Samukh district, at the Ganja Regional Agrarian Science and Innovation Center of the Ministry of Agriculture of the Republic of Azerbaijan, in irrigated gray-brown (chestnut) soil as replanting after harvesting soybeans with Umanskaya-1 variety of barley.

The experiment is 2-factorial and was conducted after the autumn barley harvest (after the 1$^{st}$ decade of June).

Factor A: Soil cultivation: 1. Cultivation at a depth of 8-10 cm; 2. 13-15 cm deep disc harrow; 3. Plow to a depth of 20-22 cm.

Factor B: mineral fertilizer rates: 1. Control (without fertilizer); 2. $N_{30}P_{60}K_{30}$; 3. $N_{60}P_{90}K_{60}$; 4. $N_{90}P_{120}K_{90}$.

Experiments were conducted with inter-row cultivation method, in 3 repetitions, with the area of 54.0 m$^2$ (30x1.80 m) in the registration section for each option, 45x10 cm planting scheme, 30 kg of seeds taken per hectare.

The following forms of mineral fertilizer were used for the experimental area: potassium-potassium sulfate form (46%), nitrogen-ammonium nitrate form (34.7%), phosphorus-simple superphosphate form (18.7%). From mineral fertilizers, it was considered appropriate to give N fertilizer once at the exit time, and P and K fertilizers for the most part 70% before sowing, and the remaining 30% during the branching period at feeding process. Agrotechnical measures were carried out according to the rules established for the area. In total, phenological observations were carried out on twenty-five plants.

Key findings derived from the research-Physical-chemical, water-physical and agrochemical properties of the experimental area soil ;

- The effect of soil cultivation and mineral fertilizer dosages on soybean development phases on moisture content, volume mass and total porosity change in 0-10; 10-20; 20-30 cm soil layers.

-The effect of soil cultivation methods and mineral fertilizer doses on the field weeding in connection with the soybean development phases, soybean height, branching, leaf surface and structural indicators;

-The effect of soil cultivation and mineral fertilizers on soybean yield, quality, protein and fat yield;

- Determination of economic efficiency.

***Scientific novelty of the study.***

In the research work, for the first time, the effective norms of

soil cultivation and mineral fertilizers under soy were determined in the conditions of Ganja-Dashkesen region after barley harvest, soil fertility increased, quality and fertility indicators escalated.

***The theoretical and practical significance of the research.*** It was ascertained that soil cultivation and mineral fertilizers have an significant effect on the crop quality and soybeans yield in repeated summer crops after the barley harvest. The highest indicators were 1479.6 AZN/ha and the level of profitability was 138.2% when plowing by turning the soil at a depth of 20-22 cm, in the $N_{60}P_{90}K_{60}$ mineral fertilizer rate.

In the soil samples brought for analysis: pH using a potentiometer device, total humus according to the method of I.V. Tyurin and granulometric composition according to the method of N.A. Kaczynski, absorbed bases according to the method of K.K. Hedroys, absorbed ammonia according to the method of D.P. Konev, activated phosphorus according to the method of B.P. Machigi, Determination of nitrate nitrogen by Grandval-Liajou, total potassium based on Smith's method, exchangeable potassium was determined according to P.B. Protasov's flame photometer method, total phosphorus and nitrogen were determined by the method of K.E.Ginzburg, G.M.Sheglova, V.S.Zaytsev's simplified calculation and N.A. Kaczynski's modification, and the soil moisture content was determined by drying in a 105°C thermostat. The amount of protein, fat, cellulose and ash in soybean grain was determined by generally accepted methods. The accuracy of the obtained results was confirmed through mathematical calculations.



**Figure 1.** Description of Experimental Plots for Studying the Effects of Tillage Practices and Mineral Fertilizer Rates on Soybean Branching
*(Ganja Regional Center for Agricultural Science and Innovation Advisory Services, 2018–2020)*

The effects of soil cultivation methods and mineral fertilizers on soybean tillering after barley harvesting were studied on irrigated light brown (chestnut) soils. The results of the study are presented in the table. As seen from the table, based on the 3-year average during the grain

maturation phase, the number of tillers in the control (no fertilizer) variant was 8.8 tillers in the plots cultivated at 8-10 cm depth, 9.4 tillers in the plots with disk harrowing at 13-15 cm depth, and 11.4 tillers in the plots plowed at 20-22 cm depth The application of mineral fertilizers caused a relatively significant increase in these values compared to the unfertilized control. Specifically, in the plots cultivated at 8-10 cm depth, the $N_{30}P_{60}K_{30}$ treatment resulted in 9.7 tillers; in the disk-harrowed plots at 13-15 cm depth, 10.5 tillers; and in the plowed plots at 20-22 cm depth, 13.4 tillers. The highest numbers of tillers were observed under the $N_{60}P_{90}K_{60}$ treatment, with 12.6, 13.0, and 16.4 tillers respectively.With further increases in mineral fertilizer rates ($N_{90}P_{120}K_{90}$), the number of tillers decreased in all three soil cultivation treatments, resulting in 10.9 tillers for 8-10 cm cultivation, 12.3 tillers for 13-15 cm disk harrowing, and 14.7 tillers for 20-22 cm plowing.

**Table 4.** The Effect of Tillage Practices and Mineral Fertilizers on Branching in Summer-Planted Soybean

| Ss | Mineral fertilizer norms | Grain ripening (2018) | | | Grain ripening (2019) | | | Grain ripening (2020) | | |
|---|---|---|---|---|---|---|---|---|---|---|
| | | 8-10 sm Cultivation | 13-15 sm disc harrow | 20-22 sm tillage | 8-10 sm Cultivation | 13-15 sm disc harrow | 20-22 sm Tillage | 8-10 sm Cultivation | 13-15 sm disc harrow | 20-22 sm tillage |
| 1 | Control (without fertilizer) | 8,5 | 9,3 | 10,7 | 9,2 | 10,1 | 12,4 | 8,8 | 8,8 | 11,0 |
| 2 | $N_{30}P_{60}K_{30}$ | 9,3 | 10,4 | 12,5 | 10,2 | 11,4 | 14,5 | 9,7 | 9,7 | 13,2 |
| 3 | $N_{60}P_{90}K_{60}$ | 12,6 | 13,6 | 15,5 | 13,5 | 14,7 | 17,5 | 13,0 | 13,0 | 16,3 |
| 4 | $N_{90}P_{120}K_{90}$ | 10,6 | 12,3 | 13,7 | 11,2 | 13,8 | 15,8 | 10,8 | 10,8 | 14,5 |

**Table 5.** The effect of soil tillage practices and mineral fertilizer rates on soybean branching

| Ss | Mineral fertilizer norms | Grain ripening (Three-Year Average, 2018,2019,2020) | | |
|---|---|---|---|---|
| | | 8-10 sm Cultivation | 13-15 sm disc harrow | 20-22 sm tillage |
| 1 | Control (without fertilizer) | 8,8 | 9,4 | 11,4 |
| 2 | $N_{30}P_{60}K_{30}$ | 9,7 | 10,5 | 13,4 |
| 3 | $N_{60}P_{90}K_{60}$ | 12,6 | 13,0 | 16,4 |
| 4 | $N_{90}P_{120}K_{90}$ | 10,9 | 12,3 | 14,7 |

## 3. RESULT AND DISCUSSION

In the conditions of the Ganja-Dashkesen region, on irrigated light brown (chestnut) soils, soil cultivation methods and mineral fertilizers significantly affect soybean tillering after barley harvesting. Among all three soil cultivation methods, the number of tillers was highest under

the mineral fertilizer rate of $N_{60}P_{90}K_{60}$. Compared to the control (without fertilizer), the average increase in tiller number over three years was 4.1–4.3 tillers in the plots cultivated at 8-10 cm depth, 4.9–5.6 tillers in the plots disk-harrowed at 13-15 cm depth, and 4.0–4.1 tillers in the plots plowed at 20-22 cm depth. This increase contributes to a greater leaf area and vegetative biomass, which in turn substantially enhances productivity. A correlation was observed between soybean grain yield (kg/ha) and the number of tillers, confirming the reliability of the obtained results.

A comprehensive study was conducted in the Ganja-Dashkasan region to investigate the effects of soil cultivation practices and mineral fertilizers on the branching process of soybean during summer planting. Soybean, possessing a taproot system, is highly sensitive to soil conditions, and its productivity largely depends on soil properties and nutrient availability.

The research demonstrated that the combination of plowing at a depth of 20–22 cm and the application of $N_{60}P_{90}K_{60}$ (60 kg/ha nitrogen, 90 kg/ha phosphorus, 60 kg/ha potassium) mineral fertilizer optimally enhanced the branching characteristics of soybean plants. This soil cultivation depth improved the physical properties of the soil, promoting better root development, which in turn increased branching intensity and overall vegetative growth of the plants.

Balanced application of mineral fertilizers ensured adequate supply of nitrogen, phosphorus, and potassium, meeting the nutritional needs of the plants. As a result, this fertilizer rate created optimal conditions during the branching phase and contributed to maximizing soybean yield.

The findings suggest that in the agroecological conditions of the Ganja-Dashkasan region, the combined use of plowing at 20–22 cm depth and $N_{60}P_{90}K_{60}$ mineral fertilizer is recommended to effectively stimulate branching and achieve maximum productivity of summer soybean crops. This approach also represents an optimal agricultural technology contributing to sustainable soil resource management and environmental protection.

**REFERENCES**

Alakbarov, F. Sh., Hasanova, A. O., Huseynov, M. M., Huseynova, A. M., Aslanova, D. H., Isayeva, D. A., Zeynalova, A. I., & Orucova, R. N. (2025). *Scientific works of ADAU*. Ganja.

Alakbarova, M. M. (2014). Study of agrobiological and economic-technological characteristics of French grape varieties under the conditions of Goygol district [Abstract of dissertation for the Doctor of Agricultural Sciences]. Ganja.

Alakbarova, Z. A. (2013). Mineral nutrition of cucumber and tomato plants under greenhouse conditions of the Ganja–Gazakh region [Abstract of dissertation for the Ph.D. in Agricultural Sciences]. Baku.

Aliyeva, A. A. (2017). Development of some elements of soybean cultivation technology in the Ganja–Gazakh region [Abstract of dissertation for the Ph.D. in Agricultural Sciences]. Baku.

Aslanov, H. A. (2015). *Application of the natural zeolite mineral together with fertilizers in agriculture.* Baku: Elm.

Babayev, M., Ismayilov, A., & Huseynova, S. (2017). Integration of the Azerbaijani national soil classification into the international system. Baku: Elm.

Hasanova, A. O. (2012). Agrochemical characteristics of experimental field soils. *Azerbaijan Agrarian Science, (1)*, 168–169.

Hasanova, T. A. (2013). *Effect of fertilizers on productivity, potential, and effective fertility of soil in cotton–lucerne crop rotations* [Abstract of dissertation for the Ph.D. in Agricultural Sciences]. Baku.

Jafarov, Y. A., & Mehdiyeva, E. Kh. (2014). Agrochemical analysis methods. Baku: Military Publishing House.Ahmadov, Sh. H., Rzayev, M. Y., & Abdullayeva, Z. M. (2016, May 12–13). Influence of irrigation methods and fertilizer rates on the productivity of soybean cultivated in stubble fields. In *Proceedings of the International Scientific Conference "Current Problems of Modern Chemistry and Biology"* (Part IV, pp. 240–244). Ganja: Ganja State University Publishing.

Kalmykov, A. V. (2009). *Improvement of soybean cultivation technologies ensuring increased productivity and technological properties of seeds in the foothill zone of the Kabardino-Balkarian Republic* [Dissertation for the Candidate of Agricultural Sciences]. Vladikavkaz.

Kazimov, N. N., Nagiyev, J. A., & Marlamova, D. S. (2006). Possibilities of obtaining two crops from one area. *Azerbaijan Agrarian Science, (3–4)*, 43–44.

Mammadov, G. Sh. (2007). *Fundamentals of soil science and soil geography.* Baku: Elm.

Mammadov, G. Y., & Ismayilov, M. M. (2012). *Crop production.* Baku: Sharq-Qarb Publishing.

Nasirova, T. A. (2019). Effect of cultivation factors on branching of soybean under Absheron conditions. *Azerbaijan Agrarian Science, (2)*, 159–160.

The State Statistical Committee of the Republic of Azerbaijan. (n.d.*). Official statistical data. Retrieved from* [https://www.stat.gov.az](https://www.stat.gov.az)

Kobazayeva, T. P. (2007). *Creation of the northern ecotype of soybean and its introduction into the Non-Chernozem zone of Russia.* Moscow: MGAU.

Medvedev, A. M. (2006). Report of the chairman of the council of plant breeders. *Information Bulletin,* (9–10), 24–36.

Shchuchka, R. V. (2006). *Influence of biological preparations and growth stimulants and methods of their application on the yield and quality of soybean seeds in the Central Black Earth Region* [Dissertation for the Candidate of Agricultural Sciences]. Voronezh.

# CHAPTER 6

# A SUSTAINABLE ALTERNATIVE ANIMAL FEED SOURCE: ALGAE

Prof. Dr. Gülcan DEMİROĞLU TOPÇU[1], Res. Assist. Esra DURU[2]

[1] Ege University, Faculty of Agriculture, Department of Field Crops, İzmir, Türkiye
Orcid: 0000-0002-5978-4183, gulcan.demiroglu.topcu@ege.edu.tr
[2] Ege University, Faculty of Agriculture, Department of Field Crops, İzmir, Türkiye
Orcid: 0009-0000-1481-9998, esra.duru@ege.edu.tr

## 1.  INTRODUCTION

The global population is increasing rapidly. Climate change and the gradual depletion of soil, water, and forest resources have driven people to seek new and sustainable resources. It is estimated that the demand for food and agricultural products will increase by approximately 50% between 2013 and 2050 (Vos and Bellù, 2019). However, expanding arable land in most regions of the world does not seem feasible due to water scarcity in these areas. Furthermore, expanding agricultural land is inconsistent with sustainability principles, as it increases greenhouse gas emissions and reduces biodiversity (Alexandratos and Bruinsma, 2012).

Along with the growing population, the demand for animal protein sources is increasing each day, in parallel to the demand for plant production. This situation increases the global livestock industry's need for sustainable feed sources every day. As a result of this increasing need, interest in alternative feed sources has risen significantly in recent years, and importance has begun to be given to the use of agricultural by-products and feed alternatives (Kazemi, 2025). In this context, the use of algae in animal feed has emerged as a promising solution due to its nutritional properties, production efficiency, positive effects on animal health, and contribution to environmental sustainability (Gurau et al., 2025).

Algae are a large and diverse group of organisms capable of photosynthesis, living in both freshwater and marine ecosystems, as well as terrestrial and extreme habitats. Algae can be considered a plant group known for centuries, dating back to ancient civilizations. The term was first introduced by Linnaeus in 1753, and A. L. De Jussieu (1789) distinguished algae from the rest of the plant kingdom. These organisms play a critical role in aquatic and terrestrial food chains as primary producers in the ecosystem. Algae are generally divided into different taxonomic groups based on their pigment composition, cell structure, and physiological characteristics. Basically, there are two different types of algae, ranging from single-celled microscopic species called microalgae to large multicellular organisms called macroalgae. Marine macroalgae species, also known as seaweeds, are divided into three main groups based on their pigment composition: green algae (Chlorophyta), red algae (Rhodophyta), and brown algae (Ochrophyta/Phaeophyceae) (Baweja and Sahoo, 2015). There are significant differences between macroalgae and microalgae as represented in Figure 1.1.
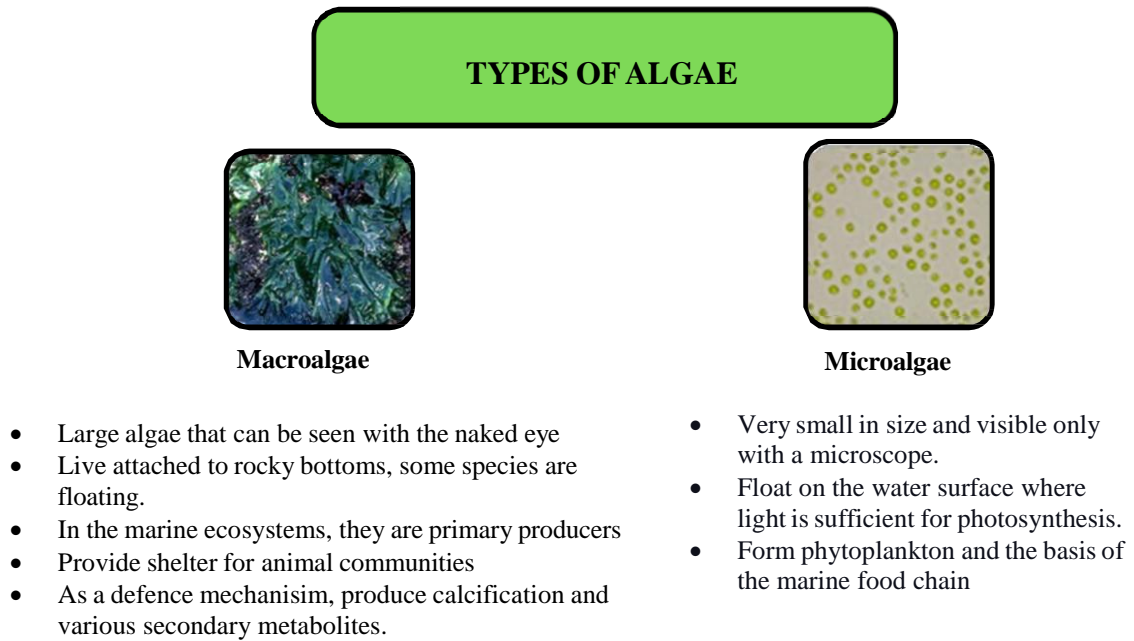
**Figure 1.1.** Types of algae and their significant differences (Pereira, 2021), macroalgae (Anonim, 2021a) and microalgae (Rezaei et al., 2024).
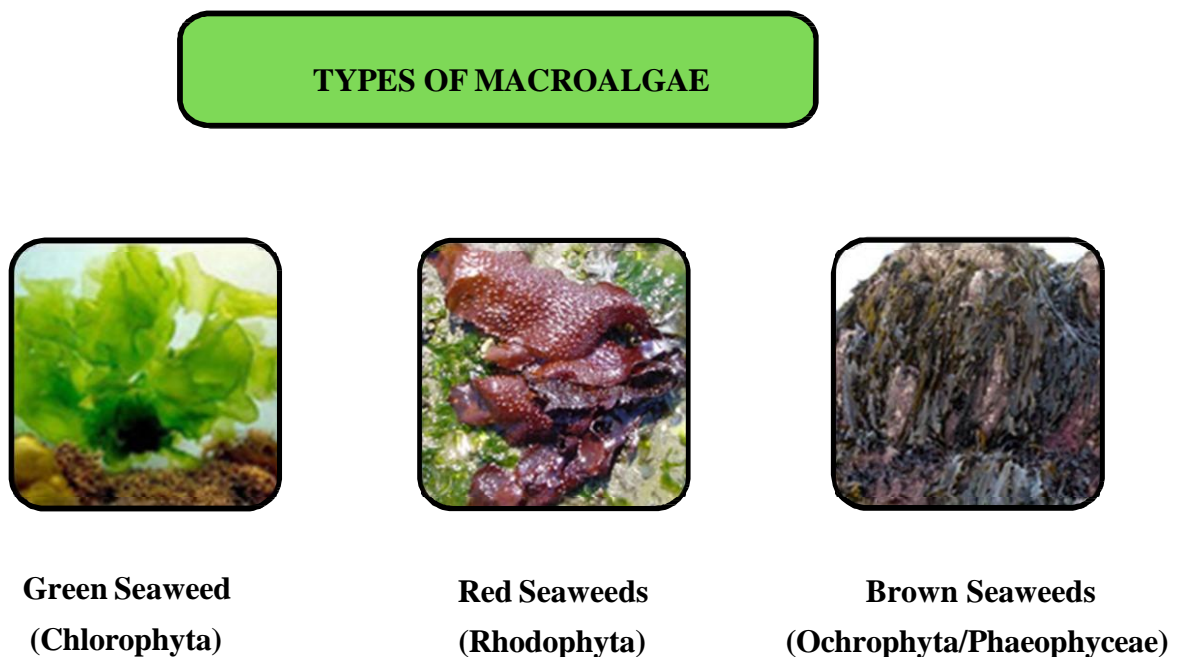


**Figure 1.2.** Different types of macroalgae, green seaweed (Van Ginneken and Vries, 2018), red seaweeds (Kasanah et al., 2022), brown seaweeds (Anonim, 2021b)

In recent years, algae have been gaining increasing attention as a sustainable alternative feed source for animal production. Among the reasons for this are their high nutritional value and mineral richness. Furthermore, their rapid growth rates and high biomass yield, which contain protein, fiber, minerals, and bioactive compounds, are known to improve animal health

and productivity without requiring freshwater and arable land resources. For example, some microalgae, such as Spirulina (*Arthrospira* sp.), *Chlorella* sp., and *Schizochytriu*m sp., can reach up to 70% protein content, making them the most widely used microalgae in animal production, capable of competing with traditional feed sources such as soybean, which is one of the main protein sources in animal husbandry. Furthermore, these microalgae are rich in omega-3 fatty acids, which are crucial for animal health and productivity (Barta et al. 2021; Martins et al., 2021). Microalgae can be used as a feed source as well as a feed supplement. In fact, as stated by Saadaoui et al. in their 2021 review, when microalgae are used in animal feed supplements, they have been shown to lower cholesterol in animals, improve immune response, increase milk yield in cows, improve meat and egg quality, exhibit antibacterial and antiviral effects against diseases, improve digestive functions, and increase probiotics. In addition, it has been stated that they increase reproductive functions and help animals control their weight. Unlike microalgae, macroalgae are multicellular organisms that can be seen without a microscope. Macroalgae, which are classified as green, red, and brown based on their pigmentation, have different nutritional properties. Some species can exceed 60 meters in length and can be found in large masses, such as seaweed forests (Pereira, 2021). Also use of macroalgae in animal diet positively affects health and product quality (Vahedi et al., 2021).

## 2. ALGAE PRODUCTION TECHNIQUES

Algae production techniques vary depending on the type of algae desired to be cultivated (microalgae or macroalgae), the desired products, resource availability, and the intended purpose. Microalgae production systems are commonly classified as open, closed, and hybrid systems (Kazemi, 2025). Macroalgae production systems are categorized as hatchery and at-sea cultivation. At-sea cultivation is also divided into three categories: Off-Shore Cultivation, On-Shore Cultivation, and Near-Shore Cultivation (Khan et al., 2024).

### 2.1 Microalgae Production Systems

#### a) Open Systems

They are used in large-scale algae cultivation. Installation is relatively simple and cost-effective compared to other systems. There are three types of ponds: unstirred ponds, circular or stirred ponds, and raceway ponds. Unstirred ponds are shallow ponds where water and algae naturally remain. These ponds are generally built under the sunlight, and nutrients are not distributed homogeneously, resulting in lower production efficiency. Circular or stirred ponds, on the other hand, distribute nutrients and light evenly to the algae, ensuring uniform growth. Raceway ponds, another type of pond, utilize continuous mechanical circulation of the water. It is one of the most used ponds in microalgal production. In these ponds, algae sedimentation is prevented, and the distribution of light and nutrients is homogeneous. While the use of pond types in open systems offers many advantages, they also come with some disadvantages (Kazemi, 2025; Sharma et al., 2025).

**Advantages:**
- Its most important advantage is its simplicity and low installation cost.

- Maintenance is easier and operating costs are more economical than other systems.
- Because of natural sunlight usage, it does not require a supplemental lighting system.
- Algae can be fed with wastewater or directly added nutrients. This reduces the need for additional nutrient sources.
- Algae can meet their carbon dioxide needs from the atmosphere.
- Production can be achieved economically without technical obstacles.

**Disadvantages:**
- One of the biggest disadvantages is the high risk of contamination. There is a risk of proliferation of undesirable microorganisms.
- Yield is lower compared to other systems.
- Because of lighting, nutrient levels, and carbon dioxide levels are not consistent, yield may decrease due to climate or weather conditions.
- It is highly dependent on environmental conditions. High temperature, pH, and nutrient control may be problematic. Furthermore, high temperatures cause water evaporation, resulting in excessive water consumption.
- Open systems require large areas of land. Land costs can be high.



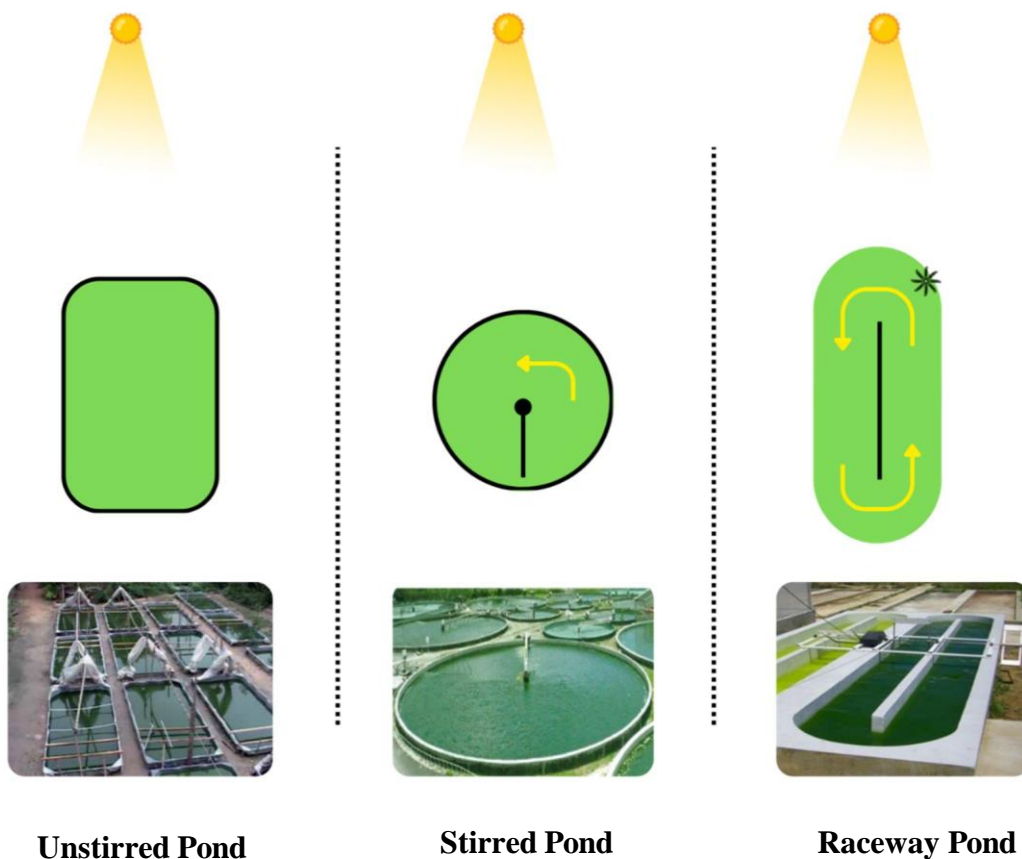| **Unstirred Pond** | **Stirred Pond** | **Raceway Pond** |

**Figure 2.1.** Three open algal cultivation systems: an unstirred pond (Anonim, 2009), a stirred pond (Alami et al., 2021), and a raceway pond (Bwapwa et al., 2019). The illustrations adapted from Kumar et al., (2024).

### b) Closed Systems

Closed systems allow for greater control of microalgae cultivation conditions compared to open systems, resulting in higher efficiency. Various photobioreactors are used in closed systems. These photobioreactors are enclosed structures made of glass or plastic. Sensitive variables such as light intensity, pH, temperature, and nutrient levels can be easily controlled. One of the most significant advantages of closed systems is preventing contamination, ensuring the smooth growth of valuable algae. Furthermore, higher biomass densities can be achieved in photobioreactors, which are highly efficient. There are a variety of systems of photobioreactors that may be used with various combinations of light sources and sunshine, increased nutrition, and metabolic efficiency, such as horizontal, vertical, stirred tank, and flat plate. However, all of these systems, the installation cost, is considerably more expensive than open systems. The energy consumption costs for maintaining a controlled environment are also quite high. Therefore, such systems are generally preferred for applications with high returns where the risk of contamination can be a problem. However, their use in animal feed production can be disadvantageous due to low returns (Kazemi, 2025). In short, closed systems offer many advantages, but they also have some disadvantages.



| **Vertical Photobioreactor** | **Horizontal Photobioreactor** | **Stirred Photobioreactor** | **Flat Panel Photobioreactors** |

**Figure 2.2.** Different microalgae closed cultivation systems, vertical photobioreactor (Huo et al., 2018), horizontal photobioreactor (AlgaePARC Wageningen UR, 2013, as cited in Young-Lorenz, 2013), stirred photobioreactor (Benner et al., 2022), flat panel photobioreactors (Ojamae, 2011).

**Advantages:**
- They provide a controlled and closed growth environment.
- Minimizes the risk of external contamination.
- Increases photosynthetic efficiency.
- Can produce more dense algae biomass than open systems

- Because of lighting, nutrient levels, and carbon dioxide levels are not consistent, yield may decrease due to climate or weather conditions.
- Vertical systems can be used, they don't require as large an area as open systems.
- The quality and market price of the algae produced are higher

**Disadvantages:**
- Expensive installation and operating costs.
- High energy consumption due to lighting and temperature regulation requirements.
- Requires technical knowledge and labor.
- May not be suitable for all algae species
- Difficult to establish and produce large-scale production facilities.

### c) Hybrid Systems

Hybrid systems offer a new and advantageous approach to algae production by combining low-cost open systems with high-yield closed systems. In these systems, algae first reach high biomass density in closed systems (photobioreactors) and are grown contamination-free. They are then transferred to open ponds for continued growth and harvesting. While hybrid systems offer many advantages, they also have disadvantages (Jayaraman et al., 2024; Kazemi, 2025).

**Advantages:**
- They combine the advantages of open and closed systems.
- They provide a control during the initial growth phase
- They support high-quality and pure production.
- They are not as costly as closed systems
- Environmental factors are not as effective as open systems
- They can be applied to larger areas than closed systems.

**Disadvantages**
- Energy consumption and establishment costs are higher.
- The system is more difficult to operate and requires knowledge and labor.
- Management of two different systems can be challenging.
- While a small area is required initially, adapting to larger scales in later stages can be difficult.

## 2.2. Macroalgae Production Systems

In the past, seaweed cultivation could not be conducted in a controlled manner due to the unknown reproductive cycle of algae. The discovery of this cycle paved the way for seaweed production. Today, depending on the variety, some species can be propagated in a single stage, while others require multiple stages of production. Macroalgae cultivation consists of two components: hatchery and sea cultivation. Sea cultivation, on the other hand, consists of three different types: offshore cultivation, onshore cultivation, and nearshore cultivation (Khan, 2024)

### a) Hatchery Cultivation

Hatchery cultivation is the stage in which the growth phase of seaweed or aquatic plants is initiated in a controlled and safe environment. Here, seaweed in its initial growth phase is cultivated in special tanks, provided with appropriate light, temperature, water quality, and nutrients, and grown into young seedlings. These seedlings are then transported to the open sea or field for cultivation. The culture facility is the first and critical step in ensuring the healthy and productive growth of seaweed (Tealman et al., 2015; Khan, 2024).

### b) At Sea Cultivation

Seaweeds are cultivated in a natural marine environment using natural factors such as sunlight, temperature, wave action, and nutrients. Initial seaweeds grown in hatcheries are used here. These can be cultivated offshore, in shallow coastal areas, or onshore. Seaweed cultivation in offshore systems involves attaching seaweeds to ropes or similar structures suspended a few meters below the water surface. Mature seaweeds are harvested from boats using mechanical equipment. Nearshore cultivation, which utilizes areas near the shore as well as the open sea, involves planting seaweed seedlings in net-like growing environments along the shallow shore. Harvesting is also done using boats and mechanical equipment. In coastal cultivation, coastal water pools are used to raise young seedlings. This provides a more controlled environment compared to offshore or coastal cultivation. Manual or mechanical harvesting methods can be used (Gutierrez et al., 2006; Khan, 2024).

**TYPES OF MACROALGAE PRODUCTION SYSTEMS**



| Off-Shore Cultivation | Near-Shore Cultivation | On-Shore Cultivation |

**Figure 2.3.** Different seaweed cultivation systems, off-shore (Anonim, 2021c), near-shore (Anonim, 2014) and on-shore cultivation systems (Anonim, 2022).

## 3. BIO-ACTIVE COMPONENTS AND BENEFITS OF ALGAE FOR ANIMAL HEALTH

Algae contain a variety of bioactive components, including amino acids, proteins, carbohydrates, fatty acids, minerals, vitamins, antioxidants, sterols, pigments, and phenolic compounds. These components provide significant advantages for the use of algae as animal feed.

Being rich in protein and amino acids, algae are found in high concentrations of essential nutrients for animal growth and development. This is because algae contain a high amount of protein comparable to soybeans, one of the most important feed sources. Although there are many algae species, Arthrospira and Chlorella are considered important protein sources for animal consumption because they contain essential amino acids similar to traditional protein sources such as soybeans, fish, and eggs. Microalgae such as *Spirulina*, *Dunaliella*, *Chlamydomonas*, and *Scenedesmus* are also used in animal feed, and most of them have high protein content (Dineshbabu et al., 2019). In addition to microalgae, which are high in protein and used in animal nutrition, macroalgae for example *Porphyra*, *Ulva*, *Palmaria*, and *Gracilaria*, can also contain quite high protein content, as mentioned in Das and Ghosh's review in 2024. Among green, red, and brown algae, brown algae generally have the lowest protein content. Besides being a good source of protein, algae are also a good source of carbohydrates, providing an energy source for animals and, due to their specialized polysaccharides, have immune-supporting properties. The carbohydrate content and polysaccharide composition vary depending on the algae species. Algal fatty acids are notable for maintaining heart health and reducing inflammation. They also play a significant role in increasing animals' tolerance to stress. Sterols and pigments also contribute significantly to animal health by providing antibacterial and immune-boosting properties. Phenolic compounds are known to act as natural preservatives in feed and prevent spoilage. These information reveals that algae not only contribute to animal nutrition but also contribute to animal health, support growth, and reduce the risk of illness. Considering all the features, algae's versatility stands out as a tool that supports both ecological and sustainable animal husbandry practices.
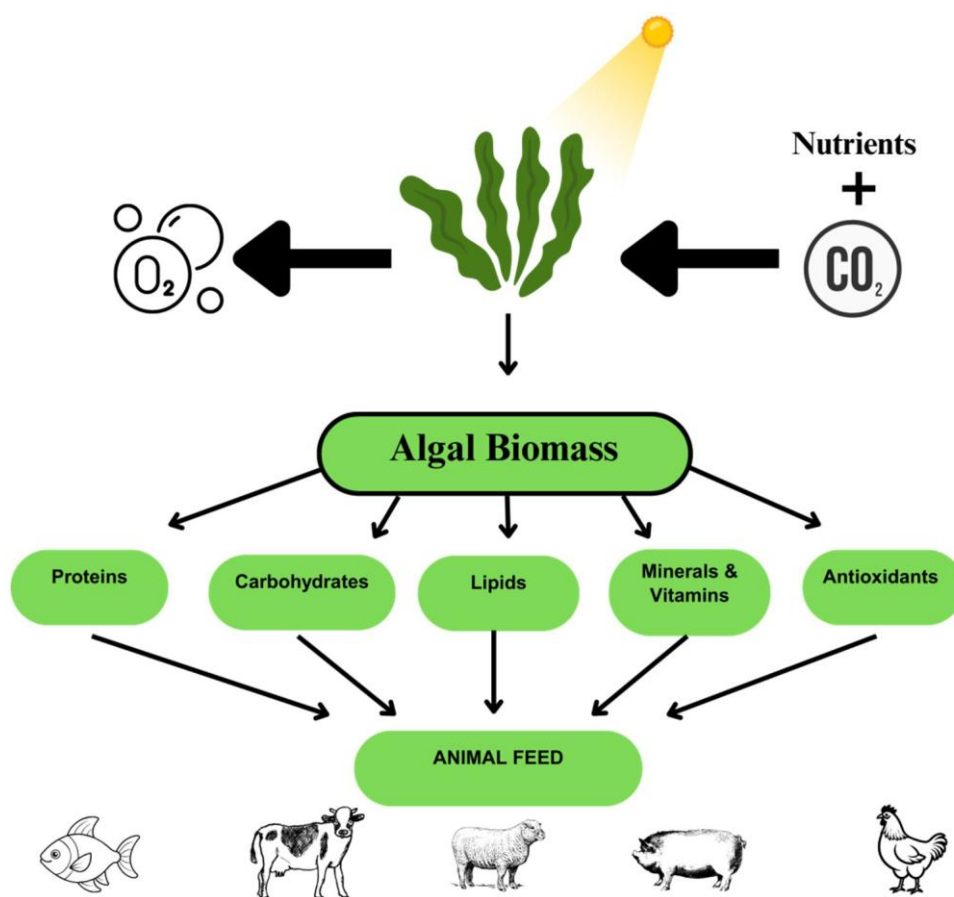
**Figure 3.1.** Key groups of bioactive components derived from algal biomass and their potential functional roles in animal nutrition. The visual is adapted from the original figure by Das and Ghosh, 2024.

To summarize the benefits of algae for animal health:

• The amino acids and proteins that it contains support animal growth and tissue regeneration.
• Some of the pigments it contains improve meat and egg color.
• Omega-3 fatty acids strengthen the immune system.
• Carbohydrates support intestinal health.
• Vitamins and minerals boost immunity.
• Antioxidants improve animal health and product quality.

## 4. BENEFITS OF USING ALGEA IN ANIMAL HUSBANDRY

Review of the studies indicates that seaweed has the potential to supplement the protein and energy supply of farm animals such as ruminants, pigs, poultry and supports prebiotics in the digestive systems of both ruminants and monogastric animals (Makkar et al., 2016).

A comprehensive review of studies on ruminants indicates that the use of algae supplements in ruminant diets improves milk quality, enhances meat color and quality, and

offers numerous advantages such as supporting lower cholesterol levels and healthier liver function in animals. For example, while some algae species, such as *Schizochytrium*, have been found to increase the omega-3 content in milk, the effect of some species is limited. In other words, the effects of algae species on animals can vary greatly. It is certain that the physiological responses of ruminants are dose-dependent and that the appropriate doses may vary between species, which is why extensive and comprehensive studies are needed. In addition to all this, the use of algae in ruminant diets stands out for its potential to reduce methane gas emissions, one of the sustainability problems in animal husbandry. It has been stated that it contributes to sustainability without affecting animal health and productivity (Kazemi, 2025). Red algae, with their distinct chemical properties, have been identified as the algae species with the highest potential for reducing methane gas production (Machado et al., 2016). It has been reported that the red algae species *Asparagopsis taxiformis*, when fed in appropriate amounts, reduces enteric $CH_4$ emissions in cattle by 80% (Roque et al., 2021).

The effect of algae may vary depending on the type of algae, whether it is macroalgae or microalgae, the form in which it is administered, the ruminant being fed, and the sex and physiological condition of the animal. Furthermore, differences have been observed in analyses depending on the amount and duration of algae feeding to animals. For example, adding microalgae and macroalgae to the diets of some sheep was found to increase milk protein content (Harahap et al., 2024). It has been stated that algae have many benefits in the nutrition of ruminants. However, changes in nutrient composition, the presence of non-nutritive harmful substances, heavy metal accumulation, and economic constraints in production processing still exist. Continued research will help algae be used more efficiently in ruminant feed systems.

In poultry farming, where parameters such as egg production and meat quality are important, the use of different algae has been targeted to improve these parameters. The use of an algae called *Chlorella vulgaris* in the diet of laying hens has been found to increase egg production (Zheng et al., 2011). *Undaria pinnatifida*, a brown algae species, has been found to increase egg laying and egg weight, but no changes were observed in eggshell color or hardness, or yolk color (Heo et al. 2005). Other studies related to egg quality have also reported that algae such as *Entermorpha* spp., *Chlorella vulgaris*, and *Enteromorpha prolifera* improve egg quality parameters such as weight, brighter yolk, and shell thickness (Coudert et al., 2020).

Since a large portion of fishing operation costs is allocated to feed expenses, alternative sources have been researched in recent years. However, it has been found that feed produced by traditional methods does not meet all the nutritional requirements of fish. With increasing research in recent years, seaweed has been targeted for use as an alternative method. In a review reporting on numerous studies on seaweed species, feeding concentrations, and levels of incorporation into fish feed, the types of algae used in fishing activities were reported. As a result of these studies, it has been stated that this type of seaweed has different effects depending on the dosage level and fish species. The contributions of algae to fish development can be listed as increasing growth, improving lipid metabolism, improving physiological activities, regulating stress responses, providing resistance to diseases, and improving carcass quality. In conclusion, the use of algae in animal feed provides nutritional, health, and environmental advantages, increasing animal production efficiency and reducing antibiotic use. However, it is recommended that the variations in the components of algae species, the risk of heavy metal

accumulation they may pose, and the challenges encountered in their production be carefully addressed and further research be conducted (Morais et al., 2020).

## 5. USE OF ALGAE AS SILAGE

In recent years, there has been increasing interest in algae as an alternative feed source. When freshly harvested, algae have a high moisture content, leading to post-harvest decay, enzymatic degradation, and loss of nutritional value. Therefore, different techniques are being employed to utilize algae as feed. Preservation by drying is one of the frequently used methods, but it is impractical due to seasonal challenges, varying weather conditions, and the high energy demand and space requirements. In addition to this storage method, ensiling algae can be considered a more effective and sustainable strategy. Ensiling is used in many forage crops by using fermentation, and it is a strategy that allows nutrients to be preserved independently of weather conditions for later use. This method allows for the preservation of algae after harvest, independent of seasonal and weather conditions. Studies on two different brown algae, *Fucus vesiculosus* and *Saccharina latissima*, showed differences in fermentation, but the pH level of silage made with *Saccharina latissima* was reported to be acceptable. This indicated that there are bottlenecks in ensiling of algae because silageability is variety-specific. Although with some nutritional degradation during ensiling, it is a sustainable method for a specific variety of algae (Campbell et al., 2020).

The high iodine content of some types of algae is a key consideration when making silage. The presence of iodine is a significant limiting factor in the use of algae as animal feed, as high iodine levels can be toxic to animal health. Therefore, the use of various pretreatments plays a critical role in silage to reduce the iodine content of the algae. Reducing iodine levels can be achieved through boiling, soaking, freezing, and oven drying. Each method has its advantages and disadvantages. When making silage, these should be evaluated and the appropriate method selected. These methods can be listed as follows:

- Blaching
- Soaking
- Oven Drying
- Freeze-Drying

As shown in a review which considers different pre-silage techniques for decreasing iodine content, the blanching method, algae are soaked in water at 30-80 degrees Celsius for 30-300 seconds, and a significant decrease in iodine levels is observed. In the soaking method, algae are held at approximately 32 degrees Celsius for a specific period of time to remove excess salt, minerals, and iodine. In drying methods, algae are dried at low temperatures in ovens or by freezing (Dhakal et al., 2024). In summary, ensiling is considered a highly sustainable preservation method that largely preserves the nutritional content of algae and protects animal health. However, as studies have shown, the presence of varietal-specific ensiling differences is still a significant limitation.

## 6. COMMERCIAL ALGAE-BASED FEED PRODUCTS

It is clear that the need for sustainable feed sources is increasing daily with the growing global population. At this point, algae has emerged as an alternative feed source, gaining importance in the livestock sector because it is high in protein and does not require water or land for cultivation like traditional feed sources. Algae boasts high sustainability and a low carbon footprint. Today, products derived from various algae species are available worldwide, and they are marketed in different forms such as flour, extracts, pellets, crisps, and mineral supplements. There are some examples of products shown in Figure 6.1.
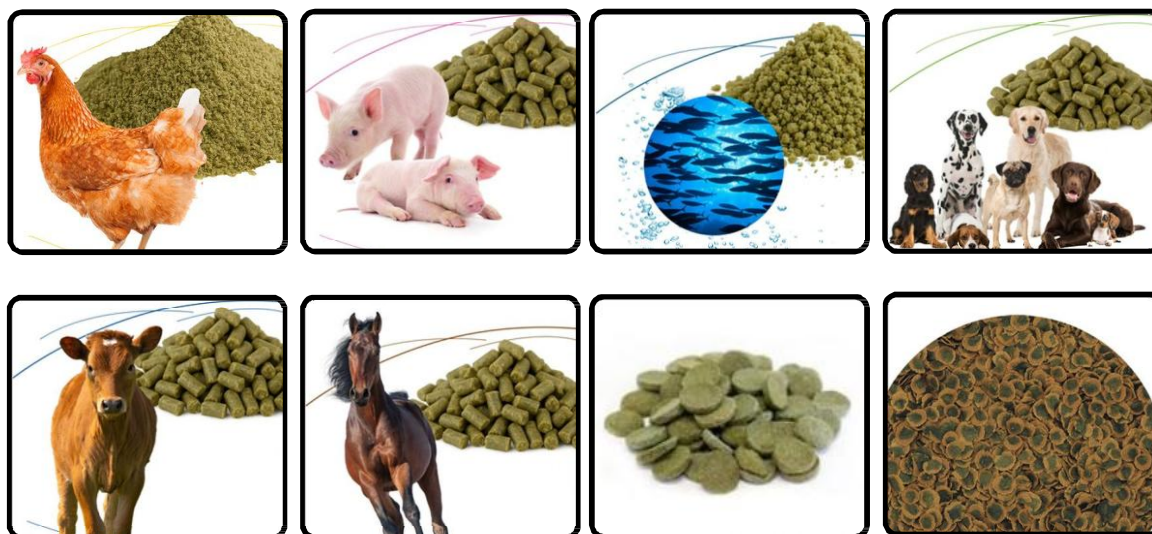


**Figure 6.1.** Commercially available algae-based feed products (Anonim, 2024a), Algae Disc® for aquaculture (Anonim, 2024b) and Algae Crisp® algae-derived supplemental feed tablets (Anonim, 2024c).

## 7. FUTURE STRATEGIES FOR IMPROVEMENT OF ALGAE-BASED ANIMAL FEED

Algae can be considered a promising source for the future of sustainable animal husbandry as an alternative feed source providing high protein, bioactive plants beneficial for animal health, and rapid growth ability. Most of the time they don't need an arable land and fresh water sources unlike traditional animal feed sources.

Advances in technology and research on the genetics of living organisms have led to significant developments over time, enabling humanity to directly manipulate target genes. These innovative methods have created numerous opportunities for new discoveries. For example, microalgae are organisms that can produce pigments, lipids, proteins, and other valuable components. However, their natural production levels are not always sufficient for commercial applications. Therefore, many studies have been conducted with the aim of increasing production levels by developing gene editing methods. Although these studies have the potential to deliver high-quality and efficient products, there are still challenges to overcome. Current algal strains are limited, and new breeding techniques are needed to develop

high-quality strains. Furthermore, the consistency of genetically modified algae in producing the desired components still needs improvement. The integration of omics technologies, machine learning, and artificial intelligence tools into biology will accelerate the development of next-generation microalgal feedstocks. Public acceptance of genetically modified organisms is another factor limiting research. To ensure consumer acceptance, it is important to select appropriate regulatory techniques for genetic studies and to conduct developments transparently (Qin et al., 2023; Raj et al., 2025).

## 8. CONCLUSION

Microalgae and macroalgae stand out as an alternative feed source with high nutritional content, including protein, lipids, and vitamins. These features make algae suitable for feeding animals across a wide range of applications, from ruminants to monogastric animals, poultry, and aquaculture. Also, from another aspect, algae production systems require minimal land and freshwater resources, making them a more sustainable and environmentally friendly solution compared to traditional feed sources. It provides significant benefits such as increasing the digestive efficiency of ruminants, reducing methane gas emissions, and improving growth and egg quality in poultry. Furthermore, the possibility of ensiling algae, as well as using them dry, creates new opportunities in the storage process and makes their use more practical. Future work on genetic engineering to modify, optimize, and increase the efficiency of algae's nutritional profiles holds promise for the breeding of new algae suitable for commercial use.

The use of algae in animal husbandry as a feed source is an innovative approach in terms of environmental sustainability and economic efficiency. Research in this field will enable the animal husbandry sector to develop more sustainable production models for future generations.

## REFERENCES

Alami, A. H., Alasad, S., Ali, M., & Alshamsi, M. (2021). Investigating algae for $CO_2$ capture and accumulation and simultaneous production of biomass for biodiesel production. *Science of the Total Environment*, 759, 143529.

Alexandratos, N., & Bruinsma, J. (2012). World agriculture towards 2030/2050: the 2012 revision

Anonim, (2009), Growing *Spirulina* algae in PET bottles. https://tk.noblogs.org/post/2009/09/24/growing-spirulina-algae-in-pet-bottles-2/

Anonim, (2014), PortalExport. The development of seaweed industry in Indonesia [Photograph]. https://portalexport.wordpress.com/2014/08/19/the-development-of-seaweed-industry-in-indonesia/

Anonim, (2021a). Watanabe, J. Chlorophyta - green algae Stanford SeaNet. https://seanet.stanford.edu/Chlorophyta

Anonim, (2021b). Watanabe, J. *Phylum ochrophyta* Stanford SeaNet. https://seanet.stanford.edu/Ochrophyta

Anonim, (2021c). Eyevine. Floating offshore seaweed farm. The Economist.https://www.economist.com/science-and-technology/floating-offshore-farms-may-increase-production-of-seaweed/21805108

Anonim, (2022). Cyanotech Corporation. Microalgae cultivation facility along the Kona Coast of Hawaii's Big Island. Cornell University News. https://news.cornell.edu/stories/2022/10/onshore-algae-farms-could-feed-world-sustainably

Anonim, (2024a). Ocean Harvest Technology. Species-specific seaweed feed solutions. https://oceanharvesttechnology.com

Anonim, (2024b). Zeigler Feed. Algae Disc® aquaculture feed. https://www.agriexpo.online/prod/zeigler-feed/product-185939-105915.html

Anonim, (2024c). TetraPro Algae Multi-Crisps. https://www.tetra.net/en-roa/products/tetrapro-algae-multi-crisps

Barta DG, Coman V, Vodnar DC (2021) Microalgae as sources of omega-3 polyunsaturated fatty acids: bio-technological aspects. *Algal Re*s 58:102410. https:// doi. org/ 10. 1016/j. algal. 2021. 102410

Baweja, P., & Sahoo, D. (2015). *Classification of algae*. In The algae world (pp. 31-55). Dordrecht: Springer Netherlands.

Benner, P., Meier, L., Pfeffer, A., Krüger, K., Oropeza Vargas, J. E., & Weuster-Botz, D. (2022). Lab-scale photobioreactor systems: principles, applications, and scalability. *Bioprocess and biosystems engineering*, 45(5), 791-813.

Bwapwa, J. K., Akash, A., & Trois, C. (2019). Jet fuel from domestic wastewater treatment using microalgae: A review. *Green Materials for Wastewater Treatment*, 321-360.

Campbell, M., Ortuño, J., Ford, L., Davies, D. R., Koidis, A., Walsh, P. J., & Theodoridou, K. (2020). The effect of ensiling on the nutritional composition and fermentation characteristics of brown seaweeds as a ruminant feed ingredient. *Animals*, *10*(6), 1019.

Coudert, E., Baéza, E., & Berri, C. (2020). Use of algae in poultry production: A review. *World's Poultry Science Journal*, 76(4), 767-786.

Das, J., & Ghosh, K. (2024). Potential Use of Algae in the Diets of Farmed Animals and Fish: An Overview. *In Proceedings of the Zoological Society* (Vol. 77, No. 4, pp. 443-462). New Delhi: Springer India.

De Jussieu, A. L. (1789). Genera Plantarum: Secundum ordines naturales disposita, juxta methodum in Horto regio parisiensi exaratam, anno M.DCC.LXXIV. Paris: Author. https://www.biodiversitylibrary.org/item/7125

Dhakal, S., Jüterbock, A. O., Lei, X., & Khanal, P. (2024). Application of the brown macroalga *Saccharina latissima* (Laminariales, Phaeophyceae) as a feed ingredient for livestock: A review. *Animal Nutrition*, 19, 153-165.

Dineshbabu, G., Goswami, G., Kumar, R., Sinha, A., & Das, D. (2019). Microalgae–nutritious, sustainable aqua-and animal feed source. *Journal of Functional Foods*, *62*, 103545.

Gurau S, Imran M, Ray RL (2025) Algae: a cutting-edge solution for enhancing soil health and accelerating carbon sequestration–a review. *Environ Technol Innov* 37:103980. https://doi.org/10.1016/j.eti.2024. 103980

Gutierrez, A., Correa, T., Munoz, V., Santibanez, A., Marcos, R., Cáceres, C., & Buschmann, A. H. (2006). Farming of the giant kelp *Macrocystis pyrifera* in southern Chile for development of novel food products. *Journal of Applied Phycology*, 18(3), 259-267.

Harahap, M. A., Widodo, S., Handayani, U. F., Altandjung, R. I., Wulandari, Sakti, A. A., ... & Baihaqi, Z. A. (2024). Examining performance, milk, and meat in ruminants fed with macroalgae and microalgae: A meta-analysis perspective. *Tropical Animal Health and Production*, 56(7), 243.

Heo, S. J., E. J. Park, K. W. Lee, and Y. J. Jeon. (2005). Antioxidant Activities of Enzymatic Extracts from Brown Seaweeds. *Bioresource Technology* 96: 1613–1623. doi:10.1016/j.biortech.2004.07.013

Huo, S., Wang, Z., Zhu, S., Shu, Q., Zhu, L., Qin, L., ... & Dong, R. (2018). Biomass accumulation of Chlorella zofingiensis G1 cultures grown outdoors in photobioreactors. *Frontiers in Energy Research*, 6, 49.

Jayaraman, J., Kumaraswamy, J., Rao, Y. K., Karthick, M., Baskar, S., Anish, M., ... & Ammarullah, M. I. (2024). Wastewater treatment by algae-based membrane bioreactors: a review of the arrangement of a membrane reactor, physico-chemical properties, advantages and challenges. *RSC advances*, 14(47), 34769-34790.

Kasanah, N., Ulfah, M., Imania, O., Hanifah, A. N., & Marjan, M. I. D. (2022). Rhodophyta as potential sources of photoprotectants, antiphotoaging compounds, and hydrogels for cosmeceutical application. *Molecules*, 27(22), 7788.

Kazemi, M. (2025). Algae as a sustainable feed resource: revolutionizing animal nutrition. *Aquaculture International*, 33(6), 1-56.

Khan, N., Sudhakar, K., & Mamat, R. (2024). Macroalgae farming for sustainable future: Navigating opportunities and driving innovation. *Heliyon*, 10(7).

Kumar, C., Sharma, M., Kaur, M., Arya, S. K., & Khatri, M. (2024). Cultivation of algae: techniques and challenges. In Value added products from bioalgae based biorefineries: opportunities and challenges (pp. 43-65). Singapore*: Springer Nature* Singapore.

Linnaeus C (1753) Species plantarum, vol 1 and 2, In Stearn WT (1957), *Carl Linnaeus Species Plantarum*. Royal Society, London.

Machado, L., M. Magnusson, N. A. Paul, R. Kinley, R. de Nys, and N. Tomkins. (2016). Identification of bioactives from the red seaweed *Asparagopsis taxiformis* that promote antimethanogenic activity in vitro. J. *Appl. Phycol*. 28:3117–3126. doi:10.1007/s10811-016-0830-7

Makkar, H. P., Tran, G., Heuzé, V., Giger-Reverdin, S., Lessire, M., Lebas, F., & Ankers, P. (2016). Seaweeds for livestock diets: A review. *Animal Feed Science and Technology*, 212, 1-17.

Martins, C. F., Ribeiro, D. M., Costa, M., Coelho, D., Alfaia, C. M., Lordelo, M., ... & Prates, J. A. (2021). Using microalgae as a sustainable feed resource to enhance quality and nutritional value of pork and poultry meat. *Foods*, 10(12), 2933.

Ojamae, K. (2011). *Growth physiology and photosynthetic performance of green microalgae mass culture grown in a thin-layer cascade*. University of Tartu.

Pereira, L. (2021). *Macroalgae*. Encyclopedia, 1, 177–188. https://doi.org/10.3390/encyclopedia1010017

Qin, S., Wang, K., Gao, F., Ge, B., Cui, H., & Li, W. (2023). Biotechnologies for bulk production of microalgal biomass: from mass cultivation to dried biomass acquisition. Biotechnology for Biofuels and Bioproducts, 16(1), 131.

Raj, S., Jyothsna, P., Lasya, V., Ramya, V., Sreenikethanam, A., Gobi, M., ... & Bajhaiya, A. K. (2025). The role of microalgae and genetic engineering in transforming sustainable animal nutrition: a comprehensive review. *Discover Applied Sciences*, 7(11), 1-21.

Rezaei, A., Cheniany, M., Ahmadzadeh, H., & Vaezi, J. (2024). Evaluation of lipid composition and growth parameters of cold-adapted microalgae under different conditions. *BioEnergy Research*, 17(1), 557-569.

Roque, B. M., M. Venegas, R. D. Kinley, R. de Nys, T. L. Duarte, X. Yang, E. Kebreab. (2021). Red Seaweed (*Asparagopsis taxiformis*) supplementation reduces enteric methane by over 80 percent in beef steers. *PLoS One* 16:1–20. doi:10.1371/journal.pone.0247820

Saadaoui, I., Rasheed, R., Aguilar, A., Cherif, M., Al Jabri, H., Sayadi, S., & Manning, S. R. (2021). Microalgal-based feed: promising alternative feedstocks for livestock and poultry production. *Journal of Animal Science and Biotechnology*, 12(1), 76.

Sharma, A. K., Jaryal, S., Sharma, S., Dhyani, A., Tewari, B. S., & Mahato, N. (2025). Biofuels from microalgae: A review on microalgae cultivation, biodiesel production techniques and storage stability. *Processes*, 13(2), 488.

Taelman, S. E., Champenois, J., Edwards, M. D., De Meester, S., & Dewulf, J. (2015). Comparative environmental life cycle assessment of two seaweed cultivation systems in North West Europe with a focus on quantifying sea surface occupation. *Algal Research*, 11, 173-183.

Vahedi, V., Hedayat-Evrigh, N., Holman, B. W., & Ponnampalam, E. N. (2021). Supplementation of macro algae (*Azolla pinnata*) in a finishing ration alters feed efficiency, blood parameters, carcass traits and meat sensory properties in lambs. *Small Ruminant Research*, 203, 106498.

Van Ginneken, V., & de Vries, E. (2018). Seaweeds as biomonitoring system for heavy metal (HM) accumulation and contamination of our oceans. American Journal of Plant Sciences, 9(7), 1514-1530.

Vos, R., & Bellù, L. G. (2019). Global trends and challenges to food and agriculture into the 21st century. *Sustainable food and agriculture*, 11-30.

Young-Lorenz, J. D. (2013). Portfolio analysis of carbon sequestration technologies and barriers to adoption (Doctoral dissertation, University of Western Australia).

Zheng, L., Oh, S. T., Jeon, J. Y., Moon, B. H., Kwon, H. S., Lim, S. U., ... & Kang, C. W. (2012). The dietary effects of fermented *Chlorella vulgaris* (CBT®) on production performance, liver lipids and intestinal microflora in laying hens. *Asian-Australasian journal of animal sciences*, 25(2), 261.

# CHAPTER 7

# SURFACE ROUGHNESS AND LUBRICATION IN INTERNAL COMBUSTION ENGINES

Lecturer Buse SERGEK[1], Prof. Dr. A.Engin ÖZÇELİK[2]

[1]Baskent University, Anatolia Organized Industrial Zone Vocational School, Welding Technology Program, Ankara, Türkiye Orcid: 0000-0002-5773-4553, e-mail: busesergek@baskent.edu.tr
[2]Selcuk University, Technology Faculty, Mechanical Engineering Department, Konya, Turkey Orcid: 0000-0002- 8646-0950, e-mail: eozcelik@selcuk.edu.tr

## 1. INRODICTION

Tribology is a multidisciplinary science that examines the interconnected phenomena of friction, wear, and lubrication within mechanical systems. It aims to improve the operational efficiency and service life of machinery by minimizing frictional losses and preventing wear between interacting surfaces. To achieve this, tribological principles are applied to maintain friction at an optimum level and ensure that the wear occurring in sliding machine components remains negligible. This is primarily achieved through the application of appropriate lubricants (Shah & Shukl, 2021).

In internal combustion engines, an increase in the number of dynamic components, their contact surface areas, and their surface roughness results in more complex tribological challenges. The main objective of an engine tribologist is to achieve efficient lubrication across all moving engine parts while simultaneously reducing environmental impacts, frictional losses, and wear. This task is particularly demanding because engines operate under diverse and fluctuating conditions, including variations in load, speed, and temperature (Johansson et al., 2011), (Burunsuzoğlu & Cesur, 2023).

Enhancing the tribological performance of engines yields several key advantages, such as:

•Lower fuel consumption,

• Increased engine power output,

• Reduced oil consumption,

• Decreased emission of harmful exhaust gases,

• Improved durability, reliability, and engine lifespan, and

• Reduced maintenance costs with extended service intervals (Tung & McMillan, 2004).

As shown in Figure 1, a linear-motion internal combustion engine is a fundamental mechanical unit used not only in automobiles but also in various land and marine vehicles, including motorcycles, trucks, agricultural machines, construction equipment, and ships (Tung & McMillan, 2004).
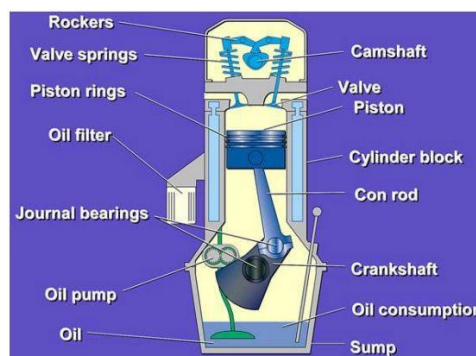


**Figure 1.** Tribological components of an internal combustion engine (Tung & McMillan, 2004).

The distribution of fuel energy is illustrated in Figure 2. Approximately 38% of the total fuel energy in a passenger vehicle is converted into mechanical power to overcome aerodynamic drag and frictional losses. Of this, about 5% is utilized to counteract air resistance caused by both external and internal flows, including cooling and electrical systems, while the remaining 33% compensates for internal frictional losses within the vehicle (Holmberg et al., 2012).
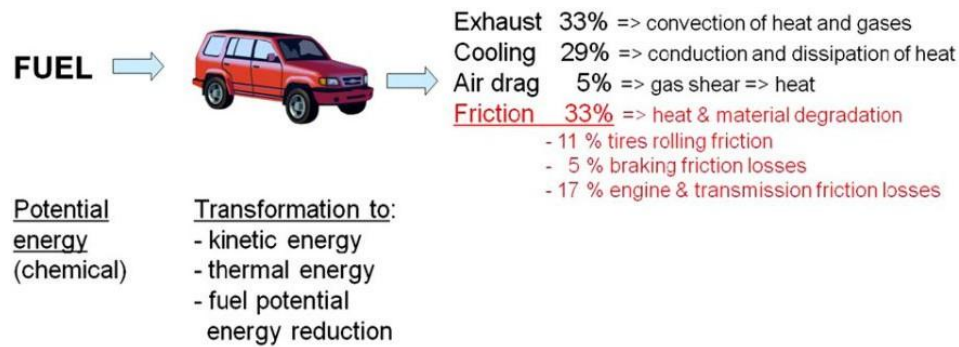


**Figure 2.** In passenger vehicles, the fuel energy distribution for a speed of 60 km/h is approximately (Holmberg et al., 2012).

As presented in Figure 3, around 35% of the total fuel energy lost to friction corresponds to the losses occurring in the engine system itself.
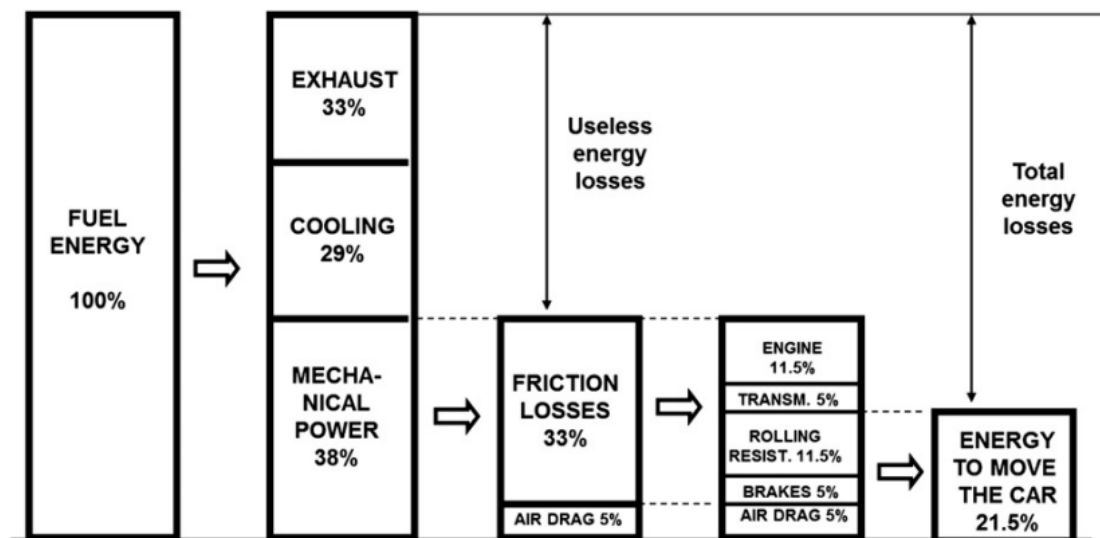


**Figure 3.** Distribution of energy consumption in passenger vehicles (Holmberg et al., 2012).

In most vehicles, the engine's internal systems are grouped into three primary subsystems: the piston group, the valve system, and the bearings and seals. According to Figure 4, approximately 45% of frictional losses originate from the piston group, 30% from hydrodynamic components such as bearings and seals, 15% from the valve train, and 10% from viscous losses due to oil pumping (Holmberg et al., 2012).

When considering an average passenger vehicle utilizing 100 units of energy, approximately 11.5 units are consumed due to frictional losses within the internal combustion engine. Of this, around 2.9 units are spent overcoming bearing friction alone. Although this may seem small on a macro scale, the energy dissipated through bearing friction in dynamically loaded parts is considerably significant (Taylor, 1998).
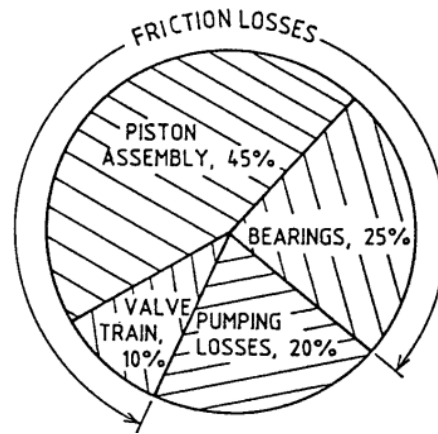


**Figure 4.** Distribution of Friction Losses in an Internal Combustion Engine (Taylor, 1998).

## 2. LITERATURE REVIEW

The relationship between surface roughness and lubrication within internal combustion engines has been extensively investigated by various researchers, focusing on minimizing frictional losses and enhancing wear resistance in sliding components.

Liu et. al., (2022), the frictional behavior between the piston ring and cylinder liner was analyzed in depth. A dynamic friction model was established for the liner–ring interface, taking into account both the surface roughness and deformation of these components. Through comparative analysis and the Box-Behnken response surface methodology, it was determined that increasing the roughness of the piston ring slightly increases asperity friction but decreases fluid friction, ultimately reducing the total frictional loss. Conversely, an increase in the cylinder liner's surface roughness results in lower asperity friction but higher fluid friction, thereby raising total frictional losses (Liu et. al., 2022).

Aoki et al., (2018). explored how machined grooves on the piston skirt influence lubrication performance. Using Elastohydrodynamic Lubrication (EHL) theory, they analyzed the effects of groove geometry and orientation on oil film thickness and friction coefficient. Their results demonstrated that higher groove coverage leads to a reduced friction coefficient, as the horizontally oriented grooves promote smoother lubricant flow between the flat surfaces. This reduces both the solid contact load (Ns) and the fluid friction force (Ff'). Furthermore, they observed that groove width had a more substantial influence than depth, suggesting that controlling groove geometry in the lateral direction is a practical way to minimize friction. Overall, shallow and wide grooves were found to be the most effective in lowering the friction coefficient (Aoki et al., 2018).

In another study, Cho et al. investigated how different surface roughness values of the piston skirt and surface coatings affect lubrication. They compared skirts ground to three distinct roughness levels and coated them with either graphite or diamond-like carbon (DLC) films. Their findings indicated that commercial piston skirts with coarse surfaces experience

increased friction losses due to asperity contact between peaks. In contrast, smoother skirts showed reduced friction and wear, demonstrating a direct link between lower friction and enhanced wear resistance (Cho et al., 2009).

Jocsak et al., (2006) simulated how piston surface texture influences engine friction using three-dimensional honing patterns. Their analysis revealed that reducing the cross-hatch angle—thereby aligning the grooves more perpendicularly to the flow direction—lowers friction in the ring pack system. However, these surface modifications may also introduce drawbacks such as increased scuffing tendency and higher oil consumption (Jocsak et al., 2006).

Meng et al., (2019)careful optimization of both run-in processes and surface roughness during piston skirt design is essential for minimizing friction and wear. Their findings suggested that while extremely smooth surfaces theoretically reduce friction, they are more prone to seizure and sensitive to debris. Conversely, maintaining a moderate level of initial roughness combined with a soft surface coating provides better tribological performance and reliability (Meng et al., 2019).

Garcial et al.,(2021) surface texturing was proposed as a promising method to improve engine tribological behavior. Texturing modifies the topography of the contact surface by introducing dimples and grooves, which enhance lubricant retention and debris trapping. Their experiments demonstrated that applying textured surfaces on the cylinder liner reduced maximum asperity contact forces by 9.43% and total frictional forces by 5.29%, while simultaneously increasing the oil film thickness—thereby mitigating wear (Johansson et al., 2011).

## 3. FRICTION AND LUBRICATION IN INTERNAL COMBUSTION ENGINES

### 3.1. Lubrication and Its Importance

Lubrication refers to the process of forming a thin, slippery film between two interacting surfaces to reduce friction and facilitate smooth motion. The primary purpose of lubrication in engines is to minimize wear caused by direct metal-to-metal contact and to ensure efficient energy transfer by decreasing frictional losses (Halis, 2016). For any power-transmitting mechanism that depends on a liquid lubricant, the key tribological factor is the oil film thickness that separates the mating surfaces (Tung & McMillan, 2004).

Figure 5 illustrates the correlation between the coefficient of friction and the oil film thickness ratio commonly expressed by the Summerfield number (viscosity × speed / load). The diagrams above the curve depict various lubrication states between two sliding surfaces. The far-left image represents direct surface contact, while the right side depicts full film lubrication; between these extremes lies mixed lubrication, where intermittent contact occurs. The curved line below demonstrates how the friction coefficient changes with the Summerfield number (Tung & McMillan, 2004).
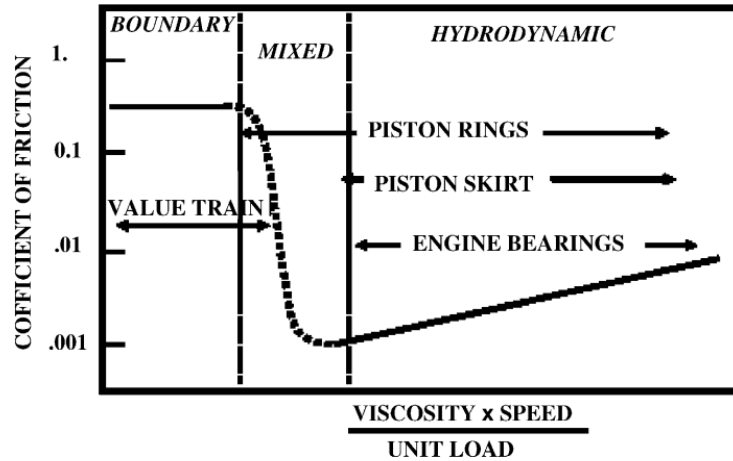
**Figure 5.** Lubrication regimes for engine components and their relationship with friction.

Different engine components rely on specific lubrication regimes to operate efficiently, and these regimes often vary throughout the engine's duty cycle. For instance, main bearings and thrust bearings typically function under hydrodynamic lubrication, in which a continuous oil film separates the metal surfaces. Metal-to-metal contact occurs only under low-speed or high-load conditions or when using low-viscosity oils. In contrast, piston rings, valve systems, and clutch interfaces generally experience mixed or boundary lubrication, where some asperity contact occurs and surface films or chemical layers play an essential protective role (Tung & McMillan, 2004).

The Stribeck curve in Figure 6 schematically shows how lubrication modes transition as a function of lubricant viscosity ($\eta$), shear rate ($v$), and surface pressure ($s$) (Folle et. al., 2022).
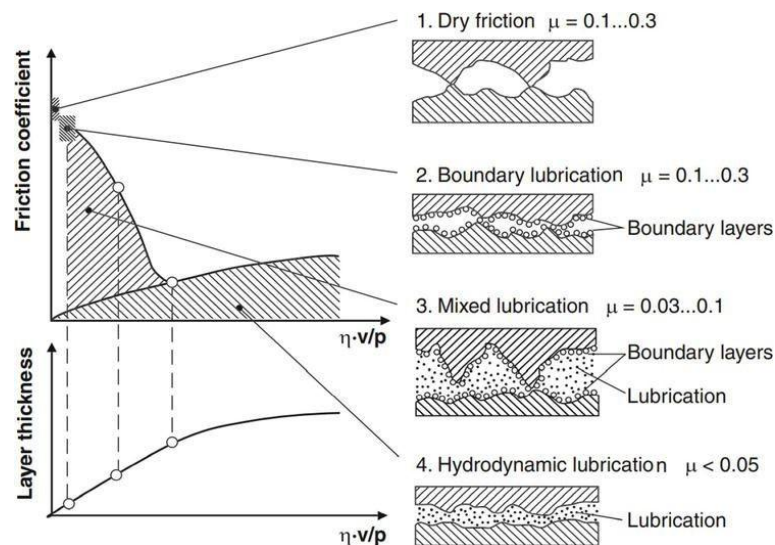


**Figure 6.** Stribeck diagram for different lubrication conditions with dynamic viscosity, shear rate, and pressure/surface pressure (Folle et. al., 2022).

The dominance of particular lubrication regimes for each engine part depends on the surface roughness, wear condition, and degradation of the lubricant (Tung & McMillan, 2004). During operation, oil continuously circulates through the engine system. The oil stored in the crankcase first passes through the oil filter, which removes harmful contaminants. A pump then increases the pressure and directs the oil toward critical components such as the crankshaft bearings, connecting rods, and cylinder walls, providing lubrication between the piston and liner. The oil also lubricates the camshaft bearings, gears, valve mechanism, and oil pump before returning to the crankcase to complete the cycle (Halis, 2016). The main elements of this system are depicted in Figure 7.
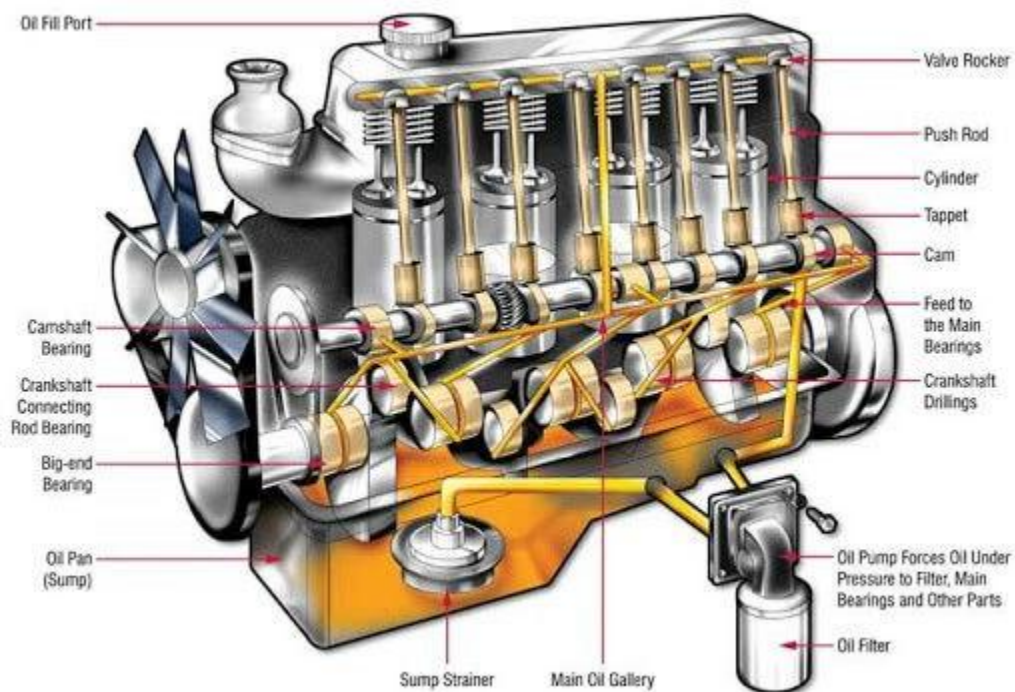
**Figure 7.** Engine Lubrication System (Halis, 2016).

## 3.2. Piston assembly system

The piston assembly, shown schematically in Figure 8, comprises the piston, piston rings, piston pin, connecting rod, and bearings. The key frictional interfaces are:

(a) the piston skirt sliding against the cylinder liner,

(b) the piston rings moving axially within the liner, and

(c) the piston pin and connecting rod bearings.

Friction in the piston group primarily arises from interactions between the piston skirt and liner, and between the piston rings and liner. Radial sliding within the ring grooves alsocontributes to wear, though it is minor in terms of total energy loss (Wong & Tung, 2016).
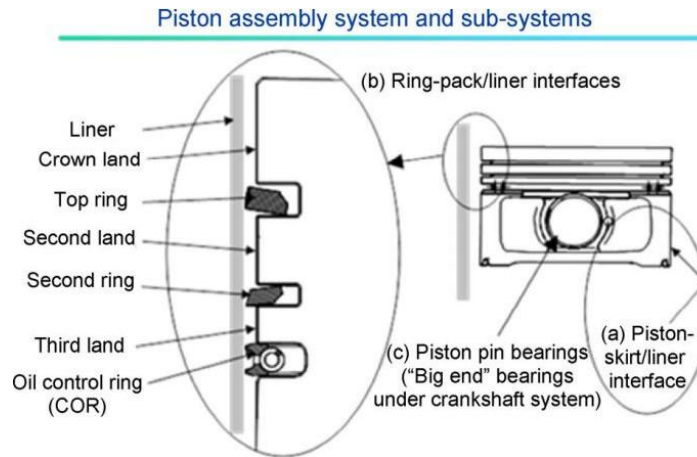
**Figure 8.** Piston assembly system; (a) piston skirt/cylinder liner subsystem, (b) ring assembly/cylinder liner subsystem, and (c) piston pin/piston bearing surfaces are shown (Wong & Tung, 2016).

Factors determining ring–liner friction include surface topography, surface roughness, ring geometry, and lubricant properties. Since the piston ring behaves as a flexible body, deformations caused by oil film pressure must also be considered (Wong & Tung, 2016). For designs dominated by boundary lubrication, increasing oil viscosity generally reduces boundary friction but increases hydrodynamic resistance. Thus, an optimal viscosity must be achieved for minimal total friction (Moughon, 2006).

Minimizing friction between the piston skirt and liner requires maintaining hydrodynamic lubrication. When sufficient oil is supplied, surface profile and roughness become less influential. Consequently, ensuring adequate lubrication is the most effective way to prevent boundary contact and reduce frictional losses (Mansouri & Wong, 2005).

The lubrication regime changes dynamically during the piston's stroke. Boundary lubrication dominates near top dead center (TDC) and bottom dead center (BDC), where sliding speed approaches zero and oil film thickness is minimal. In contrast, hydrodynamic lubrication prevails mid-stroke. Typically, the oil control ring operates under boundary lubrication due to its high tension and narrow contact bands, while the top compression ring and second ring experience mixed regimes. Overall, the top and oil control rings contribute most to total friction, whereas the second ring contributes the least due to lower gas pressure and tension (Wong & Tung, 2016).

## 3.3. Engine bearings

In most engines, bearings are lubricated either by direct oil feed through drilled passages or by oil spray. When lubrication is sufficient, wear remains negligible after a brief run-in phase. However, shaft misalignment or contaminants in the oil can accelerate wear. Another potential failure mode is corrosive attack (Tung & McMillan, 2004).

Crankshaft bearing friction arises primarily in the main bearings that support the shaft's rotation. Additional friction occurs at seal interfaces, where contact is constant. The bearing eccentricity, defined as the offset between the shaft and bearing centers, generates hydrodynamic pressure that sustains the oil film. Adequate lubrication ensures that the

minimum oil film thickness remains greater than the surface roughness amplitude, avoiding mixed or boundary lubrication conditions (Wong & Tung, 2016).

The frictional losses at bearing seals are typically constant, as the contact remains solid-to-solid. The frictional power loss depends on the rotational speed, bearing diameter, and total contact area (Wong & Tung, 2016).

Figure 9 illustrates the interfaces among the piston, piston pin, and connecting rod. The piston pin bearings endure some of the highest dynamic loads in the engine (Wang, 2006). Unlike crankshaft bearings, these do not benefit from oil's cooling function, which complicates lubrication. The interaction between surface roughness and bearing deformation has been modeled using elastohydrodynamic lubrication (EHL) theory. Considering these effects under mixed lubrication has become essential for accurate simulation and design (Wang, 2006).
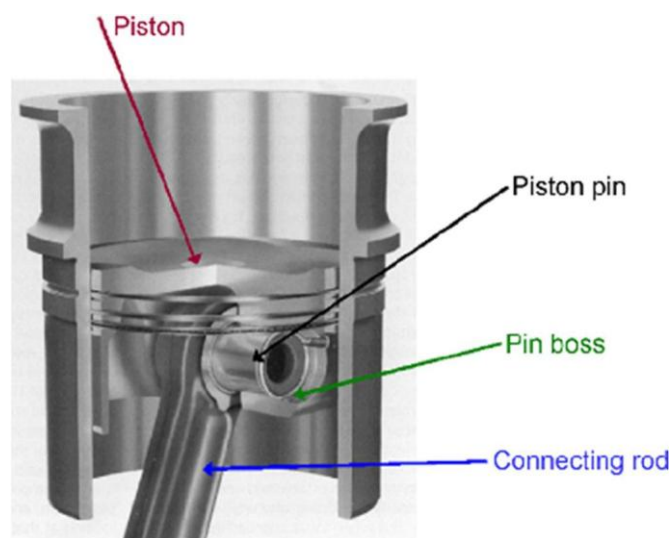


**Figure 9.** Schematic drawing showing the bearing interface surfaces of the piston, piston pin, and connecting rod (Wang, 2006).

The big-end bearings at the connecting rod–crankshaft interface generally operate under hydrodynamic lubrication, supplied continuously with oil via channels within the crankshaft (Wong & Tung, 2016).

## 3.4. Valve system

The valve train comprises several components that convert the rotational motion of the camshaft into the reciprocating motion of the valves. It includes the camshaft, followers, valve springs, retainers, seals, and the valves themselves, as depicted in Figure 10 (Wang, 2006).
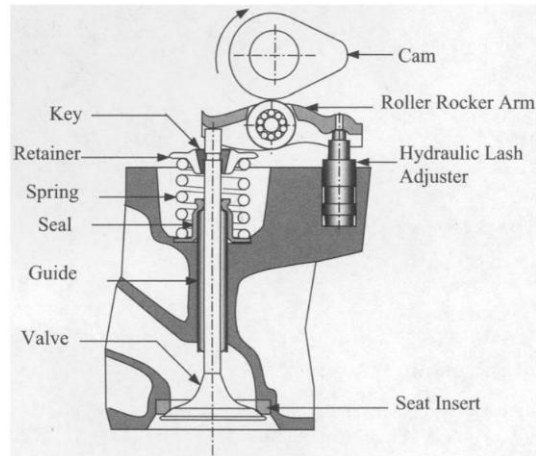
**Figure 10.** Diagram and nomenclature of the valve system (Wang, 2006).

Multiple contact points within the valve system experience different lubrication regimes, from hydrodynamic to boundary lubrication. On average, valve train friction accounts for 15–20% of the total mechanical losses of an engine, though in some cases this can reach up to 40%. Friction in this subsystem becomes more dominant at low speeds, indicating that mixed and boundary lubrication play a significant role in its operation (Wong & Tung, 2016).

## 4. WEAR MECHANISMS IN INTERNAL COMBUSTION ENGINES

### 4.1. Abrasive wear in internal combustion engines

Abrasive wear is a type of wear that occurs when relatively harder particles create a cutting effect on a softer surface, removing surface material. Grinding, sanding, and polishing processes can be cited as examples of controlled abrasive wear. In lubricated systems, abrasive wear mostly results from the contamination of the oil with sand particles. To prevent such wear problems, it is necessary first to change the oil and filter, and then to identify and eliminate the source of the abrasive particles (El-Sherbiny & Ali, 2010).

In internal combustion engines, the most common wear mechanism on piston rings and cylinder bores is abrasion caused by hard particles in the oil film. These particles originate either from the combustion chamber or from the wear itself. Abrasive wear usually concentrates on the piston ring surface and the cylinder bore at the top dead center. If there are hard phases (carbide or phosphide) in cast iron, different wear rates are observed at the top of the cylinder. Abrasive wear is more pronounced during the engine's break-in period and rarely occurs during long-term operation, but it can be observed when there are significant changes in operating conditions (Eyre et al., 1990).

### 4.2. Adhesive wear in an internal combustion engine

Adhesive wear, referred to as adhesion wear, occurs when the asperities on a surface that have welded (or adhered) together break during the relative motion of one metal surface over another (Demirtaş, 2017). Various studies indicate that the typical type of wear observed in

internal combustion engine valves is adhesive wear, which results from high contact stress, insufficient lubrication, and the relative sliding of contact surfaces (Cavalier et al., 2016).

When using lubricants, the durability of the oil film should be taken into account. These lubricants should be viscous enough to form a thick film in fluid or semi-fluid states and should contain some load-carrying additives to prevent metal-to-metal contact under boundary lubrication conditions. This type of wear occurs directly between metal surfaces when the oil film, which provides durability, fails to separate the two surfaces. The piston ring-cylinder liner area is the region where continuous and effective lubrication is the hardest to achieve. Therefore, it is logical to assume that adhesive wear mainly occurs at the top and bottom dead centers. In fact, wear sections on the cylinder liner are particularly noticeable at these points (Müjdeci, 2003).

## 4.3. Corrosion wear in internal combustion engines

Corrosive wear is defined as the material loss that occurs on worn surfaces additionally due to chemical reactions. Chemical wear can occur alone or in combination with other types of wear (Demirtaş, 2017). This type of wear results from chemical effects caused by some products present in the atmosphere (air, humidity, $CO_2$) or due to oxidation, phase changes, etc., in the lubricant (Eyre et al., 1990).

The operating conditions of engines at low or high speeds, the formation of acidic products as a result of sulfur in the fuel or oxidation of the lubricating oil, lead to corrosion wear. In this context, critical components are parts that operate under high temperature fluctuations. These are the piston rings, cylinders, and valves. Surfaces are coated with reactive metals, which are friction-reducing alloys used in bearings. Generally, lubricants are used to protect the surface against corrosion wear and to eliminate this wear (Schilling, 1972).

## 4.4. Fatigue wear in internal combustion engines

Fatigue occurs over time in machine parts due to repeated loads or vibrations. In particular, the continuous and variable loading of surfaces causes fatigue cracks to form just beneath the surface. Fatigue wear occurs on surfaces such as rolling bearings, gears, and cam mechanisms (Demirtaş, 2017).

Surface cracks, the most basic form of fatigue wear, occur at the most sensitive points of the engine, such as the cam and valves. This phenomenon also occurs in bearings. Preventing these deteriorations lies not only in selecting the right oil but also in the surface metallurgy. Materials with fatigue resistance and heat treatments on the surface characterize the durability of contact points. Additionally, lubrication can be improved by enhancing EHD (Elastohydrodynamic) lubrication conditions (Cesur, 2008).

The piston ring-cylinder pair is a significant source of energy loss due to friction and wear in internal combustion engines. Therefore, the friction and wear mechanisms between the cylinder and piston ring pair need to be thoroughly examined. The friction between the piston ring and cylinder directly affects engine efficiency and fuel consumption. Additionally, the

friction between the piston ring and cylinder is a parameter that affects engine lifespan. Therefore, understanding and controlling the friction and wear mechanisms between the piston ring and cylinder play a critical role in preventing the increase in surface roughness of engine parts and in enhancing engine performance and longevity (Burunsuzoğlu & Cesur, 2023).

## 5. LUBRICATING OIL IN INTERNAL COMBUSTION ENGINES

Internal combustion engines are power units widely used in the automotive, maritime, aviation, and industrial sectors. These engines require proper lubrication systems to provide high efficiency, power, and durability (Burunsuzoğlu & Cesur, 2023). Engine oils are a critical component that directly affects the performance, efficiency, and lifespan of internal combustion engines. Therefore, the proper selection of lubricants used in engines and the evaluation of their performance are of great importance (Johansson et al., 2011).

Motor oils are classified as mineral oils, synthetic oils, and semi-synthetic oils based on their production method: mineral oils are obtained by blending base oils derived from the distillation of crude oil with various additives, synthetic oils are produced through chemical processes in a laboratory environment, and semi-synthetic oils are a mixture of both. Mineral oils are cheaper and provide average performance, while synthetic oils are resistant to high/low temperatures and high pressure, have a longer lifespan, and offer high performance. Semi-synthetic oils, produced by mixing 70–80% mineral oil with 20–30% synthetic oil, fall between the two in terms of price and performance. The advantages of synthetic oils include higher purity, lower friction, compatibility with engine requirements, and durability under demanding operating conditions (Halis, 2016).

Additives used to prevent wear become increasingly important as the power of engines increases. Anti-wear additives in mixed or partial oil films aim to minimize wear. As temperature rises, the tendency towards boundary lubrication increases due to the viscosity-temperature relationship, and low contact speeds, high contact pressures, and rough surfaces contribute to the formation of boundary lubrication. If these conditions are extreme and there is little or no oil film, maximum surface contact will occur. This phenomenon is defined as extreme pressure (EP) contact and is usually observed along with very high temperatures and pressures. Additives that prevent extreme pressure contact typically require higher activation temperatures and pressures compared to anti-wear additives. Anti-wear and extreme pressure additives function through thermal decomposition, producing compounds that react with the metal surface. These active-surface compounds preferably form a thin layer that is sheared under boundary lubrication conditions (Müjdeci, 2009).

## 6. CONCLUSION

In this study, friction, wear, and lubrication in the mechanical system of engines were examined. As a result of the adhesive wear of engine parts, small wear particles can remain fixed on the opposite surface. This situation increases the surface roughness of engine parts in areas where boundary lubrication conditions occur. The surface roughness, which is negatively affected by hardened and oxidized particles resulting from adhesive wear, causes abrasive wear to worsen. Similarly, fatigue wear occurring under excessive loads leads to the formation of

wear particles, causing abrasive wear and negatively affecting surface roughness; this, in turn, triggers adhesive wear.

In conclusion, all wear mechanisms that negatively affect surface roughness in engine mechanisms trigger each other's development, and without effective development and use of lubrication systems, the efficient and long-lasting operation of the engine's mechanical system cannot be considered.

In conclusion, all wear mechanisms that adversely affect surface roughness in engine components accelerate each other's progression, and without the effective development and utilization of lubrication systems, the efficient and durable operation of the engine's mechanical system cannot be ensured. It has been evaluated that by improving the lubrication systems in internal combustion engines to reduce wear, it is possible to reduce the processes followed to improve the surface metallurgy of engine parts and to lower the costs in this area.

## REFERENCES

Aoki, H., Hayakawa, K., & Suda, N. (2018). Numerical analysis on effect of surface asperity of piston skirt on lubrication performance. *Procedia Manufacturing*, *15*, 496-503.

Burunsuzoğlu, İ., & Cesur, İ. (2023). Farklı Motor Yağlayıcının Segman-Silindir Çifti Arasındaki Sürtünme Ve Aşınma Özelliklerine Etkisinin İncelenmesi. *1st International Conference on Pioneer and Innovative Studies*, June 5-7, 2023 : Konya, Turkey

Cavalieri, F. J., Zenklusen, F., & Cardona, A. (2016). Determination of wear in internal combustion engine valves using the finite element method and experimental tests. *Mechanism and machine theory*, *104*, 81-99.

Cesur, İ. (2008). *Investigation of the effects of different fuel mixtures on the friction and wear characteristics between the ring-cylinder pair*, Master's thesis, Sakarya University Institute of Science, (Turkey).

Cho, D. H., Lee, S. A., & Lee, Y. Z. (2009). The effects of surface roughness and coatings on the tribological behavior of the surfaces of a piston skirt. *Tribology Transactions*, *53*(1), 137-144.

El-Sherbiny, M. H., & Ali, W. Y. (2010). Abrasive Wear of Internal Combustion Engines. *Journal of the Egyptian Society of Tribology*, *7*(1), 1-13.

Eyre, T. S., Dutta, K. K., & Davis, F. A. (1990). Characterization and simulation of wear occurring in the cylinder bore of the internal combustion engine. *Tribology international*, *23*(1), 11-16.

Folle, L. F., dos Santos Silva, B. C., Batalha, G. F., & Coelho, R. S. (2022). The role of friction on metal forming processes. In *Tribology of Machine Elements-Fundamentals and Applications*. IntechOpen.

García, C. P., Rojas, J. P., & Abril, S. O. (2021). Analysis of the influence of textured surfaces and lubrication conditions on the tribological performance between the compression ring and cylinder liner. *Lubricants*, *9*(5), 51.

Halis, S. (2016). *Experimental investigation of the effect of vehicle usage times on engine oil viscosity,* Master's thesis, Pamukkale University Institute of Science. Turkey

Holmberg, K., Andersson, P., & Erdemir, A. (2012). Global energy consumption due to friction in passenger cars. *Tribology international*, *47*, 221-234.

Jocsak, J., Li, Y., Tian, T., & Wong, V. W. (2006). Modeling and optimizing honing texture for reduced friction in internal combustion engines. *SAE Transactions*, 335-347.

Johansson, S., Nilsson, P. H., Ohlsson, R., & Rosén, B. G. (2011). Experimental friction evaluation of cylinder liner/piston ring contact. *Wear*, *271*(3-4), 625-633.

Liu, N., Wang, C., Xia, Q., Gao, Y., & Liu, P. (2022). Simulation on the effect of cylinder liner and piston ring surface roughness on friction performance. *Mechanics & Industry*, *23*, 8.

Mansouri, S. H., & Wong, V. W. (2005). Effects of piston design parameters on piston secondary motion and skirt-liner friction. *Proceedings of the Institution of Mechanical Engineers, Part J: Journal of Engineering Tribology*, *219*(6), 435-449.

Meng, Z., Zhang, L., & Tian, T. (2019). Study of break-in process and its effects on piston skirt lubrication in internal combustion engines. *Lubricants*, *7*(11), 98.

Moughon, L. L. F. (2006). Effects of piston design and lubricant selection on reciprocating engine friction (Doctoral dissertation, Massachusetts Institute of Technology).

Müjdeci, S. (2009). *Experimental investigation of the effects of commercial oil additives on friction, wear and engine performance in internal combustion engines*. Doctoral thesis, Yıldız Technical University, Institute of Science, Turkey.

Müjdeci, S. (2003). *Wear mechanisms occurring in internal combustion engines and microscopic examination of wear on piston, piston ring and cylinder surfaces in sample engines*. Master's thesis, Yıldız Technical University, Institute of Science, Turkey.

Ö.Çağlayan. (2014). *Hydrodynamic lubrication analysis of crankshaft main bearing in internal combustion engines*, Master's thesis, Istanbul Technical University, Institute of Science. Turkey

S. Demirtaş. (2017). Experimental analysis of the wear mechanisms at top dead center in internal combustion engine, Master's thesis, Yıldız Technical University, Institute of Science, Turkey.

Schilling, A. (1972). Automobile Engine Lubrication–Engine Wear.

Shah, K. R., & Shukl, A. (2021). Analysis of Friction and Wear as a System Response Using Indigenously Fabricated Tribometer. *Tribology in Industry*, *43*(3).

Taylor, C. M. (1998). Automobile engine tribology—design considerations for efficiency and durability. *Wear*, *221*(1), 1-8.

Tung, S. C., & McMillan, M. L. (2004). Automotive tribology overview of current advances and challenges for the future. *Tribology international*, *37*(7), 517-536.

Wang, Y. (2006). Introduction to engine valvetrains. SAE international.

Wong, V. W., & Tung, S. C. (2016). Overview of automotive engine friction and reduction trends–Effects of surface, material, and lubricant-additive technologies. *Friction*, *4*(1), 1-28.

# CHAPTER 8

# CULTIVATION AND USES OF FODDER BEET (*Beta vulgaris* var. *rapacea* Koch) AS AN ALTERNATIVE FORAGE CROP

Asst. Prof. Dr. Bülent BUDAK[1]

[1]Ege University, Ödemiş Vocational Training School, İzmir, Türkiye
Orcid:  0000-0002-2728-9049, e-mail: bulent.budak@ege.edu.tr

## 1. INTRODUCTION

Fodder beet (*Beta vulgaris* var. *rapacea* Koch.), also known as goosefoot, saltbush, or spinach, is a forage plant belonging to the Chenopodiaceae family (Ayaz, 2015). Worldwide, this family includes 103 genera and approximately 1,400 species (Yıldırımlı, 2003). In Türkiye, this family is represented by 33 genera and 120 taxa. Fodder beet is a biennial plant, completing vegetative growth in the first year and generative growth in the second year. It includes both halophytic (salt-tolerant) and xerophytic (drought-tolerant) species. Fodder beet originates from the Middle East and is known to have been used as cattle feed in Ancient Greece around 500 BC (Henry, 2010). It was recorded to have been grown as a root crop in Germany and Italy in the 16th century. Today, this plant is widely cultivated in temperate climate zones worldwide (Anonymous, 2006).

Fodder beet has emerged as a valuable alternative forage crop in temperate regions due to its high yield potential, excellent energy content, and adaptability to diverse agro-climatic conditions. While beet varieties have traditionally been grown for sugar production, specialized varieties have been developed for animal feeding, providing a cost-effective and nutrient-dense feed source for ruminants and other livestock species. The increasing demand for sustainable and energy-rich forage crops has made fodder beet a strategic component in modern livestock production systems (Kır et al., 2007; Dalley et al., 2016; Woods et al., 2021).

This crop is particularly advantageous in regions where traditional forage crops, such as corn or alfalfa, are limited due to soil or climate constraints. Fodder beet provides a high dry matter yield per hectare and can be grazed locally or harvested and stored for later use. The roots are rich in soluble carbohydrates; The upper parts provide additional fiber and protein, making it a balanced feed option when included in animal feed (Edwards et al., 2018).

### 1.1. Botanical Characteristics

Fodder beet belongs to the family Amaranthaceae, the genus Beta, and the species *Beta vulgaris*. It exhibits a biennial growth habit, forming a large storage root in the first year and flowering in the second year under vernalization conditions. Root morphology varies from cylindrical to spherical depending on the cultivar, and root color can be white, yellow, or orange. It has a deep taproot that enhances drought tolerance. The plant produces large green leaves that contribute significantly to total biomass.

### 1.2. Ecological Requirements

Fodder beet thrives in temperate climates, in moderately rainy, well-drained soils. Optimum growth occurs in deep, fertile loamy soils with a pH of 6.5-7.5. The plant is sensitive to waterlogging, but thanks to its deep root system, it is moderately drought tolerant. Forage beet requires temperature requirements of 5–10°C for germination, 15–20°C during the vegetative stage, and 18–22°C for root development.

The most suitable soil type for fodder beet cultivation is light to medium soils; it does not perform well in excessively clayey, sandy, stony, or gravelly soils. The highest yields are achieved in regions with a long growing season (120-150 days). The optimal planting time for fodder beet is April-May in regions where sugar beet is grown and September-November in

temperate regions. The planting rate is calculated as 1 kg per decare when planting with a drill and 2-3 kg per decare when planting by hand. Because fodder beet seeds are very small, the recommended planting depth is 2-3 cm. Fertilization for fodder beet should be applied at the time of planting: 2-3 tons of farm manure, 5-10 kg of phosphorus, and a total of 15-20 kg of nitrogen per decare. Half of this amount should be applied at planting, and the remainder after the first hoeing. Planting fodder beets in the same field for two consecutive years is not recommended (Gülümser, 2024).

The first hoeing and thinning operations are carried out when the plants reach a height of 3-4 cm above the soil surface. Fodder beets should be planted with 40-45 cm spacing between rows and 30-35 cm spacing between rows. Irrigation is essential in regions with insufficient rainfall. Especially in arid regions, the plant should be irrigated 4-5 times throughout the growing season. High yields require adequate soil moisture and nutrient availability. Fodder beet is a nutrient-heavy crop requiring significant inputs of nitrogen, phosphorus, and potassium. Balanced fertilization ensures optimal root development and sugar accumulation

## 1.3. Harvesting and Storage

Fodder beet is usually harvested in late autumn, 150-180 days after planting, when the roots have reached maximum size and sugar content. Root size and weight: Most varieties reach 8-12 kg per root under optimal conditions. Dry matter content: Generally 12-18%. Yellowing of the lower leaves indicates physiological maturity. Harvest should be done before severe frosts, which can damage root tissues and reduce forage quality. Delayed harvesting can increase root size but reduces storage capacity and increases disease risk (Dalley et al., 2016).

## 1.4. Harvesting Methods

Two basic methods are used for harvesting fodder beets.

**a) Mechanical harvesting:** Beet harvesters remove the roots, remove excess soil, and usually trim the leaves from the top. This is suitable for large-scale operations but requires a significant investment.

**b) Manual harvesting:** Common in small-scale or resource-limited systems. Roots are loosened with a fork and lifted by hand, minimizing mechanical damage.

## 1.5. Postharvest Handling

Proper handling is essential to prevent physical damage and microbial contamination. Roots should be cleaned of soil, and damaged or diseased roots should be removed. Excessive washing is not recommended, as residual moisture during storage can cause rot.

## 1.6. Storage Conditions

Due to their high moisture content, fodder beet roots are susceptible to fungal rot and frost damage. Storage conditions for fodder beets require a temperature of 2–5°C and a relative humidity of 90–95%. Adequate airflow is necessary to reduce condensation and maintain constant temperatures. Roots should be stored in compacted or silaged conditions, covered with straw and plastic sheeting to protect against frost and rain.

**Figure 1.1.** Planting of Fodder Beet



**Figure 1.2.** Appearance of Fodder Beet Flowers and Seed Structure

## 1.7. Storage Techniques

a) **Compaction:** The traditional method involves insulating open-air piles with soil or straw. Cost-effective but requires careful monitoring.

b) **Silage Production:** Fodder beets can be ensiled with other feeds (e.g., grass or corn) to improve fermentation and reduce spoilage.

c) **Frost Protection:** Additional insulation or indoor storage is required in cold climates.

### 1.8. Storage Duration and Losses

Under optimal conditions, fodder beets can be stored for 4–6 months with minimal nutrient loss. Inadequate storage can result in:

- Weight loss: Due to respiration and moisture evaporation.
- Sugar degradation: Decreased energy value.
- Microbial spoilage: Especially by Botrytis and Rhizopus species.

Efficient harvesting and storage practices are essential to maintain forage quality and ensure availability during the winter months.

### 1.9. Nutritional Value and Role in Animal Nutrition

Fodder beet roots are characterized by high concentrations of soluble carbohydrates (mostly sucrose), which constitute 50-70% of the dry matter. This provides an excellent and easily fermentable energy source for ruminants.

The composition of fodder beet includes: Dry Matter (DM): 12-18%, Crude Protein (CP): 6-9% of DM, Neutral Detergent Fiber (NDF): 10-15% of DM, Metabolizable Energy (ME): 12-13 MJ/kg DM. The composition of fodder beet (Beta vulgaris var. rapa L.) leaves and petioles includes: Crude Protein: 12-18% of DM, Fiber: Higher than roots, supports rumen health, and Minerals: Rich in calcium, potassium, and magnesium.

### 1.10. Digestibility and Energy Value

Fodder beet roots have high digestibility (up to 90%) due to their low fiber and high sugar content. This promotes rapid ruminal fermentation, which can significantly increase energy intake in dairy and beef cattle. However, rapid fermentation, when not balanced with sufficient fiber, can predispose animals to ruminal acidosis (Dalley et al., 2016; Woods et al., 2021).

### 1.11. Role in Animal Nutrition

Fodder beet improves milk yield and fat content by increasing energy intake during lactation in dairy cattle. Its high energy density contributes to effective weight gain in beef cattle. It is suitable for finishing diets in sheep and goats, but requires careful adaptation to prevent digestive issues. In non-ruminants, its use should be limited due to the high fiber content in the upper parts and the risk of digestive upset. To maximize benefits and minimize risks: Animals should be acclimated for 10-14 days to prevent acidosis. Fodder beet should be mixed with high-fiber feeds (e.g., hay or silage). Phosphorus and trace minerals may also be needed.

**Figure 1.3.** General view of Fodder Beet






**Figure 1.4.** Harvesting of Fodder Beet

## 2. ADVANTAGES AND DISADVANTAGES OF FODDER BEET

The advantages of fodder beet include: High energy density, high palatability, and feeding from grazing or stored tubers. Despite its numerous benefits, fodder beet also presents some limitations that should be considered:

- High risk of ruminal acidosis due to rapid sugar fermentation when not balanced with fiber (Dalley et al., 2016).
- Mineral imbalances: Low phosphorus in roots and excess potassium in leaves can cause hypophosphatemia or grass tetany (Edwards et al., 2018).
- Susceptibility to frost damage, which reduces fodder quality and storability.
- Storage difficulties due to high moisture content and susceptibility to fungal rot
- High initial setup costs, including precision planting, fertilization, and specialized machinery.
- Limited protein content requires supplementation with protein-rich feeds.
- Potential nitrate accumulation under drought stress or excessive nitrogen fertilization.

## 3. CURRENT SITUATİON IN TÜRKİYE AND THE WORLD

Fodder beet remains a niche crop in Türkiye, where fodder production is dominated by alfalfa, sainfoin, vetch, and silage corn. As of 2020, Türkiye's total fodder area reached approximately 2.31 million hectares, representing 6.1% of total agricultural land and 12.3% of cultivated area (Tan and Yolcu, 2021). Despite a significant increase of over 200% in fodder cultivation since the early 2000s thanks to government subsidies, Türkiye still faces a shortage of high-quality forage for livestock (Geren et al., 2002; Koçak, 2023).

Fodder beet is primarily grown in regions with suitable soil and irrigation facilities, such as the Central and Eastern Anatolia regions. Its adoption remains limited for the following reasons:

- Low awareness among farmers about its high energy value and yield potential,
- Higher installation costs compared to traditional forage crops,
- Requirement for specialized machinery,
- Storage difficulties in regions experiencing harsh winters.

However, interest in fodder beet is increasing due to:

- Government incentives supporting alternative forage crops,
- Demand for energy-rich forages in intensive dairy and fattening systems,
- Better drought tolerance compared to corn,
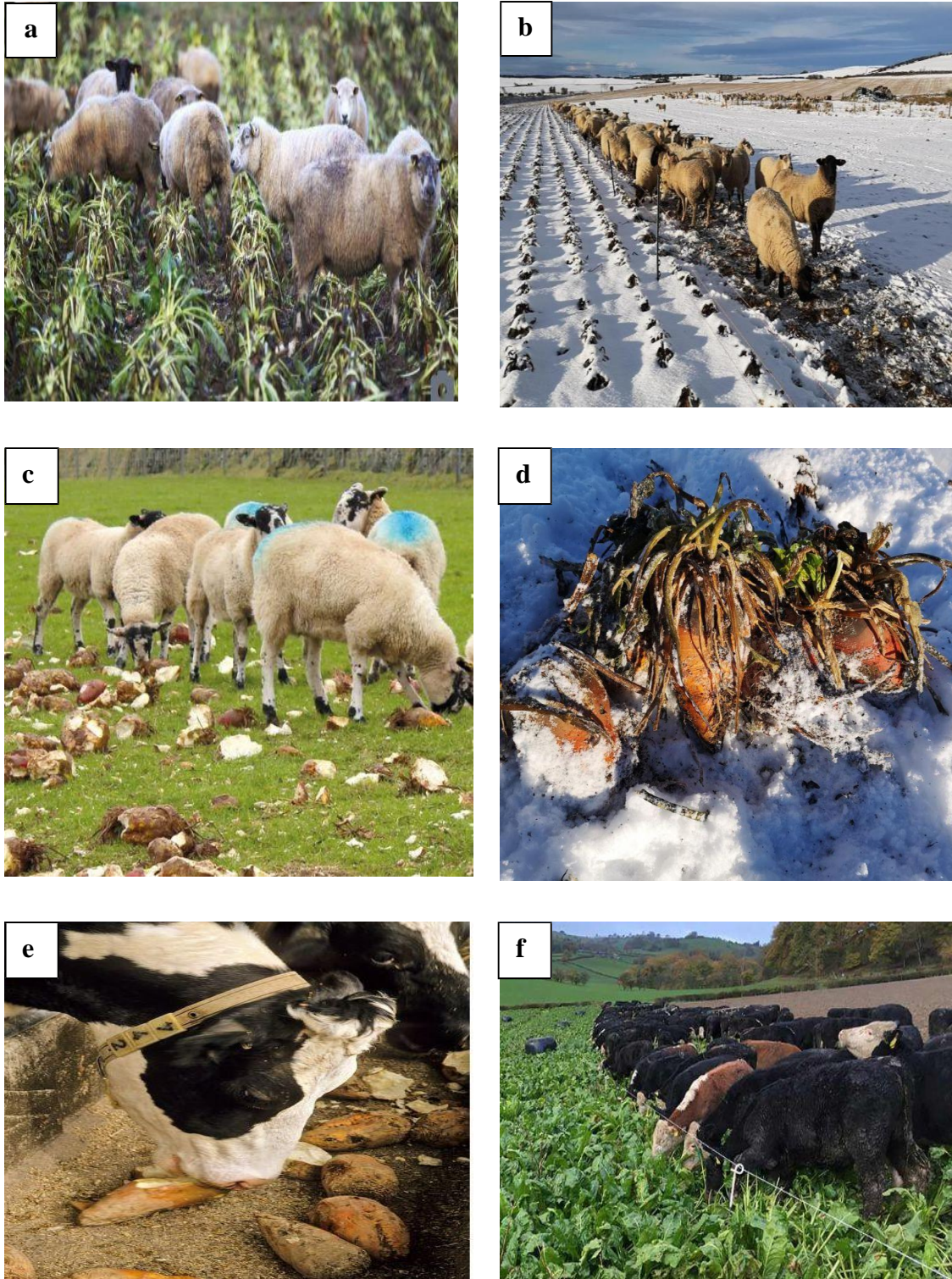- Utilization of fallow lands.

**Figure 3.1.** The importance of Fodder Beet in the nutrition of livestock (Anonymous, 2025-5 a,b,c,d,e,f)

According to TÜİK (Turkish Statistical Institute), fodder beet production has historically been much lower than sugar beet. While sugar beet covers tens of thousands of hectares annually, fodder beet plantings are estimated to be only a few thousand hectares, mostly in

irrigated areas. Integrating fodder beet into crop rotations could significantly help close Türkiye's fodder gap, especially when supported by extension services (Çelik, 2020).

Fodder beet is widely cultivated in Europe (UK, Germany, France, Poland) and New Zealand. It is considered one of the highest-yielding forage crops, producing up to 20-25 tons of dry matter per hectare under optimal conditions. In these regions, fodder beet plays an important role in winter feeding systems for dairy and beef cattle, often replacing or supplementing corn silage. The popularity of fodder beet is driven by its high energy density and palatability, flexibility in feeding systems (grazing or stored roots), and economic benefits in intensive livestock operations.In contrast, adoption in Türkiye and other Mediterranean countries is limited due to agricultural challenges and farmers' lack of familiarity with the crop. However, fodder beet is increasingly recognized as a strategic crop for sustainable livestock production under climate change scenarios requiring drought-resistant, high-yielding forages.

## 4. CONCLUSION AND RECOMMENDATIONS

Fodder beet is a highly promising alternative forage crop for modern livestock systems thanks to its exceptional energy density, high yield potential, and adaptability to diverse agroecological environments. Its ability to provide significant amounts of dry matter and metabolizable energy makes it particularly valuable in intensive dairy and cattle production systems.

However, its successful integration into feeding programs requires careful management to reduce risks such as rumen acidosis, mineral imbalances, and storage losses. Gradual dietary adaptation, appropriate fiber and mineral supplementation, and adherence to best practices during harvesting and storage are essential.

While fodder beet requires fertile soils, adequate irrigation, and meticulous crop management (factors that increase initial production costs), its superior yield and feed quality can offset these costs in high-performance livestock farms. Despite its potential to address feed shortages and increase feed efficiency, fodder beet is underutilized in Türkiye. Broader adoption requires farmer training and extension services, government incentives to reduce establishment costs, and research and development focused on regionally improved varieties, disease resistance, and cost-effective storage solutions.

Globally, fodder beet is a cornerstone of winter feeding systems in countries such as New Zealand and the United Kingdom. With increasing pressure on feed resources and increasing climate variability, its role as a component of sustainable livestock production strategies is expected to expand.

# REFERENCES

Anonymous, (2006). www.biologie.uni-hamburg.de/bonline/schaugaren/varalba/fodder-beet 2006.

Anonymous, (2025):https://www.agricom.co.nz/management-advice/fodder-beet-management/fodder-beet-establishment

Anonymous, -2, ,(2025): https://cs.wikipedia.org/wiki/Soubor:Illustration_Beta_vulgaris_var._rapacea0.jpg

Anonymous-3a,,2025:https://www.myseeds.co/products/red-mammoth-fodder-beet-beta-vulgaris?variant=47656735310017

Anonymous 3b, (2025): https://www.farmlands.co.nz/Winter-Agronomy/fodder-beet/

Anonymous 4a, (2025): https://www.jholdawaycontracting.com/fodder-beet-harvesting.html

Anonymous 4b, (2025): https://www.pflanzen-vielfalt.net/ackerpflanzen-a-z/ruebe-futterruebe/

Anonymous 4c, (2025): https://www.agricom.co.nz/management-advice/fodder-beet-management/fodder-beet-establishment

Anonymous 5a,(2025):https://www.farmersjournal.ie/sheep/news/sheep-farmers-furious-as-prices-1-kg-behind-2022-icsa-743260

Anonymous 5b, (2025): https://www.farmersguide.co.uk/livestock/sheep/fodder-beet-keeps-sheep-on-a-roll/

Anonymous-5c, (2025): https://www.thescottishfarmer.co.uk/features/23351281.new-zealand-stock-45-dry-cows-hectare-fodder-beet

Anonymous, 5d, (2025):https://www.feedipedia.org/node/534

Anonymous, 5ef, (2025): https://www.fwi.co.uk/livestock/beef/a-guide-to-overwintering-beef-cattle-on-fodder-beet

Ayaz, H. (2015). *Determination of Yield, Quality, and Some Agronomic Characteristics of Different Fodder Beet Genotypes under Erzurum Conditions*. Master's Thesis, Institute of Science, Department of Field Crops, Atatürk University, Erzurum..

Çelik, Ş. (2020). Estimation modelling of the amount of fodder beet production in Turkey: Comparative analysis of artificial neural networks and trend analysis methods. *Journal of Multidisciplinary Engineering Science Studies*, 6(7), 134–142.

Dalley, D. E., Edwards, J. P., & Woods, R. R. (2016). Fodder beet feeding systems for dairy cows in New Zealand. Proceedings of the New Zealand Society of Animal Production, 76, 91–96.

Edwards, J. P., Dalley, D. E., & Pinxterhuis, J. B. (2018). A survey of fodder beet use and feeding practices on dairy farms in Canterbury, Otago and Southland. *Proceedings of the New Zealand Society of Animal Production*, 78, 91–98.

FAO (2023). Crop and livestock products: Sugar and fodder beet statistics. Food and Agriculture Organization of the United Nations.

Geren, H., Demiroğlu, G., & Avcıoğlu, R. (2002). Investigations on the yield characteristics of some forage turnip (*Brassica rapa* L.) cultivars. *Journal of Agriculture Faculty of Ege University*, 39(1).

Gülümser, E. (2024). *Alternative Forage Crops Book*. Sugar Beet Chapter, pp. 121–131. Publication No: 5647, ISBN: 978-625-371-824-7. First Edition, October 2024.

Henry, K. (2010). Fodder beet. In J. E. Bradshaw (Ed.), *Root and tuber crops: Handbook of plant breeding* (pp. 221–246). Springer. https://doi.org/10.1007/978-0-387-92765-7_7

Kır, B., Demiroğlu, G., & Soya, H. (2007). An investigation on yield characteristics of some forage turnip (*Brassica rapa* L.) cultivars. *Journal of Agriculture Faculty of Ege University*, 44(1), 87-97.

Koçak, A. (2023). *An overview of fodder resources and animal production in Tu*rkey. Options Méditerranéennes: Série A, 102, 15–22.

Tan, M., & Yolcu, H. (2021). Forage crop production and utilization in Turkey. *Turkish Journal of Agriculture and Forestry*, 45(2), 123–135.

Yıldırımlı, Ş. (2003). The chorology of the Turkish species of Chenopodiaceae, Cistaceae, Convolvulaceae, Cornaceae and Corylaceae families. *The Herb Journal Systematic Botanic*, 10, 203-15.

Woods, R. R., Dalley, D. E., & Judson, H. G. (2021). Fodder beet: Nutritional characteristics and feeding strategies for dairy cattle. *Journal of New Zealand Grassland*, 83, 45–52.

# CHAPTER 9

# THE EFFECT OF FERTILIZER RATES ON THE PRODUCTIVITY OF INTERCROPPING AND SOIL FERTILITY

Prof.Dr. Elkhan Rajaf oglu Allahverdiyev[1], Aghayeva Malahat Ali[2],
Bayramov Bahruz Surkhay oglu[3]

[1]Azerbaijan State Agrarian University, Doctor of Agricultural Sciences, Azerbaijan
ORCID: 0009-0000-6666- 8255, e-mail: elxan_recebli@mail.ru

[2]Lankaran State University, Doctor of Philosophy in Biological Sciences, Azerbaijan
ORCID: 0000-0001-7968- 0472, e-mail: zooloq.60@mail.ru

[3]Nakhchivan State University, PhD in Agrarian Sciences, Azerbaijan
ORCID:  0009-0007-7495-1756, e-mail: behruzbayramov67@gmail.com

## 1. INTRODUCTION

The arable land resources of our republic are very limited. According to statistical data, there is 0.18 hectares of arable land per capita in our republic, which is much less than the world average. Providing the country's population with food, livestock with feed, and industry with raw materials with the products obtained from such areas is considered one of the urgent issues of the day. This requires the intensification of agriculture, increasing the productivity of arable land, its quality, and at the same time increasing soil fertility.

The importance of using intercropping and applying the correct fertilizer norms in increasing soil fertility, improving its physical and chemical properties, and increasing the productivity and quality of plants is very great (Allahverdiyev et al., 2014; Rawnsley et al., 2019).

Intercropping has many advantages, including increasing the efficiency of using natural resources such as nutrients, radiation, climatic conditions, and water, reducing the use of fertilizers, preventing soil erosion, and increasing the durability and quality of the product. At the same time, intercropping significantly increases the organic matter content of the soil (Christie et al, 2020; Ibrahim et al, 2019).

 In this regard, the Head of State has decided to increase the amount of the discount for fuel and motor oils used in the production of agricultural products in the country and to stimulate the implementation of repeated (intermediate) sowing in the country, and in accordance with the order issued by the Cabinet of Ministers, in accordance with subparagraph 1.10.1.3 of the Decree of the President of the Republic of Azerbaijan No. 413 dated December 22, 2014 "On the implementation of the Law of the Republic of Azerbaijan "On the State Budget of the Republic of Azerbaijan for 2015", to ensure a 25 percent increase in the amount of assistance provided to agricultural producers from the state budget for fuel and motor oils used in the cultivation of each hectare of arable land and in the implementation of perennial crops (FAO).

Currently, one of the most important complex measures envisaged in the field of agricultural development in our republic is the expansion of the area of intermediate sowing and its productivity increase. The effective application of intercropping ensures that a single plot of land can be harvested two or three times a year. As a result, grain production, especially fodder, increases, and land and other means of production are used more intensively and efficiently.

The results of science and advanced practice show that in order to obtain high and quality products from agricultural crops, it is necessary to use progressive and efficient technology in

the cultivation of these plants. Taking this into account, more efficient technological methods have been developed based on the experience of domestic and foreign researchers. Among them, the development of technologies and devices for direct (no-till) sowing and application of organic fertilizers to the soil is of great practical importance (Rezaei-Chiyaneh et al, 2021).

The total active temperature in the plain and foothill regions of Azerbaijan exceeds 4000-45000C. In the eastern part of the Araz-bayu plain in the Nakhchivan Autonomous Republic, this indicator reaches 50000C. Therefore, it should be noted that, due to its soil and climatic conditions, our republic is considered a very favorable country for the cultivation of field fodder crops, especially legumes and grain fodder crops, and for obtaining high yields from them.

In order to obtain high and quality products in different regions of our republic, the components, proportions, sowing methods, and plant density of plants to be cultivated in mixtures have been studied through experiments. As a result of the experiments, it was determined that it is more expedient to cultivate corn or sorghum in mixtures with legumes rather than pure crops (Phelan et.al 2015).

P.B. Zamanov et al. conducted studies, it was determined that agricultural plants, on average, annually remove 500 kg of humus, 75-80 kg of nitrogen, 25-30 kg of phosphorus, and 60-70 kg of potassium from one hectare. In order to restore and restore nutrients and humus taken from the soil by plants, it is important to apply the necessary amount of organic and mineral fertilizers to the soil (Zamanov, 2011). The use of organic fertilizers alone or in combination with chemical fertilizers helps to improve the physical and chemical properties of the soil and improves the efficient use of applied fertilizers, as a result of which plant productivity and quality increase.

## 2. MATERIAL AND METHODOLOGY

Taking these into account, in order to create conditions for using atmospheric nitrogen in the biological cycle in the lower part of the Karabakh region, where the effective and potential fertility of the soil is very low, to increase the productivity of intercropping and to study ways to protect soil fertility in order to provide livestock with green fodder, we conducted an experiment at the Elvin farm in the Hindarkh settlement of the Agjabedi region. One of the most important requirements for protecting and increasing soil fertility is the application of cultivation methods that do not destroy the structure of the soil.

The experimental work used the Zagatala-514 variety of corn (*Zea mays* L) and the Imeritin variety of soybean (*Glycine max* L). During sowing, 30 kg of corn and 30 kg of soybean seeds were sown per hectare.

Soil samples were collected from five locations within the experimental area in a cross-sectional manner and were analyzed for their agrochemical properties. The following parameters were analyzed in the soil samples: total humus content using the I.V. Tyurin method, total nitrogen using the Kjeldahl method, total phosphorus using the Lorenz method, total potassium using the Smith method, nitrate nitrogen using the Grandval-Lajoux method, easily hydrolyzable nitrogen using the Tyurin and Kononov method, mobile phosphorus using the Machigin method, exchangeable potassium using the P.V. Protasov method, adsorbed ammonium nitrogen using the Konev method with Nessler's reagent via colorimetric analysis, soil pH in an aqueous solution measured potentiometrically (Jafarov et al., 2014; Huseynov et al., 2018).

The results of field experiments were calculated using the mathematical calculation method of B.A. Dospekhov. Correlations between many indicators were implemented in the Excel program.

## 3. DISCUSSIONS

During the experiment, we determined that after the harvest of cereal crops, those areas remain empty until new cereal crops are sown, and favorable solar energy, active temperature, irrigation water, and fertile soils allow for the planting and cultivation of fodder plants with a short vegetation period in those areas. The conducted studies prove that soils where leguminous plants are not cultivated dry out excessively due to the heat of the sun, and become cracked. becomes, its structure is destroyed. In addition, in rainy years, weeds germinate and develop in such areas, and the fields are littered with weeds. Even some weeds spread their ripe seeds around since the vegetation period is short. This worsens the environment for the plants planted later, causing weeds to spread more in the area. One of the main importance of intercropping is the weed control measure. This has been reflected in studies conducted in various countries.

The effect of fertilizer norms and irrigation quantities on the yield of green mass of mixed crops of corn and soybean was studied. The conducted studies prove that the right choice of crops in mixed crops, the implementation of complex agrotechnical measures in the right order and the use of mineral and organic fertilizers greatly increase the quantity and quality of the total crop (Liu et al 2020).

The use of organic fertilizers against the background of various amounts of irrigation during the study had a positive effect on the yield of mixed crops of corn and soy.

As a result of the studies, it was determined that against the background of 4 vegetation irrigation (4200 m$^3$), if the yield of mixed crops in the control variant without fertilizers was

357 cen/hec, the yield increased under the influence of mineral and organic fertilizers, varied between 455 cen/hec and 616 kg/hec. Thus, as a result of the study, it becomes clear that in the economy during the shortage of water against the background of 4-fold vegetation irrigation (4200 m$^3$), the use of organic and mineral fertilizers significantly increases the yield of mixed crops of corn and soy. So, if the yield of mixed crops of the control variant without fertilizers was 357 kg/hec, then with the application of fertilizer standards $N_{120}P_{150}K_{150}$ the yield of 616 kg/hec was achieved, which indicates an increase of 259 kg/hec or 73.2% compared with the control variant.

When using mineral and organomineral fertilizers, a sharp increase in productivity was noticed. So, in the application of 10 t/hec of manure + $N_{70}P_{125}K_{90}$, a yield of 585 kg/hec was obtained. And this means a yield increase of 228 kg/hec or 63,8% compared with the control without fertilizers.

If the yield amounted to 378 kg/hec in the control variant without fertilizers against the background of 6-fold vegetation irrigation, while using mineral and organic-mineral fertilizers, the green mass, increasing, varied between 488 and 655 kg/hec.

**Table 1.** Influence of irrigation and fertilizer norms on the yield of green mass of plants of mixed crops (corn and soy) stubble (2023-2024)

| Options | 4 times watering (4200 m$^3$) | | | 6 times watering (6300 m$^3$) | | |
|---|---|---|---|---|---|---|
| | Average producti-vity, cent/hec | increase | | Average producti-vity, cent/hec | increase | |
| | | cent/hec | % | | cent/hec | % |
| Control option | 357 | - | - | 378 | - | - |
| $N_{40}P_{60}K_{60}$ | 455 | 98 | 27,4 | 488 | 110 | 29,1 |
| $N_{60}P_{90}K_{90}$ | 522 | 165 | 46,7 | 537 | 159 | 42,0 |
| $N_{90}P_{120}K_{120}$ | 608 | 251 | 70,3 | 637 | 259 | 68,5 |
| $N_{120}P_{150}K_{150}$ | 616 | 259 | 73,2 | 655 | 277 | 73,2 |
| manure 10 t/hec +$P_{35}$ | 425 | 68 | 19,3 | 457 | 79 | 20,9 |
| manure 10 t/hec +$N_{10}P_{65}K_{30}$ | 506 | 149 | 41,73 | 525 | 147 | 38,9 |
| manure 10 t/hec +$N_{40}P_{95}K_{60}$ | 578 | 221 | 61,9 | 619 | 241 | 63,7 |
| manure 10 t/hec +$N_{70}P_{125}K_{90}$ | 585 | 228 | 63,8 | 628 | 250 | 66,1 |

P=2,2                    P=0,65

Against the background of 6-fold vegetation irrigation (6300 m3 / ha), a manifestation of a similar effect is visible. So, when applying the $N_{120}P_{150}K_{150}$ fertilizer norms, a yield of 655 kg/hec was achieved, which, compared to the control version without fertilizers, indicates a yield increase of 277 kg/hec and 73.2%.

Against the background of 6-fold vegetation irrigation (6300 $m^3$ / ha) with the use of mineral and organomineral fertilizers, a multiple increase in yield also became clear. So, in the application of 10 t/hec of manure + $N_{70}P_{125}K_{90}$, a yield of 628 kg/hec was achieved. And this amounts to an increase of 250 kg/hec or 66.1% compared with the control variant without fertilizers.

But it should be noted that irrigation water in our country is lacking mainly in the Aran zone. Therefore, with a 6-fold watering, the resulting crop is not very economically sound.

The mathematical calculations carried out at the end of the experiment prove the accuracy of the experiment. The indicator E (kg/hec) obtained from fertilizer is many times high.

Based on the results of the study, we can say that during the simultaneous sowing of corn and soybeans to obtain a high yield of green mass, the optimal irrigation and fertilizer rates were determined.

Cumshdov et al., (2005) note that soil fertility is related to the amount of organic residues in it. Thus, the root and rotting residues of plants, under favorable conditions, decompose under the influence of microorganisms and turn into organic matter. As a result, the soil is enriched with organic matter

A simple and inexpensive way to restore soil fertility is to use legumes. According to literature data, each hectare of legume crops collects about 100-150 kg of nitrogen from the air, which in turn is equivalent to 15-20 tons of high-quality manure. Legumes enrich the soil with biological nitrogen and root mass, which indicates that the soil is of great importance in terms of ecological and economic efficiency.

As a result of our research in recent years, it has been found that during the joint planting of corn and soybean, sorghum and peas in intercropping, a significant amount of root and root residues accumulate, which, when decomposed and mixed with the soil, play a major role in increasing nutrients and preserving soil fertility. This also shows that intercropping is a good predecessor for the plants to be planted after it.

In the low-lying region of the Karabakh zone on gray-meadow soils, stubble residues were taken from the mixed crops of corn and soy according to the monolithic method and, drying, weighed in the open air. The stubble residues in the control variant without fertilizers, if they amounted to 5 kg/hec, as a result of the introduction of organic and mineral fertilizers

amounted to a significant increase. So, in the variant of fertilizer application in the norm $N_{90}P_{120}K_{120}$, stubble residues in the amount of 8 kg/hec were accumulated, when applying $N_{120}P_{150}K_{150}$ 9 kg/hec, and with the combined use of organic and mineral fertilizers in the norm of 10 t/hec of manure + $N_{70}P_{125}K_{90}$ - 8.7 kg/hec. Thus, it was found that with the introduction of organic and mineral fertilizers against the background of 4 irrigation during the growing season on mixed crops of corn and soybean, the mass of stubble residues increased significantly.

As a result of the analyzes, it was determined that the amount of nitrogen, phosphorus and potassium in the composition of the stubble residues thoroughly varies depending on the norms of fertilizers. If in the control variant the amount of total nitrogen, total phosphorus and total potassium in the norm of $N_{120}P_{150}K_{150}$ was 0.95%, 0.35%, and 0.96%, respectively, with the combined use of organic and mineral fertilizers in the norm of 10 t/hec of manure + $P_{35}$ amounted to 0.96%; 0.36% and 0.99%, in the case of organic fertilizers, the norm of 10 t/hec of manure + $N_{10}P_{65}K_{30}$ was 1.07%; 0.41% and 1.22%. And this, in turn, fundamentally affects not only the amount of accumulated nutrients in the stubble, but also the improvement of the water-physical properties of the soil and its structure.

In the variants, when applying 6 waterings during the growing season, a similar situation was also created. If the stubble residues in the control version without fertilizers were 5.6 cen/hec, then when using mineral fertilizers in the norm $N_{120}P_{150}K_{150}$ they were 9.4 cen/hec, and when combined with organic and mineral fertilizers in the 10 t / ha version of manure + $N_{70}P_{125}K_{90}$ the stubble residue was accumulated in the amount of 9.3 cen/hec.

As a result of the analyzes, it was determined that in the composition of the stubble residues, the amount of total nitrogen, total phosphorus and total potassium substantially changes depending on the norms of fertilizers. In the control variant without fertilizers, if the amounts of total nitrogen, total phosphorus and total potassium were 0.96%, 0,97% and 0.36%, respectively, when applying fertilizers in the norm $N_{120}P_{150}K_{150}$ 1.07%, 0.46% and 1,21%, with the combined use of organic and mineral fertilizers in the norm of 10 t/hec of manure + $N_{70}P_{125}K_{90}$, these indicators amounted to 1.08%, respectively; 0.42% and 1.22%. And this, in turn, fundamentally affects not only the amount of accumulated nutrients in the stubble, but also the water-physical properties of the soil and the improvement of its structure.

Studies have shown that the use of organic and mineral fertilizers in mixed crops significantly affects not only the stubble mass, but also the root mass so that it plays a large role in increasing soil fertility.

If the root mass in the control version at 4 waterings accumulates in an amount of 23 kg/ha, using organic and mineral fertilizers is a significant increase. So, when using mineral

fertilizers in the norm of $N_{120}P_{150}K_{150}$, the root mass if it was 30 kg/hec, then when combined with organic and mineral fertilizers in the norm of 10 t/hec of manure + $N_{70}P_{125}K_{90}$, the root mass was accumulated in the amount of 29 kg/hec.

The amount of total nitrogen, total phosphorus and total potassium in the composition of the root mass varies significantly depending on the norms of fertilizers. So, in the control version without fertilizers, if the content of total nitrogen, total phosphorus and total potassium was 0.84%, 0.19% and 0.72%, when applying fertilizers in the norm $N_{120}P_{150}K_{150}$ amounted to 1.00%, 0.24% and 0.96%, and when using 10 t/hec of manure + $N_{70}P_{125}K_{90}$ was 0.91%, 0.23% and 0.98%, respectively.

During the growing season, 6 irrigations were applied. If in the control version without fertilizers the root mass is accumulated in an amount of 23.5 cen/hec, then with the use of organic and mineral fertilizers this amounted to a significant increase. In particular, when applying the norms of fertilizers, the $N_{120}P_{150}K_{150}$ was 30.5 cen/hec, while the combined use of organic and mineral fertilizers in the norm of 10 t/hec of manure + $N_{70}P_{125}K_{90}$, the root mass was accumulated in the amount of 29.7 cen/hec. And this, in turn, as a result of microbiological processes, decomposing, will be of great importance in the accumulation of biological nitrogen, in maintaining soil fertility. So in the control version without fertilizers, if the amount of total nitrogen, total phosphorus and total potassium was 0.84%, 0.18% and 0.73%, with a fertilizer rate of $N_{120}P_{150}K_{150}$ these indicators were 1.01%; 0.24%; 0.97%, and with the combined use of organic and mineral fertilizers in the amount of 10 t/hec of manure + $N_{70}P_{125}K_{90}$ amounted to 0.93%, 0.24% and 0.99%.

The use of organic and mineral fertilizers at the optimum rate, along with a positive effect on the root mass and stubble residues of mixed crops significantly increases the soil fertility in quantitative and qualitative terms. And this proves that corn and soy are good precursors for subsequent sowing crops.

Intercropping also has a positive effect on improving the water-physical properties of the soil by increasing the amount of organic matter in the soil. The great importance of intercropping in improving the water-physical properties of the soil is evident in many studies. According to literature, intercropping significantly increases the amount of water-resistant aggregates in the soil and improves its structural condition. Studies have shown that in areas where leguminous crops are cultivated, the amount of water-resistant aggregates in the 0-10 cm layer of soil increases by 12-17%, which leads to an increase in biological activity (Allahverdiyev, 2019).

Here, in order to improve the soil structure, organic fertilizer is applied to the subsoil and the cultivated plants are used as phytomeliorants. With this method, the potential and effective fertility of the soil is restored by biological methods. The water-holding capacity of the soil is improved, and conditions are created for plant residues to rot and mix with the soil. On the other hand, this is more important in arid regions. Since plants shade the soil surface, evaporation from the field is reduced.

## 4. CONCLUSION

Thus, the application of organic fertilizers and the cultivation of green manure (siderate) crops on degraded soils accelerates biological processes in the soil, increases the amount of organic matter, and improves soil structure. Based on this, we recommend that farming enterprises cultivate cover crops after harvesting grain crops in order to make efficient use of soil and other natural resources. This not only helps meet the feed demand of livestock farming but also preserves soil fertility.

**REFERENCES**

Abdul Hassan, SN. (2018). Effect of zeolite mineral and organic fertilizer in some physical and chemical in different Soils Texture and growth of wheat plant (*Triticm aestivum* .L). MSc. Thesis.

Allahverdiyev, E.R. (2019).The Role of Post-Cereal Residues in Raising Soil Fertility / Bulletin of Science and Practice. Vol. 5. No. 12. pp. 191-196.

Allahverdiyev, E.R., S.F. Aliyeva, M.A. Behbudova. (2014). The Impact of Fertilizer Norms and Irrigation on Soil Fertility and the Green Biomass Yield of Sorghum and Pea Intercropping. Dedicated to the 91st Anniversary of National Leader Heydar Aliyev's Birth and the 85th Anniversary of ADAU. Scientific Works of ADAU. Ganja, , pp. 43-45.

Christie, K.M.; Smith, A.P.; Rawnsley, R.P.; Harrison, M.T.; Eckard, R.J. (2020). Simulated seasonal responses of grazed dairy pastures to nitrogen fertilizer in SE Australia: N loss and recovery. *Agric. Syst. 182*, 102847.

Cumshdov I.M., Rzayev M.Y., Abdullayeva Z.M. (2005). The effect of short-rotation alternating and continuous crops on some soil fertility indicators and plant productivity. Azerbaijan Agrarian Scientific Journal, , No. 1-2, pp. 60-62 http://axar.az/news/49432

Huseynov A.M., Huseynov N.V., Mammadova K.Y. (2018). Agrochemistry Baku. 440s

Ibrahim, A.; Harrison, M.T.; Meinke, H.; Zhou, M. (2019). Examining the yield potential of barley near-isogenic lines using a genotype by environment by management analysis. *Eur. J. Agron.* , *105*, 41–51.

Jafarov Y.A., Mehdiyeva E.Kh., (2014). Methods of agrochemical analysis, Baku, 264 p.

Liu, K.; Harrison, M.T., Hunt, J., Angessa, T.T., Meinke, H., Li, C., Tian, X,, Zhou, M. (2020). Identifying optimal sowing and flowering periods for barley in Australia: A modelling approach. *Agric. For. Meteorol. 282–283*, 107871.

Phelan, D.C.; Harrison, M.T.; Kemmerer, E.P.; Parsons, D. (2015). Management opportunities for boosting productivity of cool-temperate grazed dairy farms under climate change. *Agric. Syst. 138*, 46–54.

Rawnsley, R.P.; Smith, A.P.; Christie, K.M.; Harrison, M.T.; Eckard, R.J. (2019). Current and future direction of nitrogen fertiliser use in Australian grazing systems. *Crop Pasture Sci.*, *70*, 1034–1043.

Rezaei-Chiyaneh, E.; Amirnia, R.; Fotohi Chiyaneh, S.; Maggi, F.; Barin, M.; Razavi, B.S. (2021). Improvement of dragonhead (*Dracocephalum moldavica* L.) yield quality through a coupled intercropping system and vermicompost application along with maintenance of soil microbial activity. *Land Degrad. Dev. 32*, 2833–2848.

Zamanov P.B. (2011). The need for soil and plants for basic nutrients. Collection of works on soil science and agrochemistry. Volume XIX. Baku - Science-.p367-371.

**CHAPTER 10**

**STRENGTHENING SMALL RUMINANT HEALTH: CURRENT VACCINATION PRACTICES AND FUTURE PROSPECTS IN TURKEY**

Dr. Fatma ATLI[1]

[1] Ege University Faculty of Agriculture, Department of Animal Science, Bornova-İzmir
ORCID: 0000-0001- 6536-5594 e-mail: atli.fatma@ege.edu.tr

## 1. INTRODUCTION

Sheep and goat farming constitutes a cornerstone of Turkey's livestock industry, contributing significantly to rural livelihoods, food security, and the national economy. According to FAO and Turkish Statistical Institute (TÜİK) data, Turkey hosts one of the largest small ruminant populations worldwide, with more than 43 million sheep and 10,5 million goats as of 2024 (TUIK, 2024). These animals provide essential products including meat, milk, cheese, and fiber, while also supporting cultural traditions and sustainable use of marginal lands (Sevik, 2023).

Despite their economic and social importance, small ruminant production faces major constraints from infectious diseases that reduce fertility, milk yield, and survival rates. Diseases such as peste des petits ruminants (PPR), brucellosis, enterotoxemia, and bluetongue have historically caused significant economic and animal welfare losses (OIE, 2021; Bayir and Gürcan, 2023). Vaccination programs have emerged as the most effective strategy to control these diseases, especially in resource-limited rural settings where treatment and biosecurity measures are less feasible.

Turkey has implemented several national vaccination campaigns, including widespread use of Brucella melitensis Rev-1 vaccine in sheep and goats since 2009, and the launch of PPR eradication programs in 2013 under FAO and OIE guidelines (FAO, 2022). These programs have markedly reduced disease incidence and improved productivity, as illustrated by the parallel rise in small ruminant populations (see Figure). However, challenges such as cold-chain maintenance, uneven regional coverage, farmer awareness, and logistical constraints continue to limit vaccine effectiveness (Akkaya et al., 2021; FAO 2022).

This review provides an overview of current vaccination practices in sheep and goat farming in Turkey, covering bacterial, viral, and parasitic diseases. Seasonal and age-specific schedules are discussed, alongside challenges in implementation and opportunities for improvement.

The paper emphasizes the need for thermostable and multivalent vaccines, enhanced farmer education, and integration of serological surveillance into herd health programs to ensure sustainable small ruminant production and align with global eradication initiatives.

# 2. MAJOR INFECTIOUS DISEASES OF CONCERN AND VACCINES USED IN TURKEY

## 2.1 Viral diseases

Peste des petits ruminants (PPR) — PPR is a high-priority transboundary viral disease of sheep and goats with high morbidity and variable mortality; live attenuated homologous vaccines provide long-lasting immunity (commonly ≥3 years under field conditions) and are the backbone of control/eradication strategies promoted by FAO/OIE. National vaccination campaigns across endemic regions are central to eradication goals (global PPR eradication by 2030). Field performance depends on correct dose, storage and coverag. (Imanbayeva et al., 2025)

Sheep/goat pox and capripoxviruses — Live attenuated capripox vaccines (sheep pox/goat pox strains) are used regionally when outbreaks or risk warrants; capripox vaccine platforms are also being investigated as vectors for multivalent vaccines (Boshra et al., 2024).

Bluetongue virus (BTV) — BTV seroprevalence studies in Turkey show circulation of BTV in many regions, and BTV control is complicated by multiple serotypes and vector (Culicoides) ecology; vaccination with serotype-specific inactivated vaccines is the common approach where available and indicated by surveillance. Recent seroprevalence work in Antalya and other provinces confirms ongoing exposure of small ruminants (Sevik, 2023)

## 2.2 Bacterial diseases

Brucellosis (*Brucella melitensis*) — Brucellosis remains a significant zoonosis and animal health problem in parts of Turkey. The live attenuated Rev-1 vaccine is the most widely used and effective vaccine for sheep and goats; in Turkey, Rev-1 has been applied in mass campaigns and in some studies evaluated via conjunctival administration (to reduce interference with serological diagnostics and reduce abortion risk). Control programs combine vaccination with test-and-slaughter, movement controls and surveillance. Evidence points to persistent hotspots and the need for improved, targeted strategies (Fernandez-Georges et al., 2025)

Clostridial (enterotoxemia, tetanus, malignant oedema, etc.) — Multicomponent toxoid vaccines (C, D, C+D, and broader clostridial polyvalent vaccines) are standard for routine flock health to prevent sudden death syndromes; recent research continues on recombinant and improved antigens. These vaccines are widely used in Turkish flocks as part of routine prophylaxis (Akkaya et al., 2021).

Pasteurellosis/Mannheimiosis — Bacterins and toxoid bacterin combinations targeting Pasteurella/Mannheimia species are commonly used to reduce respiratory disease and peracute deaths — especially during stress periods (weaning, transport) (Abdolmohammadi Khiav and Zahmatkesh, 2021).

### 2.3 Parasitic vaccines (research stage / limited use)

Commercial vaccines for some parasitic diseases (e.g., certain multivalent experimental vaccines for Fasciola hepatica) have shown promise in trials, but routine parasitic vaccination remains limited; integrated parasite control usually combines strategic anthelmintic use, pasture management and selective breeding. Research on multivalent and subunit vaccines continues (Zafra et al., 2021).

## 3. NATIONAL AND REGIONAL VACCINATION PROGRAMS IN TURKEY — CURRENT STATUS AND İMPACT

Turkey has implemented national vaccination campaigns for priority diseases (notably PPR and brucellosis) and routine vaccination for clostridial and other endemic conditions. Reports and peer-reviewed studies indicate that these campaigns have led to measurable improvements in disease control where coverage is adequate, but uneven regional uptake and persistent hotspots remain. For brucellosis, national control efforts using Rev-1 and other control measures have reduced incidence in many areas, but human brucellosis and animal reservoirs persist in some regions, requiring sustained action. Similarly, PPR vaccination is central to national control plans aligned with the FAO/OIE eradication strategy; vaccine availability and campaign implementation have been effective where logistics and coverage targets were met (Akkaya et al., 2021; Bayır and Gürcan, 2023).

## 4. IMPLEMENTATOON DETAILS: SCHEDULES, SEASONAL TIMING AND PRACTICAL RECOMMENDATIONS

### 4.1 Typical vaccine schedule considerations (generalized)

• PPR: Single dose of live attenuated vaccine (minimum protective dose per OIE recommendations) for lambs/kids at an age determined by maternal antibody waning (commonly at 3 months) and for adults in mass campaigns; booster strategies depend on campaign design and epidemiological situation (Kumar et al., 2017).

• Brucellosis (Rev-1): Standard protocol is vaccination of young replacement animals (e.g., 3–6 months), with caveats for pregnant animals; conjunctival vaccination has been used

to reduce some adverse events and interference with milk/serology. Rev-1 in adults is typically under organized control programs (Saboor et al., 2024; Fernandez-Georges et al., 2025).

- Clostridial polyvalent toxoids: Primary series for young animals, then annual boosters prior to risk periods (e.g., before lambing, turnout to pasture) (Fanelli et al., 2022).

- Mannheimia/Pasteurella bacterins: Given pre-stress periods (weaning, transport, acaricide dips) and as part of herd health plans (Goncagül et al., 2021).

*Note:* Exact timing should be adapted to local epidemiology, maternal antibody interference and manufacturer instructions (dose, route). OIE/FAO manuals and vaccine producers provide detailed protocols and quality control requirements (OIE, 2021).

## 5. OPERATIONAL CHALLENGES IN TURKEY (EVIDENCE AND PRACTICAL IMPLICATIONS)

### 5.1 Farmer awareness and compliance

Multiple studies in low- and middle-income settings show that farmer knowledge, attitudes and practices strongly influence vaccine uptake; Turkey shares similar challenges in rural and remote districts where veterinary access, literacy and perceived vaccine benefit vary. Community engagement and targeted education increase participation in campaigns (Yilmaz and Wilson, 2012; Akkaya et al., 2021).

### 5.2 Cold-chain and logistics

Preserving vaccine potency requires an unbroken cold chain from manufacturer to field; studies and program reviews globally emphasize cold-chain failures as a major cause of reduced vaccine effectiveness. Rural delivery in Turkey faces logistical hurdles (distance, transport, electricity reliability), calling for investment in cold-chain infrastructure, temperature monitoring and contingency measures (solar refrigerators, cold boxes) in remote districts. Thermostable vaccine formulations would ease these constraints (see next section) (Sharma and Agrawal, 2024).

### 5.3 Regional disparities in coverage and surveillance gaps

Surveillance data and seroprevalence studies reveal geographic heterogeneity for BTV, brucellosis and other infections; passive surveillance underestimates true incidence and can mask pockets of infection that sustain transmission. Integration of active serological surveillance into routine programs is needed for data-driven targeting (Fernandez-Georges et al., 2025).

### 5.4 Diagnostic interference and vaccine choices (example: Rev-1)

Live vaccines such as Rev-1 can complicate serological surveillance because vaccine-induced antibodies may be indistinguishable from field infection in some tests. Alternative strategies are used to reduce this problem. Studies from Turkey have evaluated conjunctival Rev-1 administration as a field-practical approach (Akkaya et al., 2021).

### 6. OPPORTUNITIES: TECHNOLOGY, PROGRAM DESIGN AND SURVEILLANCE

#### 6.1 Thermostable vaccines

Thermostable formulations (or technologies that maintain potency outside strict cold chains) are a major innovation for veterinary vaccination campaigns in areas with weak cold-chain infrastructure. Reviews and experimental data indicate that thermostable PPR formulations and other heat-stable approaches can simplify logistics, reduce wastage and increase effective coverage. Turkey could benefit from piloting thermostable formulations in remote provinces (Fanelli et al., 2022).

#### 6.2 Multivalent and vectored vaccines

Developments in multivalent vaccine platforms — including capripoxvirus-vectored constructs and other recombinant vectors — aim to protect against multiple pathogens with a single inoculation, reducing handling and improving compliance. Early trials provide proof-of-concept; regulatory approval and field effectiveness remain to be validated in different epidemiological contexts. Such platforms could be strategically important in Turkey to reduce the number of separate vaccinations needed per production cycle (Akkaya et al., 2021; Goncagül et al., 2021).

#### 6.3 Integration of serological surveillance (targeted, routine)

Routine incorporation of serological monitoring (targeted sampling, sentinel herds, pre- and post-campaign serosurveys) allows assessment of vaccine coverage and efficacy, identification of immunity gaps and early detection of outbreaks. Recent regional seroprevalence studies for BTV and brucellosis illustrate the value of active surveillance in Turkey. Building laboratory capacity and streamlining data flows between field services and central authorities will improve program targeting (Boshra et al., 2024).

#### 6.4 Farmer training and participatory approaches

Community platforms, farmer organizations, and local extension networks improve vaccine acceptance and compliance. Evidence from other countries demonstrates that farmer

engagement increases uptake and correct use of vaccines — a transferable strategy for Turkish rural contexts (Goncagül et al., 2021).

## 7. RECOMMENDED PRIORITIES FOR TURKEY (PRACTICAL, EVIDENCE-BASED)

1. Strengthen cold-chain and delivery systems — invest in temperature monitoring, solar-powered refrigeration in remote clinics, and training for vaccine handlers. Thermostable products should be preferentially piloted where supply chain challenges are greatest (Sevik, 2023).

2. Expand and integrate active serological surveillance — sentinel herds, pre-/post-vaccination serosurveys and routine lab reporting to detect coverage gaps and early outbreaks (Yilmaz and Wilson, 2012).

3. Optimize brucellosis control strategy — continue targeted use of Rev-1 for young stock, evaluate conjunctival vs. subcutaneous administration where appropriate, use DIVA-capable diagnostics and couple vaccination with movement controls and human health surveillance (Saboor et al., 2024).

4. Adopt mixed delivery models — mass campaigns for eradication-oriented diseases (PPR) combined with routine flock-level vaccination for clostridial and respiratory pathogens; use mobile vaccination teams and community animal health workers to increase reach (Sharma and Agrawal, 2024).

5. Promote research & regulatory pathways for multivalent and thermostable vaccines — support field trials and fast-track regulatory evaluation of promising platforms that reduce dosing events and cold-chain dependence (Abdolmohammadi Khiav and Zahmatkesh, 2021).

## 8. LIMITATIONS AND RESEARCH GAPS

• Country-specific operational data: While many programmatic recommendations are supported by global evidence, more Turkey-specific operational studies (on cold-chain failures, vaccine wastage rates, farmer KAP specifically in Turkish provinces) would allow finer targeting (Sevik, 2023).

• Field effectiveness data for new platforms: Multivalent and thermostable vaccine candidates require Turkey-based field trials to validate performance under local climatic and management conditions.

- DIVA tools and molecular surveillance: Increased investment in DIVA-compatible diagnostics and genomic surveillance would enhance ability to differentiate vaccine strains from wild-type infections and to track viral evolution (Imanbayeva et al., 2025).

## 9. CONCLUSION

Vaccination remains central to control of major small ruminant diseases in Turkey. Where adequately implemented, national campaigns (PPR, brucellosis) and routine flock vaccinations (clostridial, pasteurellosis) have demonstrably reduced disease burden; however, operational challenges — cold chain, regional coverage gaps, farmer awareness and surveillance limitations — curtail optimal impact. Priority actions should include strengthening cold-chain logistics, piloting thermostable/multivalent vaccines, integrating serological surveillance, and intensifying farmer education. Coordinated efforts by veterinary services, universities and producer organizations can translate scientific advances into sustainable improvements in small ruminant health and profitability in Turkey (FAO, 2022).

## REFERENCES

Abdolmohammadi Khiav, L., & Zahmatkesh, A. (2021). Vaccination against pathogenic clostridia in animals: A review. Tropical Animal Health and Production, 53(2), 284.

Akkaya, F., Kandemir, Ç., & Taşkın, T. (2021). Koyun ve keçi yetiştiriciliğinde uygulanan aşılar. Hayvansal Üretim, 62(2), 157-170.

Bayir, T. U. B. A., & Gürcan, İ. S. (2023). Assessment of Peste Des Petits Ruminants (PPR) in Turkey Between 2017-2019. Journal of the Hellenic Veterinary Medical Society, 74(2), 5771-5780.

Boshra, H., Blyth, G. A., Truong, T., Kroeker, A., Kara, P., Mather, A., ... & Babiuk, S. (2024). The Development of a Multivalent Capripoxvirus-Vectored Vaccine Candidate to Protect against Sheeppox, Goatpox, Peste des Petits Ruminants, and Rift Valley Fever. Vaccines, 12(7), 805.

Fanelli, A., Mantegazza, L., Hendrickx, S., & Capua, I. (2022). Thermostable vaccines in veterinary medicine: state of the art and opportunities to be seized. Vaccines, 10(2), 245.

FAO. (2022). Peste des petits ruminants global eradication programme: Contributing to food security, nutrition and poverty alleviation. Food and Agriculture Organization of the United Nations. https://www.fao.org

Fernandez-Georges, I. K., Manalo, S. M., Arede, M., Ciaravino, G., Beltrán-Alcrudo, D., Casal, J., ... & Allepuz, A. (2025). Ruminant and human brucellosis situation in Türkiye and the Caucasus. Tropical animal health and production, 57(6), 1-15.

Goncagül, G., Günaydın, E., Kardoğan, Ö., Cokal, Y., & Salcı, E. S. Ö. (2021). REV-1 conjunctival vaccine administration in Turkey.

Imanbayeva, D., Pérez Aguirreburualde, M. S., Knauer, W., Tegzhanov, A., Yustyniuk, V., Arzt, J., ... & Parida, S. (2025). A Scoping Review on Progression Towards Freedom from Peste des Petits Ruminants (PPR) and the Role of the PPR Monitoring and Assessment Tool (PMAT). Viruses, 17(4), 563.

Kumar, N., Barua, S., Riyesh, T., & Tripathi, B. N. (2017). Advances in peste des petits ruminants vaccines. Veterinary microbiology, 206, 91-101.

OIE. (2021). OIE Terrestrial Animal Health Code. World Organisation for Animal Health. https://www.oie.int

Saboor, A., Kalwar, Q., Rahimoon, M. M., Kolachi, H. A., Laghari, S. A., Kaka, A., ... & Uddin, A. (2024). Prevalence of Abortifacient Disorders in Small Ruminants: a Comprehensive Review. Journal of Bioresource Management, 11(4), 16.

Sharma, B., & Agrawal, I. (2024). Surveillance of Veterinary and Human Health in Pertaining Risk Analysis of Zoonoses Throughout the Globe. In The Handbook of Zoonotic Diseases of Goats (pp. 66-82). GB: CABI.

Şevik, M. (2023). Epidemiology of bluetongue virus infection among small ruminants in Turkey: Seroprevalence and associated risk factors. Preventive Veterinary Medicine, 213, 105871.

TUIK. (2024). https://data.tuik.gov.tr/Bulten/Index?p=Hayvancilik-Istatistikleri-Haziran-2024-53811

Yilmaz, O., & Wilson, R. T. (2012). The domestic livestock resources of Turkey: Economic and social role, species and breeds, conservation measures and policy issues. Livestock Research for Rural Development, 24(9), 157.

Zafra, R., Buffoni, L., Pérez-Caballero, R., Molina-Hernández, V., Ruiz-Campillo, M. T., Pérez, J., ... & Martínez Moreno, F. J. (2021). Efficacy of a multivalent vaccine against *Fasciola hepatica* infection in sheep. Veterinary research, 52(1), 13.

# CHAPTER 11

# GREEN SOFTWARE PRINCIPLES AND PRACTICES FOR SUSTAINABLE DIGITAL TRANSFORMATION

Tolga Furkan KILINÇ[1], Assoc. Prof. Dr. Gül Nihal GÜĞÜL[2], Assoc. Prof. Dr. Tahir SAĞ[3]

[1]Selcuk University, Graduate School of Natural and Applied Sciences, Konya, Türkiye
ORCID: 0009-0007-8035- 3322, e-mail: tolgafurkankilinc@gmail.com
[2]Selcuk University, Department of Computer Engineering, Konya, Türkiye
ORCID: 0000-0002-5927-3308, e- mail: gul.gugul@selcuk.edu.tr
[3]Selcuk University, Department of Computer Engineering, Konya, Türkiye
ORCID: 0000-0001-8266-7148, e- mail: tahirsag@selcuk.edu.tr

# 1. INTRODUCTION

The share of energy consumption of information technologies (IT) sector in global carbon emissions is gradually increasing. Recent studies indicate that information and communication technologies (ICT) are responsible for approximately 2% to 4% of global carbon emissions, and this rate may rise to 14% by 2040 (Software Carbon Intensity (SCI) Specification, 2023). These developments necessitate a re-evaluation of the processes of software design, development, and usage.

Software systems which are the structures that manage hardware resources, are components that directly affect energy consumption. Inefficient software can cause energy waste due to unnecessary processing load, high resource utilization, and unoptimized algorithms. Within this framework, the concept of **Green Software** has emerged as an approach aimed at minimizing the environmental impact of software (Kumar, 2022).

Green Software is a collection of practices, strategies, and technologies designed to reduce carbon emissions by ensuring energy efficiency during the design, development, deployment, and usage stages of software (Microsoft, 2023). This approach adds a sustainability dimension to traditional software development processes, contributing both to the reduction of environmental impacts and to the improvement of operational efficiency.

In this study, the literature in the field of Green Software has been comprehensively reviewed, and fundamental principles and implementation strategies have been presented. Within the scope of the research, technical documents from the Green Software Foundation were analyzed in addition to databases such as Google Scholar, ACM Digital Library, IEEE Xplore, and ScienceDirect.

The structure of the study is organized as follows: the second section defines the conceptual framework of Green Software; the third section discusses its fundamental principles. The fourth section examines sustainable software development strategies, while the fifth section focuses on measurement and evaluation methodologies. The sixth and seventh sections discuss industrial applications, challenges, and future directions. The eighth and ninth sections respectively focus on examples of sustainable software architecture and the integration of sustainability into software processes. Finally, the tenth section presents a case study based on the SCI (Software Carbon Intensity) metric, demonstrating with a practical example how the environmental impact of software systems can be measured quantitatively. The eleventh and final section provides a general evaluation of the study and offers recommendations in light of the findings obtained.

# 2. THE CONCEPT OF GREEN SOFTWARE

Green Software is an approach that aims to enhance the environmental sustainability of software systems. Although there are various definitions in the literature, Green Software can be most comprehensively defined as follows:

It refers to the practices, strategies, and technologies applied to minimize energy consumption and carbon emissions throughout the design, development, deployment, and usage processes of software (Pinto & Castor, 2020).
The scope of Green Software includes the following areas:
- Energy efficiency in software architecture and design

- Code optimization and efficient algorithms
- Optimization of resource usage (processor, memory, storage)
- Energy-aware programming practices
- Software sustainability and ease of maintenance
- Environmental impact assessment throughout all stages of the software lifecycle (Verdecchia et al., 2021)

The initial studies on software energy efficiency particularly focused on extending battery life in the context of mobile devices and embedded systems. However, as environmental sustainability concerns have increased over time, more comprehensive approaches have been developed to reduce the carbon footprint of software (Koçak, 2022).

In the early 2000s, academic interest in Green Software began to grow as a subfield of the "Green Computing" concept. With the establishment of the Green Software Foundation in 2021, industry-standard practices and measurement methodologies started to be developed (Green Software Foundation, 2021). Especially, standards such as the Software Carbon Intensity (SCI) specification have provided a common framework for measuring and comparing the environmental impacts of software (Green Software Foundation, 2023).

## 3. GREEN SOFTWARE PRINCIPLES

Green software development is built upon certain fundamental principles. These principles provide a sustainability framework that covers the entire lifecycle of software—from design to implementation and maintenance. Figure 1 illustrates these sustainability principles.



**Figure 1:** Green software principles

### 3.1. Efficiency Principle

Software should be designed to perform the same functionality with fewer resources (CPU, memory, storage, network). This principle aims to produce maximum value with minimal resource usage (Pereira, 2021). Software developed in accordance with the efficiency principle consumes less energy and therefore leads to lower carbon emissions.

According to the research of Pinto and Castor, focusing on software efficiency can reduce energy consumption by an average of 30–50% (Pinto & Castor). This increase in efficiency provides significant energy savings, especially in large-scale systems and continuously running applications.

### 3.2. Scalability

The scalability principle envisions designing software so that it uses only as many resources as needed and releases them when demand decreases (Capra, 2012). Systems with dynamic scaling capabilities can optimize resource usage according to workload and prevent energy waste.

This principle is particularly important in cloud-based systems and is implemented through strategies such as load balancing, auto-scaling, and demand-based resource allocation.

Research by Microsoft shows that systems using effective scaling strategies can reduce energy consumption by up to 20% (Microsoft, 2023).

### 3.3. Carbon Awareness

The carbon awareness principle aims to design software to operate during low carbon intensity periods or in low carbon intensity regions. Since the ratio of renewable energy changes over time, executing intensive operations during these periods can reduce the carbon footprint.

The SCI (Software Carbon Intensity) specification developed by the Green Software Foundation provides a standard methodology to measure and optimize the carbon intensity of software (Green Software Foundation, 2023). This methodology facilitates carbon-aware design decisions for software developers.

### 3.4. Hardware Efficiency

Software should be optimized in a way that extends hardware lifespan and reduces the need for frequent hardware replacement (Lago, 2019). Since the production of new hardware contains a significant amount of "embedded carbon," software strategies that extend the lifespan of existing hardware contribute to reducing the overall environmental impact.

Verdecchia and others have noted that mandatory hardware upgrades due to software requirements are a common issue that exacerbates the e-waste problem (Verdecchia et al., 2017). Hardware-efficient software mitigates this issue by enabling longer operation with existing resources.

### 3.5. Measurement and Transparency

The measurability and traceability of a software's environmental impact are critical for achieving sustainability goals (Hindle, 2018). Transparent reporting of energy consumption and carbon emissions enables developers and users to make informed decisions.

Kumar and others have developed various tools and methodologies to measure software energy consumption (Kumar, 2022). Such measurement tools allow software teams to evaluate the impact of their optimization efforts and develop continuous improvement strategies.

## 4. GREEN SOFTWARE DEVELOPMENT STRATEGIES AND TECHNIQUES

Various strategies and techniques have been developed to put Green Software principles into practice. This section examines the most effective green software development approaches.

### 4.1. Energy-Efficient Algorithms

The selection and optimization of algorithms are critical factors that directly affect the energy efficiency of software. Preferring algorithms that achieve the same results with fewer computations can significantly reduce energy consumption (Manotas, 2016).

For example, comparative studies between sorting algorithms have shown that the Quicksort algorithm provides significant advantages in terms of energy efficiency compared to Bubble Sort when dealing with large data sets (Lima, 2016). Similarly, in machine learning algorithms, there is a direct relationship between model complexity and energy consumption (Table 1).

**Table 1:** Comparison of Algorithm Selection and Energy Efficiency

| | | |
|---|---|---|
| Bubble Sort | O(n²) | High energy consumption |
| Insertion Sort | O(n²) | Moderate energy consumption |
| Merge Sort | O(n log n) | Low–moderate energy consumption |
| Quick Sort | O(n log n) | Low energy consumption |

In determining energy-efficient algorithms, Big O notation alone may not be a sufficient criterion; in real-world applications, energy consumption can vary depending on several factors such as memory access patterns, suitability for parallel processing, and opportunities for hardware-level optimization.

## 4.2. Demand-Based Processing

Avoiding unnecessary background operations and executing processes only when needed is an effective strategy for reducing software energy consumption (Adams, 2019). Techniques such as "lazy loading," "on-demand computation," and "event-driven architecture" are widely used in the implementation of this strategy.

Koçak et al. demonstrated that demand-based processing strategies in mobile applications can extend battery life by 15–25% (Koçak, 2022). This approach provides significant energy savings, especially in applications with continuously running background services.

## 4.3. Data Optimization

Data optimization strategies encompass various techniques aimed at ensuring more efficient use of system resources. These strategies include:

4.3.1. **Data compression:** Reduces both storage requirements and the amount of data transmitted over the network.

4.3.2. **Caching:** Keeps frequently used data in faster-access storage, preventing repetitive operations and unnecessary data transmission.

4.3.3. **Data structures:** Optimizing data structures according to application access patterns and usage improves processing efficiency.

4.3.4. **Data localization:** Keeping data close to where it is processed reduces network traffic and minimizes latency.

## 4.4. Intelligent Use of Cloud Resources

Cloud computing offers significant opportunities in terms of resource sharing and efficient utilization. However, to fully realize this potential, it is necessary to allocate cloud resources dynamically, taking into account the use of green energy, and to develop appropriate optimization strategies.

Research by Microsoft indicates that managing cloud resources with carbon-aware planning strategies can reduce a data center's carbon footprint by up to 30% (Microsoft, 2023). These strategies include:

4.4.1.    Directing workloads to regions with low carbon intensity

4.4.2.    Scheduling computation-intensive tasks during periods of high renewable energy generation

4.4.3.    Prioritizing energy-efficient hardware

4.4.4.    Consolidating resources and reducing idle capacity (Taina, 2011)

### 4.5. Energy-Aware CI/CD

Continuous Integration and Continuous Deployment (CI/CD) processes are indispensable components of modern software development. Optimizing these processes in terms of energy efficiency not only reduces the carbon footprint during the development phase but also improves the efficiency of the resulting software (Calero & Piattini, 2017). Figure 2 illustrates the operational steps of CI/CD processes within an energy-aware approach.



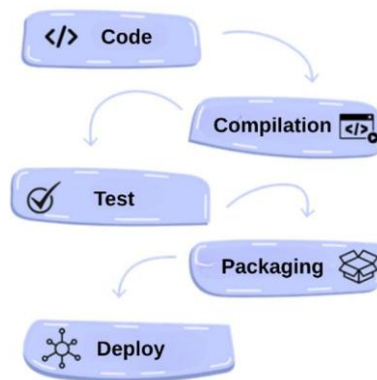**Figure 2:** Energy-Aware CI/CD

Energy-aware CI/CD practices include:
- Optimizing test automation and eliminating redundant tests
- Configuring build processes efficiently
- Designing deployment strategies to minimize energy consumption
- Integrating energy consumption metrics into the CI/CD pipeline
- Incorporating green software principles into code review processes (Calero, Moraga & Bertoa, 2013)

# 5. GREEN SOFTWARE MEASUREMENT AND EVALUATION METHODOLOGIES

Measuring and evaluating the environmental impact of software is one of the fundamental components of the Green Software approach. The methodologies and tools used to assess the energy consumption and carbon footprint of software are examined below.

## 5.1. Software Carbon Intensity Methodology

The Software Carbon Intensity (SCI) specification, developed by the Green Software Foundation, is an indicator designed to measure and compare the carbon emissions of software in a standardized manner. It is calculated using Equation (1) (Green Software Foundation, 2023).

$$Software\ Carbon\ Intensity\ (SCI) = \frac{((E \times I) + M)}{R} \tag{1}$$

Where:

E : Energy consumed (kWh)

I : Location-based carbon intensity ($gCO_2$ eq/kWh)

M : Embedded emissions (hardware manufacturing and lifecycle)

R : Scaling factor per functional unit

The SCI methodology provides software developers with the ability to set concrete goals for reducing the carbon footprint of their applications and to measure their progress (Green Software Foundation, 2022).

## 5.2. Energy Consumption Measurement Tools

Various tools and frameworks have been developed to measure the energy consumption of software. These tools provide the capability to analyze energy consumption at different levels of granularity (code block, function, application, system) (Noureddine, 2015). Commonly used energy consumption measurement tools include (Georgiou, 2019):

- Intel RAPL (Running Average Power Limit): Used for measuring energy consumption at the processor level.
- PowerAPI: A software-based power measurement library capable of measuring at different granularity levels.
- Jouleit: An energy monitoring tool for JavaScript applications.
- Android Battery Historian: Analyzes the battery usage of mobile applications.
- Cloud Carbon Footprint: Calculates the carbon emissions of cloud resources.

These tools assist software developers in analyzing and optimizing the energy consumption of their code.

## 5.3. Performance Profiling and Energy Analysis

Performance profiling tools are used to identify bottlenecks and inefficient code sections that affect the energy consumption of software. These tools analyze factors such as CPU usage,

memory access, disk I/O, and network traffic to determine the problem areas that increase energy consumption (Ournani, 2021).

Modern integrated development environments and profiling tools are increasingly incorporating energy analysis features. For example, environments such as **Visual Studio** and **IntelliJ IDEA** can provide energy efficiency recommendations through code analysis tools and plugins (Li, 2015).

## 6. INDUSTRIAL APPLICATIONS AND CASE STUDIES

The principles and strategies of Green Software have started to be adopted by both large-scale and small-scale organizations across various industries. This section examines successful Green Software applications and the benefits they provide.

### 6.1. Green Software Applications in Major Technology Companies

Major technology companies such as Microsoft, Google, and IBM have integrated Green Software principles into their corporate strategies. Microsoft's "Microsoft Cloud for Sustainability" platform helps organizations monitor and reduce their carbon emissions (Microsoft, 2023). Google optimizes the energy efficiency of its data centers through carbon-aware computing techniques (Google, 2023).

The case studies of these companies demonstrate that Green Software strategies can provide both environmental and economic benefits. For example, the carbon-aware computing strategies implemented in Microsoft's Azure cloud platform reduced energy costs by 15% while lowering carbon emissions by 25% (Althoff, 2021).

### 6.2. Energy Optimization in Mobile Applications

Applications running on mobile devices are an area where energy optimization is critically important due to limited battery life. The study conducted by Koçak et al. examined the impact of software architectures and design patterns used in mobile applications on energy consumption (Koçak, 2022).

The research results showed that optimizing database operations, minimizing background processes, and using local caching strategies can reduce the energy consumption of mobile applications by up to 30%. These optimizations not only extend battery life but also increase the lifespan of devices, thereby reducing the amount of e-waste (Pathak, 2012).

### 6.3. Green Design Principles in Web Applications

Web applications serve billions of users worldwide, and their energy efficiency has a significant impact on the global carbon footprint. Initiatives such as *The Green Web Foundation* and *Sustainable Web Design* have developed design principles and best practices to improve the energy efficiency of websites and web applications.

These practices include:
- Optimizing page size and loading times
- Compressing media content (images, videos) using efficient formats
- Reducing unnecessary HTTP requests
- Strategic use of CDNs (Content Delivery Networks)
- Implementing server-side and client-side caching strategies

Applying these practices can significantly reduce the energy consumption and carbon footprint of websites. For example, BBC's website optimization efforts reduced per-page carbon emissions by 25% (Chole Fletcher, 2021).

## 7. CHALLENGES AND FUTURE DIRECTIONS

There are several challenges to the widespread adoption of Green Software principles. At the same time, research and industrial applications in this field are rapidly evolving, and new opportunities are emerging. The main current challenges in Green Software development can be discussed under four categories:

- Measurement Challenges: Accurately and consistently measuring the energy consumption and carbon footprint of software remains a complex problem. More advanced tools and methodologies are needed to standardize the measurement of energy consumption for software operating in different environments.
- Lack of Knowledge and Awareness: Many software developers do not possess sufficient knowledge or awareness about energy efficiency and sustainability. Education and capacity-building efforts are critical to overcoming this challenge.
- Economic Incentives: The economic benefits of Green Software development may not always be visible in the short term. Stronger economic incentives and regulatory frameworks are required for organizations to adopt this approach.
- Optimization in Complex Systems: Modern software systems typically consist of numerous components and services. Performing end-to-end energy optimization in such complex systems can be technically challenging.

Future Research Directions in Green Software

The future research directions in the field of Green Software include the following topics:

- AI-Driven Energy Optimization: Developing systems that automatically optimize software energy consumption using machine learning and artificial intelligence techniques. These systems can provide energy efficiency recommendations at both code and architectural levels and create performance/energy profiles.
- Quantum Computing and Energy Efficiency: Exploring the potential of quantum computing technologies to consume less energy than classical algorithms for certain problems. In particular, evaluating quantum algorithms for optimization, cryptography, and simulation in terms of energy efficiency (Shenoy, 2019).
- Edge Computing and Green Software: With the proliferation of IoT (Internet of Things) devices, investigating the potential of the edge computing paradigm in terms of energy efficiency. Studying the impact of shifting computational processes from data centers to edge nodes on energy consumption and carbon emissions (Liu, 2020).
- Energy Efficiency of Programming Languages: Comparing different programming languages and frameworks in terms of energy efficiency and determining optimal language selection strategies for low-carbon software development.

Emerging Industrial Trends and Opportunities in Green Software

Emerging industrial trends and opportunities in the Green Software field include:

- Carbon-Neutral Software Certification: Developing programs that assess and certify the carbon footprint of software. Such certification programs can promote the adoption of sustainable software practices and enable consumers to make more informed choices.
- Expansion of Regulatory Frameworks: Regulatory frameworks such as the European Union's *European Green Deal* have begun to focus on the environmental impacts of digital technologies, including software systems. These regulations encourage organizations to adopt Green Software practices (European Commission, 2021).
- Sustainable Software Development Education: Integrating Green Software principles into computer science and software engineering curricula. Developing educational programs to ensure that future generations of software developers embrace sustainability-oriented approaches.
- Open Source Green Software Initiatives: The expansion of open-source initiatives such as the *Green Software Foundation* and similar organizations. These initiatives contribute to the growth of the Green Software ecosystem by providing tools, libraries, and best practices for sustainable software development (Green Software Foundation, 2021).

## 8.  SUSTAINABLE SOFTWARE ARCHITECTURE DESIGN EXAMPLES

The implementation of Green Software principles begins at the software architecture level. This section examines sample models and approaches for designing sustainable software architecture.

### 8.1.  Energy Optimization in Microservices Architecture

The microservices architecture allows applications to be divided into small, independently deployable, scalable, and manageable services. This architectural approach enables the execution of only the necessary services when required, ensuring more efficient use of resources (Jagroep, 2017).

Recommended strategies for energy optimization in microservices architecture include:
- **Optimization of Service Granularity:** It is important to establish an optimal balance between the communication overhead of very fine-grained services and the lack of flexibility of very coarse-grained services.
- **Asynchronous Communication Models:** Using asynchronous messaging in inter-service communication makes the system more flexible and resilient while reducing unnecessary waiting times and resource waste.
- **API Gateway Optimization:** Configuring API Gateways with intelligent routing and caching strategies can reduce unnecessary service calls and network traffic.

### 8.2.  Sustainability Advantages of Serverless Architecture

Serverless architecture (Function-as-a-Service - FaaS) allows developers to execute code units (functions) without dealing with infrastructure management. This architectural approach ensures energy efficiency by consuming resources only when the functions are executed and using no resources when they are idle (Eismann, 2021).

The sustainability advantages of serverless architecture include:
1. **On-Demand Resource Utilization:** Since functions run only when invoked, they consume less energy compared to continuously running servers.
2. **Automatic Scaling:** Functions automatically scale according to workload, ensuring efficient use of resources.
3. **Infrastructure Sharing:** Cloud providers optimize resource usage by sharing infrastructure among multiple clients (Shahrad, 2020).

## 8.3. Reactive Architectures and Energy Efficiency

Reactive architecture is an approach focused on designing asynchronous, message-driven, and event-driven systems. This architectural style provides significant advantages in terms of resource efficiency and system resilience (Bonér, 2014).

The energy efficiency advantages of reactive architectures include:
- **Asynchronous Processing:** Using asynchronous rather than blocking calls ensures more efficient use of resources.
- **Message-Driven Communication:** Using message queues instead of direct dependencies between components makes the system more flexible and robust.
- **Stream Processing:** Real-time processing of data streams reduces the resources required for storing and processing large datasets later [53].

## 9. INTEGRATION OF SUSTAINABILITY INTO SOFTWARE PROCESSES

Integrating Green Software principles into all stages of the software development lifecycle is critical for developing sustainable software systems. This section examines how a sustainability perspective can be integrated into software processes.

## 9.1. Sustainability in Requirements Analysis

Defining sustainability objectives during the software requirements analysis stage ensures that energy efficiency is treated as a fundamental quality attribute. The following approaches can be adopted at this stage (Becker, 2014):
- **Sustainability Requirements:** Measurable requirements related to energy consumption, resource utilization, and carbon footprint should be defined.
- **Quality Attributes Framework:** Sustainability should be evaluated alongside traditional quality attributes such as performance, reliability, and maintainability.
- **Requirements Prioritization:** Trade-offs between functional and sustainability requirements should be assessed, and conscious decisions should be made.

## 9.2. Sustainability in Design and Coding Stages

Applying sustainability principles during the design and coding stages directly affects the energy efficiency of the software. The following practices can be adopted at this stage [56]
- **Sustainable Design Patterns:** Utilizing design patterns that enhance energy efficiency and documenting these patterns (e.g., Event-Driven Architecture).

- **Code Reviews:** Incorporating the energy efficiency perspective into code review processes helps identify inefficient code blocks at early stages.
- **Automated Static Analysis Tools:** Integrating static analysis tools that detect code structures potentially problematic in terms of energy consumption.

### 9.3. Sustainability in Testing and Quality Assurance

Evaluating energy consumption and resource utilization in testing and quality assurance processes is important for sustainable software development. The following approaches can be adopted at this stage (Feitosa, 2018):

- Energy Profile Testing: Developing tests that measure software energy consumption under different usage scenarios.
- Load Testing and Energy Measurement**:** Monitoring and evaluating system energy consumption during load testing.
- Sustainability Benchmarks**:** Comparing the software's energy efficiency with industry-standard benchmarks.

### 9.4. DevOps and Sustainable Operations

Enriching DevOps practices with a sustainability perspective helps reduce the environmental impacts of software during the operational phase. In this context, the concept of **GreenOps** has emerged. GreenOps practices include:

- **Infrastructure Automation:** Defining infrastructure as code (Infrastructure as Code - IaC) and optimizing resource usage through automatic scaling strategies.
- **Energy Consumption Monitoring:** Continuously monitoring and analyzing energy consumption during the operational phase of the software.
- **Carbon-Aware Deployment Strategies:** Planning software updates and deployments during periods of low carbon intensity.

## 10. A SAMPLE CASE STUDY

One of the fundamental measurement methods of the Green Software approach is the SCI indicator, which provides a quantitative assessment of a software's energy consumption and carbon emissions. Below is an SCI calculation based on a sample scenario.

**Sample Scenario:**

A cloud-based application serves 1,000,000 users per month. The related data for this application are presented in Table 2.

**Table 2:** Carbon Emission Values of the Sample Case Study

| | |
|---|---|
| Energy Consumption (E) | 12.000 kWh |
| Regional Carbon Intensity (I) | 0,45 kgCO$_2$eq / kWh |
| Embedded Emission (M) | 1,500 kgCO$_2$eq |
| Number of Operations (R) | 1,000,000 user transactions |

Green Software aims to reduce the environmental impact of software. In this example, the SCI indicator is used to quantitatively analyze the carbon emission performance of a software system. The lower the SCI value, the "greener" the software. This example provides a transparent and comparable way to measure the environmental impact of software. The data can be either real or estimated, and in this case, the measured values can be used when exploring ways to improve energy efficiency.

Energy Consumption (E) represents the total amount of electricity consumed by the servers running the software, measured in kilowatt-hours (kWh). In real systems, this value can be directly measured using energy measurement tools (e.g., Intel RAPL, PowerAPI). Alternatively, it can be derived from the monthly reports of total energy consumption in data centers. In our example: *E = 12,000 kWh/month* represents the average monthly electricity consumption of a large-scale application's server infrastructure.

Carbon Intensity (I) indicates the environmental impact of the energy source used to generate electricity. Its unit is kilograms of $CO_2$ equivalent per kilowatt-hour ($kgCO_2eq/kWh$). This value can be determined from regional energy providers' carbon intensity reports (e.g., electricityMap for Europe). The average value for Türkiye ranges from 0.4 to 0.6 $kgCO_2eq/kWh$. In our example: *I = 0.45 kgCO₂eq/kWh*, indicating that electricity is primarily generated from fossil fuels.

Embedded Emissions (M) represent the total carbon emissions produced during the manufacturing and lifecycle of hardware. It is measured in kilograms of $CO_2$ equivalent ($kgCO_2eq$). This value can be obtained through lifecycle assessment (LCA) reports from hardware manufacturers. For instance, a typical server can generate approximately 18,000 $kgCO_2eq$ annually. For monthly calculations, 1,500 kg was used. In our example: *M = 1,500 kgCO₂eq*.

Number of Operations (R) represents the total number of operations performed by the software, such as user transactions, requests, or processing cycles. It can be measured through application analytics tools, API logs, or transaction counters. In this case, "one operation" is defined as a single user action (e.g., placing an order). In our example: *R = 1,000,000 user transactions per month.*

$$SCI = \frac{((E \times I) + M)}{R} = \frac{((12.000 \times 0,45) + 1.500)}{1.000.000} \cong 0,0069 \; kgCO_2eq/transaction$$

This value is considered quite low for an optimized software system running in a low-carbon-intensity region. If the same application were operated in a region with higher carbon emissions, the SCI value would increase significantly.

## 11. CONCLUSION AND RECOMMENDATIONS

This study presents a systematic approach aimed at reducing the environmental impacts of software systems, discussing the concept of Green Software together with its conceptual foundations and practical strategies. Findings obtained from the literature indicate that the implementation of efficient software architectures, energy-aware algorithms, and carbon-transparent CI/CD processes can significantly reduce the overall carbon footprint of software.

The SCI calculation example demonstrates how this theoretical framework can be applied in practice, revealing that the environmental impact of a software system can be quantitatively expressed based on energy consumption, carbon intensity, and processing volume. Such measurements are critical for integrating sustainability criteria into the software development process.

In the future, it is expected that AI-supported energy profiling systems will enable real-time carbon tracking and optimization processes. Moreover, the expansion of regulatory frameworks, the widespread adoption of sustainable software certification programs, and the integration of sustainability topics into educational curricula will further promote the large-scale adoption of Green Software practices.

Green Software should be regarded as a fundamental component in the sustainable transformation of the digital era — serving as a bridge between **environmental responsibility** and **technical excellence.**

## REFERENCES

Adams, B., McIntosh, S., Hassan, A. E., & Hindle, A. (2019). "An empirical study of integration activities in distributions of open source software." *Empirical Software Engineering*, 24(6), 3722–3772.Althoff, M. (2021). "Microsoft Cloud for Sustainability: Empowering organizations to accelerate progress toward a net-zero future." *Microsoft Azure Blog*.

Becker, C., Chitchyan, R., Duboc, L., Easterbrook, S., Mahaux, M., Penzenstadler, B., ... & Betz, S. (2014). "The karlskrona manifesto for sustainability design." *arXiv preprint arXiv:1410.6968*.

Bonér, J., Farley, D., Kuhn, R., & Thompson, M. (2014). *The reactive manifesto*. https://www.reactivemanifesto.org

Calero, C., & Piattini, M. (2017). "Puzzling out software sustainability." *Sustainable Computing: Informatics and Systems*, 16, 117–124.

Calero, C., Moraga, M. A., & Bertoa, M. F. (2013). "Towards a software product sustainability model." *arXiv preprint arXiv:1309.1640*.

Capra, E., Francalanci, C., & Slaughter, S. A. (2012). "Is software 'green'? Application development environments and energy efficiency in open source applications." *Information and Software Technology*, 54(1), 60–71.

Chole Fletcher, C. (2021). "The carbon impact of streaming: an update on BBC TV's energy footprint." *BBC Technology Blog*. https://www.bbc.co.uk/rd/blog/2021-06-bbc-carbon-footprint-energy-envrionment-sustainability

Eismann, S., Scheuner, J., Van Eyk, E., Schwinger, M., Grohmann, J., Herbst, N., ... & Kounev, S. (2021). "A review of serverless use cases and their characteristics." *ACM Computing Surveys (CSUR)*, 55(2), 1–35.

European Commission. (2021). "Digital solutions for zero pollution." *European Green Deal Action Plan*.

Feitosa, D., Ampatzoglou, A., Avgeriou, P., & Nakagawa, E. Y. (2018). *Yeşil Yazılım: Sürdürülebilir Dijital Geleceğin İnşasında Temel Yaklaşımlar*.

Georgiou, S., Rizou, S., & Spinellis, D. (2019). "Software development lifecycle for energy efficiency: Techniques and tools." *ACM Computing Surveys (CSUR)*, 52(4), 1–33.

Google. (2023). *24/7 Carbon-Free Energy: Progress and Insights*. https://sustainability.google/progress/energy/

Green Software Foundation. (2021). *Foundation Overview*. https://greensoftware.foundation/overview

Green Software Foundation. (2022). *SCI Guidance Documentation*. https://github.com/Green-Software-Foundation/sci-guidance

Green Software Foundation. (2023). *Software Carbon Intensity (SCI) Specification*. https://greensoftware.foundation/articles/software-carbon-intensity-sci-specification

Hindle, A. (2018). "Green mining: A methodology of relating software change and configuration to power consumption." *Empirical Software Engineering*, 23(2), 1494–1524.

Jagroep, E., Procaccianti, G., van der Werf, J. M., Brinkkemper, S., Blom, L., & van Vliet, R. (2017). "Energy efficiency on the product roadmap: An empirical study across releases of a software product." *Journal of Software: Evolution and Process*, 29(2), e1852.

Koçak, S. A., Alptekin, G. I., Bener, A. B., Miranskyy, A., & Doğan, E. (2022). "Yazılım Özelliklerinin Enerji Tüketimi Üzerine Etkileri." *Bilişim Teknolojileri Dergisi*, 15(1), 1–12.

Kreps, J. (2014). "Questioning the lambda architecture." *O'Reilly Radar*, 2, 3–5.

Kumar, N., et al. (2022). "Energy Efficiency in Software Engineering: A Systematic Literature Review." *IEEE Transactions on Software Engineering*, 48(5), 1822–1853.

Lago, P. (2019). "Architecture design decision maps for software sustainability." In *2019 IEEE/ACM 41st International Conference on Software Engineering: Software Engineering in Society (ICSE-SEIS)* (pp. 61–64). IEEE.

Li, D., Halfond, W. G., & Gopalakrishnan, S. (2015). "Calculating source line level energy information for Android applications." In *Proceedings of the 2015 International Symposium on Software Testing and Analysis* (pp. 78–89).

Lima, L. G., Melfe, G., Soares-Neto, F., Lieuthier, P., Fernandes, J. P., & Castor, F. (2016). "Haskell in Green Land: Analyzing the energy behavior of a purely functional language." In *2016 IEEE 23rd International Conference on Software Analysis, Evolution, and Reengineering (SANER)* (Vol. 1, pp. 517–528). IEEE.

Liu, Y., Sun, C., Wong, J. W., Qu, Y., & Liang, T. Y. (2020). "Towards green computing: A survey of energy-efficient edge systems." *ACM Computing Surveys (CSUR)*, 53(5), 1–36.

Manotas, I., Bird, C., Zhang, R., Shepherd, D., Jaspan, C., Sadowski, C., ... & Clause, J. (2016). "An empirical study of practitioners' perspectives on green software engineering." In *2016 IEEE/ACM 38th International Conference on Software Engineering (ICSE)* (pp. 237–248). IEEE.

Microsoft. (2023). *Sustainable Software Engineering Principles*. https://docs.microsoft.com/en-us/learn/modules/sustainable-software-engineering-overview/

Noureddine, A., Rouvoy, R., & Seinturier, L. (2015). "Monitoring energy hotspots in software." *Automated Software Engineering*, 22(3), 291–332.

Ournani, Z., Belgaid, M. C., Rouvoy, R., Rust, P., & Penhoat, J. (2021). "Taming energy consumption variations in systems benchmarking." In *2021 IEEE/ACM 14th International Conference on Utility and Cloud Computing (UCC)* (pp. 67–77). IEEE.

Pathak, A., Hu, Y. C., & Zhang, M. (2012). "Where is the energy spent inside my app? Fine grained energy accounting on smartphones with Eprof." In *Proceedings of the 7th ACM European Conference on Computer Systems* (pp. 29–42).

Pereira, R., Couto, M., Ribeiro, F., Rua, R., Cunha, J., Fernandes, J. P., & Saraiva, J. (2021). "Ranking programming languages by energy efficiency." *Science of Computer Programming*, 205, 102609.

Pinto, G., & Castor, F. (2020). "Energy efficiency: A new concern for application software developers." *Communications of the ACM*, 63(3), 60–70.

Pinto, G., Castor, F., & Liu, Y. D. (2014). "Mining questions about software energy consumption." In *Proceedings of the 11th Working Conference on Mining Software Repositories*, 22–31.

Shahrad, M., Fonseca, R., Goiri, Í., Chaudhry, G., Batum, P., Cooke, J., ... & Bianchini, R. (2020). "Serverless in the wild: Characterizing and optimizing the serverless workload at a large cloud provider." In *2020 USENIX Annual Technical Conference (ATC 20)* (pp. 205–218).

Shenoy, P., & Irwin, D. (2019). "Quantum computing for computer scientists and its energy implications." *IEEE Computer*, 52(10), 13–18.

Taina, J. (2011). "Good, bad, and beautiful software—In search of green software quality factors." *Cepis Upgrade*, 12(4), 22–27.

Verdecchia, R., Lago, P., Ebert, C., & De Vries, C. (2021). "Green IT and green software." *IEEE Software*, 38(6), 7–15.

Verdecchia, R., Procaccianti, G., Malavolta, I., Lago, P., & Koedijk, J. (2017). "Estimating the energy impact of software releases and deployment strategies: The KPMG case study." In *2017 ACM/IEEE International Symposium on Empirical Software Engineering and Measurement (ESEM)* (pp. 257–266). IEEE.

# CHAPTER 12


# ENDOPHYTIC BACTERIA IN PLANT STRESS MANAGEMENT AND AGRICULTURAL SUSTAINABILITY

Prof. Dr. Behçet KIR[1], Res. Assist Esra DURU[2]

[1]Ege University, Faculty of Agriculture, Department of Field Crops, İzmir, Türkiye
ORCID: 0000-0002-7282-7010, behcet.kir@ege.edu.tr
[2] Ege University, Faculty of Agriculture, Department of Field Crops, İzmir, Türkiye
ORCID: 0009-0000-1481-9998, esra.duru@ege.edu.tr

## 1. INTRODUCTION

The rapid increase in the world population has significantly increased the demand for agricultural production. This increase has led to significant losses of agricultural land to meet urbanization and industrialization needs, making it increasingly difficult to meet food needs. To increase agricultural production, high-yield crop varieties have been selected and intensive agriculture practices are increased. Due to this, the use of fertilizers and the fact that only a small portion is used by plants causes the rest to accumulate in the soil, started to pollute soil, which threatens the lives of organisms that are living in. Similarly, the residue of chemical pesticides in agricultural products poses a risk to human health and food safety. The widespread use of pesticides also contributes to the decline in biodiversity. In addition, environmental stress factors become more severe, Drought, salinity, heavy metal pollution, and high temperatures negatively affect plant growth and yield, threatening food security (Lopes et al., 2021; Hakim et al., 2021).

In recent years, with increasing land loss and environmental threats, the concept of sustainability in agriculture has gained importance, and sustainability goals in agricultural production have emerged (Demiroğlu Topçu et al., 2019). Sustainable agricultural production encompasses many practices; in general, it aims to minimize negative impacts on the environment by conserving natural resources and ensuring reliable food production. The efficient use of resources is a fundamental element of sustainable agriculture. In this context, the protection of soil, water, and biodiversity is among the primary objectives. Chemical fertilizers and pesticides should be used only in small amounts, in the correct dosage, from the right source, at the right time, and in the right place (Hakim et al., 2021).

One of the most important methods for promoting the more efficient use of resources that support sustainable agriculture is the use of beneficial microorganisms to support plant growth, particularly endophytic bacteria that promote plant growth because they are highly abundant in the soil when compared with other organisms. These bacteria live in plant tissues, mostly in parts such as roots, leaves, or stems, in a symbiotic relationship with the plant without harming it. They support growth by providing nutrients such as nitrogen and phosphorus that the plant needs and affect their growth positively. They also exhibit protective effects by increasing the plants' resistance to abiotic and biotic stresses in agriculture (Glick, 2012; Mishra et al., 2017).

In short, today's agricultural sector faces bottlenecks in terms of sustainability due to population growth and environmental issues. The excessive use of chemical fertilizers and pesticides causes environmental pollution, soil degradation, and disruption of the balance in the ecosystem. In this period, where new ways for sustainable agriculture are being sought, endophytic bacteria offering environmentally friendly solutions. Bacterial endophytes, which can increase nutrient uptake through control mechanisms that reduce dependence on chemical inputs and induce plant development under abiotic and biotic stress conditions, will play a critical role in ensuring sustainability in agriculture in the future. This section will discuss how endophytic bacteria affect plant health under abiotic and biotic stress conditions, and their potential.
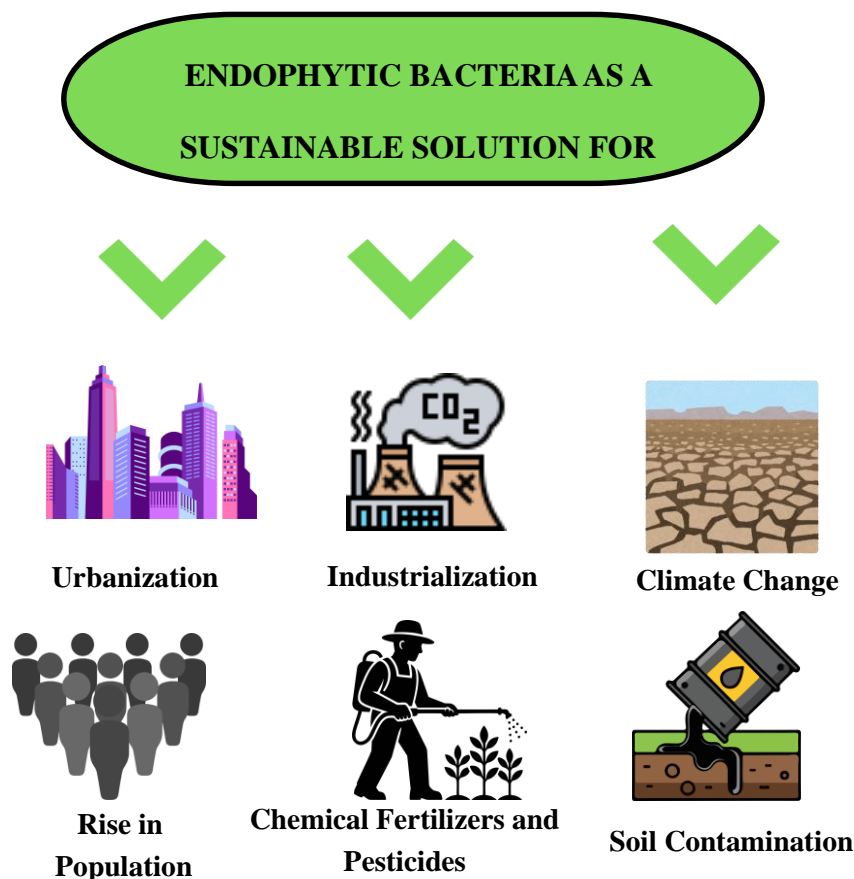
**Figure 1.1 :** Some of the environmental pressures that are threatening agricultural systems.

## 2. ENDOPHYTIC BACTERIA: DEFINITION AND ECOLOGY

The term endophyte was first used in 1866 by De Barry to describe any organism found within plant tissue, thereby terminologically distinguishing organisms living inside plants from those living on their surface. Although there are many suggestions for the definition of endophytes, the generally accepted definition is "Endophytes are microorganisms found in a wide variety of plant tissues without causing any obvious infection in the host" (Hallmann et al. 1997). Endophytic bacteria provide mutual benefit to plants, i.e., they establish symbiotic relationships. These bacteria can be found in vegetative organs such as the roots, stems, and leaves of plants. However, roots serve a very important purpose as the entry point for these bacteria. This is because roots can selectively filter the bacteria that will be taken into the plant. Although there are many endophytic bacterial communities in the soil, the number of bacteria that can enter and colonize plants is lower due to plant selectivity. The general characteristics of bacteria that can successfully enter plants can be said to be the ability to move, the ability to break down plant cell walls, and elimination efficiency of ROS(reactive oxygen species). Their colonization is classified into three types based on their dependence on plant tissue. The first one is an obligate endophyte that cannot survive in soil, and it is transferred via seeds. The second one is that facultative endophytes are generally found in soil but can colonize plants

when suitable conditions are provided. Lastly, passive endophytes can enter plants through wounds or cracks in the plant (Khan et al., 2020a; Liu et al., 2017).

In conclusion, we can say that the ecology of bacterial endophytes depends on their ability to colonize plant roots and develop symbiotic relationships with plants. Plant roots act as a filter, allowing only certain endophytes to enter. Thus, endophytic bacteria that enter and colonize the plant can facilitate nutrient uptake without causing any harm and contribute to the plant's resistance to stress conditions.



**Figure 2.1.** Endophytic bacteria in the rhizosfere and plant endophyte selectivity.

## 3. ROLE OF ENDOPHYTIC BACTERIA IN ABIOTIC STRESS MITIGATION

Plants encounter numerous abiotic stresses throughout their life cycle, and these stress conditions have negative effects on growth, development, and yield. Furthermore, abiotic stress factors pose a serious threat to agricultural productivity and global food security. The most common abiotic stress conditions observed in plants are drought, salinity, low or high temperatures, heavy metals, and nutrient deficiencies. These stress conditions generally disrupt the cellular functioning of plants and inhibit metabolic processes. Additionally, it can increase the production of stress-related proteins by altering plant gene expression. While some of these processes may force the plant to adapt to stress, the plant's biological processes may be negatively affected. As a result of these, significant declines can be seen in crop yields (Zhang et al., 2023).

Today, many methods are used to combat abiotic stresses that significantly reduce crop yields in plants. Endophytic bacteria appear to be a viable option due to the cost and time advantages they offer in supporting plant growth under stress conditions. These bacteria can function as biofertilizers, increasing nutrient uptake in plants and promoting plant growth in stressful environments. They activate the host plant's response system to reduce stress load or produce compounds that increase plant tolerance to stress. With the discovery of this phenomenon, many agricultural applications, such as biofertilizers and biostimulants, have become possible. Understanding the communication between these bacteria and plants has a
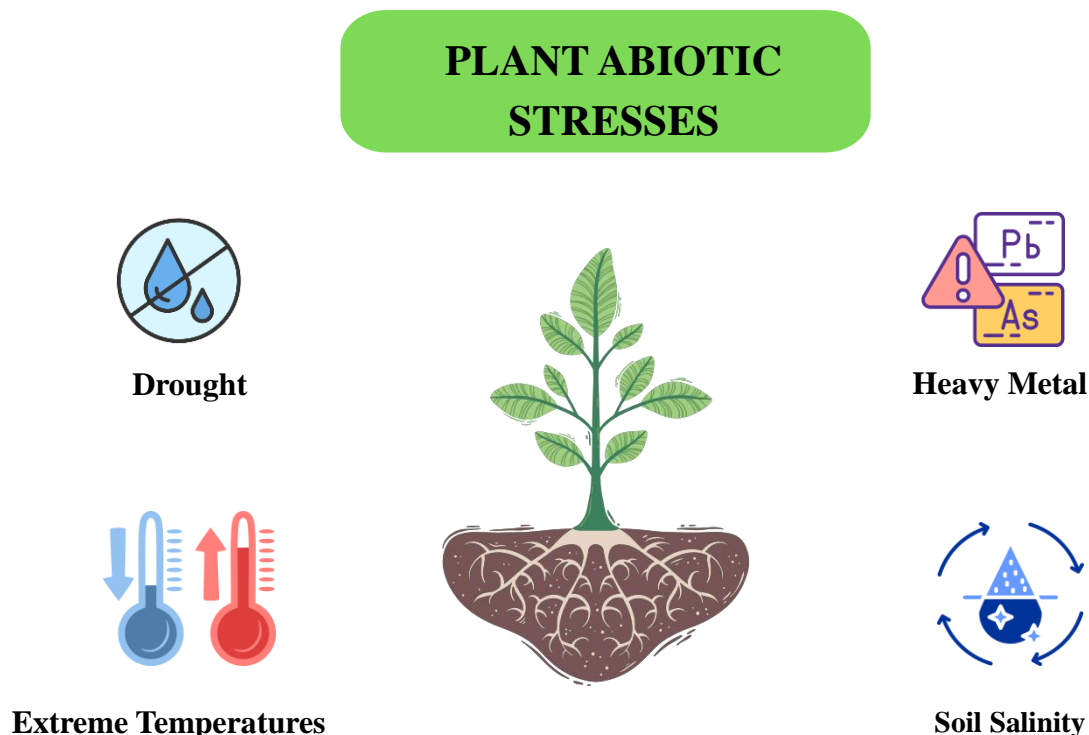
great importance for sustainable agriculture.



**Figure 3.1.** Some of the common abiotic stress factors in plants.

### 3.1. Drought Stress Mitigation Via Endophytic Bacteria

Drought stress is one of the major abiotic stress types that occurs when plants cannot obtain sufficient water and has negative effects on plant growth and yield. Plants attempt to reduce the negative impacts of drought stress by developing various physiological and molecular mechanisms. They activate stress signaling pathways and control stomatal closure to minimize water loss (Chaffai et al., 2024; Demiroğlu Topçu et al.,2024).

Endophytic bacteria aim to increase plants' drought resistance by producing phytohormones, exocelluloses, antioxidants, and osmolytes. These substances facilitate morphological changes that support shoot and root growth. Endophytic bacteria work to help plants adapt to drought by altering the plant at both the molecular and biochemical levels (Kumar et al., 2025).

There are numerous drought studies investigating the effects of endophytic bacterial inoculations. For example, a study testing the effects of *Pseudomonas* sp. and *Pantoea* sp. bacteria on *Hordeum vulgare* under dry conditions revealed the potential of these bacteria to increase plant resistance. The study found that the seeds of plant, inoculated with these bacteria showed improvements in chlorophyll content, net photosynthesis rate, and soil water retention capacity. Both bacteria offer a promising solution for supporting barley production and increasing yield under dry conditions. The findings of the study emphasize the need for careful selection of bacteria to be used to promote plant growth under drought stress conditions (Abideen et al., 2022).

In another study on the physiological characteristics and nutrient content of endophytic bacteria in pepper seedlings, isolates of the bacteria *Bacillus thuringiensis* and *Ochrobactrum* sp. were used. While drought stress negatively affects enzyme activities and mineral uptake, it was found that these bacteria had some beneficial effects on the seedlings which reverse impacts of drought stress (Sadak et al., 2021).

In conclusion, it can be said that drought stress has negative effects on the physiological characteristics and yield of plants. Endophytic bacterial inoculation can be performed both from seeds and seedlings, and application strategies can vary from plant to plant. While the performance of endophytic bacteria vary, more studies should be conducted for each variety within each plant species to reach definite results.

## 3.2. Salinity Stress Mitigation Via Endophytic Bacteria

Salt stress is one of the major abiotic stress factors that directly affects plant growth and yield by causing ion toxicity in plants. Water availability decreases with salt stress while disrupting the metabolic processes of plants. This results in reductions in photosynthesis, nutrient uptake, and protein synthesis ((Khalvati et al. 2001; Zhao et al., 2021).

The use of microorganisms in salt stress management shows promise because they offer a safe, inexpensive, and sustainable method for increasing plant productivity and growth under stress conditions. Endophytic bacteria regulate plant growth hormones and help plants absorb nutrients more efficiently by promoting the growth and yield of plants exposed to salt stress. Many bacterial species have been reported to increase salt stress tolerance in plants (Kumar et al., 2025).

In a study aimed at reducing the stress effects of soil salinity on tomato plants and increasing fruit nutritional value, the tolerance of plants to salinity was tested using a newly discovered *Agrobacterium* strain. Tomato seedlings were inoculated with the bacteria, and their tolerance to salt stress was investigated. Researchers observed that the application of the halotolerant bacterial strain conferred salt stress tolerance. Improvements in plant health were observed by increasing root growth, shoot biomass, and proline content (Potestio et al., 2024).

In another study examining the effects of halotolerant bacteria isolated from saline habitats on alleviating salt stress in wheat seedlings, it was found that the strains *Hallobacillus* sp. SL3, *Bacillus halodenitrificans* PU62, and *Bacillus sp.* (J8W) increased the growth of wheat seedlings at high salt concentrations. Specifically, strains belonging to *Hallobacillus* sp. and *Bacillus halodenitrificans* were found to increase root elongation by more than 90% and plant dry weight by 17.4%. This study clarified the potential of halotolerant bacteria isolated from saline environments to directly or indirectly increase the growth of plants under salt stress (Ramadoss et al., 2013).

One other study on endophytic bacteria that obtained from halotolerant plants were screened and applied to rice seedlings under salt stress. Bacteria helped develop salt tolerance in rice plants and caused a significant increase in growth. They also find endophytic bacteria mitigate the adverse effects of stress conditions and enhance rice growth characteristics by producing phytohormones (Khan et al., 2020b).

As a result, it is known that salt stress negatively affects plant growth and development. Studies have consistently shown that endophytic bacteria can significantly reduce the harmful effects of salinity, making them a sustainable method for supporting plant growth. It can be

concluded that these bacteria strengthen the survival ability of plants by producing various phytohormones.

### 3.3. Heavy Metal Stress Mitigation Through Endophytic Bacteria

Increased industrialization activities and extensive agricultural technologies have made heavy metal contamination one of the major problems in today's world. The growth and development of plants depend on the availability of micronutrients and macronutrients. Macronutrients are elements that plants need in large quantities, while micronutrients are elements that plants need only in small quantities. However, certain heavy metals such as cadmium(Cd), arsenic(As), zinc(Zn), aluminum(Al), nickel(Ni), chromium(Cr), and lead(Pb) are elements that cause high toxicity even when present in very small amounts in the soil or within the plant, as they are not essential for plant growth (Kumar et al., 2025).

Oxidative stress is the most prominent damage caused by heavy metals in plants. The presence of heavy metals in plants increases the production of reactive oxygen species, causing damage to cells. In addition, heavy metals negatively affect the photosynthesis process. As a result of these effects, the plant's energy production mechanism is disrupted, and its growth is inhibited. They also prevent plants from absorbing essential nutrients, leading to nutritional imbalances (Emamverdian et al., 2015).

One of the sustainable solutions for heavy metal stress in plants is the use of endophytic bacteria. They can reduce heavy metal toxicity by converting harmful heavy metals into non-toxic forms. They can increase metal uptake and mobility by stimulating specific mechanisms in plants. In this respect, endophytic bacteria can be highlighted as an environmentally friendly approach that reduces stress factors affecting phytoremediation and agricultural yield (Kumar et al., 2025).

In a heavy metal stress study conducted on *Oryza sativa* plants, metal-resistant endophytic bacteria strains2 behaviour were examined (*Enterobacter ludwigii* SAK5 and *Exiguobacterium indicum* SA22), and it was found that these bacteria support plant growth and mitigate heavy metal stress. In the study, which investigated heavy metals such as cadmium and nickel, heavy metals accumulated more in the roots, with nickel accumulation being higher. In plants inoculated with bacteria, the expression of stress-related genes associated with heavy metals was reduced. There was also no increase in plant phytohormones comparable to that seen at stress levels. The study indicates that bacterial inoculation reduces heavy metal stress in plants (Jan et al., 2019).

In another study on heavy metal pollution, endophytic root bacteria were used to increase the cadmium tolerance of the *Panicum virgatum* L. . Their effects on cadmium tolerance and accumulation were investigated. In plants treated with endophytic bacteria, increases in root, biomass, and shoot length were observed despite stress conditions. Furthermore, inoculation with these bacteria not only improved growth but also reduced Cd concentration in the plant body (Afzal et al., 2017)

In short, heavy metals have a toxic effect on plants. They cause growth retardation, reduction in biomass, and cellular damage in plants. Endophytic bacteria that promote plant growth can protect plants against heavy metal stress. These bacteria can accumulate heavy metals within themselves or convert them into a non-toxic form.
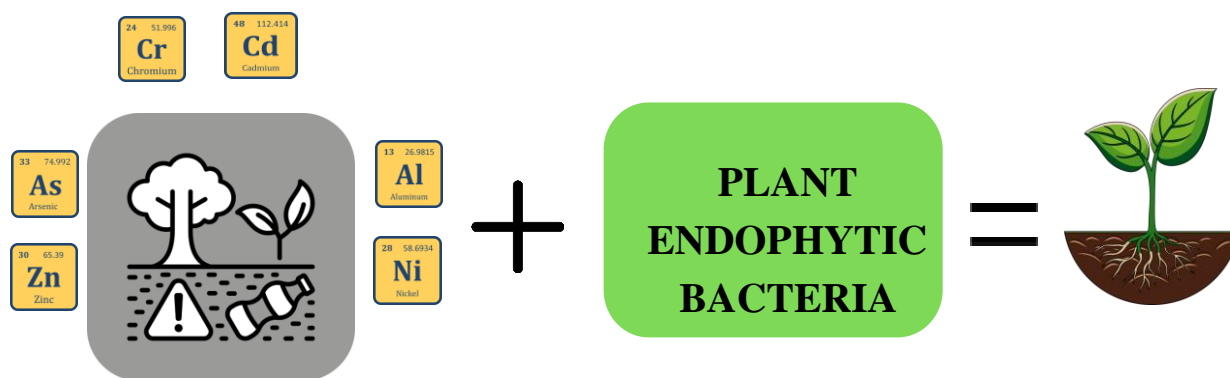
**Figure 3.2.** Deterioration of plant health under heavy metal contamination and improvement of plant growth through the application of endophytic bacteria.

### 3.4. Mitigation of Temperature Stress via Plant Endophytic Bacteria

Temperature is one of the factors that is quite important for plant development. Plant growth, development, and metabolic activities develop depending on temperature. When temperature stress occurs, plant growth slows down, or stops. Temperature stress, which directly affects crop yield, is one of the main problems faced by producers due to the effects of global climate change.

Temperature stress can be seen as high or low temperature stress. These stress factors cause structural changes in plant tissues and organelles. They can interfere with the functioning of the dark and light reactions of photosynthesis, thereby inhibiting photosynthesis. Although plants have learned to adapt to changing temperatures and environmental conditions over time, temperature stress remains one of the most important stress factors in agriculture. Furthermore, we need to consider that plants encounter multiple abiotic stress factors during their normal life cycle, temperature-related stress can significantly reduce yield losses, leading to a greater perception of the effects of other stress factors (Źróbek-Sokolnik, 2021).

Endophytic bacteria play important roles in increasing plant tolerance to heat stress. They are known to support plant growth by developing plant defense mechanisms, producing heat shock proteins, secreting osmoprotectants, activating important genes in heat stress tolerance, and producing various phytohormones (Kumar et al., 2025).

In a study investigating the use of endophytic bacteria and fertilizer to reduce the adverse effects of increasing temperature levels on *Oryza sativa* L., it was found that endophytic bacteria supported plant growth at high temperatures and significantly increased the grain weight and biomass of inoculated plants. In particular, plants inoculated with the *Bacillus paralicheniformis* strain showed an increase in yield of nearly 50%. The study indicated that thermotolerant bacterial strains increase tolerance to heat stress by regulating plant metabolism (Dlamini et al., 2025).

In another study where eight effective strains of *Acinetobacter rhizosphaerae*, which live as phosphorus solubilizers in the cold deserts of the Himalayas, were tested to alleviate cold stress in wheat. In order to test effects, in vitro and in vivo experiments were conducted. The bacteria increased plant growth and positively affected nutrient uptake and yield, thereby helping to alleviate temperature stress (Kour and Yadav, 2023).

As stated in the studies conducted, endophytic bacteria play a critical role in increasing plant tolerance to temperature stress. The use of these beneficial organisms in changing climate conditions is important both in ensuring sustainability and in increasing food security.

## 4. ENDOPHYTIC BACTERIA–MEDIATED BIOTIC STRESS MITIGATION IN PLANTS

Biotic stress is the type of stress caused by living organisms that harm plants. These harmful organisms are bacteria, viruses, insect pests, weeds, and nematodes. These living organisms generally inhibit plant growth and development and reduce photosynthesis rates, leading to yield losses. Plants develop various defense mechanisms against biotic stresses, but biotic stresses still cause serious production problems in agriculture.

Bacterial endophytes have considerable potential for use in biological control. This is because these organisms protect plants from environmental stresses by triggering immune responses against pathogens. They provide resistance against harmful organisms by affecting plant gene expression, physiological, and metabolic responses against phytopathogens in the plant. Endophytes recognize pathogens and produce various compounds to combat them. Furthermore, endophytic bacteria enhance stress tolerance by producing various phytohormones that strengthen plant immunity (Chaudhary et al., 2022).

In a study investigating the effects of endophytic bacteria on the development of tomato and pepper plants and the bacterial spot disease caused by *Xanthomonas euvesicatoria*, four different endophytic bacteria were used, and their effects against the disease were examined on both hosts. *Ochrobactrum* sp. CB36/1 endophyte was found to reduce disease severity in tomatoes by 37%. However, the same effect was not observed in peppers. Although it was determined that endophytic bacteria activate the defense mechanism of plants against biotic stress, this situation also showed that different results may be observed on different plants (Akköprü et al., 2018).

Another study investigated the biological control, insecticidal activity, and potential of *Bacillus* species bacteria against *Spodoptera frugiperda*, a pest that significantly affects corn yield. In the study, which used three different inoculation methods (seed, leaf, soil) and combinations of these application methods, laboratory experiments showed that endophytic bacteria exhibited antibacterial and insecticidal effects, killing nearly 60-65% of the pests. However, it was reported that the presence of these bacteria did not significantly affect plant growth (Fathy et al., 2024).

In conclusion, bacterial endophytes are emerging as an environmentally friendly alternative to chemical pesticides. The widespread adoption of biological control strategies based on bacterial endophytes offers a promising approach that could support environmental sustainability by reducing chemical pesticide use and enhancing agricultural productivity.
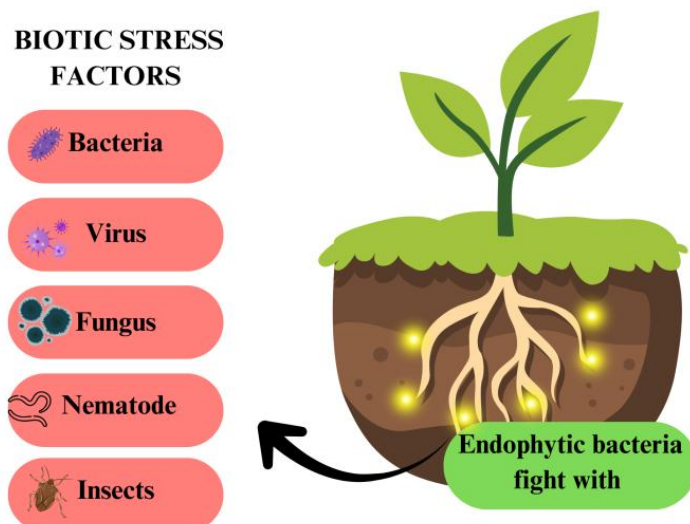
**Figure 4.1.** Biotic stress factors and the interactions of endophytic bacteria that enhance defense against these stresses in plants.

## 5.    BACTERIAL INOCULATION METHODS

The method of applying plant growth-promoting bacteria to plants is crucial for their attachment to the plant root zone and long-term survival. Since microorganisms have limited mobility, the inoculation process should be performed as close as possible to the rhizosphere. The plant's response to microorganisms that support plant growth depends on the inoculation density and method, as well as root structure, interactions between microorganisms, pH, temperature, plant species, root exudates of these plants, and the physiological state of the plant. Inoculation can be carried out with a single isolate, but multiple microorganisms can also be used because synergistic interactions between microorganisms can increase the effectiveness of inoculation and positively affect plant growth. There are three different seed inoculation methods: seed inoculation, root inoculation, and soil inoculation. Seed inoculation can be considered as an alternative method to chemical seed treatments. In this method, seeds are immersed in a solution with a known concentration of microorganisms. Chemicals released during seed germination serve as a nutrient source for these microorganisms and  enabling colonization. Secondly, root inoculation involves dipping plant roots into a microorganism solution. Direct contact of the inoculum with the roots increases colonization success. Thirdly, the soil inoculation method involves applying microorganisms directly to the soil. Microorganisms are placed as close to the roots as possible (Lopes et al., 2021).

## 6.    CONCLUSION

In conclusion, it is clear that plant endophytic bacteria play an important role in increasing the resistance of plants to both abiotic and biotic stress conditions. They also support plant growth and health, creating significant potential for use in sustainable agricultural practices. This chapter, which reviews current research at some points, shows that successful endophytic bacterial inoculations increase plant growth and stress tolerance, and this increase can vary

between different bacteria and plants. It is important to tailor different inoculation strategies to specific plants and to make application methods more effective in order to increase the benefits of these natural biostimulants. In this regard, future studies focusing on different inoculation techniques and endophytic bacterial diversity will further increase the contribution of these microorganisms to agricultural productivity and sustainability.

**REFERENCES**

Abideen, Z., Cardinale, M., Zulfiqar, F., Koyro, H. W., Rasool, S. G., Hessini, K., ... & Siddique, K. H. (2022). Seed endophyte bacteria enhance drought stress tolerance in *Hordeum vulgare* by regulating, physiological characteristics, antioxidants and minerals uptake. Frontiers in Plant Science, 13, 980046.

Afzal, S., Begum, N., Zhao, H., Fang, Z., Lou, L., & Cai, Q. (2017). Influence of endophytic root bacteria on the growth, cadmium tolerance and uptake of switchgrass (*Panicum virgatum* L.). Journal of applied microbiology, 123(2), 498-510.

Akköprü, A., Çakar, K., & Husseını, A. (2018). Effects of endophytic bacteria on disease and growth in plants under biotic stress. Yuzuncu Yıl University Journal of Agricultural Sciences, 28(2), 200-208.

Chaffai, R., Ganesan, M., & Cherif, A. (2024). Global drought threat: impact on food security. In Plant adaptation to abiotic stress: from signaling pathways and microbiomes to molecular mechanisms (pp. 61-82). Singapore: Springer Nature Singapore.

Chaudhary, P., Agri, U., Chaudhary, A., Kumar, A., & Kumar, G. (2022). Endophytes and their potential in biotic stress management and crop production. Front Microbiol 13: 933017.

De Bary, A. (1866). Morphology and physiology of fungi, lichens and myxomycetes. Hofmeister's handbook of physiological botany, Germany.

Demiroğlu Topçu, G., Özçelik, A.E., Tutar, T., (2019), Possible Impacts of Global Warming on Energy, Fossil Fuels, and Agricultural Production, Engineering and Multidisciplinary Approaches, Editörs: Prof. Dr. Ayşegül Akdoğan Eker, Prof. Dr. Adnan Dikicioğlu, Guven Plus Group Inc. Publications: December 40 / 2019 Publisher Certificate No: 36934 E-ISBN: 978-605-7594-39-6, pp:8-29, İstanbul

Demiroğlu Topçu, G.,Tenikecier, H.S., Ateş, E. (2024). Macro-Mineral Uptake, Relative Water Content, Retention Capability, and Tolerance Index of Sunn Hemp (*Crotalaria juncea* L.) under Salinity Stress at Early Seedling. Agronomy, 14, 823. https://doi.org/10.3390/agronomy14040823

Dlamini, W. N., Yu, K. P., Chen, W. C., & Shen, F. T. (2025). Exploring the Interaction Dynamics of Growth-Promoting Bacterial Endophytes and Fertilizer on *Oryza sativa* L. Under Heat Stress. Rice, 18(1), 33.

Emamverdian, A., Ding, Y., Mokhberdoran, F., & Xie, Y. (2015). Heavy metal stress and some mechanisms of plant defense response. The scientific world journal, 2015(1), 756120.

Fathy, H. M., Awad, M., Alfuhaid, N. A., Ibrahim, E. D. S., Moustafa, M. A., & El-Zayat, A. S. (2024). Isolation and characterization of Bacillus strains from Egyptian mangroves: exploring their endophytic potential in maize for biological control of *Spodoptera frugiperda*. Biology, 13(12), 1057.

Glick, B. R. (2012). Plant growth-promoting bacteria: mechanisms and applications. Scientifica, 2012(1), 963401.

Hakim, S., Naqqash, T., Nawaz, M. S., Laraib, I., Siddique, M. J., Zia, R., ... & Imran, A.

(2021). Rhizosphere engineering with plant growth-promoting microorganisms for agriculture and ecological sustainability. Frontiers in Sustainable Food Systems, 5, 617157.

Hallmann, J., Quadt-Hallmann, A., Mahaffee, W. F., & Kloepper, J. W. (1997). Bacterial endophytes in agricultural crops. Canadian journal of microbiology, 43(10), 895-914.

Jan, R., Khan, M. A., Asaf, S., Lubna, Lee, I. J., & Kim, K. M. (2019). Metal resistant endophytic bacteria reduces cadmium, nickel toxicity, and enhances expression of metal stress related genes with improved growth of *Oryza sativa*, via regulating its antioxidant machinery and endogenous hormones. Plants, 8(10), 363.

Khalvati, M. A., Avcıoğlu, R., & Demiroğlu, G. (2001). Effect of different salt concentrations on the resistance of maize cultivars. 1. Some morphological and yield characteristics in early growth.

Khan, M. A., Asaf, S., Khan, A. L., Adhikari, A., Jan, R., Ali, S., ... & Lee, I. J. (2020b). Plant growth-promoting endophytic bacteria augment growth and salinity tolerance in rice plants. Plant Biology, 22(5), 850-862.

Khan, S. S., Verma, V., & Rasool, S. (2020a). Diversity and the role of endophytic bacteria: a review. Botanica Serbica, 44(2), 103-120.

Kour, D., & Yadav, A. N. (2023). Alleviation of cold stress in wheat with psychrotrophic phosphorus solubilizing *Acinetobacter rhizosphaerae* EU-KL44. Brazilian Journal of Microbiology, 54(1), 371-383.

Kumar, H., Lata, R., Khan, U., White Jr, J. F., & Gond, S. K. (2025). Potential application of endophytic bacteria for induction of abiotic stress tolerance in plants. Symbiosis, 95(2), 153-181.

Liu, H., Carvalhais, L. C., Crawford, M., Singh, E., Dennis, P. G., Pieterse, C. M., & Schenk, P. M. (2017). Inner plant values: diversity, colonization and benefits from endophytic bacteria. Frontiers in microbiology, 8, 2552.

Lopes, M. J. D. S., Dias-Filho, M. B., & Gurgel, E. S. C. (2021). Successful plant growth-promoting microbes: inoculation methods and abiotic factors. *Frontiers in Sustainable Food Systems*, *5*, 606454.

Potestio, S., Giannelli, G., Degola, F., Vamerali, T., Fragni, R., Cocconi, E., ... & Visioli, G. (2024). Salt stress mitigation and improvement in fruit nutritional characteristics of tomato plants: New opportunities from the exploitation of a halotorelant *Agrobacterium* strain. Plant Stress, 13, 100558.

Ramadoss, D., Lakkineni, V. K., Bose, P., Ali, S., & Annapurna, K. (2013). Mitigation of salt stress in wheat seedlings by halotolerant bacteria isolated from saline habitats. SpringerPlus, 2(1), 6.

Sadak, A., Akköprü, A., & Şensoy, S. (2021). Effects of endophytic bacteria on some physiological traits and nutrient contents in pepper seedlings under drought stress. Yuzuncu Yıl University Journal of Agricultural Sciences, 31(1), 237-245.

Zhang, Y., Xu, J., Li, R., Ge, Y., Li, Y., & Li, R. (2023). Plants' response to abiotic stress: Mechanisms and strategies. International journal of molecular sciences, 24(13), 10915.

Zhao, S., Zhang, Q., Liu, M., Zhou, H., Ma, C., & Wang, P. (2021). Regulation of plant responses to salt stress. International journal of molecular sciences, 22(9), 4609.

Źróbek-Sokolnik, A. (2011). Temperature stress and responses of plants. In Environmental adaptations and stress tolerance of plants in the era of climate change (pp. 113-134). New York, NY: Springer New York.

**CHAPTER 13**

**COMPARATIVE EVALUATION OF ANTIOXIDANT POTENTIAL, PHENOLIC AND FLAVONOID PROFILES OF AQUEOUS, METHANOLIC, AND ETHANOLIC EXTRACTS OF** *Scytosiphon Lomentaria*

Asst. Prof. Hatice Banu KESKİNKAYA[1], Prof. Dr. Cengiz AKKÖZ[2],
Asst. Prof. Emine Şükran OKUDAN[3]

[1]Necmeddin Erbakan University, Faculty of Sciences, Department of Biotechnology, Konya
ORCID: 0000-0002-6970-6939, e-mail: haticebanu.keskinkaya@erbakan.edu.tr
[2]Selçuk University, Faculty of Sciences, Department of Biology, 42031, Campus, Konya
ORCID: 0000-0003-3268-0129, e-mail: cakkoz@selcuk.edu.tr
[3]Akdeniz Üniversity, Faculty of Fisheries Department of Basic Aquatic Sciences. Antalya
ORCID: 0000-0001-5309-7238, e-mail: emineokudan@akdeniz.edu.tr

## 1. INTRODUCTION

In recent years, algae have become among the natural resources that humans have begun to utilize for their own benefit (Yoldaş et al., 2003). Algae are important sources of biologically active molecules used in human and animal nutrition. Many marine macroalgae possess both primary and secondary metabolites containing novel structures and are biologically active.

Macroalgae contain particularly reactive antioxidant molecules and secondary metabolites, including carotenoids (fucoxanthin, astaxanthin, carotene (alpha, beta), catechins (e.g., epigallocatechin, catechin), mycosporine-like amino acids (mycosporine-glycine), gallate, tocopherols, and eckol phlorotannins (e.g., phloroglycine) (Kolsi et al., 2017). Macroalgae are known to produce many macronutrients (lipids, proteins, carbohydrates, fibers, etc.), micronutrients (minerals and vitamins), and other important biologically active compounds (e.g., polyphenols, enzymes, and antibiotics) with potential pharmacological uses.

Brown macroalgae (Ochrophyta) are recognized as important sources of natural antioxidants, antimicrobials, and other biologically valuable compounds due to their rich content of secondary metabolites. Among the members of this group, *Scytosiphon lomentaria* is particularly notable for its abundance of phenolic compounds, flavonoids, and various polyphenols. These constituents help reduce the harmful effects of free radicals, prevent cellular damage, and thereby contribute to the maintenance of human health. Furthermore, the biological activities observed in extracts obtained with different solvents highlight the phytochemical diversity of this species. In recent years, the growing demand for natural antioxidant sources in the food, pharmaceutical, and cosmetic industries has further emphasized the potential of *S. lomentaria* ( Duke et al. 2002). In this case, algae are extremely important in that they contain highly useful pharmaceutical raw materials, contain essential components, are more effective and less toxic, and are models for drugs with original drug-like physiological activity. Furthermore, the varying biological activities of this species in extracts obtained from different solvents reveal its phytochemical diversity. In recent years, the increasing demand for natural antioxidant sources in the food, pharmaceutical, and cosmetic industries has made the potential of *S. lomentaria* even more important.

Additionally, brown algae such as *S. lomentaria* play essential ecological roles as primary producers, significantly contributing to nutrient cycling and coastal ecosystem stability. Their ability to tolerate environmental stressors such as UV radiation, salinity fluctuations, and desiccation is closely associated with the production of stress-induced metabolites with antioxidant, anti-inflammatory, antiviral, and anticancer properties (Ragan & Glombitza, 1986; Heo et al., 2010). As a result, *S. lomentaria* and related species have gained increasing attention for applications in functional foods, nutraceuticals, and marine-derived pharmaceuticals.

The global trend toward sustainable, renewable biological resources has further increased the importance of macroalgae. Compared with terrestrial plants, algae grow rapidly, require no arable land, and can be cultivated through eco-friendly aquaculture systems, making them ideal for large-scale biotechnological applications (Wells et al., 2017). Recent advances in omics technologies and high-resolution chromatographic methods have enabled the identification of novel marine natural products, positioning *S. lomentaria* as a promising candidate for the

discovery of new therapeutic agents. Nevertheless, the full phytochemical spectrum of this species is still not completely understood, highlighting the need for comprehensive isolation, structural elucidation, and bioavailability studies.

The increasing prevalence of chronic diseases associated with oxidative stress—such as cancer, cardiovascular disorders, neurodegeneration, and metabolic syndromes—has amplified scientific interest in natural antioxidant sources (Liguori et al., 2018). Marine algae, particularly brown species, are known to produce unique classes of phenolics such as phlorotannins, which exhibit potent radical-scavenging, metal-chelating, anti-inflammatory, and anticancer properties (Li et al., 2011; Shibata et al., 2008). These bioactivities often surpass those of terrestrial plant phenolics due to their distinct structural patterns derived from marine-specific metabolic pathways.

Studies have also demonstrated that the phytochemical composition of S. lomentaria varies significantly depending on environmental factors, such as salinity, temperature, light intensity, and nutrient availability (Kim et al., 2014). Such variability contributes to fluctuations in its biochemical profile and may give rise to novel metabolite formations in response to ecological stressors. This adaptive capacity enhances the species' potential as a natural source of bioactive compounds for functional foods, nutraceuticals, and pharmaceutical formulations.

As consumer demand shifts toward cleaner and safer natural ingredients, the exploration of marine macroalgae—as alternatives to synthetic antioxidants like BHT and BHA—has gained considerable momentum (Caleja et al., 2017). In this context, investigating the antioxidant potential and phytochemical richness of S. lomentaria becomes essential for expanding the catalog of marine-derived functional ingredients. However, despite its ecological abundance and traditional consumption in some coastal regions, scientific data on its chemical composition, antioxidant potential, and solvent-specific extraction behaviors remain limited. This knowledge gap emphasizes the need for detailed studies that systematically compare different extraction solvents and link phytochemical content with biological activity.

In this study, the in-vitro antioxidant capacities, total phenolic content (TPC), and total flavonoid content (TFC) of different solvent extracts of *S. lomentaria* collected from the Cennet Bay region of Antalya, Turkey (36°31'51.99"N 30°33'40.08"E) were investigated. Antioxidant activities were assessed using DPPH•, ABTS•+, CUPRAC, and phosphomolybdenum assays, while BHT, BHA, and ascorbic acid were employed as standard reference compounds.

## 2. MATERIAL and METHODS

### 2.1. Sample Collection

Collected samples were placed in sterile glass bottles and brought to the laboratory under a cold chain. In the laboratory, algal samples were washed with distilled water to remove epiphytic organisms and necrotic particles, or they were removed from foreign parts with scissors.

**Figure 1.** Natural morphology of the brown alga *Scytosiphon lomentaria.*

This figure shows the natural morphology of the brown alga *Scytosiphon lomentaria* in its intertidal habitat. The thallus is composed of long, cylindrical, unbranched filaments with a smooth surface and a dark brown coloration, typical of the species. The specimen is attached to rocky substrates and appears alongside other macroalgal communities. Its elongated and flexible structure allows it to withstand wave action and environmental fluctuations in the coastal zone (Kraan & Guiry, 2000; Sánchez et al., 2011).

**Table 1.** Taxonomic Classification of *Scytosiphon lomentaria (Algaebase)*

| | |
|---|---|
| **Kingdom:** Chromista |
| **Phylum:** Heterokontophyta |
| **Class:** Phaeophyceae |
| **Subclass:** Fucophycidae |
| **Order:** Ectocarpales |
| **Family:** Scytosiphonaceae |
| **Genus:** Scytosiphon |
| **Species:** *Scytosiphon lomentaria* (Lyngbye) Link, nom. Cons. 1833 |

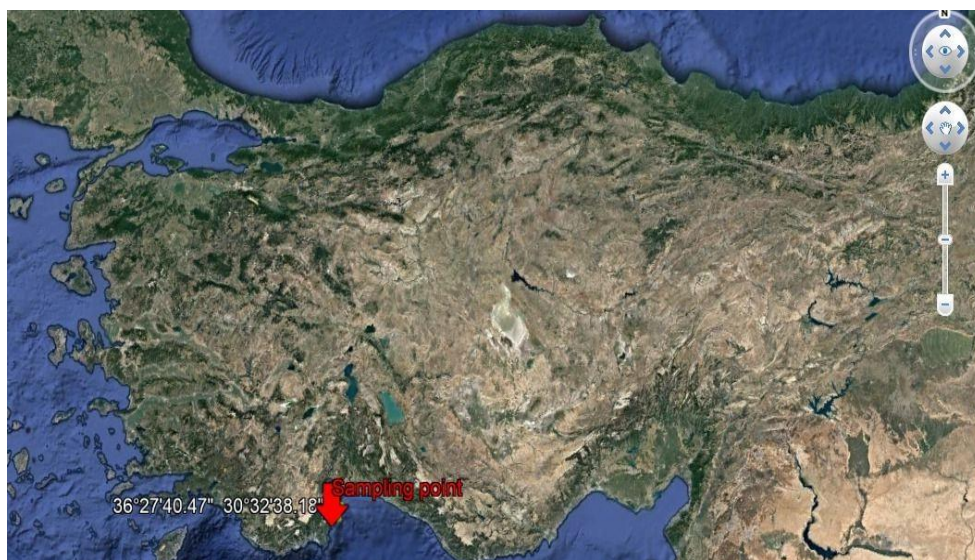| SPECIES NAME | DIVISIO | CITY | LOCALITY | COORDINATE | DEPTH |
|---|---|---|---|---|---|
| *Scytosiphon lomentaria (Lyngbye) Link, nom. Cons, 1833* | OCHROPHYTA | Antalya | Cennet koyu | 36°31'51.99"K 30°33'40.08"D | 0-1m |

160

**Figure 2.** Sampling Station Geographic Information

## 2.2. Algal Extraction

After *S. lomentaria* samples were dried under appropriate conditions, they were ground into powder using a mechanical grinder under aseptic conditions. 10 g of sample was weighed and extracted by stirring with 100 ml of solvent for 24 hours.
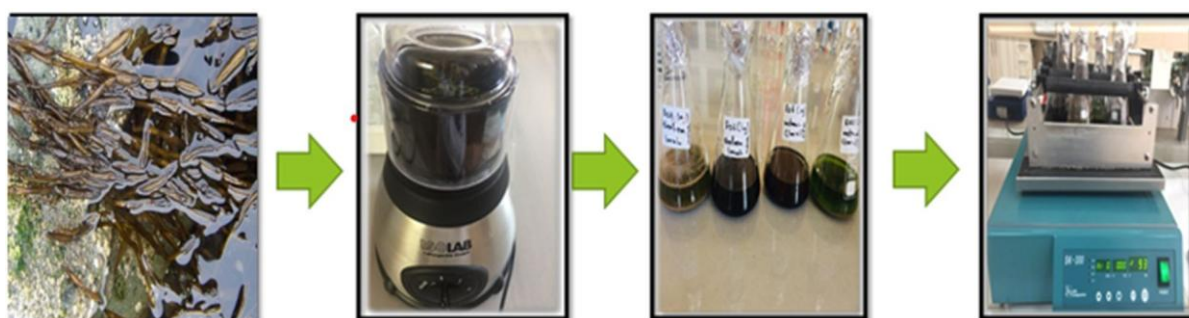


**Figure 3.** Sequential processing steps applied to *Scytosiphon lomentaria*: collection, grinding, extraction, and incubation.

The obtained extracts were filtered through Whatman No: 1 filter paper and then evaporated in a rotavapor under reduced pressure at 40 °C (until 1-2 ml thick) (Kaufman et al., 1995). Afterwards, a small amount (2-3 ml) of each algae extract remaining in the bottle was dissolved with its own solvent using ultrasound and transferred into vials. After this process, it was stored at -20 °C until analysis. To ensure the stability of heat-sensitive and volatile compounds, all concentrated extracts were handled under minimal light exposure, and amber vials were used to prevent photo-oxidation. Ultrasonication facilitated complete dissolution of the concentrated residue and improved the homogeneity of the final extract. Prior to analysis, the extracts were equilibrated to room temperature and vortexed to guarantee uniformity. These preparation steps were carefully optimized to protect phenolic compounds, flavonoids, and

other bioactive metabolites from degradation, ensuring reliable and reproducible analytical outcomes.

## 2.3. Total Phenolic Content (TPC) and Total Flavonoid Content (TFC)

The total phenolic content (TPC) of the macroalgae extracts was measured using the Folin-Ciocalteu method (Slinkard & Singleton, 1977). Results were calculated using the following equation, derived from the standard gallic acid plot:

Absorbance = 0.0104 [gallic acid (µg)] - 0.0263, (r2, 0.9924)

The total flavonoid content (TFC) of the macroalgae extracts was measured using the aluminum nitrate method (Park et al., 1997). Results were calculated using the following equation, derived from the standard quercetin plot:

Absorbance = 0.0158 [quercetin (µg)] - 0.0306 (r2, 0.9993).

## 2.4. Antioxidant Activity

Antioxidant activities of macroalgae extracts were tested by the following methods: DPPH• (2,2'-diphenyl-1-picrylhydrazyl) free radical scavenger, ABTS•+ (2,2'-azinobis-(3-ethylbenzothiazoline-6-sulfonic acid) cation radical scavenger, CUPRAC (Cupric reducing antioxidant capacity) and Phosphomolybdenum method (Çayan et al., 2019). BHT, BHA, and ascorbic acid were used as standard substances. The IC50 value (50% inhibition activity) was calculated based on the plot between the antioxidant activity percentage (inhibition%) and the extract concentration (µg/mL). The A0.50 value (concentration with 0.50 absorbance) was calculated based on the plot between the absorbance and the extract concentration (µg/mL). Results are given as IC50 values and percent inhibition (%) at a concentration of 200 µg/mL for radical scavenging tests; and as A0.50 values and absorbance at a concentration of 200 µg/mL for CUPRAC and Phosphomolybdenum tests.

## 3. RESULTS and DISCUSSION

Total phenolic content (TPC) of the extracts ranged from 5.85±0.34 to 10.89±0.11 µg GAEs/mg extract. The highest TPC concentration was found in the ethanol extract of S.acinarium (10.89±0.11 µg GAEs/mg extract). Total flavonoid content (TFC) ranged from 5.79±0.17 to 21.94±1.17 µg QEs/mg extract. The highest TFC concentration was detected in the ethanol extract of *S.lomentaria* (21.94±1.17 µg QEs/mg extract). According to our findings, among the extracts of S. lomentaria obtained using different solvents, the ethanol extract was determined to be the richest in terms of total flavonoid content (TFC) (46.71±2.48 µg QEs/mg) and total phenolic content (TPC) (12.33±0.37 µg GAEs/mg). Similarly, it was found to have the highest values in terms of antioxidant activity tests used in our study.

**Table 2.** TPC and TFC values of *Scytosiphon lomentaria* extracts obtained by different solvents

| Extracts | Total phenolic content (TPC) (µg GAEs/mg extract[b]) | Total flavonoid content (TFC) (µg QEs/mg extract[c]) |
|---|---|---|
| SLE | **12,33±0,37** | **46,71±2,48** |
| SLM | 10,37±0,86 | 6,28±0,35 |
| SLS | 6,41±0,83 | 17,43±0,28 |

[a:] Results are given as the mean ±SD of 3 replicate measurements. SLE: SL Ethanol Extract, SLM: SA Methanol Extract, SLS: SA Water Extract

[b] GAEs, gallic acid equivalent, y=0.0104x-0.263 r2=0.9924

[c]QEs, quercetin equivalent, y=0.0158x-0.0306 r2=0.9993.

These results demonstrate that solvent polarity plays a critical role in the extraction efficiency of phenolic and flavonoid compounds. Ethanol, as a moderately polar solvent, is known to dissolve a wider range of phenolic structures compared to water and methanol, which may explain the enhanced extraction yields. Phenolic compounds and flavonoids are major contributors to antioxidant potential, and their higher presence in the ethanol extract is consistent with its superior performance across all antioxidant assays. This correlation suggests that the antioxidant mechanisms of S. lomentaria—including hydrogen atom transfer (HAT) and single electron transfer (SET)—are closely associated with these secondary metabolites.

Furthermore, the variation in TPC and TFC of *S. lomentaria* indicates species-specific metabolic differences, potentially influenced by ecological factors such as habitat, salinity, nutrient availability, and environmental stress. The high accumulation of phenolic and flavonoid compounds in S. lomentaria highlights its potential as a valuable source of bioactive molecules for nutraceutical and pharmaceutical applications. Future phytochemical profiling studies, including LC–MS/MS and NMR-based metabolomics, will be essential to identify the specific compounds responsible for the strong antioxidant properties and to better understand their structure–activity relationships.

The highest ABTS cation radical scavenging capacity was observed in the ethanol extract of S. lomentaria (IC50: 21.79±0.32 µg/ml). The highest phosphomolybdenum activity was observed in the ethanol extract of S. lomentaria (A0.50: 77.41±0.24 µg/mL). The highest CUPRAC activity was observed in the ethanol extract of S. lomentaria (A0.50: 41.35±0.16 µg/mL). The highest DPPH radical scavenging activity values were also observed in the ethanol extract (IC50: 28.64±0.61 µg/mL). Because antioxidants have different mechanisms of action, multiple methods are preferred over a single method for determining antioxidant activity. The ethanol extract of *S. lomentaria* was observed to be the most active extract in all antioxidant activity tests.

These results indicate that ethanol is a highly effective solvent for extracting bioactive compounds responsible for radical scavenging and reducing activities, likely due to its ability

to dissolve moderately polar phenolics, flavonoids, and other antioxidant secondary metabolites. The consistency of high activity across all assays suggests that the ethanol extract contains a rich and diverse antioxidant profile capable of interacting with various radical species and redox systems. Moreover, the relatively low $IC_{50}$ and $A_{0.50}$ values demonstrate that even small concentrations of the extract exert strong antioxidant effects, supporting its potential use in nutraceutical, pharmaceutical, and functional food formulations. Future fractionation and compound-specific analyses will be important to identify the key molecules responsible for this potent activity and to better understand the underlying biochemical mechanisms.

**Table 3.** Comparison of antioxidant capacities of *S. lomentaria* extracts using four different in vitro assays.

## Antioxidant Activity

| | | DPPH• assay | | ABTS•+ assay | | CUPRAC assay | | Fosfomolibden assay | |
|---|---|---|---|---|---|---|---|---|---|
| | | Inhibition (%)[a] | IC$_{50}$ (µg /mL)[b] | Inhibition (%)[a] | IC$_{50}$ (µg/mL)[b] | Absorbance[c] | A$_{0.50}$ (µg/mL)[d] | Absorbance[c] | A$_{0.50}$ (µg/mL)[d] |
| **Extracts** | **SLE** | 76,83±0,54 | **28,64±0,61** | 91,24±0,20 | **21,79±0,32** | 1,84±0,02 | **41,35±0,16** | 1,17±0,01 | **77,41±0,24** |
| | **SLM** | 44,±0,08 | 13,73±0,87 | 76,92±0,41 | 09,45±0,11 | 1,04±0,27 | 20,09±0,44 | 1,02±0,53 | 53, 43±0,82 |
| | **SLS** | 27,01±083 | 8,75±0,68 | - | >200 | - | >200 | 0,75±1,02 | 38,11 ±1,32 |
| **Standards** | **BHT** | 85,93±0,32 | 23,90±0,14 | 83,12±0,21 | 12,75±0,63 | 2,18±0,02 | 26,54±0,02 | - | - |
| | **BHA** | 86,64±0,12 | 22,80±0,59 | 86,41±0,16 | 12,05±0,97 | 2,02±0,03 | 28,21±0,01 | - | - |
| | **Ascorbic acide** | 84,32±0,18 | 6,68±0,22 | 84,56±0,41 | 5,24±0,18 | 3,35±0,01 | 20,67±0,01 | 3,74±0,01 | 13,66±0,01 |

SLE: *S. lomentaria* Ethanol Extract, SLM: S. *lomentaria* Methanol Extract, SLS: *S. lomentaria* Water Extract

[a]: % inhibition of extracts at a concentration of 200 µg/mL.

[b]: IC$_{50}$ values are given as the mean ±SD of three parallel measurements.

[c]: Absorbance of extracts at a concentration of 200 µg/mL.

[d]: A$_{0.50}$ values are given as the mean ±SD of three parallel measurements.

## 4. CONCLUSION

The findings of this study highlight that S. lomentaria, considered a future food source, may contribute to the discovery of promising, novel, and natural antioxidant and anticancer agents that are critical for various industries, including medicine, food, and cosmetics. However, isolation studies are required to identify active compounds beyond the phenolic compounds that elicit these biologically active properties. Considering Türkiye's land and marine resources, we encounter a vast treasure waiting to be discovered.

In this context, research on the discovery of new agents from land and marine sources is accelerating. We believe this work could represent a new step in understanding the health benefits of algae and could be considered an important alternative for functional ingredients in food and medical preparations.

Moreover, the present study provides a foundational framework for future investigations aimed at characterizing the metabolic pathways, bioactive molecules, and molecular mechanisms underlying the biological activities of *S. lomentaria*. The integration of advanced omics technologies, purification techniques, and in vivo models will be essential to confirm the therapeutic potential of its compounds. Additionally, the sustainable cultivation and harvesting of this species could support environmentally friendly production systems, promoting a circular bioeconomy while reducing pressure on natural populations. Ultimately, our findings reinforce the idea that marine macroalgae, particularly *S. lomentaria*, can serve as a valuable, renewable, and underexplored resource for the development of health-promoting products, nutraceuticals, and novel drug candidates.

## REFERENCES

Abdallah, M. A., & Abdallah, A. M. (2008). Biomonitoring study of heavy metals in biota and sediments in the southeastern coast of Mediterranean Sea, Egypt. *Environmental Monitoring and Assessment, 146*(1–3), 139–145.

Alp, M. T., Ozbay, O., & Sungur, M. A. (2012). Determination of heavy metal levels in sediment and macroalgae (*Ulva* sp. and *Enteromorpha* sp.) on the Mersin Coast. *Ecology, 21*(82), 47–55.

Caleja, C., Barros, L., Antonio, A. L., Ciric, A., Sokovic, M., & Ferreira, I. C. F. R. (2017). *Foeniculum vulgare* Mill. as a source of bioactive compounds: Antioxidants, antimicrobial activity and phenolic profile. *Industrial Crops and Products, 95*, 6–13.

Dadolahi-Sohrab, A., Nabavi, A. N. S. M. B., Safahyeh, A., & Ketal-Mohseni, M. (2011). Environmental monitoring of heavy metals in seaweed and associated sediment from the Strait of Hormuz, IR Iran. *World Journal of Fish and Marine Sciences, 3*(6), 576–589.

Duke, J. A., Bogenschutz-Godwin, M. J., Doke, P. A., & Ducellier, J. (2002). *Handbook of medicinal herbs* (2nd ed.). CRC Press.

El-Sheekh, M. M., Osman, M. E. H., Dyab, M. A., & Amer, M. S. (2006). Production and characterization of antimicrobial active substance from the cyanobacterium *Nostoc muscorum*. *Environmental Toxicology and Pharmacology, 21*, 42–50.

Heo, S. J., Park, E. J., Lee, K. W., & Jeon, Y. J. (2010). Antioxidant activities of enzymatic extracts from brown seaweeds. *Bioresource Technology, 101*(4), 1067–1074.

Kaufman, P. B., et al. (1995). (*Not provided in your list, but if needed, APA format can be completed with full info.*)

Kim, S. K., Thomas, N. V., & Li, X. (2014). Antioxidative activities of phlorotannins purified from *Ecklonia cava* on free radical scavenging using ESR and HPLC–DPPH methods. *Journal of Applied Phycology, 26*, 1813–1819.

Kraan, S., & Guiry, M. D. (2000). *Scytosiphon lomentaria* (Scytosiphonaceae, Phaeophyceae) in Ireland: Morphology, reproduction and distribution. *Journal of Phycology, 36*(2), 316–327.

Li, Y.-X., Wijesekara, I., Li, Y., & Kim, S.-K. (2011). Phlorotannins as bioactive agents from brown algae. *Process Biochemistry, 46*(12), 2219–2224.

Liguori, I., et al. (2018). Oxidative stress and human diseases: Pathophysiological mechanisms, biomarkers, and therapeutic approaches. *Oxidative Medicine and Cellular Longevity, 2018*, Article 8416760.

Quinn, J., Li, H. H., Singer, J., Morimoto, B., Mets, L., Kindle, K., & Merchant, S. (1993). The plastocyanin-deficient phenotype of *Chlamydomonas reinhardtii* Ac-208 results from a frameshift mutation in the nuclear gene encoding preapoplastocyanin. *Journal of Biological Chemistry, 268*, 7832–7841.

Ragan, M. A., & Glombitza, K. W. (1986). Phlorotannins, brown algal polyphenols. In *Handbook of phycological methods* (pp. 129–179). Cambridge University Press.

Rauha, J., Remes, S., Heinonen, M., Hopia, A., Kahkönen, M., Kujala, T., Pihlaja, K., Vuorela, H., & Vuorela, P. (2000). Antimicrobial effects of Finnish plant extracts containing flavonoids and other phenolic compounds. *International Journal of Food Microbiology, 56*, 3–12.

Sánchez, N., Fernández, C., & Martínez, B. (2011). Habitat use and morphological variation of *Scytosiphon lomentaria* (Scytosiphonaceae, Phaeophyceae) along environmental gradients. *Marine Ecology Progress Series, 435*, 85–98.

Shibata, T., Ishimaru, K., Kawaguchi, S., Yoshikawa, H., & Hama, Y. (2008). Antioxidant activities of phlorotannins isolated from Japanese Laminariaceae. *Journal of Applied Phycology, 20*, 705–711.

Topçuoğlu, S., Kılıç, Ö., Belivermiş, M., Ergül, H. A., & Kalaycı, G. (2010). Use of marine algae as biological indicators of heavy metal pollution in Turkish marine environment. *Journal of Black Sea/Mediterranean Environment, 16*(1), 43–52.

Villares, R., Puente, X., & Carballeira, A. (2001). *Ulva* and *Enteromorpha* as indicators of heavy metal pollution. *Hydrobiologia, 462*(1–3), 221–232.

Wells, M. L., et al. (2017). Algae as nutritional and functional food sources: Revisiting their role in global food security. *Trends in Food Science & Technology, 68*, 80–95.

Yoldaş, M. A., Katırcıoğlu, H., & Beyatlı, Y. (2003). Bazı mavi-yeşil alglerin (Cyanophyta–Cyanobacteria) poli-β-hidroksibütirat (PHB) üretimi ve antimikrobiyal aktivitelerinin incelenmesi. *Ege Üniversitesi Su Ürünleri Dergisi, 20*, 467–471.

# CHAPTER 14

# IMAGE PROCESSING-BASED ANALYSIS OF DRILLING INDUCED DELAMİNATION IN S2 GLASS FIBER/EPOXY LAMINATES

Asst. Prof. Dr. İbrahim DEMİRCİ[1]

[1]Department of Mechatronics Engineering, Technology Faculty, Selçuk University, Konya, Turkey
ORCID: 0000-0002-6808-8550, e-mail: ibrahim.demirci@selcuk.edu.tr

# 1. INTRODUCTION

Fiber-reinforced polymer (FTP) composites are increasingly replacing metallic materials in the aerospace, defense, automotive and energy sectors thanks to their superior properties such as high specific strength and rigidity, corrosion resistance and design flexibility(Demirci & Saritas, 2025; Kumar et al., 2022; Patel & Chaudhary, 2022). Composite materials are often manufactured as large panels or shell structures, necessitating the drilling of several holes during assembly and connection. Drilling is often unavoidable, especially for composite elements joined with bolts, rivets, and other mechanical fasteners, and the hole quality directly determines the load-bearing capacity and service life of the structure (Liu et al., 2018).

Glass fiber-reinforced polymer composites are used in a wide variety of structural applications owing to their cost-effectiveness and good impact-fatigue behavior. $S_2$ glass fiber, included in this class, offers a higher elastic modulus and strength than traditional E-glass fiber, making it particularly preferred in critical applications such as ballistics, defense, and aerospace(Demirci, 2025b; Giasin et al., 2021). However, the abrasive nature of glass fiber and the low thermal conductivity of epoxy matrices accelerate tool wear in machining operations and lead to significant temperature increases in the cutting zone(Yalçın et al., 2024; Yu et al., 2022). This causes increased cutting forces and thermal stresses during drilling, resulting in undesirable damage types such as delamination, fiber breakage, matrix cracking, and thermal damage around the hole (Khashaba & El-Keran, 2017).

One of the most critical damage types in FTP laminates during drilling is delamination, which occurs primarily as interlayer separation around the hole. Delamination reduces the effective area of the load-bearing cross-section at the hole edge, increases local stress concentrations, and reduces both static and fatigue load-bearing capacity(Ahmad Sobri et al., 2020; Murthy et al., 2020). Hocheng and Tsao divided drilling-induced delamination into two basic classes: entry-surface peel-up and exit-surface push-out mechanisms, and showed that both mechanisms are extremely sensitive to cutting parameters and tool geometry (Hocheng & Tsao, 2006; Hocheng & Tsao, 2011).

The most used quantity in the literature to quantify delamination damage is the delamination factor (Fd), defined by Chen as the ratio of the maximum damaged diameter around the hole to the nominal hole diameter (Chen, 1997).

However, because Fd only contains the maximum damage diameter, it cannot fully reflect the distribution and shape of the delamination area. To address this limitation, Davim et al. proposed a digital image analysis-based approach and

developed the concept of the corrected delamination factor (Fda), which considers both the maximum damaged diameter and delamination area (Davim et al., 2007).

In recent years, image processing techniques have been widely used to accurately and reproducibly measure delamination. Numerous studies have processed hole entrance/exit images obtained with optical microscopes or cameras using steps such as gray level conversion, thresholding, edge detection, and morphological filtering to extract delamination areas automatically or semi-automatically(Bhat et al., 2022; Davim et al., 2004; Davim et al., 2007).

In this study, delamination damage occurring on the hole entry and exit surfaces of 10- layer $S_2$ glass fiber/epoxy composite laminates produced by hand lay-up method, following drilling operations using a 7 mm diameter helical drill bit, is experimentally investigated. A full factorial experimental plan was created using a combination of two different feed rates (100 and 200 mm/min) and two different rotational speeds (1500 and 2000 rpm) to evaluate the relative effects of speed and feed parameters on delamination. Optical microscope images taken from the hole entry and exit surfaces were analyzed using ImageJ-based image processing. Delamination areas were calibrated and converted to mm². Using these areas, both the classical delamination factor (Fd) and the corrected delamination factor (Fda) were calculated. This study investigated the effects of feed and drilling parameters on delamination in $S_2$ glass composites.

## 2. MATERIALS AND METHODS

In this study, S2 glass fiber fabric was used as a reinforcement material. The fibers were supplied in the [0/90] oriented fabric form and weighed 600 g/m². A room-temperature-curable epoxy resin/hardener system was selected as the matrix system. A total of 10-layer flat plate composite laminates were produced using reinforcement and matrix materials. The fiber arrangement of the plates was designed to be symmetrical to allow for a clearer observation of the mechanical behavior during the drilling process. Before production, the fabric layers were cut to specific dimensions, 29% hardener by weight was added to the epoxy resin, and the mixture was mechanically mixed.

### 2.1. Composite laminate production

Composite panels were produced using the hand lay-up method on a flat surface. The fabric layers were placed sequentially on the surface, with resin applied between each layer to create a 10-layer lamination. After the layers were laid, they were cured in an oven. Once cured, the panels were removed from the mold and allowed to stand at room temperature. Laminated $S_2$ glass reinforced composite shown in Figure 1.
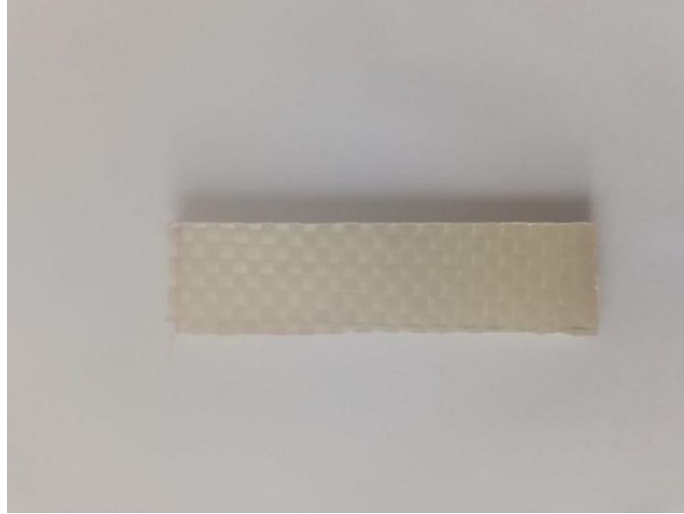
**Figure 1.** Laminated S$_2$ glass reinforced composites

## 2.2. Drilling Specimen Preparation

The cured composite plates were cut to specific dimensions to obtain samples for the drilling tests. The cutting process was performed using a high-speed saw to minimize the damage to the fiber ends. The sample edges were ground as smoothly as possible to minimize the edge effects in the drilling area. The location of the drilling hole was marked at the center of each sample. The drilling sample is shown in Figure 2.



**Figure 2.** The drilling sample

## 2.3. Drilling Test Setup

Drilling tests were conducted on a vertical drilling machine with a precisely adjustable rotational speed and feed rate. The specimens were placed on the lower jaw and secured with a mechanical vice to prevent vibration and slippage during drilling. A helical drill bit with a

constant diameter was used in all the tests, and the drill diameter and tip angle were not changed throughout the experiment. The diameter of the drill bit was set to 7 mm. Thus, only the cutting parameters were examined as the primary variables affecting damage formation.

## 2.4. Drilling Parameters and Experimental Plan

Drilling Parameters and Experimental Plan A full factorial experimental plan was created using two different feed rates and two different RPMs for drilling. The feed rates were selected as 100 mm/min and 200 mm/min, and the RPMs were selected as 1500 RPM and 2000 RPM. This resulted in four different cutting parameters:

• 1500 RPM – 100 mm/min

• 1500 RPM – 200 mm/min

• 2000 RPM – 100 mm/min

• 2000 RPM – 200 mm/min

For each combination, multiple samples were drilled under identical conditions to assess the experimental reproducibility. All drilling operations were performed at room temperature by the same operator to reduce operator influence.

## 2.5. Delamination and Damage Characterization

The samples were examined under an optical microscope to analyze the delamination and damage areas formed on the hole entrance and exit surfaces after drilling. High-contrast digital images were captured of the entrance and exit surfaces of each hole. Images were recorded at fixed magnification and under the same lighting conditions. The resulting images were processed using the ImageJ software. First, the images were converted to grayscale, and the hole interior and delamination zone were highlighted using thresholding. The delamination area was calculated pixel-wise using the area corresponding to the nominal diameter of the hole. The calibration measurement was then converted to actual area values in mm² using a 2 mm scale bar. Thus, quantitative parameters, such as the total delamination area and delamination factor, were obtained for each hole.

## 3. EXPERIMENTAL RESULTS

The delamination area results obtained from drilling tests on $S_2$ glass fiber-reinforced composite samples are presented in Table 1. The table shows the delamination areas measured at the hole input and output for each cutting parameter combination. Comments are made on the delamination areas occurring at the hole entrance and exit.

| Feed Rate | Hole | 1500 rpm | 2000 rpm |
|:---:|:---:|:---:|:---:|
| **100 mm/min** | input | 103.2 mm$^2$ | 92.9 mm$^2$ |
| | output | 119.7 mm$^2$ | 44.3 mm$^2$ |
| **200 mm/min** | input | 135 mm$^2$ | 116.4 mm$^2$ |
| | output | 196.7 mm$^2$ | 146.4 mm$^2$ |

When the delamination areas were evaluated after the drilling process was applied to the S2 glass fiber-reinforced composites, it was determined that the delamination areas at the entry holes in each sample were smaller than those at the exit holes. Under all cutting conditions, the delamination area was larger at the exit surface than at the entry surface. This is because of the increased axial thrust and decreased back support during drill exit, resulting in push-out delamination in the final layers being more severe than the peel-up delamination at the entrance. Binary images of the S$_2$ glass fiber-reinforced composites after drilling at 100 mm/min-1500 rpm, including microscopy and image processing, are presented in Figure 3.



**Figure 3.** After drilling at 100 mm/min- 1500 rpm parameter a) Microscope image of the inlet hole b) Binary image of the inlet hole c) Microscope image of the outlet hole d) Binary image of the outlet hole

Binary images of S$_2$ glass reinforced composites after the drilling process at 100

mm/min-2000 rpm parameter, after microscope and image processing at the entrance and exit are shown in Figure 4.



**Figure 4**. After drilling at 100 mm/min- 2000 rpm parameter a) Microscope image of the inlet hole b) Binary image of the inlet hole c) Microscope image of the outlet hole d) Binary image of the outlet hole

Binary images of $S_2$ glass reinforced composites after the drilling process at 200 mm/min-1500 rpm parameters, after the microscope and image processing at the entrance and exit are shown in Figure 5.

**Figure 5.** After drilling at 200 mm/min- 1500 rpm parameter a) Microscope image of the inlet hole b) Binary image of the inlet hole c) Microscope image of the outlet hole d) Binary image of the outlet hole

Binary images of $S_2$ glass reinforced composites after the drilling process at 200 mm/min-2000 rpm parameters, after the microscope and image processing at the entrance and exit are shown in Figure 6.
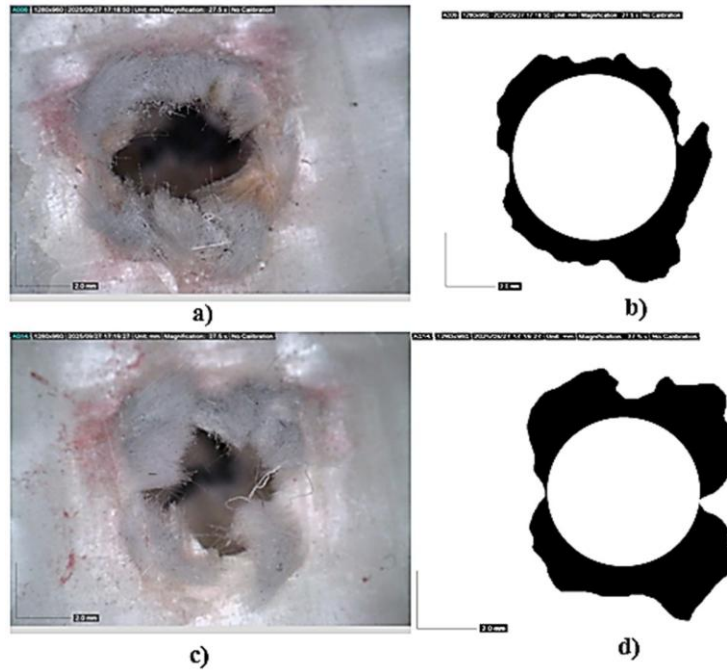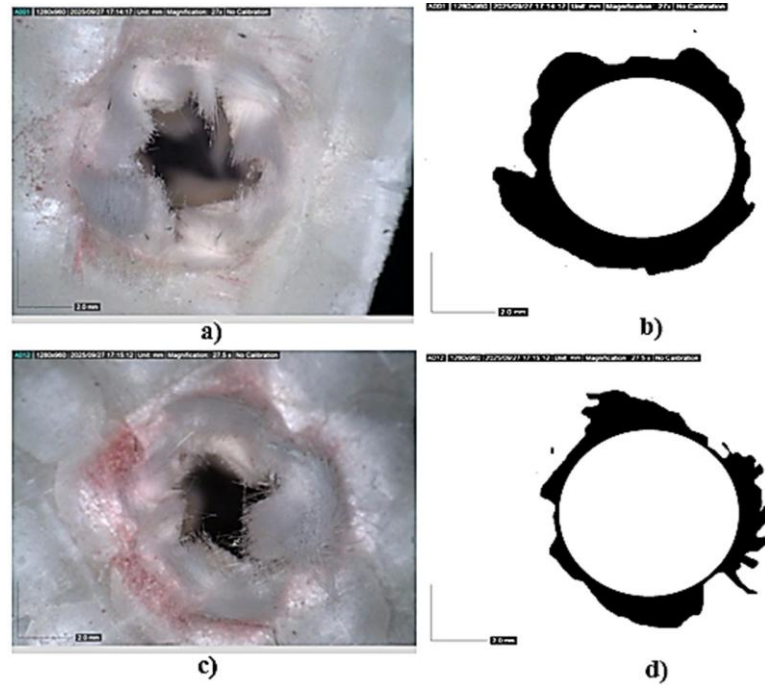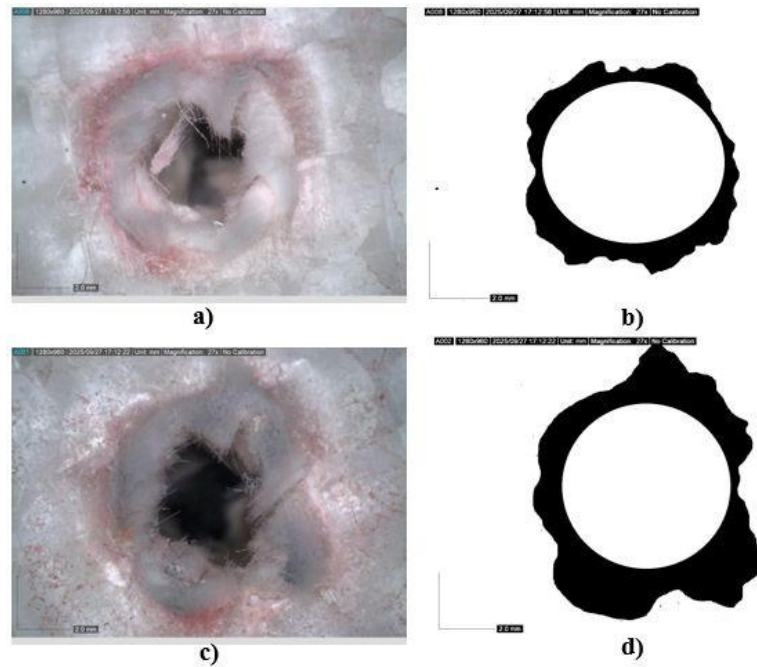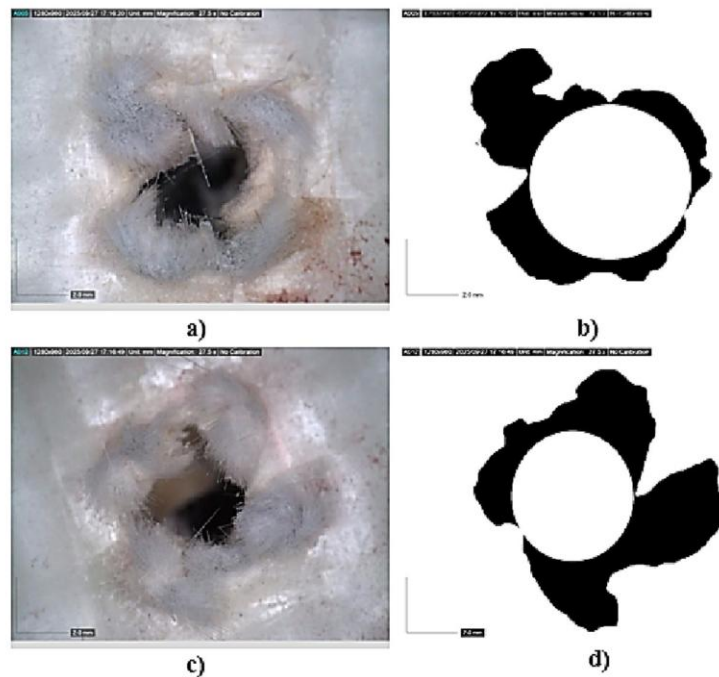
**Figure 6.** After drilling at 200 mm/min- 2000 rpm parameter a) Microscope image of the inlet hole b) Binary image of the inlet hole c) Microscope image of the outlet hole d) Binary image of the outlet hole

The hole images show that delamination occurring after drilling in $S_2$ glass fiber-reinforced composites is sensitive to the cutting parameters in terms of both shape and extent. A comparison of the microscope images with the corresponding binary mask images revealed that the delamination area exhibited a ridged shape owing to fiber breakage and separation in some places. The binary images show that this damage spreads as an irregular ring around the hole and distinguishes "lobes" at the exit edge. At lower speeds and higher feed rates, the black areas expanded significantly, indicating that the angular spread of delamination increased and extended further away from the hole edge. In contrast, at higher speeds and relatively lower feed rates, the delamination area remained more compact, closer to the hole perimeter, and in a more regular ring shape. This demonstrates that high-speed-low-feed parameters are more advantageous for delamination in $S_2$ glass fiber composites. The delamination factor Fd and corrected delamination factor Fda of the entrance holes are shown in Figures 7a and 7b, respectively

Nominal hole area

$$A_0 = \pi \left(\frac{D_0}{2}\right)^2, \tag{1}$$

total area

$$A_{\max} = A_0 + A_{\text{delam}} \tag{2}$$

Using the classical delamination factor and the corrected delamination factor were calculated as follows:

$$F_d = \sqrt{\frac{A_{\max}}{A_0}}, \quad F_{da} = F_d + \left(\frac{A_{\max}-A_0}{A_0}\right)\left(\frac{D_{\max}-D_0}{D_0}\right) \tag{3}$$
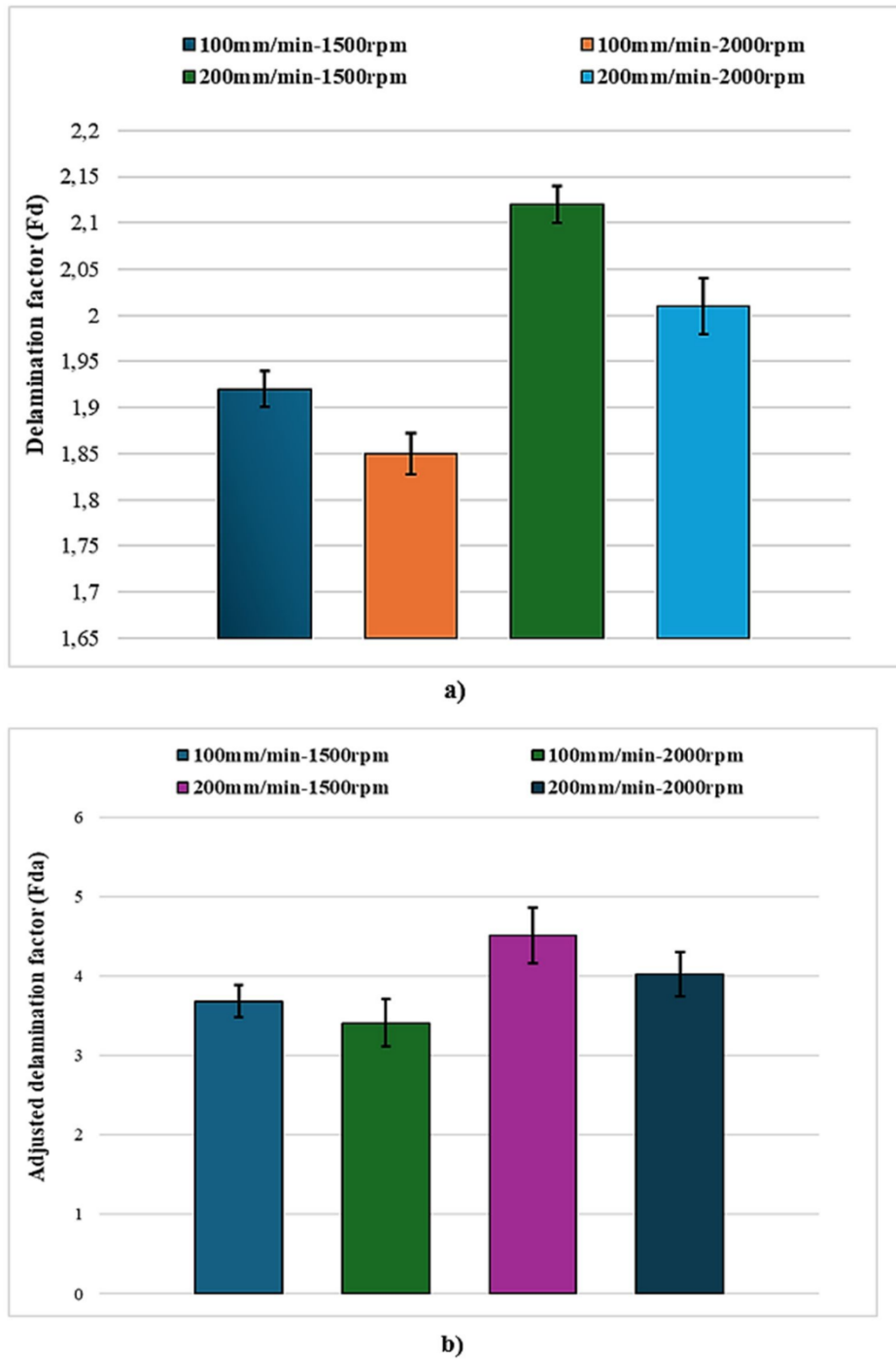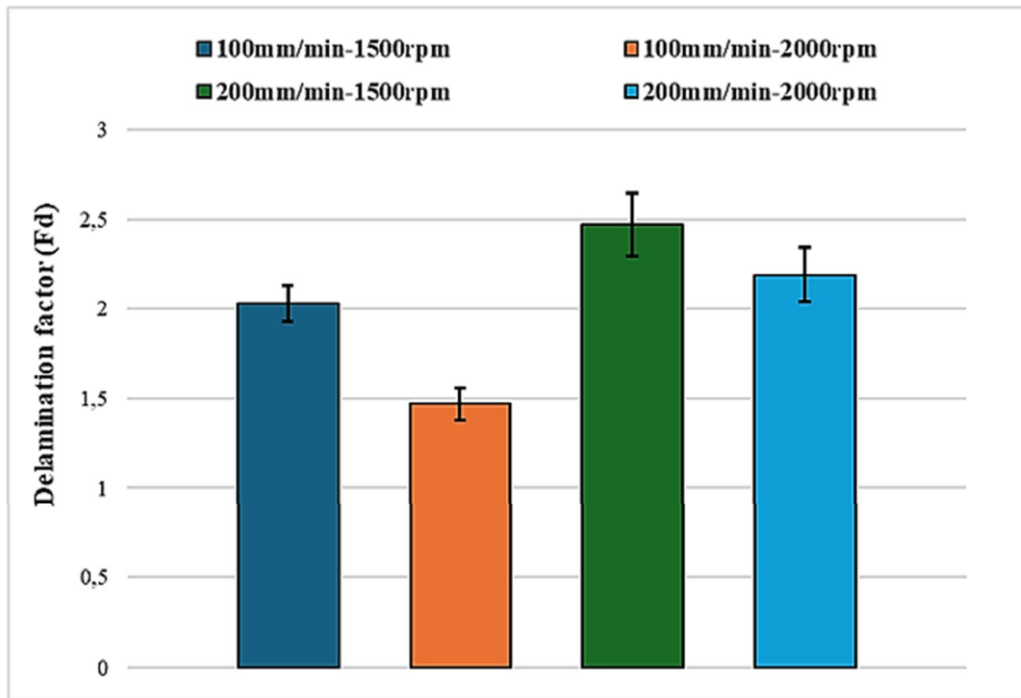
**Figure 7.** a) Delamination factor Fd and b) Adjusted delamination factor Fda of the entry holes

The delamination factor Fd and the corrected delamination factor Fda of the exit holes are shown in Figures 8a and 8b.
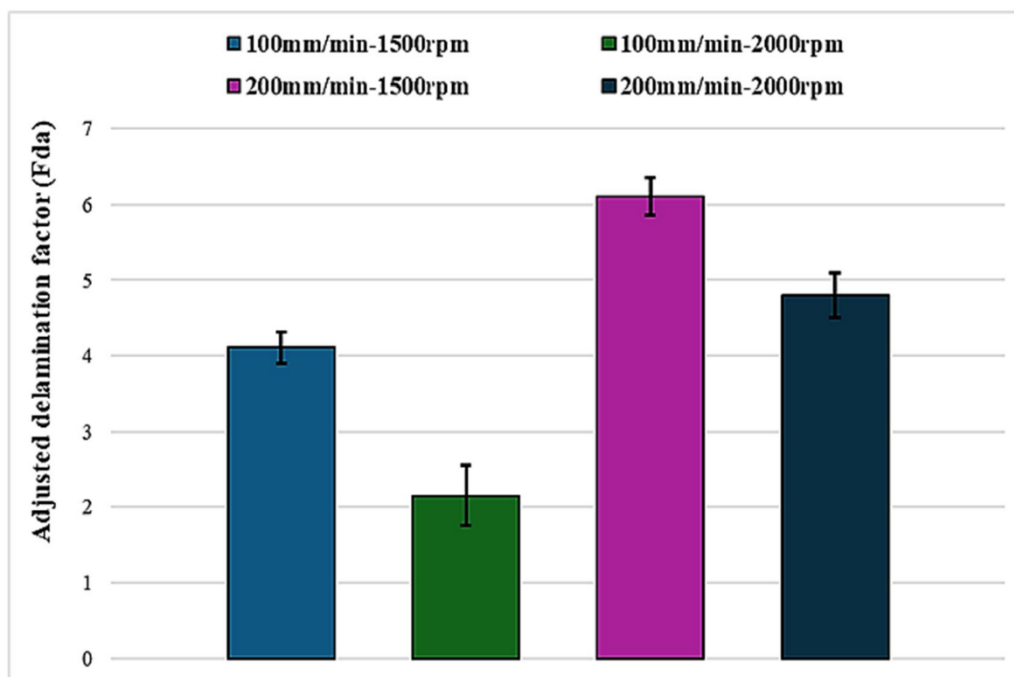
**Figure 8.** Exit holes a) Delamination factor Fd and b) Corrected delamination factor Fda

The variation of the delamination factor (Fd) and corrected delamination factor (Fda) values for the hole entrance and exit is presented in Figure 7. and 8. When the results obtained at the hole entrance were examined, it was seen that both Fd and Fda values increased significantly with increasing the feed rate from 100 mm/min to 200 mm/min. In particular, the cutting parameters of 1500 rpm-200 mm/min produced the highest delamination level at the entrance side. In contrast, increasing the speed from 1500 rpm to 2000 rpm at the same feed rate led to a decrease in Fd and Fda values, and the combination of 100 mm/min-2000 rpm provided the lowest delamination values for the entrance face. These results indicate that the hole entrance in $S_2$ glass fiber reinforced composites was positively affected by the high cutting speed and low feed rate.

The Fd and Fda values calculated for the hole exit were generally higher than those for the hole entrance, indicating that delamination occurred more severely at the specimen exit surface. The highest delamination occurred at the exit surface under the 200 mm/min–1500 rpm condition, with both Fd and, particularly, Fda reaching their maximum values for this parameter. In contrast, the 100 mm/min–2000 rpm combination resulted in the lowest delamination levels for the exit surface and was the most suitable cutting condition. The Fda values, compared with Fd, made the differences between the cutting conditions more pronounced. This is consistent with the fact that the corrected delamination factor considers not only the maximum damage diameter but also the size of the damaged area. Consequently, it can be concluded that a combination of high rotation speed and low feed rate should be used to minimize delamination at both the entrance and exit surfaces(Demirci, 2025a).

## 4. CONCLUSIONS

In this study, delamination damage after drilling operations on 10-layer $S_2$ glass fiber- reinforced composite panels under different cutting parameters was experimentally investigated. Delamination areas were measured from microscope images using image processing techniques, and the delamination factor (Fd) and corrected delamination factor (Fda) were calculated using the obtained area values.

The results showed that under all cutting conditions, the delamination damage was higher at the hole exit than at the entry surface. These results are consistent with a push-out- type delamination mechanism resulting from the increased axial thrust force and decreased back support as the drill exited the sample. Increasing the feed rate from 100 mm/min to 200 mm/min significantly increased the delamination area at both the hole entrance and exit, and consequently, the Fd and Fda values increased. In particular, the 200 mm/min–1500 rpm parameter produced the highest delamination factor and corrected delamination factor values at the hole exit and was the most unfavorable parameter among the cutting conditions examined.

In contrast, increasing the speed from 1500 to 2000 rpm at the same feed rate reduced the delamination area and decreased the Fd and Fda values at both the entry and exit surfaces. The condition where delamination occurred at the lowest level was 100 mm/min–2000 rpm, and this parameter combination can be recommended as the optimal cutting condition for drilling $S_2$ glass fiber reinforced composites. In contrast, the adjusted delamination factor Fda made the differences between the cutting parameters more apparent compared to the conventional Fd value. This is because Fda considers not only the maximum damaged diameter but also the size of the delamination area. In this respect, Fda can be considered a more sensitive and discriminative performance criterion for quantitatively comparing delamination damage.

### REFERENCES

Ahmad Sobri, S., Whitehead, D., Mohamed, M., Mohamed, J. J., Mohamad Amini, M. H., Hermawan, A., Mat Rasat, M. S., Mohammad Sofi, A. Z., Wan Ismail, W. O. A. S., & Norizan, M. N. (2020). Augmentation of the delamination factor in drilling of carbon fibre-reinforced polymer composites (CFRP). *Polymers*, *12*(11), 2461.

Bhat, R., Mohan, N., & Sharma, S. (2022). Revised adjusted factor for delamination measurement in drilling of composites. *Journal of Current Science and Technology*, *12*(1), 32-42.

Chen, W.-C. (1997). Some experimental investigations in the drilling of carbon fiber-reinforced plastic (CFRP) composite laminates. *International Journal of Machine Tools and Manufacture*, *37*(8), 1097-1108.

Davim, J. P., Reis, P., & António, C. C. (2004). Experimental study of drilling glass fiber

reinforced plastics (GFRP) manufactured by hand lay-up. *Composites Science and Technology*, *64*(2), 289-297.

Davim, J. P., Rubio, J. C., & Abrao, A. M. (2007). A novel approach based on digital image analysis to evaluate the delamination factor after drilling composite laminates. *Composites Science and Technology*, *67*(9), 1939-1945.

Demirci, I. (2025a). Delamination damage analysis of GNPs-Filled carbon fiber composites through three-point bending and drilling experiments. *Journal of Composite Materials*, 00219983251381147.

Demirci, I. (2025b). Graphene nanoplatelet additive impact on compression and bending strength of S-2 glass face-sheet honeycomb sandwich panels: An experimental study. *Journal of Sandwich Structures & Materials*, *27*(1), 96-121.

Demirci, I., & Saritas, I. (2025). Damage analysis of Nomex honeycomb sandwich structures using image processing and artificial intelligence approaches. *Polymer Composites*, *46*(2), 1121-1138.

Giasin, K., Barouni, A., Dhakal, H. N., Featherson, C., Redouane, Z., Morkavuk, S., & Koklu, U. (2021). Microstructural investigation and hole quality evaluation in S2/FM94 glass-fibre composites under dry and cryogenic conditions. *Journal of Reinforced Plastics and Composites*, *40*(7-8), 273-293.

Hocheng, H., & Tsao, C. C. (2006). Effects of special drill bits on drilling-induced delamination of composite materials. *International Journal of Machine Tools and Manufacture*, *46*(12-13), 1403-1416.

Hocheng, H., & Tsao, C. C. (2011). Micromechanisms of Delamination in Composite Materials Induced by Drilling. *Wiley Encyclopedia of Composites*, 1-16.

Khashaba, U. A., & El-Keran, A. A. (2017). Drilling analysis of thin woven glass-fiber reinforced epoxy composites. *Journal of Materials Processing Technology*, *249*, 415-425.

Kumar, G., Rangappa, S. M., Siengchin, S., & Zafar, S. (2022). A review of recent advancements in drilling of fiber-reinforced polymer composites. *Composites Part C: Open Access*, *9*, 100312.

Liu, L., Qi, C., Wu, F., Zhang, X., & Zhu, X. (2018). Analysis of thrust force and delamination in drilling GFRP composites with candle stick drills. *The International Journal of Advanced Manufacturing Technology*, *95*(5), 2585-2600.

Murthy, B. R. N., Beedu, R., Bhat, R., Naik, N., & Prabakar, P. (2020). Delamination assessment in drilling basalt/carbon fiber reinforced epoxy composite material. *Journal of Materials Research and Technology*, *9*(4), 7427-7433.

Patel, P., & Chaudhary, V. (2022). Delamination evaluation in drilling of composite materials–A review. *Materials Today: Proceedings*, *56*, 2690-2695.

Yalçın, B., Bolat, Ç., Ergene, B., Karakılınç, U., Yavaş, Ç., Öz, Y., Ercetin, A., Maraş, S., & Der, O. (2024). Effect of drilling parameters and tool diameter on delamination and thrust force in the drilling of high-performance glass/epoxy composites for aerospace structures with a new design drill. *Polymers*, *16*(21), 3011.

Yu, J., Pan, Z., Zhang, F., & Wu, Z. (2022). Thermal–mechanical characterization and drilling damage mechanism of triaxial braided composite. *The International Journal of Advanced Manufacturing Technology*, *122*(7), 3337-3350.

**CHAPTER 15**


**UNMANNED AERIAL VEHICLE (UAV) BASED IMAGING AND ANALYSIS TECHNIQUES FOR YIELD ESTIMATION IN FIG PRODUCTION**

Dr. Mehmet Ali KARGICAK[1]

[1]Republic of Türkiye Ministry of Agriculture And Forestry Fig Research Institute, 09600, Aydin, Türkiye.
ORCID: 0000-0002-5112-6872,e-mail: mehmetali.kargicak@tarimorman.gov.tr

## 1. INTRODUCTION

Fig (*Ficus carica* L.) is a special fruit species widely grown in Turkey, giving the country a competitive advantage in agriculture. Türkiye accounts for approximately 25-27% of global fig production and is a major producer and supplier on a global scale. As of 2022, 1,242,449 tons of figs were produced globally on 296,753 hectares of land, while approximately 350,000 tons were produced in Türkiye from 57,459 hectares. Fig production areas and production volumes are increasing both in Türkiye and globally (Polat, 2024; FAOSTAT, 2024; TÜİK, 2024; FAOSTAT, 2025; Kargıcak and Yılmaz, 2025). The Aegean Region dominates the spatial distribution of production in Türkiye, followed by the Mediterranean and Southeastern Anatolia regions. While the highest income from dried fig production is obtained in the Aegean Region, the Mediterranean Region stands out in terms of fresh fig production (Çalışkan, 2012; Aksoy, 2019; Kargıcak and Yılmaz, 2025).

A UAV is an integrated system comprised of three components: a pilotless aircraft system, a remote piloting control system, and a command-and-control communication environment between the two. The global UAV market, currently valued at $10.1 billion, is expected to grow by 8.12%, in contrast to overall economic growth, reaching approximately

$15 billion by 2020 (Torun, 2017). Initially used solely for military and surveillance purposes, unmanned aerial vehicles have begun to find a place in engineering applications, scientific studies, and civilian applications in recent years, thanks to the decreasing costs and increasing accessibility of advanced technology. Developed for non-military uses, unmanned aerial vehicles are now frequently used in fields such as mapping, agriculture, mining, construction, natural disaster monitoring, meteorology, and archaeology. Unmanned aerial vehicles (UAVs) are equipped with various active and passive sensors to collect data from these areas, and with these sensors, they can obtain highly accurate data. They can also produce low-cost, sensitive, fast, and analytical solutions compared to manned aircraft or satellite imagery. Numerous applications are implemented in agricultural activities using UAV and sensor-based systems. These applications include pesticide application, planting planning based on soil structure, determining plant

irrigation strategies, and biomass extraction. Furthermore, processes such as plant height measurements, soil moisture and temperature measurements, creation of various index maps, early diagnosis of plant diseases, water stress detection, chlorophyll and nitrogen concentration measurements, determination of mineral deficiencies, and yield estimation can also be performed with high accuracy with these technologies. Additionally, applications such as plant classification and development monitoring studies, forestry activities, and plant and tree counting are also supported by UAV-based systems (Villi and Yakar, 2022). UAVs, which have become widely used as a new carrier platform in recent years, offer many advantages, such as speed, flexibility, and real-time data acquisition, particularly in small areas. High-resolution digital images are obtained with the help of UAVs. Evaluating these dense images is a very difficult and time-consuming process using software with a traditional photogrammetric approach. To this end, image processing techniques have become widely used in the evaluation of UAV images to process dense datasets (Yaşayan et al., 2011).

Image processing is a technique that emerged with the development of computer technology and has become widely used. This method involves first digitally transforming a moving or still image captured by a camera, camcorder, or scanner, and then interpreting this digital data using algorithms (Demir et al., 2016). The advantages of image processing technologies include the high speed and accuracy they provide, along with the significant reduction in labor costs (Yaşayan et al., 2011).

Nowadays, image processing techniques that emerged with the development of computer technology are also used in agricultural applications such as monitoring plant growth and root development, determining leaf area, color analysis of fruits, determining fruit maturity, classification, determining weed density, detection of weeds and spraying (Karabacak, 2007; Mustafa et al., 2008; Zhao et al., 2009; Örge, 2012; Kuncan et al., 2013; Ağın, 2014; Sabancı and Aydın, 2014).

In agricultural research, many studies have been conducted on different types of plants, yield estimation, image processing techniques, and UAVs.

In a study conducted by Demirci et al. (2015), the aim was to determine the number of plants in low-altitude areas under field conditions. The accuracy rates were 86.3%, 80%,

and 86.9% for the K-Means method, and 89.2%, 70.9%, and 91.3% for the color-based segmentation method.

Song et al. (2014) developed a two-stage method for detecting and counting fruit. In stage one, they identified fruit from a single image; in stage two, they used a statistical approach to estimate data from multiple images. In the second stage alone, a 74.2% correlation was observed between automatically and manually counted fruit numbers across 435 plots. In stage one, manually counting fruit from the images yielded a 94.6% correlation.

A study conducted by Aggelopoulou et al. (2010) aimed to predict fruit yield in apple (*Malus domestica* Borkh.) orchards based on flower density determined during the flowering period. The primary objective of the study was to examine the variability in flower density within an apple orchard using image analysis and to model the relationship between the obtained flower density data and actual fruit yield. The study was conducted in a commercial apple orchard in Central Greece. Photographs of the orchard trees were taken during April 2007, when the trees were in full bloom, using a systematic uniform random sampling method. Yields were also measured for every ten trees, and the location information of these trees was recorded to create a yield map. Using the obtained data, an image processing-based algorithm was developed that analyzes images of trees in full bloom and estimates yield per tree. The developed algorithm was tested on 53 apple trees, and an error margin of approximately 18% was detected in the estimated yield values. This result demonstrates that apple yield can be successfully estimated through the analysis of images from the blooming period.

In a study conducted by Cömert (2013), an artificial intelligence-based yield prediction model was developed for the Red Chief apple variety (Malus domestica Borkh.). The aim of the research was to predict fruit yield by analyzing images obtained from apple trees. In the study, images of the selected apple trees were collected, and the data obtained from these images were compared with actual harvest values.

Image processing and analysis were conducted using MATLAB software. Images taken from a total of 20 different apple trees were converted into datasets created by analyzing the processed pixels. In this context, the AI algorithm used visual data from the

186

general appearance of each tree to estimate yield. According to the results, the model underestimated the yield of a tree with an actual yield of 56.37 kg by 4.36 kg. This finding demonstrates the high accuracy of the developed AI-based system, but small deviations can occur, especially in high-yielding trees. The study demonstrates that the combined use of image processing techniques and AI provides an effective approach to yield estimation in apple production.

In a study conducted by Payne et al. (2013), an image processing-based approach was developed for determining fruit number on mango (Mangifera indica L.) trees. The aim of the study was to use daylight images of trees to perform machine vision-based yield estimation. Approximately three weeks before harvest, images were taken from 15 trees in a designated mango orchard from four different angles over a three-day period, and the fruit on each tree was manually counted. Color segmentation was applied to the resulting images to separate fruit pixels from background pixels, allowing the fruit to be identified using image processing techniques. A dataset of 555 images was generated and analyzed. After fruit counting was completed, an average weight was determined for each mango, and the number of fruits detected was multiplied by this value to calculate the estimated total fruit weight per tree. The study results indicated that the developed algorithm produced highly accurate estimates when fruit density was low. However, the model's performance decreased as the number of fruits increased. The researchers also discussed the effects of lighting conditions on fruit detection during image acquisition.

A study conducted by Nuske et al. (2011) aimed to estimate the total grape yield in vineyards using a radial symmetry-based approach using image processing techniques. The study examined two different grape varieties and evaluated a vineyard area with a total of 224 vines. A small vineyard vehicle with cameras mounted on its side was used for data collection, allowing the grape clusters to be viewed from different angles. The resulting images were subjected to radial symmetry analysis, and the distance factor was incorporated into these calculations to increase the model's accuracy. The model's performance was tested by comparing the calculated estimated grape yields with the actual harvest values. The results showed that the developed system could estimate the total yield with a 9.8% error margin. These findings demonstrate that image processing and radial

symmetry-based methods can be effectively used in precision agriculture applications such as yield forecasting and harvest planning in viticulture.

In their study, Bargoti and Underwood (2017) compared the two processes by counting apples and counting using image processing. The comparison yielded stable results that were very close to the actual results.

In a study conducted in a greenhouse with crops longer than three meters, in dense and complex rows, it was observed that image analysis could potentially provide a good correlation with manual measurement (94.6%) and the proposed method provided a correlation without any linear adjustment (74.2%) for a large dataset (Song et al., 2014).

In their study, Kurtulmus et al. (2011) developed an image processing algorithm to identify green lemon fruits in their natural habitat by examining their color, texture, and shape characteristics. The developed algorithm appears promising for detecting green lemons on trees.

In a study conducted by Kahya and Arın (2014), a sample application of MATLAB's Image Processing Toolbox was implemented for robotic harvesting. The resulting system processed images captured from a camera using the Image Processing Toolbox. The study observed that light reflection in the processed images affected the results. It was determined that light from different angles resulted in different results when using the same image processing codes. It was understood that the solution required achieving the same lighting system. The experiments were repeated with another system. It was observed that the success rate of the study increased by incorporating a lighting system into the system.

Demir et al. (2016) compared the color properties of the weeds Sirken (*Chenopodium album* L.), Wild Lettuce (*Lectuca serriola*) and Donkey Lettuce (*Sonchus hierrensis*) obtained from digital camera images and color measurement device using image processing technique. In their study, Kulu et al. (2018) aimed to determine the number of reference fruits and determine the health status of the fruits (sound, rotten, spotted, unblemished) using real-time photographs or recorded videos taken with a UAV. Image processing techniques were used to distinguish between sound and rotten, spotted, and unspotted fruits in orange and apricot trees. They performed fruit identification using

Haar cascade, local binary pattern (LBP), and directional gradient histogram (HOG) classifiers and compared these processes. In this study, which was conducted by scanning orange and peach with a UAV, the health status and quantity of the fruits were determined. The performance of the Haar cascade classifier was found to be 68%, LBP 50%, and HOG 25%.

Saranya and Sujatha (2017) presented a technique for determining citrus fruit yield from tree images. Manual counting for yield estimation is time-consuming for marketing and other management tasks and requires more human labor. Furthermore, this process is not cheaper. Many methods have been used for yield estimation. Separating the fruit from the background presents challenges, which can lead to inaccuracies. In this study, the bicubic interpolation technique was used to segment the image, resulting in more accurate fruit detection and fruit counting. This technique, presented for citrus fruit detection and yield, demonstrated 95% accuracy on three different datasets.

Tarale and Bavaskar (2017) used image processing to identify fruit on trees, examining the challenges of counting fruit due to varying outdoor light conditions and the possibility of fruit being obscured by leaves, branches, and other fruit. Because appearance is a key factor in consumers' decision-making process, adapting this system to the packaging process allows for the identification of damaged fruit before it reaches consumers. Furthermore, this study also allows for the distinction between diseased and healthy fruit. Because MATLAB-based image processing is effectively used to determine the number of different objects, fruit counting has traditionally been done manually or with expensive electronic systems. This situation may change with the proposed algorithm. The developed method is fast and can be implemented with a low budget. Experimental results have yielded accurate results. In the traditional method, fruit quality control is performed manually, but this produces less accurate results, requires more time, and is relatively more expensive. With this developed algorithm, automatic counting using image processing was achieved and damaged fruit was identified.

In the study conducted by Donmez et al. (2021), a multispectral camera was integrated onto an octocopter-type unmanned aerial vehicle (UAV) to obtain images from a test field containing orange trees. The obtained images were processed using Pix4D

software, and orthophoto images were created in different spectral bands (red, green, blue, near-infrared (NIR), and red-edge (RedEdge) using a digital surface model (DSM), normalized difference vegetation index (NDVI). The researchers performed analyses for each band using the tree counting algorithm they developed in MATLAB software. The results revealed that the lowest error rate was obtained in the inverse color image of the digital surface model (DSM) and near-infrared (NIR) band.

In a study conducted by Tanut et al. (2021), a model for sugarcane yield estimation was developed. For this purpose, aerial images taken from an altitude of 200–300 meters using a Phantom 4 RTK quadcopter were integrated with data obtained from sugar factories and relevant government institutions. The obtained data were analyzed using the Random Forest (RF) classification algorithm in MATLAB. The researchers tested the model on images obtained from the 2018–2019 and 2019–2020 production periods and reported that this new approach, dubbed "Wondercane," achieved 98.69% accuracy in sugarcane yield estimation.

In another study, Furukawörgesaranya et al. (2020) used UAV data to estimate corn yield. They compared NDVI values generated from UAV images with harvest data and found an $R^2$ value of 0.51. They reported that this value is quite acceptable for UAV yield.

When examining the studies, factors such as the angle of light, fruit color, camera quality, the artificial intelligence prediction model used, the image processing technique used, and the prepared data sets have had positive or negative effects on the prediction results. Using appropriate methods could have yielded higher results (Ataç & Kayabaşı 2023).

In parallel with today's developing technologies, satellite imagery is often used in agricultural productivity estimation. UAVs, which have been used in many areas in recent years, have also found their place in agricultural applications. Thanks to their unique features, UAVs offer many advantages over satellite imagery. Images obtained from UAVs have higher resolution, are time-saving, less costly, and are less affected by adverse weather conditions.

Monitoring agricultural land productivity using traditional methods is both time-consuming and often fails to achieve the desired level of effectiveness. Therefore, utilizing

remote sensing techniques in monitoring agricultural lands significantly contributes to overcoming these limitations. Analyzing images obtained from a specific altitude using image processing methods allows for objective assessment of land conditions and plant development (Tabanlıoğlu et al., 2014). These approaches allow for faster, more economical, and more accurate crop yield predictions.

## 2. UAV-BASED IMAGING AND ANALYSIS TECHNIQUES FOR YIELD ESTIMATION

In agriculture, yield (harvest) is the total quantity of any product obtained in a given year. Today, a team of approximately ten people is formed to estimate fig yields. This team must travel the entire field for a week under challenging conditions. This is both costly and labor-intensive. Accurately estimating the yield of figs, one of our most important export crops, is crucial for our country's economy. Export-oriented businesses can accurately forecast the season's crop yield and manage their operations accordingly. It also enables policymakers to make accurate crop plans. Yield estimation and mapping in orchards are important for growers because they facilitate the efficient use of resources and improve returns per unit of time and area. Accurately knowing the fruit set rate and the amount of fruit on the tree allows producers to effectively manage processes such as fertilization and pesticide application. Yield estimation also allows producers to plan product logistics, storage, and sales in advance. Currently, the standard approach for yield estimation is labor-intensive and expensive manual sampling. Constrained by these costs, sampling is typically performed on several individual crops, and measures are calculated across all farms. Due to human nature, sampling bias can lead to inaccurate yield estimates (Bargoti and Underwood, 2017).

The yield of crops grown under field conditions and their determination can be determined at harvest time. Knowing the number of plants per hectare is crucial for

forecasting. Remote sensing and image processing are widely used for this purpose. Yield estimates can be generated from both satellite imagery and photographs taken by unmanned aerial vehicles using image processing methods.

It is anticipated that yield can be reliably estimated in fig production areas using two different methods, using UAV-based remote sensing and advanced image analysis techniques.

## 2.1.     First Method: Crown Area Based Estimation Method

In the first method, the number of fruits per tree, the amount of fruit weight and crown projection (CP) data will be taken, these trees will be photographed from two different directions and the fruits on the tree will be counted using the image processing method. The ratio of the number of fruits found by counting the fruits on the shoots on the tree by eye (NF) and the number of fruits counted by image processing method (INF) will be determined for each tree and the average (ANF) will be calculated. Then, the crown areas (CA) of these trees will be determined by image processing using photographs taken by the UAV. The CP/CA value will be calculated for each tree and the Crown Projection Index Value (CPV), which is the average of the 4 trees we selected as examples for this data, will be found. Finally, the average fruit weight (Akçay, 2001) and the number of fruits falling on the projection will be calculated using the CPV/FNR calculation. These operations will be performed once to find this ratio. In the area where the yield will be calculated, the crown areas of all trees within the area will be found with a UAV equipped with a NIR camera. The efficiency of the area will be found by multiplying the CPV/FNR value and the total crown area (TCA) of the trees calculated from the area. MATLAB's image processing tools will be used for image processing. This estimation, based on all trees, will create a estimation method that will produce more accurate results. As a result:

Yield= CPVxTCA will be determined by the formula.

## 2.2.  Second Method: Estimation of the Number of Fruits per Tree

In the second method, at least three trees with different canopy sizes representative

of the area to be yielded will be selected as samples. These trees will then be photographed from two different angles. These photographs will be analyzed using image processing, and the fruit on the trees will be counted. After this process, the average number of fruits per tree (NF) of the area whose yield will be calculated will be found. The yield per tree (TY) will be found by multiplying the average fruit weight (AFW) determined in Akçay (2001) by the calculated number of fruits, the number of trees (NT) in the area will be determined by image processing technique from the photographs taken by the UAV, and the yield of the area will be calculated by multiplying this number by AFW. To formulate;

Yield= AFWxNFxTF will be determined by the formula.

In the study carried out on 4 trees with different crown volumes in the parcel of Sarılop variety located in the Fig Research Institute Central Enterprise using the first of these 2 methods, the number of fruits per tree, the amount of fruit weight and crown projection data were taken.

Based on this study, very similar values were obtained for fruit weights per unit crown area of trees in the same area.

The study proposes that yield estimation can be achieved using two different estimation approaches. In these two methods, UAV images are captured using a device equipped with an NIR camera, and image processing is performed using MATLAB software.

In the plot of Sarilop variety, in our preliminary study on 4 trees with different crown volumes, we made calculations using the number of fruits per tree, the amount of fruit weight and crown projection data, and it was observed that there was a correlation between the projection crown, the number of fruits and the average fruit spacing (Table 1).

**Table 1.** Data from the crown area-based estimation method on fig trees

| Tree (avg.) | Number of Fruits (pieces) | Weight (kg) | Crown Area (m²) | Crown Area/Fruit Weight |
|---|---|---|---|---|
| 1 | 955 | 63,0 | 14,94 | 0,2371 |
| 2 | 721 | 47,8 | 11,34 | 0,2372 |
| 3 | 610 | 40,4 | 8,94 | 0,2212 |
| 4 | 745 | 49,3 | 11,74 | 0,2381 |

In a preliminary study conducted during the harvest period, the first tree produced 955 fruits, weighing 63 kg, and a crown area of approximately 14.94 square meters. According to these data, there was an average of 0.2371 kg of fruit per unit crown area. The second tree produced 721 fruits, weighing 47.8 kg, and a crown area of 11.34 square meters. There was an average of 0.2372 kg of fruit per unit crown area. The third tree produced 610 fruits, weighing 40.4 kg, and a crown area of 8.94 square meters. The fourth tree produced 745 fruits, weighing 49.3 kg, and a crown area of 11.74 square meters. There was an average of 0.2381 kg of fruit per unit crown area. By multiplying the TİD value with the ATA value, the yield of the entire orchard could be estimated. The accuracy of fruit detection using image processing varied between 85-95%.

Yield estimation aided by UAV image processing demonstrates a high correlation with manual measurements (Song et al., 2014; Saranya and Sujatha, 2017). The developed models have provided time, labor, and cost advantages. The ability to cover entire trees, especially in large areas, makes this method superior to traditional sampling-based methods. Furthermore, image data offers the potential for additional analyses such as fruit health and maturity (Kulu et al., 2018).

Since this technology is faster and less costly than traditional imaging studies, yield estimation studies using UAV are increasing nowadays (Stroppiana et al., 2015).

### 3.    CONCLUSION

This study sets an example for use on all fruit trees in our country. It also has potential for early diagnosis of diseases and stress factors in fruit species using UAVs. The aim is to replace the traditional, manual yield estimation of figs with UAVs. This study will enable export associations to make accurate crop plans, and export-oriented businesses to accurately forecast their seasonal yields.

Based on the results of the study, it is anticipated that yield estimation using a UAV will be easier and more accurate than the traditional method. Instead of estimating yield (yield) with a large team in today's fig yield estimation studies, these two methods will minimize labor and time, minimize costs, and create an innovative approach to fruit trees, enabling the development of new estimation methods.

Accurately predicting the yield of figs, one of our most important export products, is crucial for our country's economy. By accurately predicting the seasonal crop yield, export- oriented businesses can manage their operations accordingly. Furthermore, this will enable policymakers to make accurate crop planning.

The estimation methods are directly applicable to practice, and their outputs are easily implementable. They have the potential to be used in all fig cultivation areas and serve as a reference study for other fruit trees, enabling more accurate yield estimation with less manpower, time, and funding requirements.

Yield forecasting methods will enable export-oriented businesses to estimate the amount of product to be produced in a given season and tailor their planning accordingly. This will increase the country's foreign exchange inflow.

By scanning entire fig fields with a two-person team in a very short time, fig yields can be determined. This study has demonstrated the reliability and applicability of UAV-assisted image processing methods for fig yield estimation. It provides faster, more accurate, and more cost-effective results than traditional methods. The developed method has the potential to be used not only with figs but also with other fruit species. In this context, the widespread use of UAV technology in fruit growing is recommended.

When all fruit species are evaluated, leaf/branch overlap, sensor calibration, phenological stage selection, varietal differences, and image quality are thought to impact

output. To mitigate these effects, standard flight plans and fixed ground checks, band calibration with reflectance panels, and periodic updates of site-specific AFW and CPV calibrations are recommended.

In conclusion, the two approaches presented here appear ripe for producing timely and reliable yield mapping for figs at the orchard and regional scales. With appropriate calibration and standardization steps, the method could be developed into an operational yield forecasting infrastructure that would enhance both functional and export competitiveness.

**REFERENCES**

Akçay, M. (2001). *Fig variety catalog. Central Supply Directorate Printing Press.*

Aksoy, U. (2019). Dried fig industry: progress and challenges. *VI International Symposium on Fig*, Rovinj, Croatia.

Ağın, O. (2014). *Determination of weed density in wheat production using image processing techniques. (Master's thesis, Ondokuz Mayis University, Institute of Science).*

Aggelopoulou A. D., Bochtis D., Fountas S., Swain K. C., Gemtos T. A., & Nanos G. D. 2010. Yield prediction in apple orchards based on image processing, Precision Agriculture 12(3), 448-456.

Ataç, Ş., & Kayabaşı, A. (2023). Yield Prediction Using Image Processing Based Artificial Intelligence Techniques: Apple Tree Application. *Karamanoğlu Mehmetbey University Journal of Engineering and Natural Sciences*, 5(1), 67-84.

Bargoti, S., & Underwood, J. P. (2017). Image segmentation for fruit detection and yield estimation in apple orchards. *Journal of Field Robotics, 34*(6), 1039–1060. https://doi.org/10.1002/rob.21709

Çalışkan, O. (2012). Current situation and future of table fig cultivation in Türkiye. *Uludag University Faculty of Agriculture Journal*, *26*(2), 71-87.

Cömert, O. 2013. *Digital Imaging-Assisted Red Chief Apple Harvest Estimation*, Gaziosmanpaşa University.

Demir, B., Çetin, N., & Kuş, Z. A. (2016). Determining weed color characteristics using image processing techniques. *Alınteri Agricultural Sciences Journal*, *31*(B), 59–64.

Demirci, O., Varul, M., Senyer, N., & Odabaş, M. S. (2015, 16-19 Mayıs). Plant counting with low altitude image processing. *23th Signal Processing and Communications Applications Conference (SIU)*. https://doi.org/10.1109/SIU.2015.7129803

Donmez, C., Villi, O., Berberoglu, S., & Cilek, A. (2021). *Computer Vision-Based Citrus Tree Detection in a Cultivated Environment Using UAV Imagery.* Computers and Electronics in Agriculture, Volume 187 (2021), 106273.

FAOSTAT. (2024). *World Fig Production Quantities* Retrieved 11.10.2025 from https://www.fao.org/faostat/en/#data

FAOSTAT. (2025). *World Fig Production Quantities* Retrieved 15.10.2025 from https://www.fao.org/faostat/en/#data

Furukawa, F., Maruyama, K., Saito, Y. K., & Kaneko, M. (2020) *Corn Height Estimation Using UAV for Yield Prediction and Crop Monitoring.* Unmanned Aerial Vehicle: Applications in Agriculture and Environment (e-book). 51- 69.

Kahya, E., & Arın, S. (2014). A study on determining the location of fruits on the branch using image processing. *Tekirdağ Faculty of Agriculture Journal, 11*(2), 1–7.

Karabacak, H. (2007). *Determination of plant residue coverage ratio using image processing techniques*. (Master's thesis, Ankara University, Institute of Science).

Kargıcak, M. A., & Yılmaz, S. (2025, 25-27 May). Geographically Indicated Figs of Türkiye. [Full Text]. ISPEC 17th International Conference On Agriculture, Animal Sciences and Rural Development. Kırşehir, Türkiye. Liberty Publishing House, pp. 2182-2201. https://en.ispeco.org/_files/ugd/614b1f_e5d9b66604d8402fb07dc96754b95ffa.pdf

Kulu, N., Başkaya, M., Keleş, A., Altan, A., & Hacıoğlu, R. (2018). Determination of fruit health status and yield with unmanned aerial vehicle. *2nd International Symposium on Multidisciplinary Studies and Innovative Technologies (ISMSIT)*, 1–4. https://doi.org/10.1109/ISMSIT.2018.8567174

Kuncan, M., Ertunç, H. M., Küçükyıldız, G., Hızarcı, B., Ocak, H., & Öztürk, S. (2013). *Image processing-based olive sorting machine. (Master's thesis, Kocaeli University, Institute of Science).*

Kurtulmuş, F., Lee, W. S., & Vardar, A. (2011). An advanced green citrus detection algorithm using color images and neural networks. *Tarım Makinaları Bilimi Dergisi, 7*(2), 145–151.

Mustafa, N. B. A., Fuad, N. A., Ahmed, S. K., Abidin, A. A. Z., Ali, Z., Yit, W. B., & Sharrif, Z. A. M. (2008). Image processing of an agriculture produce: Determination of size and ripeness of a banana. In *2008 International Symposium on Information Technology* (Vol. 1, pp. 1–7). https://doi.org/10.1109/ITSIM.2008.4632002

Nuske S., Achar S., Bates T., Narasimhan S., & Singh S. (2011). Yield estimation in vineyards by visual grape detection, 2011 IEEE/RSJ International Conference on Intelligent Robots and Systems, IEEE.

Örge, G. (2012). *Determination of color characteristics of different cultivated plants and weeds using image processing techniques. (Master's thesis, Namık Kemal University,*

*Institute of Science).*

Payne, A. B., Walsh, K. B., Subedi, P. P., & Jarvis, D. (2013). Estimation of mango crop yield using image analysis–segmentation method. Computers and electronics in agriculture, 91, 57-64.

Polat, A. A. (2024). Fig industry in Turkey: production and marketing. In M. J. H.Q. Ma, D. Zhao Weiyuan, Sichuan, China.

Sabancı, K., & Aydın, C. (2014). Image processing-based precision spraying robot. *Journal of Agricultural Sciences. 20*(4), 406–414.

Saranya, A., & Sujatha, N. (2017). An analysis of fruit detection and yield estimation using on tree image. *International Journal of Scientific Research and Management, 5*(7), 6524–6530. https://doi.org/10.18535/ijsrm/v5i7.03

Song, Y., Glasbey, C. A., Horgan, G. W., Polder, G., Dieleman, J. A., & van der Heijden, G. W. A. M. (2014). Automatic fruit recognition and counting from multiple images.

*Biosystems Engineering, 118*, 203–215. https://doi.org/10.1016/j.biosystemseng.2013.12.003

Stroppiana, D., M. Migliazzi, V. Chiarabini, A. Crema, M. Musanti, C. Franchino, & P. Villa. 2015. Rice Yield Estimation Using Multispectral Data from UAV: A Preliminary Experiment in Northern Italy." Proceedings of the Geoscience and Remote Sensing Symposium (IGARSS), 4664–4667, The Institute of Electrical and Electronics Engineers, Inc., Milano.

Tabanlıoğlu, A., Yücedağ, A. Ç., Tüysüz, M., & Tenekeci, M. E. (2014). Multicopter Usage for Analysis Productivity in Agriculture on GAP Region. 23nd Signal Processing and Communications Applications Conference (SIU). Malatya: IEEE.

Tanut, B., Waranusast, R., & Riyamongkol, P. (2021). High Accuracy Pre-Harvest Sugarcane Yield Forecasting Model Utilizing Drone İmage Analysis, Data Mining, And Reverse Design Method. Agriculture, 11(7), 682.

Tarale, K., & Bavaskar, A. (2017). Fruit detection using morphological image processing technique. *International Journal of Advanced Engineering, Management and Science (IJAEMS), Special Issue-3*, 61–64.

Torun, A. (2017). Trends in the Unmanned Aerial Vehicle (UAV) Sector: From the Perspective of UAV Photogrammetry. *Afyon Kocatepe University Journal of Science and Engineering (AKÜ FEMÜBİD), 17(Special Issue),* 35–52.

TUİK. (2024). *Plant Production Statistics.* Turkish Statistical Institute. Retrieved 01.10.2025 from https://biruni.tuik.gov.tr/bitkiselapp/bitkisel.zul

Villi, O., & Yakar, M. (2022). Applications and Sensor Types of Unmanned Aerial Vehicles.

*Turkish Unmanned Aerial Vehicles Magazine,* 4(2), 73-100.

Yaşayan, A., Uysal, M., Varlık, A., & Avdan, U. (2011). *Photogrammetry (Publication No. 2295). Anadolu University Publications.*

Zhao, Y., Wang, D., & Qian, D. (2009). Machine vision based image analysis for the estimation of pear external quality. In *2009 International Conference on Intelligent Computation Technology and Automation* (Vol. 1, pp. 629–632). https://doi.org/10.1109/ICICTA.2009.340

# CHAPTER 16

# INVESTIGATION OF INTERNAL PRESSURE BURST AND FATIGUE DAMAGES IN FILAMENT-WOUND COMPOSITE PIPES

Assoc. Prof. Dr. Mehmet Turan DEMİRCİ[1]

[1]Selcuk University, Technology Faculty, Metallurgical and Materials Engineering Department, Konya, Turkiye
ORCID: 0000-0003-1941-9277, e-mail: turandemirci@selcuk.edu.tr

# 1. INTRODUCTION

Composite materials are preferred due to the advantages they offer in many areas such as aviation, space, maritime, defense, and energy. Polymer-based fiber-reinforced composite materials offer high mechanical strength, high rigidity, good corrosion resistance, high thermal insulation, high impact resistance, and fatigue strength. Polymer-based fiber-reinforced composite materials have different production methods. Among these composite production methods, the filament winding process is used in applications requiring high internal compressive strength with cylindrical geometry. It is used to achieve higher strengths than other fiber fabrics. The most common areas of use are in aircraft fuselages, front dome sections of aircraft, fuel tanks, spacecraft fuselages, rocket and missile fuselages, AUAV/UAV fuselages, rocket launchers, tank barrels, liquefied and pressurized gas pipelines and tanks, acidic-basic liquid pipe discharge lines and nuclear power plants (Chairi et al., 2025; Colombo et al., 2012; Jia et al., 2016; Khalili et al., 2011; Khan & Kumar, 2025; Lopresto et al., 2011; Pavlovski et al., 2007; Raghuvanshi et al., 2025; Subagia et al., 2014; Wei et al., 2010a, 2010b). Filament winding method is the process of winding fiber bundles, wetted with matrix resin, around a cylinder mandrel or mold with a certain fiber tension and winding angle by passing the fiber bundles side by side through a resin bath from reels where different types of fibers in the form of yarn bundles are wound, depending on the winding width and tex values of the fiber bundles. The tension of the fiber bundles is crucial in the filament winding process. Too much tension prevents the fibers from being adequately wetted by the matrix resin. Fiber tension is generally maintained at 10N. The winding angle is also an important factor in determining the internal pressure resistance of cylindrical composites. The windings take on angle values in the + and - directions by moving back and forth on the cylindrical mold. One layer is formed by moving back and forth in the ± angle directions. Theoretical experimental studies on winding angles in closed tubes or tanks have determined the optimum angle for bursting strength and fatigue resistance to be 55°. In open-end tubes, increasing the winding angle increases the bursting pressure and fatigue strength.

After the winding processes of the fiber bundles wetted with matrix resin are carried out according to the desired ± layer number and winding angle, the curing processes are completed in the rotary curing oven by starting the curing processes at the pre-curing temperature and hours and the final curing temperature and hours according to the catalog values of the resin. After the hardening, i.e. curing, of the matrix resin is completed, the filament winding production process is completed by cutting and grinding to the desired dimensions. Carbon, glass, and basalt fibers are generally preferred as fiber reinforcements for filament-wound composite tubes and

pipes. E-glass is the most commonly used type of glass fiber reinforcement (Demirci, 2015).
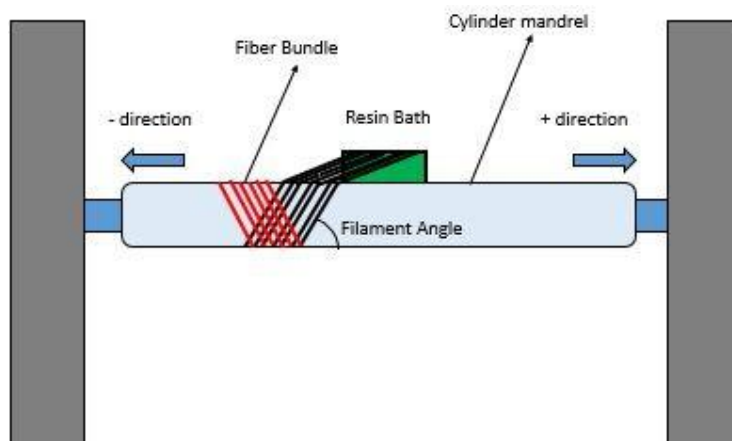


**Figure 1.** Filament winding production method in cylindrical composites.

## 2. FIBER REINFORCEMENTS USED IN FILAMENT WINDING COMPOSITES

E-glass, carbon, and basalt fibers are generally preferred as fiber reinforcements in filament-wound composite tubes and pipes. High-modulus carbon fiber reinforcements offer the highest modulus of elasticity, impact resistance, and mechanical strength. The most prominent properties of carbon fibers, which are wound into bundles, are their high strength and modulus of elasticity despite their low weight. Because of these properties, carbon fiber reinforcements are highly preferred in the aerospace and defense industries. Carbon fiber- reinforced filament-wound composites are used in the fuselages of rockets and missiles, aircraft, UAVs (unmanned aerial vehicle, and AUAVs (armed unmanned aerial vehicle) (Boopathy et al., 2025) (Almeida Jr et al., 2016; Bunsell & Thionnet, 2010; Kim et al., 2025; Leslie, 2011; Pandya, 2021; Soutis, 2005). However, their high cost paves the way for the use of E-glass and basalt fiber reinforcements when higher mechanical strength and elasticity are required and low weight is not desired. E-glass fiber-reinforced filament-wound composite tubes and pipes are the most commonly used type of fiber reinforcement in the general industry due to their low cost. They are particularly preferred in marine vessels, power plants, compressed gas and liquefied natural gas tanks and lines, and in the transfer of corrosive liquids from chemical plants, where corrosion resistance is highly desired. In addition, they are also used in electricity poles and similar structures on seashores with humid weather and corrosive conditions (Arikan, 2010; Demirci, 2020, 2022; Mehmet Turan Demirci & Ömer Sinan Şahin, 2022; Krishnan et al., 2015; Manikandan et al., 2012; Samanci et al., 2012; Sari et al., 2012; Uyaner et al., 2014; Üstün et al., 2016; Zhu et al., 2010). Although basalt fiber reinforcements have lower

mechanical properties than carbon fiber reinforcements, they exhibit higher mechanical and impact strengths than E-glass fiber reinforcements. Their cost is significantly lower than carbon fibers but slightly higher than E-glass fibers. Studies show that their strength is approximately 30% higher than E-glass fibers. The use of basalt fibers as fiber reinforcement has gained prominence in recent years and can be considered an alternative to E-glass fiber reinforcements in terms of mechanical performance and cost. While fiber reinforcements generally offer thermal, sound, vibration insulation, and corrosion resistance, basalt fibers exhibit the best performance. This has made it an important alternative fiber reinforcement. Although basalt fibers and E-glass fibers have similar chemical compositions, some chemical compositions differ because basalt fibers are produced by melting basalt rocks. The high percentages of ceramic components such as $AlO_2$, $SiO_2$, and $TiO_2$ found in the chemical composition of basalt fibers result in better mechanical performance compared to E-glass fibers (Demirci et al., 2021; Demirci, 2020, 2022; Mehmet Turan Demirci & Ömer Sinan Şahin, 2022; Mehmet T Demirci & Ömer S Şahin, 2022; Demirci et al., 2017; Demirci et al., 2014). Comparative values for carbon, E-glass, and basalt fibers are provided in Table 1 below.

**Table 1.** Mechanical properties of Carbon, E-Cam and Basalt fibers (Colombo et al., 2012; Demirci, 2015; Demirci, 2020; Pavlovski et al., 2007).

| Reinforcement materials | Tensile strength (MPa) | Elastic modulus (GPa) | Elongation failure (%) | Density (g/cm$^3$) |
|---|---|---|---|---|
| Carbon fiber | 4800 | 230 | 1.48 | 1.75 |
| Basalt fiber | 3200 | 109 | 2.31 | 2.6−2.7 |
| E-Glass fiber | 2600 | 74 | 2.05 | 2.5−2.6 |

## 3. Mechanical Tests of Filament Wound Composites

Various tests are performed according to ASTM standards to determine the mechanical, impact, and fatigue properties of filament-wound composite tubes and pipes. The split-disk test method, according to ASTM D 2290-22, is used to determine the tensile strength of filament-wound composite tubes. Tensile strengths and deformation properties can be determined by applying tensile tests to ring-shaped samples cut from filament-wound composite pipes according to ASTM D 2290-2 standards using a split-disk test apparatus. This method is practical and provides a general idea of the mechanical properties that composite tubes and pipes can exhibit before burst testing. It forms the basis for theoretical analyses (Demirci et al., 2017).
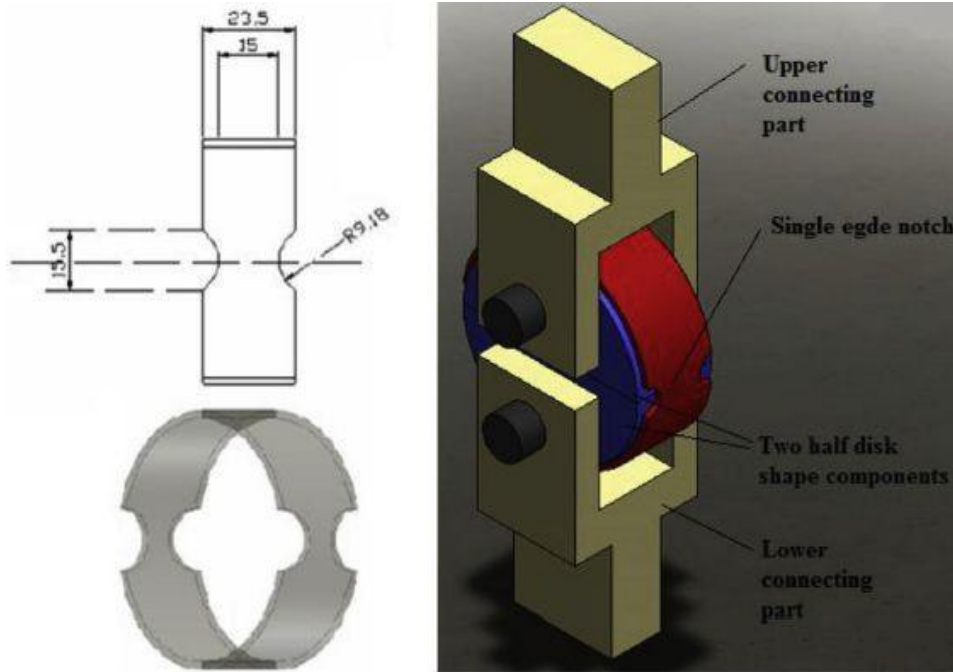
**Figure 2.** Split-disk specimen and apparatus (Demirci et al., 2017).

Another test applied to filament-wound composite pipes is burst tests, which are performed using specialized apparatus, particularly before fatigue tests. These tests involve filling hydraulic oil into a specially designed apparatus, as shown in Figure 3. It is then connected to a hydraulic pump and pressurized. Free-end static internal pressure burst tests are conducted according to ASTM D 1599-99. According to the standard, bursting of the composite pipe must occur within 60-70 s, and the pressurization must be linear. Pressure values are obtained using a manometer and a pressure sensor mounted on the apparatus (Demirci, 2015). The pressurization unit is shown in Figure 4.
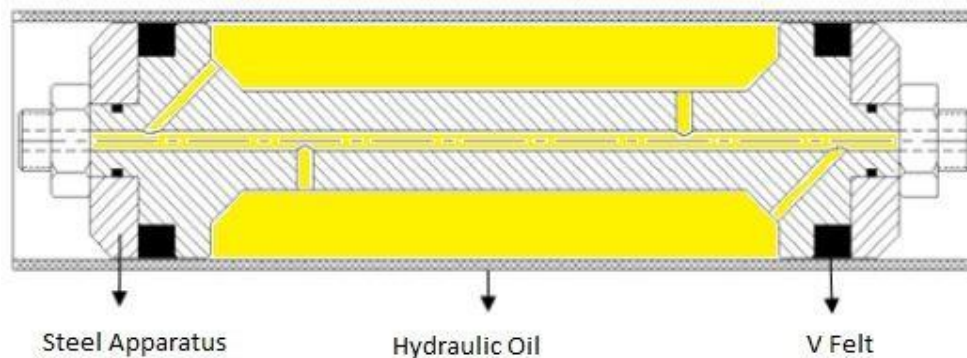


**Figure 3.** Free-end static internal pressure bursting apparatus according to ASTM D 1599-99 (Demirci, 2015).

**Figure 4.** Free-end static internal pressure burst test unit (Demirci, 2015).

When the bursting pressure obtained as a result of free-end internal pressure tests is substituted into equation 1 given below, tangential stress under internal pressure is obtained(Demirci, 2015).

$$\sigma_{statik\theta\theta} = p(D-t_r)/2t_r \qquad (1)$$

$\sigma_{\theta\theta\ static}$; tangential maximum stress (MPa), D is the outer diameter of the composite pipe; $t_r$ (mm) is the wall thickness of the composite pipe (mm), and p is the maximum internal pressure (kPa).

Percentage stress ratios ($\sigma_{\theta\theta\ static}$ x 70%, 60%, 50%, 40%, 30% etc.) of free-end internal pressure fatigue tests are determined according to the average of the maximum tangential stress values obtained in the static free-end internal pressure burst tests. Based on these obtained stress ratios, fatigue tests on filament-wound composite pipes are performed according to ASTM D 2992-12. The number of cycles per minute and the frequency are crucial in fatigue tests. In fatigue tests, it is very important to obtain the sinusoidal stress curve when pressurizing filament wound composite pipes with hydraulic oil and draining the oil from the pipe. The fatigue testing device must have a PLC unit, a display showing upper and lower pressure values, a display showing instantaneous pressure values, a frequency displays, a panel showing the number of cycles, and a panel showing the current number of cycles.

Fatigue life is determined by the fluid jet and burst damage that occurs as a result of damage to the composite pipes (Demirci, 2015).

In open-ended pressure burst tests and fatigue tests on filament-wound composite pipes, composite pipes are subject to two types of damage. Therefore, these damages are characteristic of the failures that terminate the burst and fatigue tests. n internal pressure burst and fatigue tests, fiber fractures resulting from explosion constitute the primary damage type. Catastrophic damage results from fiber fractures and a complete loss of internal pressure following explosion. The winding angles of filament-wound composite pipes also play a significant role in explosion damage. Similarly, the winding angle of filament winding fiber bundles is crucial for catastrophic damage in fatigue tests. Changing the winding angle affects the swelling of composite pipes under internal pressure, like a bottleneck in the central regions, thus changing their diameter (Demirci, 2015; Gemi et al., 2009; Sahin et al., 2009). In the internal pressure burst and fatigue tests of open-ended composite pipes, it can be stated that the greatest increase in diameter in the middle regions of the composite pipes occurs with a decrease in the winding angle. The findings in theoretical and experimental studies are in this direction (Kaynak et al., 2005; Sahin et al., 2009). The damage that occurred in BFR composite pipes resulting in explosions as a result of internal pressure tests is shown below. The types of damage that occurred in filament-wound BFR composite pipes that suffered catastrophic damage are presented in Figure 5 below. Generally, although the final damage in composite pipes varies depending on the winding angle or nano-additive content, the result is an explosion. As the internal pressure in composite pipes increases linearly, swelling occurs in the central region of the composite pipe, causing it to bulge. This means the internal diameter of the composite pipe increases. With increasing internal pressure, the fibers in filament-wound composite pipes are forced to move in the $\pm$ winding angle directions. These movements, in turn, cause radial stresses in the inner layers of the composite pipe.
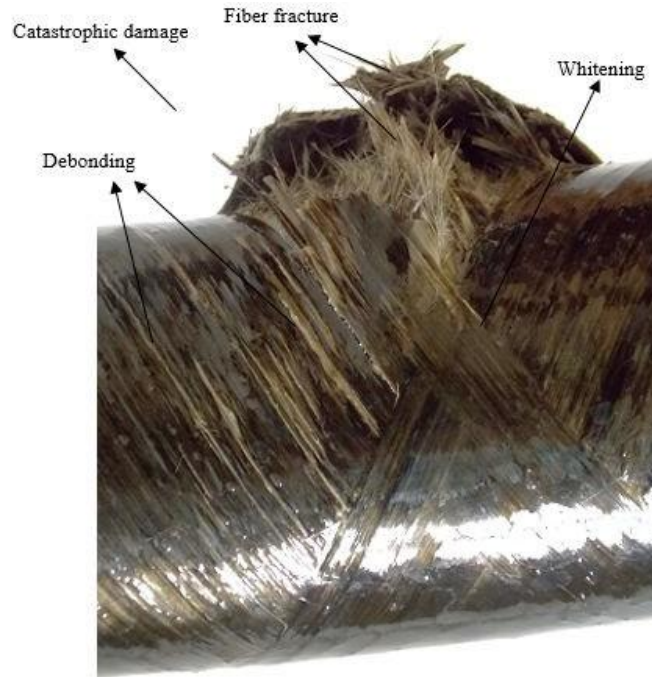
**Figure 5.** Damages resulting from the internal pressure burst test

This movement, which causes radial stresses, is similar to the opening and closing of scissors. These movements cause shear stresses, forcing the fiber bundles to move apart or closer together. Therefore, resistance to this shear movement underscores the strength of the fiber bundles and the matrix resin that binds them together. Under internal pressure, damage begins first in the matrix resin, which exhibits the weakest strength. Therefore, matrix cracks initially form as the pipe diameter increases. These matrix cracks coalesce, leading to debonding damage along the fiber direction. Debonding damage manifests itself as whitening in filament- wound composite pipes, particularly in E-glass and basalt fiber-reinforced composite pipes. As internal pressure increases, separation becomes more pronounced, and it can be determined that separation eventually occurs. Debonding damage can be clearly seen in Figure 5. Debonding damage accumulates and spreads along the fiber bundles, causing delamination damage between layers. This situation is particularly evident in fatigue tests under cyclic pressure. The fluid providing the internal pressure travels through the debonding damage, furthering the delamination damage. Shear stresses resulting from radial shear movements play a significant role in the formation of inter-laminar delamination damage. Delamination damage generally begins in areas where debonding damage is concentrated. Therefore, the scissor movements cause shear stresses, which pave the way for the formation of radial stresses along with tangential stresses in the middle sections of the composite pipes under internal pressure and consequently the formation of combined stresses. Figure 6 and Figure 7 show schematic pictures showing the stress directions and scissor

movements of the fiber bundles.
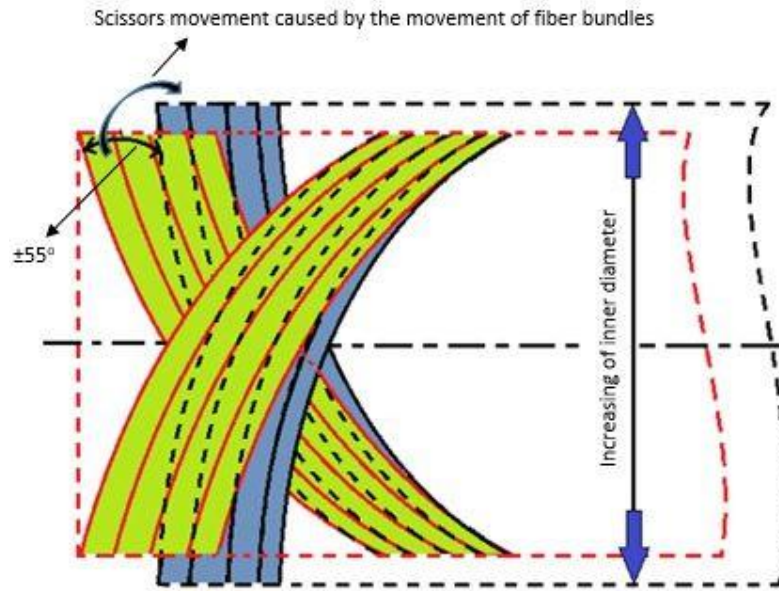


**Figure 6.** Scissor movement of fiber bundles with ±55° winding angle with increasing internal pressure.
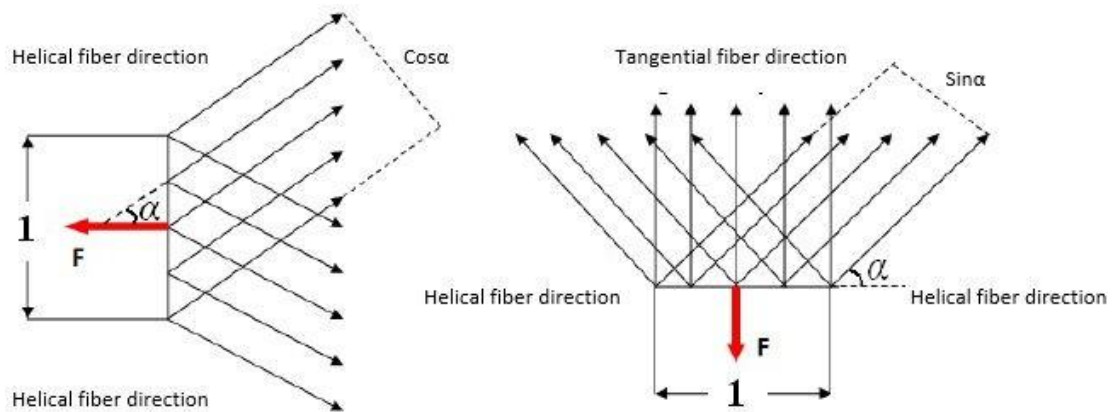


**Figure 7.** Helical and tangential fiber directions (Demirci, 2015; Zu, 2012).
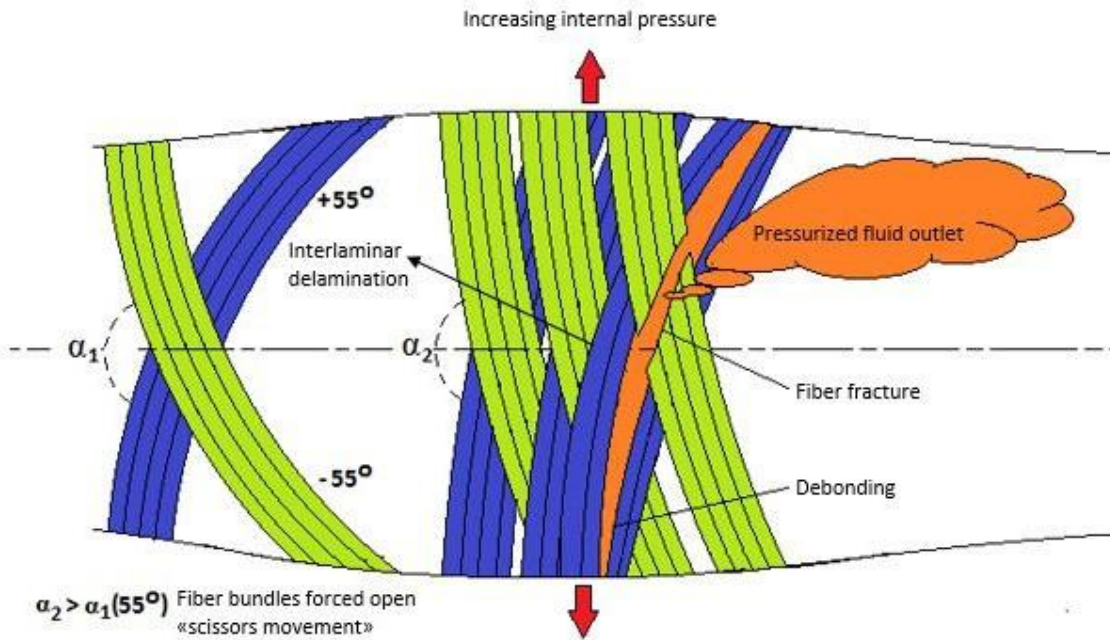
**Figure 8.** Fluid jet and damages formed in the filament winding composite pipe as a result
of fatigue tests (Demirci, 2015).

While interlayer delamination damage progresses in the direction of the angle of
the fiber bundle in filament wound composite pipes, it can also progress in the other axial
direction as a result of shear movements between the fiber bundles. Ultimately, the final
damage occurs as catastrophic fiber fracture damage or debonding damage between fiber
bundles, depending on the fatigue stress ratio of the composite pipes, as a result of fluid
jets as seen in Figure 8 and Figure 9.
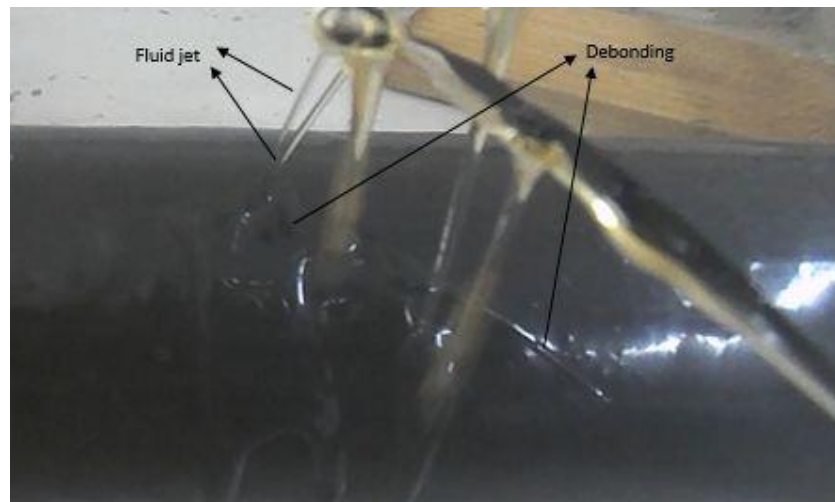


**Figure 9.** Fluid jet and debonding failure at the end of fatigue tests.

## 4. CONCLUSION

Filament-wound composites possess very high internal compressive strength, fatigue, and impact resistance. However, as with other composites, delaying and preventing damage to these composites is crucial, and researchers are continuing their work in this direction. The main damages that occur in filament wound composite pipes start with matrix cracks, followed by debonding damages in the direction of the winding angle of the fiber bundles, and interlayer delamination damages occur as these damages intensify and cluster. In internal pressure burst and fatigue life tests, fiber breakage damage or fluid jet damage occurs as the final result damage.

## REFERENCES

Almeida Jr, J. H. S., Souza, S. D., Botelho, E. C., & Amico, S. C. (2016). Carbon fiber-reinforced epoxy filament-wound composite laminates exposed to hygrothermal conditioning. *Journal of materials science*, *51*(9), 4697-4708.

Arikan, H. (2010). Failure analysis of (±55) 3 filament wound composite pipes with an inclined surface crack under static internal pressure. *Composite structures*, *92*(1), 182-187.

Boopathy, G., Srinivasan, V., Ganesan, B., & Kumar, M. H. (2025). Innovative Strategies in Lightweight Materials for High-Performance Defence Applications. In *Innovative Materials for Next-Generation Defense Applications: Cost, Performance, and Mass Production* (pp. 225-272). IGI Global Scientific Publishing.

Bunsell, A. R., & Thionnet, A. (2010). Life prediction for carbon fibre filament wound composite structures. *Philosophical magazine*, *90*(31-32), 4129-4146.

Chairi, M., Piperopoulos, E., Di Bella, G., & Proverbio, E. (2025). Mechanical Performance of Recycled Woven Basalt Fiber-Reinforced Composites for Sustainable Manufacturing Applications. *Applied Composite Materials*, 1-22.

Colombo, C., Vergani, L., & Burman, M. (2012). Static and fatigue characterisation of new basalt fibre reinforced composites. *Composite structures*, *94*(3), 1165-1174.

Demirci, I., Avcı, A., & Demirci, M. T. (2021). Investigation of nano-hybridization effects on low velocity impact behaviors of basalt fiber reinforced composites. *Journal of Composite Materials*, *55*(3), 401-414.

Demirci, M. (2015). *The effects of SiO2 nanoparticle addition on the fatigue behaviors of surface cracked and uncracked basalt fiber reinforced composite pipes* Ph. D. Thesis. Konya, Turkey: The Graduate School of Natural and Applied …].

Demirci, M. T. (2020). Low velocity impact and fracture characterization of SiO2 nanoparticles filled basalt fiber reinforced composite tubes. *Journal of Composite Materials*, *54*(23), 3415-3433.

Demirci, M. T. (2022). Investigation of low-velocity impact behavior of aluminum honeycomb composite sandwiches with GNPs doped BFR laminated face-sheets and interfacial adhesive for aircraft structures. *Polymer Composites*, *43*(8), 5675-5689.

Demirci, M. T., & Şahin, Ö. S. (2022). Effect of oil pressure upon filament wound basalt/glass fibers hybrid polymer based composite pipes subjected to low velocity impact. *Composite structures*, *288*, 115395.

Demirci, M. T., & Şahin, Ö. S. (2022). Low-velocity impact response and inspection of damage propagation for basalt fiber reinforced filament wound pipes. *Polymer Composites*, *43*(7), 4626-4644.

Demirci, M. T., Tarakçıoğlu, N., Avcı, A., Akdemir, A., & Demirci, I. (2017). Fracture toughness (Mode I) characterization of SiO2 nanoparticle filled basalt/epoxy filament wound composite ring with split-disk test method. *Composites Part B: Engineering*, *119*, 114-124.

Demirci, M. T., Tarakçıoğlu, N., Avcı, A., & Erkendirci, Ö. F. (2014). Fracture toughness of filament wound BFR and GFR arc shaped specimens with Charpy impact test method. *Composites Part B: Engineering*, *66*, 7-14.

Gemi, L., Tarakçioğlu, N., Akdemir, A., & Şahin, Ö. S. (2009). Progressive fatigue failure behavior of glass/epoxy (±75) 2 filament-wound pipes under pure internal pressure. *Materials & Design*, *30*(10), 4293-4298.

Jia, Z., Hui, D., Yuan, G., Lair, J., Lau, K.-t., & Xu, F. (2016). Mechanical properties of an epoxy-based adhesive under high strain rate loadings at low temperature environment. *Composites Part B: Engineering*, *105*, 132-137.

Kaynak, C., Erdiller, E. S., Parnas, L., & Senel, F. (2005). Use of split-disk tests for the process parameters of filament wound epoxy composite tubes. *Polymer testing*, *24*(5), 648-655.

Khalili, S., Daghigh, V., & Eslami Farsani, R. (2011). Mechanical behavior of basalt fiber-reinforced and basalt fiber metal laminate composites under tensile and bending loads. *Journal of Reinforced Plastics and Composites*, *30*(8), 647-659.

Khan, S., & Kumar, A. (2025). Failure analysis in advance cylindrical composite pressure vessel under pressure & temperature for hydrogen storage: A comprehensive review. *Polymer Composites*, *46*(4), 2933-2973.

Kim, B.-J., Lee, J. E., Oh, C.-B., Choi, D. H., Lee, M. Y., Jo, D. Y., & Kim, S. (2025). Development of silicon carbide fiber-reinforced silicon oxycarbide composites for low-observable unmanned aerial vehicle exhaust nozzles via filament winding, and polymer infiltration and pyrolysis. *Defence Technology*.

Krishnan, P., Majid, M. A., Afendi, M., Gibson, A., & Marzuki, H. A. (2015). Effects of winding angle on the behaviour of glass/epoxy pipes under multiaxial cyclic loading. *Materials & Design*, *88*, 196-206.

Leslie, J. (2011). Filament Winding Technology Learned. *Composite Filament Winding*, 81-94.

Lopresto, V., Leone, C., & De Iorio, I. (2011). Mechanical characterisation of basalt fibre reinforced plastic. *Composites Part B: Engineering*, *42*(4), 717-723.

Manikandan, V., Jappes, J. W., Kumar, S. S., & Amuthakkannan, P. (2012). Investigation of the effect of surface modifications on the mechanical properties of basalt fibre reinforced polymer composites. *Composites Part B: Engineering*, *43*(2), 812-818.

Pandya, G. (2021). *Basics of Unmanned Aerial Vehicles: Time to start working on Drone Technology*. Notion Press.

Pavlovski, D., Mislavsky, B., & Antonov, A. (2007). CNG cylinder manufacturers test basalt fibre. *Reinforced plastics*, *51*(4), 36-39.

Raghuvanshi, V., Singh, M., Dodla, S., & Khan, D. (2025). Investigation of Seawater Environment Effects on Basalt Fiber-Reinforced Epoxy Composites and the Influence of Surface Treatment on Performance. *Fibers and Polymers*, *26*(2), 855-868.

Sahin, O. S., Akdemir, A., Avci, A., & Gemi, L. (2009). Fatigue crack growth behavior of filament wound composite pipes in corrosive environment. *Journal of Reinforced Plastics and Composites*, *28*(24), 2957-2970.

Samanci, A., Tarakçioğlu, N., & Akdemir, A. (2012). Fatigue failure analysis of surface-cracked (±45°) 3 filament-wound GRP pipes under internal pressure. *Journal of Composite Materials*, *46*(9), 1041-1050.

Sari, M., Karakuzu, R., Deniz, M. E., & Icten, B. M. (2012). Residual failure pressures and fatigue life of filament-wound composite pipes subjected to lateral impact. *Journal of Composite Materials*, *46*(15), 1787-1794.

Soutis, C. (2005). Fibre reinforced composites in aircraft construction. *Progress in aerospace sciences*, *41*(2), 143-151.

Subagia, I. A., Kim, Y., Tijing, L. D., Kim, C. S., & Shon, H. K. (2014). Effect of stacking sequence on the flexural properties of hybrid composites reinforced with carbon and basalt fibers. *Composites Part B: Engineering*, *58*, 251-258.

Uyaner, M., Kara, M., & Şahin, A. (2014). Fatigue behavior of filament wound E-glass/epoxy composite tubes damaged by low velocity impact. *Composites Part B: Engineering*, *61*, 358-364.

Üstün, T., Eskizeybek, V., & Avci, A. (2016). Enhanced fatigue performances of hybrid nanoreinforced filament wound carbon/epoxy composite pipes. *Composite structures*, *150*, 124-131.

Wei, B., Cao, H., & Song, S. (2010a). RETRACTED: environmental resistance and mechanical performance of basalt and glass fibers. In: Elsevier.

Wei, B., Cao, H., & Song, S. (2010b). Tensile behavior contrast of basalt and glass fibers after chemical treatment. *Materials & Design*, *31*(9), 4244-4250.

Zhu, L., Sun, B., Hu, H., & Gu, B. (2010). Constitutive equations of basalt filament tows under quasi-static and high strain rate tension. *Materials Science and Engineering: A*, *527*(13-14), 3245-3252.

# CHAPTER 17

# THE EFFECT OF COMPLEX AGROTECHNICAL MEASURES ON THE FORMATION OF SEEDLINGS IN SUNFLOWER VARIETIES

Prof. Dr.  Nizami SEYIDALIYEV[1], Assoc. Prof. Dr. Maharram ISMAYILOV[2], Asst. Prof. Dr. Dunya ISAYEVA[3]

[1]Azerbaijan State Agricultural Universitety, Azerbaijan
Orcid: 0009-0000-2167-4782, e-mail: n.seyid55@gmail.com
[2]Azerbaijan State Agricultural Universitety, Azerbaijan
Orcid: 0009-0000-3047-2496, e-mail: ismayilov.maharram@gmail.com
3Azerbaijan State Agricultural Universitety, Azerbaijan
Orcid: 0000-0003-2346-0854, e-mail: isazade1987@gmail.com

## 1.   INTRODUCTION

In the conditions of globalization of the world economy and in the perspective, if Azerbaijan becomes an equal member of the World Trade Organization, its opportunities for integration into world economic relations will be significantly expanded. It which will enable the differentiation of agricultural product producers in terms of competitiveness parameters, the implementation of an innovative development strategy of the agricultural sector based on new world realities and principles aimed at increasing the competitiveness of agricultural products, the formation of an export-oriented agricultural production network, the formation of the Agricultural Industrial Complexs requires the creation of favorable conditions for the export of processing industry products, as well as the creation of a more advanced and international mechanism of protection of domestic producers from imports in the domestic food market.

All of these points indicate that the wide involvement of the country's economic regions in foreign economic activity, taking into account the export opportunities, the development and implementation of a measured foreign economic strategy of the agricultural sector, a systematic approach to the regulation and support of foreign economic activity by the state, the improvement of the country's export parameters, and the urgent need to solve these problems.

One of the urgent problems in modern conditions is the development of new concepts and priorities of agrarian policy based on real methods, which can ensure the increase of the competitiveness of the agricultural sector, as well as the social development of the village.

In the "Strategic Roadmap for the production and processing of agricultural products in the Republic of Azerbaijan" are defined the development goals of AEC in our country for the near, medium and long term approved by the Decree of the President of the Republic of Azerbaijan dated December 6, 2016 1 (Aliyev, 2016).

Achieving these goals is impossible without a strong flow of investment into the agricultural sector, which is the leading sector of the economy, and without its modernization. At the same time, all these are necessary conditions for effective state regulation and support of agriculture.

By applying the achievements of scientific and advanced practice, the yield of sunflower can be greatly increased. In addition to increasing the product, it should be given ample space for improving its quality, introducing new technologies and other measures.

The sunflower plant is of special importance in the social and economic development of our country. By applying the achievements of science and advanced experience to the cultivation of sunflower, its productivity can be further increased. In addition to the increase of the product, it should be given a lot of space to improve its quality, to plant fast-growing varieties, to harvest the product in the optimal period, to apply new technologies and other measures (Aliyev,1999).

The cultivation of sunflower in the world is aimed at increasing the genetic potential for productivity, product stability, health safety and food quality at the same time with the increase of production economy. *(*Hladnı*, 2010).*

In 2024 the cultivated area of sunflower in Azerbaijan was 13658.8 hectares, and the productivity was 21.9 centners/hectare *(https://www.stat.gov.az).*

Sunflower is a high water needing plant and grows well with irrigation in fertile soil with at least 500-600 mm (annual) rainfall or in less fertile soil (Banerjee et al. 2014). In addition, too little or too much irrigation water can affect crop growth, seed yield, and oil quality. Moisture stress causes a sharp decline in sunflower yield, especially at the most critical stages such as seedling, flowering bud initiation and seed filling. (Moitra et al. 2012).

In general, the demand for nutrients of sunflower is high and the crop is characterized by high plasticity in the presence of various nutrients. Calculations showed that hybrid sunflower plants extract about 47, 10 and 54 kg of N, P and K respectively to produce one tonne of seeds. *(Bhattacharyya et al. 2015).*

It is very important to ensure the nutrition of plants at the level of high agrotechnical measures in increasing productivity in agriculture.

In this regard, the application of mineral fertilizers in the cultivation of any plant is very relevant. Correct application of fertilizers ensures high yield in sunflower crops. The effectiveness of fertilizers depends on the correct determination of the annual fertilizer rate, taking into account the characteristics of the soil, the preceding crops, the distribution of

fertilizers to be applied to the soil in the pre-sowing period and during the growing season, the intended productivity and agrotechnical level (Marlamova. et al., 2023).

Sunflower is a valuable plant. In addition to increasing its productivity, organizing its sale is one of the important issues faced by entrepreneurs. The high yield of a quality product depends more on the quality and management of the energetic and productive flow in the working chambers of the machines and mechanisms used in the production of commercial sunflower seeds (Ismayilova. et al., 2013).

Sunflower is mainly cultivated as an oilseed. The oil content of modern varieties reaches 50-52%. Vegetable oils have great food and technical importance. Sunflower oil is widely used in the food industry, canning, confectionery, margarine. At the same time, is used varnish, soap making, perfumery, weaving, etc. industries. The shell of sunflower seeds is used as a raw material in the industry to obtain hexose and pentose sugars, which are used to make artificial fiber, plastic, unbreakable glass, etc. is used in the purchase.

Oilseeds are also a source of plant protein. 35-40% protein is found in the sunflower oil cake and sunflower meal, which remains when the oil of the seeds is processed.

One centner of the remaining sunflower meal after oil processing is equal to 102 feed units or 3.6 kg of protein. From the green mass of the sunflower, fodder and high-quality silage are obtained for cattle. The feed unit of 1 centner of basket flour is equal to 80 kg, and easily digestible protein is equal to 3.8-4.3 kg (Ismayilova et.al.,2017).

The rate of sowing depends on the biological characteristics of the variety or hybrid, soil-climate conditions, cultivation of the soil according to agrotechnical rules.

The rate of sowing is determined according to the soil-climatic conditions of the area, therefore, sowing rate of the plant should be set, sowing rate should not be taken excessively for growing a plant with a good healthy stem.

Sowing with appropriate plant density under favorable sowing conditions and using quality techniques and devices has a positive effect on productivity.

If the weather conditions during the sowing period are favorable (no wind, no precipitation, high soil moisture), optimal plant density can be obtained by reducing the sowing rate.

Depending on the hybrid and variety of the seed material in sowing: in hybrid crops, the sowing rate can be reduced by 15-20 percent, taking into account the soil-climate conditions and the indicators of the hybrid material's sowing rate.

In optimal sowing conditions for hybrid sunflowers, around February and early March, the ideal sowing rate is 2-3 plants from 1 meter of area, and for quality varieties, 3-4 plants are obtained from 1 meter.

Depending on the time of sowing, the rate of sowing should be increased or decreased. In late sowing, the sowing rate should be increased, and during the optimal sowing period, sowing should be carried out with the normal sowing rate.

The optimal sowing rate of sunflower varieties should be 2-3 plants per 1 meter. This means 40-50 thousand plants per hectare, depending on the fertility of the soil, the time of sowing and the previous crop. For hybrid sunflower, this means 65-70 thousand plants per hectare, depending on soil fertility and sowing time (Mammadov et al., 2015) .

Healthy and ripe seeds should be used for sowing. The germination capacity of the seeds should be at least 96%, and the purity should be 99%. Since sunflower seeds quickly lose their ability to germinate, only last year's seeds should be used for sowing. To increase the germination capacity, the seeds are spread and dried in hot air.

The seeds are treated against pests and fungal diseases. Correct regulation of plant density lays the foundation for obtaining high yields. Plant density is one of the most important agrotechnical measures. It cannot be replaced by any agrotechnical measures (Astakhov et. al.,2019).

If the agrotechnical calendar plan is followed correctly, productivity and product quality will increase significantly. High-quality implementation of sowing has a positive effect on the interphase periods of the plant (Blinohvatov et. al.,2018).

The sowing period of sunflower depends on weather conditions. When the temperature in the cultivated layer of the soil is 5-7°C, it is necessary to prepare for sowing. Sowing is done when the soil temperature is 8-12°C.

Sowing with appropriate plant density under favorable sowing conditions and using quality techniques and devices has a positive effect on productivity.

If the weather conditions during the sowing period are favorable (no wind, no precipitation, high soil moisture), optimal plant density can be obtained by reducing the sowing rate (Zhidkov et. al.,2022).

After sowing the sunflower, until the sprouts are received, if a crack is formed in the field and there are weed sprouts, it should be harrowed immediately. If the sowing is carried out by row method, harrowing is carried out in the direction perpendicular to the rows. If the field is weedy, it is possible to carry out the knowledge until 2-4 leaves are formed in the sunflower. When the row spacing is 70 cm, the first cultivation is carried out at a width of 50 cm, and the second cultivation at a width of 45 cm.

The first irrigation is carried out in the 4-8 leaf phase, the second irrigation when the basket is formed, the third irrigation at the beginning of flowering and the fourth irrigation at the time of seed formation at the rate of 800-1000 $m^3$ per hectare (Osipenko,2016).

In order to produce sunflower in Hungary today it is important to develop hybrid-specific cropping technologies. The ever widening number of hybrids makes the constant examination of genotypes necessary from the viewpoint of genotypeenvironment interactions and critical elements. Plant density as a complex factor puts strain on the pathological features, yield and quality of sunflower. The experiment's main objective is to find the optimal plant density for both the genotype and external factors.

As a result of the experiment's in Hungary to find the optimal plant density for both genotype and external factors, it can be stated that the optimal crop density is between 45,000- 75,000 plant/ha. In 2001 the optimal density was 55,000 plant/ha. The Aréna PR and the Alexandra PR hybrids produced the greatest yields (3511 kgha-1; 3338 kgha[-1]). In the growing season of 2002, the yields were higher than in the previous year and the optimal crop density was 45,000-65,000 plant/ha. The best yields were produced by the Aréna PR and Alexandra PR hybrids in this year again (4102 kgha[-1]; 4267 kgha[-1]) and in 2003, 45,000-65,000 plant/ha proved to be the best crop density. The highest yield was produced by the Alexandra PR.

Analyzing the growing seasons of 2001, 2002 and 2003 it can be declared that as a result of dry climate of the three years yields were higher. It can be stated that the yield is decreased by higher than average of precipitation in the growing season (András Szabó et.al., 2005).

## 2. MATERIALS AND METHODS

The comparative study of complex agrotechnical measures, including organic fertilizer norms, irrigations, different forms of plant density, is one of the most urgent issues.

Therefore, we have set ourselves the goal of studying the effect of complex agrotechnical measures on the quality indicators of the ecologically clean sunflower product under the conditions of the Ganja-Dashkasan economic region.

In practice, the varieties "Alazan", "Oreshka" and "Casio" are studied comparatively by applying the mentioned complex agrotechnical measures.

İn each of the varieties were planned control-5 tons of manure, 10 tons of manure, 15 tons of manure options, 42, 47 and 56 thousand plant density per hectare, 3, 4 and 5 times irrigation.

It is known that the implementation of each agrotechnical measure in the optimal period lays the groundwork for obtaining an abundant and high-quality product.

The experiment consists of 9 variants and each variant has 4 repetitions. In the experimental field, each replicate is 50 meters long and 2.8 meters wide (4 rows, 70 cm between rows), the area of one replicate is 140 $m^2$, the area of one option is 140x4=560 $m^2$, and the total area of the experimental field is 560x9=5040$m^2$.

**Table 1.** Scheme of the experiment

| Variants | | | | Repetition | | | |
|---|---|---|---|---|---|---|---|
| *Varieties* | *Sowing scheme and plant density, thousand units/ha* | *Organic fertilizer rates* | *Irrigations* | *I* | *II* | *III* | *IV* |
| | 70X35-1(42 thousand plants) | Control-5 tons of manure | 3 time | 1 | 10 | 19 | 28 |
| Alazan | 70X30-1(47 thousand plants) | 10 tons of manure | 4 time | 2 | 11 | 20 | 29 |
| | 70X25-1(56 thousand plants) | 15 tons of manure | 5 time | 3 | 12 | 21 | 30 |
| | 70X35-1(42 thousand plants) | 5 tons of manure | 3 time | 4 | 13 | 22 | 31 |
| Oreshka | 70X30-1(47 thousand plants) | 10 tons of manure | 4 time | 5 | 14 | 23 | 32 |
| | 70X25-1(56 thousand plants) | 15 tons of manure | 5 time | 6 | 15 | 24 | 33 |
| | 70X35-1(42 thousand plants) | 5 tons of manure | 3 time | 7 | 16 | 25 | 34 |
| Casio | 70X30-1(47 thousand plants) | 10 tons of manure | 4 time | 8 | 17 | 26 | 35 |
| | 70X25-1(56 thousand plants) | 15 tons of manure | 5 time | 9 | 18 | 27 | 36 |

### 3. RESULT AND DISCUSSION

The agrotechnical measures we applied had different effects on the formation of seedling in the field, depending on the biological and morphological characteristics of the varieties. This is a regularity that depends on the genotype of the varieties.

As can be seen from table No. 2, 50% seedling in Alazan variety were produced on March 18,19, and 100% sprouts on March 22,23.

In the Oreshka variety, 50% seedling were formed on March 21,22, and 100% seedling were formed on March 22,24.

In Kazio variety, 50% seedling were observed on March 19, 20, 22, and 100% seedling were observed on March 22,24.

The regularity of the formation of 50 and 100% seedling in sunflower varieties depends on the biological and morphological characteristics of the varieties, as well as certain climatic conditions. Varieties have different growing seasons. The rates of organic and mineral fertilizers did not significantly affect the formation of sprouts.

**Table 2.** The effect of complex agrotechnical measures on the formation of 50 and 100% seedlings in sunflower varieties

| Varieties | Sowing scheme and plant density, thousand units/hectare | Organic fertilizer rates | İrrigations | Seedlings | |
|---|---|---|---|---|---|
| | | | | 50% | 100% |
| Alazan | 70X35-1(42 thousand plants) | Control-5 tons of manure | 3 times | 19.03.2023 | 23.03.2023 |
| | 70X30-1(47 thousand plants) | 10 tons of manure | 4 times | 19.03 | 23.03 |
| | 70X25-1(56 thousand plants) | 15 tons of manure | 5 times | 18.03 | 22.03 |
| Oreshka | 70X35-1(42 thousand plants) | 5 tons of manure | 3 times | 21.03. | 24.03 |
| | 70X30-1(47 thousand plants) | 10 tons of manure | 4 times | 22.03 | 22.03 |
| | 70X25-1(56 thousand plants) | 15 tons of manure | 5 times | 21.03 | 22.03 |
| Casio | 70X35-1(42 thousand plants) | 5 tons of manure | 3 times | 22.03 | 24.03 |
| | 70X30-1(47 thousand plants) | 10 tons of manure | 4 times | 20.03 | 22.03 |
| | 70X25-1(56 thousand plants) | 15 tons of manure | 5 times | 19.03 | 22.03 |

# REFERENCES

Aliyev, H.A. (1999). *Decree on some issues related to acceleration of agrarian reforms*. Baku: Presidential Decree of the Republic of Azerbaijan.

Aliyev, I.H. (2016). *Strategic Roadmap for the production and processing of agricultural products in the Republic of Azerbaijan*. Baku: Presidential Decree of the Republic of Azerbaijan.

Astakhov, A.A., & Konovalenko, S.A. (2019). Plant density and sunflower productivity. *Bulletin of the agrarian and industrial complex of the Volgograd region*, 22(208).

Banerjee, H., Dutta, S.K., Pramanik, S.J., Ray, K., Phonglosa, A., & Bhattacharyya, K. (2014). Productivity and profitability of spring planted sunflower hybrid with nitrogen, phosphorus and potassium fertilizer. *Annuals of Plant and Soil Research*, 16(3), 250–256.

Bhattacharyya, K., Mandal, J., Banerjee, H., Alipatra, A., Ray, K., & Phonglosa, A. (2015). Boron fertilization in sunflower (*Helianthus annuus* L.) in an Inceptisol of West Bengal, India. *Communications in Soil Science and Plant Analysis*, 46(4), 528–544.

Blinohvatov, A.F., Butylkin, F.A., et al. (2018). *Cultivation of sunflower in the Penza region.* Penza: A.S. Afanasyev.

Hladni, N. (2010). *Genes and sunflower yield*. Beograd: Foundation Andrejevi.

Ismayilova, H.R., & Mammadov, N.N. (2013). A dynamic model of the interaction of energetic and productive flows in the working chambers of machines and mechanisms in the production of seed commodity sunflower seeds. *News collection of the Ganja branch of ANAS*, 54, 67–75.

Ismayilova, H.R., & Mammadov, N.N. (2017). Justification of the economic efficiency of post-harvest processing of sunflower seeds. *Scientific Works of ADAU*, 4, 115–119.

Mammadov, N.N., & Ismayilova, H.R. (2015). Some issues of preparation of sunflower seeds for sowing. In *Teaching and application of creative industrial technologies: International scientific and practical conference materials* (pp. 110–112). Ganja, AMU.

Marlamova, D.S., Nabiyev, I.R., & Huseynova, L.R. (2023). Effect of mineral fertilizer rates on sunflower plant productivity. *Materials of the scientific-practical conference dedicated to the 100th anniversary of the birth of national leader Heydar Aliyev*, 183–185.

Moitra, A., Puste, A.M., Mandal, T.K., Gunri, S.K., Banerjee, H., & Pramanik, B.R. (2012). Yield, water use and economics of summer sunflower (*Helianthus annuus* L.) as influenced by

irrigation and integrated nutrient management. *World Journal of Science and Technology*, 2(7), 81–86.

Osipenko, D.A. (2016). *Resource-saving technology for cultivating sunflower on irrigated ordinary black soils* (Doctoral dissertation). Novocherkassk.

State Statistics Committee. (n.d.). *Agriculture, forestry and fisheries*. Retrieved, 2025, from https://www.stat.gov.az/source/agriculture/

Szabó, A., & Pepó, P. (2005). Test of the plant density reaction of genotype sunflower hybrids. *Acta Agraria Debreceniensis*, 16, 3298. https:// doi.org/ 10.34101/ actaagrar/ 16/3298.

Zhidkov, V.M., Astakhov, A.A., & Konovalenko, S.A. (2022). Plant density and timing of sunflower sowing on black soils of the Volgograd region. *Scientific Bulletin of Volgograd: VGSHA*, 3, 116–119.

# CHAPTER 18

# PHOSPHORUS RECOVERY FROM BIOMASS COMBUSTION ASH: THERMAL PROCESSES AND FERTILIZER POTENTIAL

Asst. Prof. Dr. Ozben Kutlu[3*], Prof. Dr. Hayati Olgun[2], Senior Researcher Dr. Niculina Mihaela Balanescu[3] and Senior Researcher Dr. Georgeta Predeanu[4]

[1]Ege University Solar Energy Institute, 35100, İzmir, Türkiye
ORCID: 0000-0002-0361-6949 e-mail: ozben.kutlu@ege.edu.tr
[2]Ege University Solar Energy Institute, 35100, İzmir, Türkiye
ORCID: 0000-0002-1777-2010 e-mail: hayatiolgun1958@gmail.com
[3]National University of Science and Technology POLITEHNICA Bucharest (UNSTPB), Bucharest, Romania
ORCID: 0000-0003-4479-8459 e-mail: niculina.balanescu@upb.ro
[4]National University of Science and Technology POLITEHNICA Bucharest (UNSTPB), Bucharest, Romania
ORCID: 0000-0001-8550-8417 e-mail: gpredeanu@gmail.com

# 1. INTRODUCTION

## THE GLOBAL PHOSPHORUS PRODUCTION AND EMERGING CHALLENGES

Phosphorus (P) presents a fundamental duality in the context of global sustainability. On one hand, it is indispensable for all known life and is a core building block of living matter alongside carbon, hydrogen, nitrogen, and oxygen. This essentiality directly links P to global food security, as it is a primary and non-substitutable input for modern agriculture, supplied to croplands via fertilizers to maintain high yields. On the other hand, the same element is a key pollutant in surface waters. Inefficient use and runoff from agricultural lands lead to the enrichment of rivers, lakes, and coastal waters, triggering eutrophication—a process that induces harmful algal blooms, oxygen depletion, and severe degradation of aquatic ecosystems.

The primary source of P for meeting global demand is the mining of finite phosphate-rich mineral rocks. This non-renewable resource is the starting point for virtually all P fertilizers and industrial P compounds. The quality and commercial value of these geological deposits are typically classified by their phosphorus pentoxide ($P_2O_5$) content. Unprocessed phosphate rock generally contains between 4% and 20% $P_2O_5$, whereas economic exploitation for fertilizer production requires a considerably higher grade, usually above 20% $P_2O_5$ (Eroglu, 2023; Desmidt et al., 2025).

The global phosphate rock market is overwhelmingly driven by the agricultural sector, with approximately 90% of all mined phosphate rock used for fertilizer manufacture. Roughly half of this extracted rock is chemically converted to phosphoric acid ($H_3PO_4$), which is the key precursor for high-quality, water-soluble phosphate fertilizers such as diammonium phosphate (DAP) and monoammonium phosphate (MAP). The growing demand is satisfied by finite geological reserves, estimated at around 72 billion tons in 2023. However, the pronounced geographical concentration of these reserves raises concerns regarding the resilience and security of global P supply. The Kingdom of Morocco holds the largest share of known reserves, controlling a substantial majority of the global total. Other countries with significant reserves include China, the United States, Egypt, Tunisia, Russia, and Algeria (US Geological Survey, 2023). In comparison, Türkiye's phosphate rock reserves are modest, estimated at about 50 million tons (Eroglu, 2023).

Global phosphate rock production was approximately 220 million tons in 2022 and is similarly concentrated in a limited number of producing countries. Although Morocco controls roughly 70% of global reserves, it produced about 35 million tons in 2023, while China was the largest producer with 85 million tons. This concentration of both reserves and production underscores the vulnerability of the global P supply chain and reinforces the strategic importance of developing alternative, secondary sources of P.

Part of Morocco's phosphate reserves lies in territories along the border with Western Sahara, a region subject to international political disputes and largely under de facto Moroccan control. The Bou Craa mine, known for its high-grade phosphate rock, is at the core of these geopolitical tensions (Walsh et al., 2023). In parallel, recent periods of political instability in key producing countries such as Tunisia, Jordan, and Syria have weakened global phosphate supply and increased

the European Union's (EU) dependence on Moroccan exports. However, the unresolved legal and political status of Western Sahara introduces substantial uncertainty regarding the reliability and cost of phosphate derived from this region, creating a strategic vulnerability for Europe (Ridder et al., 2012).

In recent years, P—although not currently classified as a critical element in the short to medium term—has gained increasing importance as an input for clean energy technologies, especially due to its role in lithium iron phosphate (LFP) cathodes and as a component of electrolytes in many lithium-ion batteries (U.S. Department of Energy, 2023). Demand projections for 2020–2035 indicate four scenarios combining different climate-policy pathways—specifically the International Energy Agency's Stated Policies and Net Zero Emissions scenarios—with high and low material-intensity assumptions based on electric vehicle and stationary storage deployment. According to these projections, P's market share for energy applications is expected to remain below 10%. Given that current demand from the energy sector is relatively low, existing capacity is considered sufficient in the near term. However, under the IEA Net Zero Emissions pathway, total demand is expected to approach or exceed projected future P production capacity, with an estimated annual growth rate of around 3%.

The EU faces a particularly high supply risk for elemental phosphorus ($P_4$), as it is 100% dependent on imports from China, Vietnam, and Kazakhstan, while its import dependency for phosphate rock is reported at 84% (EC, 2020). In its 2020 public consultation on Critical Raw Materials, the European Commission (EC) identified $P_4$ and phosphate rock as critical raw materials for the EU, emphasizing the geopolitical risks arising from both high import dependence and the concentration of supply in a small number of countries. To build a more resilient and sustainable supply chain for P-based raw materials, the EC proposed strategic actions to secure supply and enhance extraction, refining, processing, and recovery capacities within the EU. These actions include support for mining, refining, and processing projects, as well as the development of recycling technologies and P recovery from secondary sources such as wastewater sludge and animal wastes. In this context, the European Sustainable Phosphorus Platform (ESPP) has called for $P_4$ and purified phosphoric acid to be recognized as Strategic Raw Materials due to their critical role in batteries, renewable energy, electronics, aerospace, and other industrial applications. The ESPP has also highlighted the need for clear targets related to supply, recycling, and resilience for key nutrients, and has underlined the importance of increasing investment in phosphoric acid purification capacity and research into producing high-purity $P_4$ from secondary resources (ESPP, 2023).

This strong reliance on finite, geographically concentrated, and increasingly exploited resources poses a critical challenge. P thus lies at the nexus of food security, environmental protection, and resource management, underscoring the urgent need to develop sustainable P recovery and recycling technologies.

## 2. P-RICH BIOMASS ASHES

The ash composition of biomass and waste-derived fuels differs significantly from that of coal ashes and can vary considerably depending on the origin of the fuel (woody, agricultural, or animal waste). To accurately characterize ash formation from a given fuel, it is necessary to understand the reactions of inorganic elements during combustion and their bonding behavior as a function of temperature.

In biomass, the relatively high contents of P and calcium (Ca) are often present in low-reactivity mineral forms, most commonly as hydroxyapatite. During combustion, the overall chemical composition may not change dramatically, but crystal formation leads to a marked decrease in the specific surface area of the ash (Deydier et al., 2005; Masiá et al., 2007).

Other major inorganic elements in biomass—such as potassium (K) and silicon (Si)—together with minor amounts of sulphur (S) and chlorine (Cl), tend to promote deposit formation on heat-transfer surfaces. Organically bound K in biomass volatilizes during combustion and forms low-melting oxides, hydroxides, chlorides, and sulphates. These compounds can adhere to boiler walls and tubes, causing slagging and fouling. When biomass is co-fired with coal, these elements can lower the ash melting temperature and increase the rate of deposit formation. Therefore, in co-firing processes, the fuel composition and blending ratios are critical for achieving stable combustion behavior.

The chemical composition of biomass is highly variable and depends on factors such as species, growing conditions, soil properties, fertilizer use, plant age, and external contamination. In general, however, biomass has a simpler composition than fossil fuels (Vassilev et al., 2010). On a dry and ash-free basis, biomass mainly consists of carbon (C), oxygen (O), and hydrogen (H), with nitrogen (N) and S present at lower levels. The inorganic fraction typically contains Ca, K, Si, P, Cl, magnesium (Mg), aluminum (Al), iron (Fe), sodium (Na), manganese (Mn), and titanium (Ti) (Phyllis2, 2025).

Woody biomass species generally have low ash contents and relatively low levels of Ca, K, and Cl. In contrast, agricultural residues (straw, stalks, grasses, etc.) tend to have higher ash contents and elevated K, Si, N, and Cl levels. Fast-growing species are known to accumulate greater amounts of elements such as K, Na, Mg, P, Cl, and S. P is typically low in wood and woody biomass but becomes one of the dominant elements—together with Ca—in animal-derived biomasses (e.g., bone meal, poultry litter) and in sewage sludge (Table 1). The compositional differences between biomass types, especially in the inorganic fraction, span a wide range and strongly influence thermochemical conversion processes and ash formation. Furthermore, specific groups of elements tend to co-occur in biomass, reflecting important chemical relationships that govern fuel behavior during combustion (Vassilev et al., 2010).

**Table 1.** Chemical ash composition of typical biomass groups (Vassilev et al. 2010)

| Biomass group, MEAN | $SiO_2$ | CaO | $K_2O$ | $P_2O_5$ | $Al_2O_3$ | MgO | $Fe_2O_3$ | $SO_3$ | $Na_2O$ | $TiO_2$ |
|---|---|---|---|---|---|---|---|---|---|---|
| Wood and woody biomass | 22.22 | 43.03 | 10.75 | 3.48 | 5.09 | 6.07 | 3.44 | 2.78 | 2.85 | 0.29 |
| Herbaceous and agricultural biomass | 33.39 | 14.86 | 26.65 | 6.48 | 3.66 | 5.62 | 3.26 | 3.61 | 2.29 | 0.18 |
| Animal biomass | 2.90 | 49.04 | 7.67 | 28.17 | 1.69 | 2.75 | 0.35 | 3.91 | 3.50 | 0.02 |

**Table 2.** Chemical dry ash composition of selected P-rich biomasses (%)

| Biomass | Ash content | $P_2O_5$ | $SiO_2$ | CaO | $K_2O$ | $Al_2O_3$ | MgO | $Fe_2O_3$ | $SO_3$ | $Na_2O$ | $TiO_2$ | Ref |
|---|---|---|---|---|---|---|---|---|---|---|---|---|
| Meat and bone meal | 23.95 | 41.50 | <0.02 | 41.80 | 3.20 | 2.40 | 1.40 | 0.25 | 4.30 | 6.50 | 0.01 | Masiá et al. 2007 |
| Palm kernels | 5.14 | 30.60 | 18.00 | 9.20 | 16.30 | 6.10 | 6.50 | 9.10 | 2.50 | 0.14 | 0.12 | Masiá et al. 2007 |
| Sewage sludge | n.d. | 23.51 | 28.99 | 7.39 | 3.35 | 22.20 | 4.42 | 7.76 | 0.57 | 0.04 | n.d. | Yang et al 2025 |
| Sewage sludge | 48.06 | 15.40 | 26.52 | 16.04 | 0.93 | 10.34 | 2.05 | 17.83 | 2.83 | 2.16 | 0.75 | Wei et al. 2005 |
| Sewage sludge | n.d. | 12.10 | 43.60 | 5.61 | 2.34 | 16.60 | 1.40 | 10.40 | 0.24 | 0.82 | n.d. | Chen et al 2006 |
| Macroalgae *Fucus vesiculosus* | 22.82 | 21.99 | 1.26 | 5.73 | 17.34 | 0.93 | 4.91 | 1.33 | n.d. | 15.20 | n.d. | Ross et al 2008 |
| Poultry litter | 13.12 | 12.24 | 0.88 | 16.63 | 12.07 | n.d. | 3.60 | 0.80 | 3.07 | 2.14 | 0.05 | Adamczyk et al. 2021 |
| Chicken litter | 37.79 | 12.00 | 4.50 | 44.30 | 9.50 | 0.79 | 3.20 | 0.35 | 2.80 | 0.47 | 0.02 | Masiá et al. 2007 |
| Pistachio shells | 1.41 | 11.80 | 8.22 | 10.01 | 18.20 | 2.17 | 3.26 | 35.37 | 3.79 | 4.50 | 0.20 | Miles et al 1995 |
| Olive tree wood | 1.50 | 10.75 | 10.24 | 41.47 | 25.16 | 2.02 | 3.03 | 0.88 | 2.65 | 3.67 | 0.13 | Vamvuka and Zografos (2004) |
| Willow | 0.95 | 10.04 | 8.08 | 45.62 | 13.20 | 1.39 | 1.16 | 0.84 | 1.15 | 2.47 | 0.06 | Miles et al 1995 |
| Walnut blows | 2.36 | 8.30 | 5.18 | 22.32 | 28.00 | 1.82 | 11.58 | 0.85 | 1.88 | 0.74 | 0.09 | Miles et al 1995 |
| Groundnut plant | 87.79 | 8.24 | 22.05 | 17.95 | 8.46 | 6.43 | 11.79 | 10.86 | 1.16 | 0.92 | 1.58 | Trivedi et al 2016; Kamble et al 2017 |
| Pepper plant | 14.44 | 5.20 | 12.60 | 32.20 | 24.60 | 4.90 | 7.40 | 2.00 | n.d. | 0.90 | 0.50 | Masiá et al. 2007 |
| Olive residue | 7.17 | 4.90 | 17.90 | 10.40 | 34.40 | 3.30 | 4.70 | 1.60 | 3.00 | 0.10 | 0.12 | Masiá et al. 2007 |
| Bamboo *Phyllostachys nigra (4,5 year)* | 0.41 | 20.70 | 16.30 | 5.06 | 33.60 | 0.42 | 6.66 | 0.42 | 2.32 | 0.71 | <0.01 | Scurlock et al. 2000 |
| Bamboo branches | 10.18 | 4.12 | 62.45 | 2.83 | 17.67 | 1.96 | 3.91 | 1.81 | 2.30 | 0.39 | 0.13 | Hu et al. 2020 |
| Plastic and greenhouse waste | 31.79 | 3.84 | 28.40 | 25.80 | 9.70 | 3.90 | 5.70 | 18.40 | n.d. | 0.80 | 0.81 | Masiá et al. 2007 |

n.d. = not detected

Characterization studies indicate that P in ash is generally present in discrete crystalline phases, such as Ca-based phosphates (e.g., hydroxyapatite) or mixed Mg–K phosphates (e.g., whitlockite). This speciation largely governs the plant-availability of P in ash-derived products. Certain agricultural and animal waste-derived ashes (Table 2), as well as municipal sewage sludge (SS), exhibit high P contents. However, the use of such ashes as P fertilizers can be limited by elevated heavy metal concentrations (e.g., Cd, Pb) and by the low solubility of some P species (Vassilev et al., 2010). Consequently, advanced analytical methods are needed to elucidate P bonding forms within the ash matrix and to track phase transformations during thermal processing, in order to select the most suitable recovery technology.

SS and poultry litter are particularly valuable secondary sources of P (Table 2). A study on Polish SS reported that $P_2O_5$ contents in ash can vary between 8 and 29%, with composition strongly dependent on the combustion technology, flue gas cleaning system, and, consequently, ash collection units (Kominko et al., 2025). Spent mushroom compost is another rapidly growing waste stream that is not yet widely utilized in other sectors. Approximately 5 kg of waste compost are generated for every 1 kg of mushroom produced, making sustainable management of this material essential (Finney et al., 2009). With an ash content of around 30%, this waste contains approximately 0.6–1.65% (w) total P (Pan et al., 2023), which becomes concentrated in the corresponding ash and can therefore be considered a potential secondary P source.

As shown in Table 2, the P contents of ashes derived from the same biomass type can be highly variable. This variability is closely related to the geographical and environmental origin of the biomass, but also to combustion technology (e.g., bed type), bed temperature, agglomeration mechanisms, and the presence of additives. These factors collectively influence both the total P content and the specific mineral forms in which P is retained in the ash.

### 3. Effect of Combustion Parameters on Ash Chemical Composition

Although biomass typically has a lower ash content than coal, it is generally richer in alkali and alkaline earth elements. Common operational problems in biomass combustion differ from those in coal-fired systems and include pronounced slagging and fouling. The mineralogical composition of the fuel significantly affects ash fusion temperatures and, consequently, boiler design and operation.

To minimize deposit formation in convective passes, it is often recommended that the flue gas temperature at the furnace outlet be kept at least 100°C below the ash softening temperature or 50°C below the initial deformation temperature (Rayaprolu, 2013). In general, acidic oxides tend to increase ash melting temperatures, whereas basic oxides lower them. Biomass— especially herbaceous species—typically exhibits lower ash melting temperatures than coal, a characteristic attributed to its high alkali content.

228

Biomass ash is usually enriched in Ca, Cl, K, Mg, Mn, Na, P, phosphate phases, carbonates, and organically bound inorganic species, while coal ash is more dominated by Al, Fe, N, S, Si, Ti and the corresponding sulphide, sulphate, and silicate phases. During combustion, these ash- forming components may partially volatilize and/or be transported with the flue gas, contributing to the formation of fly ash (Lachman et al., 2021).

Several mathematical methods have been developed to predict slagging and fouling tendencies based on ash chemistry. Once the concentrations of oxidized ash components (expressed as oxides) are determined on a dry basis, slagging (SI) and fouling (FI) indices can be calculated (Alves et al., 2021):

$$Equation\ (1): SI = \frac{CaO + MgO + Fe_2O_3 + K_2O + Na_2O}{SiO_2 + Al_2O_3 + TiO_2} \times S$$

$$Equation\ (2): FI = \frac{CaO + MgO + Fe_2O_3 + K_2O + Na_2O}{SiO_2 + Al_2O_3 + TiO_2} \times [K_2O + Na_2O]$$

Lachman et al. (2021) performed a statistical analysis of ash fusion temperatures and chemical compositions of biomass grouped into six categories (woody biomass, grasses, straw, husk, organic residues, and others) and modelled indices relevant to combustion. Their analysis showed that in the studied biomass ashes, $SiO_2$ and $K_2O$ contents tended to decrease with increasing ash fusion temperatures, while CaO, MgO, and $Al_2O_3$ contents increased. In ashes with the highest fusion temperatures, CaO was identified as the dominant oxide. In samples with the lowest softening temperatures (<800 °C), $P_2O_5$ was the dominant oxide (often exceeding 30%), although it was also noted that $P_2O_5$-rich samples were associated with the lowest model accuracy. In low-melting ashes, a large temperature interval was observed between softening temperature and hemispherical temperature, which negatively affects the predictive power of statistical models. The authors suggested that more extensive data sets are needed to improve model reliability and cautioned against applying these models directly to biomass-based fuels, although their proposed classification diagram (Figure 1) could be used as an indicative tool once sufficient validation is achieved.
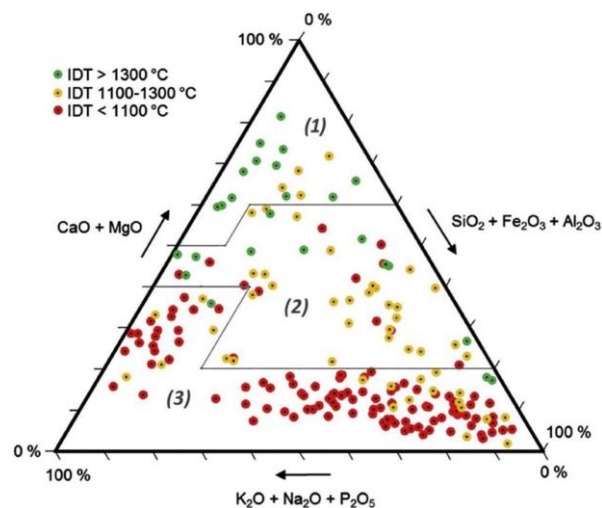
**Figure 1.** Classification of average ash oxide composition as a function of initial deformation temperature (adapt from: Lachman et al., 2021)

In fluidized bed combustors, efficient and trouble-free operation requires careful control of the volatility and retention behavior of alkali metals, particularly K and Na. Among these, K is especially problematic: at relatively low temperatures, K tends to accumulate in the bed ash, but above approximately 800 °C it volatilizes significantly. Gaseous K compounds can react with $SiO_2$ in the bed material to form low-melting potassium silicates, which deposit as sticky

layers on particle surfaces, promoting bed agglomeration. In contrast, Na remains largely in the ash, and the relative proportions of Ca, Mg, Si, Al, and Fe in the ash increase with temperature, though these elements generally have a less pronounced effect on agglomeration.

P is present at high levels only in certain biomass types. At typical fluidized bed combustion temperatures below 1000°C, P is largely retained in the solid ash. Literature reports indicate that high-P biomasses tend to form high-melting Ca–Mg–K phosphate compounds, which can reduce slagging behavior. Thus, P may have a beneficial effect on mitigating slagging while simultaneously providing favorable reaction pathways for subsequent P recovery from ash (Tan and Lagerkvist, 2011).

## 4. DISTRIBUTION AND SPECIATION OF P IN ASH

In biomass combustion systems, ash is commonly classified into bed ash and fly ash; depending on the flue gas cleaning system, fly ash can be sub-divided into cyclone ash, bag filter ash, or electrostatic precipitator (ESP) ash. P is often enriched in the fly ash fraction—particularly in cyclone and bag filter ashes—where it is typically associated with micron particles (Khan et al., 2009). This fine secondary fly ash is usually the most P-rich fraction and is therefore a primary target for P recovery processes.

Within the ash, P is stabilized in different mineral phases depending on fuel composition and operating conditions. In systems with high Ca contents, P is predominantly bound in apatite- like calcium phosphate phases (e.g., tricalcium phosphate-type Ca–P compounds), which are characterized by high melting points and substantial thermal stability. In contrast, in fuels or blends enriched in K, P can shift towards K-based phosphate phases (e.g., $K_2PO_4$), which have lower melting points and significantly influence ash fusion behavior and slagging propensity. Variations in the Ca/P ratio during ash formation further indicate that P is not necessarily confined to a single Ca-phosphate phase but may be distributed among mixed phosphates involving Ca and alkali metals.

In ashes derived from high-P biomasses such as sewage sludge, P is predominantly associated with cations that readily form phosphates, including Ca, K, and Fe. In sewage sludge, P is often considered to be present mainly as $Ca_3(PO_4)_2$ in a relatively inert and poorly reactive form. In addition, smaller amounts of $K_2PO_4$, Mg-based phosphates (e.g., $Mg_3P_2O_8$), and $AlPO_4$ are frequently reported. At elevated temperatures, a fraction of P may volatilize into the gas phase as $P_4O_{10}$, $P_2O_5$, and related species. In secondary cyclone ash, iron–calcium phosphates such as $Ca_9Fe(PO_4)_7$ and $Fe_7(PO_4)_6$ have also been identified (Tan and Lagerkvist, 2011; Magdziarz et al., 2016).

Fuel blends can further modify P speciation. In the study by Falk et al. (2020), ashes from two sewage sludge mixtures were dominated by Ca–P phases, with relatively low amounts of other cations. In contrast, ashes produced from blends including dried grain contained not only Ca– P phases but also significant quantities of K- and Mg-bearing phosphates.

Leng et al. (2019) reported that the dominant crystalline phase in ash derived from meat and bone meal is hydroxyapatite ($Ca_5(PO_4)_3(OH)$). However, other $Ca_5(PO_4)_3X$ compounds with similar crystal structures (X = Cl, F, Br) may also be present. These phases act as stable, decomposition-resistant P carriers on the bed material. Additional phases identified in such ashes include calcite ($CaCO_3$), portlandite ($Ca(OH)_2$), and calcium sulphate ($CaSO_4$), which are interpreted as products of reactions between hydrated lime and acidic gas components during combustion.

In ashes derived from swine manure, olive kernels, and pruning residues, calcite is often reported as a dominant phase, with Ca present in anhydrite, fairchildite, and calcite forms. P is chiefly associated with Ca, Mg, and Fe, forming phosphates such as whitlockite (notably in swine manure ash) and hydroxyapatite (especially in olive kernel and pruning ash), as well as rodolicoite and newberyite, which bind P with Fe and Mg (Vamvuka et al., 2017).

Studies on poultry manure combustion have reported $P_2O_5$ contents in ash as high as 28–29%. In a fluidized bed system operated with quartz sand as bed material, up to 96% of the ash was recovered as bed ash. Within this bed ash, the crystalline fraction (about 43%) was dominated by phosphate phases such as potassium magnesium phosphate,

nonacalcium magnesium sodium heptakis phosphate, and nagelschmidtite (Adamczyk et al., 2021). When poultry litter was co-fired with bark residues, hydroxyapatite was the dominant P phase in bottom ash; co-firing with wheat straw led to fly ash enriched in both hydroxyapatite and whitlockite (Häggström et al., 2020).

In another study, combustion of poultry manure at 500–900°C yielded ashes with 75–85% crystalline phases, among which whitlockite was the dominant phosphate (21–23%). With increasing temperature, the proportion of crystalline phases increased, and above 700°C the formation of calcium phosphate, calcium silicate, and aluminum phosphate became pronounced. Additional phosphate species identified included iron(II) phosphate and sodium phosphate. Higher temperatures were associated with greater total P retention and with an increased fraction of P in crystalline phases. However, the highest concentration of plant- available P was found in the amorphous fraction of ash obtained at 500°C (Więckol-Ryk et al., 2020). High-temperature combustion processes have also been shown to produce crystalline hydroxyapatite and carbonate apatite phases (Cempa et al., 2022).

## 5. RECOVERY TECHNIQUES OF P FROM ASH

Although biomass ash is recognized as a promising secondary source of P, the fraction of plant- available P is often low, limiting its direct use as a fertilizer (Massa et al., 2024). Therefore, reducing heavy metal contents and enhancing P bioavailability are critical objectives in P recovery from ash. The most widely studied recovery methods include wet chemical extraction, thermochemical processes, and electrodialysis-based extraction (Jupp et al., 2021; Zhu et al., 2022).

*5.1 Wet Chemical Extraction:* Wet chemical extraction is a mature and industrially established route for P production from phosphate rock, valued for its high efficiency and relatively low cost. It is also the most frequently proposed technique for P recovery from combustion ashes. Phosphoric acid is produced from phosphate rock via acidification, concentration, and purification steps. In a typical industrial process, phosphate rock is treated with sulphuric acid according to:

Equation (3): $Ca_5(PO_4)_3F + 5H_2SO_4 + 5nH_2O \rightarrow 3H_3PO_4 + 5CaSO_4 \cdot nH_2O + HF$
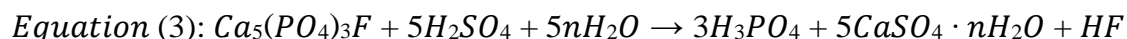
resulting in phosphoric acid as the main product and calcium sulphate hydrates (gypsum) and hydrogen fluoride as by-products (Jupp et al., 2021).

Pramanik et al. (2019) proposed an acid or alkali leaching approach in which valuable P compounds are first precipitated as struvite crystals, followed by separation using a forward osmosis membrane to create a selective counter-flow. However, such processes may require large amounts of chemicals and often exhibit limited efficacy in removing heavy metal contaminants (Massa et al., 2024).

*5.2 Thermochemical Processes:* Thermochemical methods are particularly recommended for P recovery from sewage sludge and related wastes and are already

applied at pilot or industrial scale. In these processes, the mineralogical structure of ash is transformed at elevated temperatures (typically 900–2000°C), allowing for P separation and purification.

Notable examples include the AshDec and Mephrec processes. The Outotec AshDec process, developed with the Federal Institute for Materials Research and Testing (Berlin) and ASH DEC Umwelt AG (Vienna), remains under development but offers advantages such as the absence of acidification and limited contaminant accumulation. The Mephrec process, on the other hand, is constrained by its high energy demand (approximately 1.2 kWh per kg P recovered) and by the relatively limited applicability of its acidic product in soils, which hampers further implementation (Havukainen et al., 2016; Massa et al., 2024). In the Thermphos process, an electric arc furnace operating at around 1500°C achieves $P_4$ production with recovery efficiencies reported as high as 95%. The process generates a reusable slag predominantly consisting of calcium and silicon compounds (Xu et al., 2023; Fahimi et al., 2025).

Pyrolysis and hydrothermal carbonization (HTC) are additional thermochemical conversion routes that are considered cost-effective, sustainable, and less toxic, particularly for recovering P from agricultural biomass. The resulting biochar or hydrochar is typically enriched in more plant-available P species compared to conventional combustion ash. For example, co-pyrolysis of sewage sludge and straw has been reported to increase the proportion of plant-available P in the total P pool to up to 95%, generating monetite, hydroxyapatite, and pyrocoproite forms that are more easily utilized by plants (Xu et al., 2024).

Among thermal methods, microwave heating technology has recently attracted growing attention (Qiu et al., 2016). Microwaves enable rapid and efficient internal heating of materials with high dielectric constants, thereby improving energy efficiency. Fiameni et al. (2022) demonstrated the production of bioavailable $NaCaPO_4$ from wastewater using microwave- assisted processes. Microwave technology offers effective heating with minimal thermal losses and is considered a promising technology for future P recovery applications (Fiameni et al., 2022; Massa et al., 2024). Predeanu et al. (2025) investigated microwave-assisted high- temperature reactions of calcium phosphate with carbon and silica, based on the following redox reaction:

$Equation$ (4): $2Ca_3(PO_4)_2 + 10C + 3SiO_2 \rightarrow 3Ca_2Si + 10CO_{(g)} + 2P_{2(g)}$
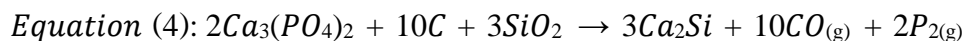
achieving successful volatilization of P, in line with earlier work (Beral and Zapan, 1962). The resulting slag was evaluated for its potential use as a cement additive, suggesting additional value streams.

*5.3 Electrodialytic Extraction:* Electrodialysis is another promising technique for P recovery, particularly suited for enhancing P solubility in acidic conditions while simultaneously promoting heavy metal removal. In this approach, an appropriate amount of acid is added to the ash, transforming largely insoluble heavy metals and P into ionic forms. Under an applied electric field, phosphate ions migrate towards the anode and can be separated from other ions (Zhu et al., 2022). This method therefore contributes both to P concentration and to partial decontamination of the recovered product.

## 6. CONCLUSION

The global P cycle is under increasing pressure due to the combined effects of finite phosphate rock reserves, geopolitical concentration of supply, growing agricultural and industrial demand, and emerging requirements from the clean energy sector. The EU's high import dependency for both phosphate rock and $P_4$, together with political uncertainties in major producing regions, highlight the strategic vulnerability of current P supply chains. In this context, biomass and waste-derived ashes—particularly those from sewage sludge, poultry manure, meat and bone meal, and certain agricultural residues—represent an important class of secondary P resources.

The composition and speciation of P in biomass ashes are highly variable and depend on fuel type, origin, combustion technology, and operating conditions. While high-P ashes are often dominated by thermally stable Ca- and Mg-phosphate phases such as hydroxyapatite and whitlockite, significant fractions of P may also be present in alkali phosphates and mixed Ca– Fe or Ca–Mg–K phases, especially in blended fuels. These mineralogical differences have a dual impact: they influence ash fusion behavior, slagging and fouling propensity in combustion systems, and they determine the solubility and plant-availability of P, thereby constraining the direct agronomic use of raw ashes.

A range of technological options has emerged to overcome these limitations and to transform P-rich ashes into safe fertilizer products or industrial P intermediates. Wet chemical extraction is currently the most mature and widely applied approach, although challenges remain in reducing chemical consumption and managing heavy metals. Thermochemical processes provide routes for P concentration and decontamination, and in some cases for producing elemental P or high-purity phosphates, but they are often energy-intensive. More recently, alternative routes such as pyrolysis, hydrothermal carbonization, microwave-assisted treatments, and electrodialysis extraction have shown promise in enhancing P bioavailability and enabling simultaneous P recovery and heavy metal removal, but they still require further scale-up and techno-economic validation.

Overall, the recovery of P from biomass ashes is technically feasible and offers a realistic

avenue for partially decoupling P supply from finite mined resources. However, realizing this potential at scale will require: (i) systematic characterization of ash composition and P speciation across different biomass types and combustion technologies, (ii) integration of recovery processes into existing waste management and energy systems, (iii) clear regulatory frameworks for ash-derived fertilizers and P products, and (iv) comprehensive assessments of environmental, economic, and social impacts and life cycle assessment. Within this context, the PREWA project which follows the PHIGO project (2025) has been developed and aims to promote clean and advanced process technologies for P recycling. If these conditions are met, P recovery from biomass ash can play a pivotal role in developing a more circular, resilient, and sustainable phosphorus economy.

## Acknowledgements

## REFERENCES

Adamczyk, Z. Cempa, M. Białecka, B. (2021) Phosphorus-Rich Ash from Poultry Manure Combustion in a Fluidized Bed Reactor. *Minerals* 11(7), 785; https://doi.org/10.3390/min11070785

Alves, L.S. Moreira, B.R.A. Viana, R.S. Gimenez, A.P. Dias, E.S. Noble, R. Zied, D.C. (2021) Recycling spent mushroom substrate into fuel pellets for low-emission bioenergy producing systems. *Journal of Cleaner Production* 313, 127875. https://doi.org/10.1016/j.jclepro.2021.127875

Beral, E., Zapan, M., 1962. Phosforus. In: Inorganic Chemistry. *Editura Tehnicˇa, Bucureşti*, pp. 672.360–369 (in Romanian).

Cempa, M. Olszewski, P. Wierzchowski, K. Kucharski, P. Białecka, B. (2022) Ash from Poultry Manure Incineration as a Substitute for Phosphorus Fertiliser. *Materials* 15, 3023. https://doi.org/10.3390/ma15093023

Chen, C.H. Chiou, I.J. Wang, K.S. (2006) Sintering effect on cement bonded sewage sludge ash. *Cement & Concrete Composites* 28, pp. 26–32. https://doi.org/10.1016/j.cemconcomp.2005.09.003

Desmidt, E. Ghyselbrecht, K. Zhang, Y. Pinoy, L. Bruggen, B.V. der. Verstraete, W. Rabaey, K. Meesschaert, B. (2015) Global Phosphorus Scarcity and Full-Scale P-Recovery Techniques: A Review, *Environmental Science and* Technology, 45:4, 336-384, DOI: 10.1080/10643389.2013.866531

Deydier, E. Guilet, R. Sarda, S. Sharrock, P. (2005) Physical and chemical characterisation of crude meat and bone meal combustion residue: "waste or raw material?". *Journal of Hazardous Materials*, 121, pp.141-148. https://doi.org/10.1016/j.jhazmat.2005.02.003

Eroglu, G. (2023) Dünyada ve Türkiye'de Fosfat. Maden Tetkik ve Arama Genel Müdürlüğü Fizibilite Etütleri Daire Başkanlığı Raporu Ek-1, pp.32 (in Turkish)

ESPP (2023) Phosphate Rock and P4 stay on EU Critical Raw Materials List. *Newsletter about*

*nutrient stewardship – ESPP eNews* no. 74 - March 2023, https://www.phosphorusplatform.eu/images/eNews/ESPP-eNews-no74.pdf (Access date: November 2025)

European Commission (EC) (2020) Critical Raw Materials Resilience: Charting a Path towards greater Security and Sustainability, *Communication COM (2020) 474 final,* https://eur-lex.europa.eu/legal-content/EN/TXT/HTML/?uri=CELEX:52020DC0474#footnote34 (Access date: November 2025)

Falk, J. Skoglund, N. Grimm, A. Ohman, M. (2020) Systematic Evaluation of the Fate of Phosphorus in Fluidized Bed Combustion of Biomass and Sewage Sludge. *Energy Fuels* 34, 3984−3995. https://dx.doi.org/10.1021/acs.energyfuels.9b03975

Finney, K. Sharifi, V.N. Swithenbank, J. (2009) Combustion of spent mushroom compost and coal tailing pellets in a fluidised-bed. *Renewable Energy* 34 (3), pp. 860-868. https://doi.org/10.1016/j.renene.2008.06.012

Häggström, G. Fürsatz, K. Kuba M. Skoglund, N. Öhman, M. (2020) Fate of Phosphorus in Fluidized Bed Co-combustion of Chicken Litter with Wheat Straw and Bark Residues. *Energy & Fuels* 34, 1822-1829. https://dx.doi.org/10.1021/acs.energyfuels.9b03652

Havukainen, J. Nguyen, M.T. Hermann, L. Horttanainen, M. Mikkil, M. Deviatkin, I. Linnanen, L. (2016) Potential of phosphorus recovery from sewage sludge and manure ash by thermochemical treatment. *Waste Management* 49, 221–229. https://doi.org/10.1016/j.wasman.2016.01.020.

Hu, J. Yan, Y. Song, Y. Liu, J. Evrendilek, F. Büyükada, M. (2020) Catalytic combustions of two bamboo residues with sludge ash, CaO, and $Fe_2O_3$: Bioenergy, emission and ash deposition improvements. *Journal of Cleaner Production* 270, 122418. https://doi.org/10.1016/j.jclepro.2020.122418

Jupp, A.R., Beijer, S., Narain, G.C., Schipper, W. Slootweg, J.C. (2021) Phosphorus recovery and recycling-closing the loop. *Chemical Society Reviews*, 50(1), 87–101. https://doi.org/10.1039/d0cs01150a

Kamble, M.G. Deokar, S.K. Tajane, S.P. Mandavgane, S.A. (2020) Groundnut plant ash: Characterisation and adsorption efficacy study for removal of paraquat dichloride. *Indian Journal of Chemical Technology* 27, pp. 35-42.

Khan, A.A. Jong, W. Jansens, P.J. Spliethoff, H. (2009) Biomass combustion in fluidized bed boilers: Potential problems and remedies. *Fuel Processing Technology* 90, 21–50. https://doi.org/10.1016/j.fuproc.2008.07.012

Kominko, H. Gorazda, K. Wzorek, Z. (2025) Evaluation of the potential use of sewage sludge ash in phosphoric acid production and phosphorus recovery technologies. Journal of Water Process Engineering 70, 107054. https://doi.org/10.1016/j.jwpe.2025.107054

Lachman, J. Balas, M. Lisy, M. Lisa, H. Milcak, P. Elbl, P. (2021) An overview of slagging and fouling indicators and their applicability to biomass fuels. *Fuel Processing Technology* 217, 106804. https://doi.org/10.1016/j.fuproc.2021.106804

Leng, L. Zhang, J. Xu, S. Xiong, Q. Xu, X. Li, J. Huang, H. (2019) Meat & bone meal (MBM) incineration ash for phosphate removal from wastewater and afterward phosphorus recovery. *Journal of Cleaner Production* 238, 117960. https://doi.org/10.1016/j.jclepro.2019.117960

Magdziarz, A. Wilk, M. Gajek, M. Nowak- Wozny, D. Kopia, A. Kalemba-Rec, I. Kozinski,

J.A. (2016) Properties of ash generated during sewage sludge combustion: A multifaceted analysis. *Energy* 113, 85-94. https://doi.org/10.1016/j.energy.2016.07.029

Masiá, A.A.T. Buhre, B.J.P. Gupta, R.P. Wall, T.F. (2007) Characterising ash of biomass and waste. *Fuel Processing Technology* 88, 1071–1081. https://doi.org/10.1016/j.fuproc.2007.06.011

Massa, M., Zanoletti, A., Fiameni, L., Valentim, B., Depero, L.E. Bontempi, E. (2024) Improving phosphorus availability in sewage sludge ash through a novel microwave-based technology. *Water and Environment Journal*, 1–12. https://doi.org/10.1111/wej.12956

Miles TR, Miles JTR, Baxter LL, Bryers RW, Jenkins BM, Oden LL. (1995) Alkali deposits found in biomass power plants. A preliminary investigation of their extent and nature. *Report of the National Renewable Energy Laboratory* (NREL/TZ-2-11226-1; TP-433-8142), Golden, CO, USA; 1995

Pan, X., Deng, Tf., Zhang, L. Ge, L.j. Li, L.q. Yang, L.s. Gao, M. Cao, J.f. Wei, F.x. Liu, X.l. Yan, Y.f. Yang, J. Yang, X.s. (2023) Epimedium Herbal Residue as a Bulking Agent for Lignite and Spent Mushroom Substrate Co-composting. *Waste and Biomass Valorization* 14, 2547–2555. https://doi.org/10.1007/s12649-022-02018-y

PHIGO (2025) Thermal Processing of P-rich ashes aiming for HIGH-GRADE PHOSPHORUS Products (PHIGO). ERAMIN3 Joint Call 2021. Topic 4: Recycling and Re-use of End-of-Life products and assets, Project coordinator: Guozhu Ye, SWERIM (Sweden) (ref. 2022-00072) & TUBITAK-Turkey (ref. 122N038) & UEFISCDI-Romania (ref. 310/01.03.2022) & FCT-Portugal (UIDB/04683/2020; UIDP/04683/2020). 2022 – 2025.

Phyllis2 (2025) Database for the physico-chemical composition of (treated) lignocellulosic biomass, micro- and macroalgae, various feedstocks for biogas production and biochar. *TNO Biobased and Circular Technologies*. https://phyllis.nl/

Pramanik, B.K., Hai, F.I., Ansari, A.J. & Roddick, F.A. (2019) Mining phosphorus from anaerobically treated dairy manure by forward osmosis membrane. *Journal of Industrial and Engineering Chemistry*, 78, 425–432. https://doi.org/10.1016/j.jiec.2019.05.025

Predeanu, G. Valentim, B. Popescu, L.G. Abagiu, A.T. Anghelescu, L. Bălănescu, M.N. Białecka, B. Bontempi, E. Cempa, M. Drăgoescu M.F. Guedes, A. Kutlu, O. Massa, M. Mousa, E. Nicoară, A.I. Olgun, H. Slăvescu, V. Vasile, B.S. Ye, G. (2025) *International Journal of Coal Geology* 307, 104808. https://doi.org/10.1016/j.coal.2025.104808

Rayaprolu, K. (2013) Boilers: A Practical Reference. *CRC Press, Taylor &Francis Group* Boca Raton. ISBN 978-1-4665-0053-2

Ridder, M. Jong, S. Polchar J. Lingemann, S. (2012) Risks and Opportunities in the Global Phosphate Rock Market: Robust Strategies in Times of Uncertainty. *The Hague Centre for Strategic Studies Report* No 17 12 | 12. ISBN/EAN: 978-94-91040-69-6

Ross AB, Jones JM, Kubacki ML, Bridgeman T. (2008) Classification of macroalgae as fuel and its thermochemical behaviour. *Bioresource Technology* 99, pp. 6494–6504. https://doi.org/10.1016/j.biortech.2007.11.036

Scurlock, J.M.O. Dayton, D.C. Hames, B. (2000) Bamboo: an overlooked biomass resource? *Biomass Bioenergy* 19, 229–44. https://doi.org/10.1016/S0961-9534(00)00038-6

Tan, Z. And Lagerkvist, A. (2011) Phosphorus recovery from the biomass ash: A review. *Renewable and Sustainable Energy Reviews* 15, 3588–3602

https://doi.org/10.1016/j.rser.2011.05.016

Trivedi, N.S. Mandavgane, S.A. Mehetre, S. Kulkarni B.D. (2016) Characterization and valorization of biomass ashes. *Environ Sci Pollut Res* 23, 20243–20256 (2016). https://doi.org/10.1007/s11356-016-7227-7

US Department of Energy (2023) Critical Materials Assessment. Draft report. https://www.energy.gov/sites/default/files/2023-05/2023-critical-materials-assessment.pdf (Access date: November 2025)

US Geological Survey (2023). Mineral commodity summaries 2023, US Report, doi: 10.3133/mcs2023

Vamvuka D, Zografos D. (2004) Predicting the behaviour of ash from agricultural wastes during combustion. *Fuel 83*: 2051–7 https://doi.org/10.1016/j.fuel.2004.04.012

Vassilev, S.V. Baxter, D. Andersen, L.K. Vassileva, C.G. (2010) An overview of the chemical composition of biomass. *Fuel* 89, 913–933 https://doi.org/10.1016/j.fuel.2009.10.022

Walsh, M., Schenk, G. & Schmidt, S. (2023) Realising the circular phosphorus economy delivers for sustainable development goals. *npj Sustainable Agriculture.* 1, 2. https://doi.org/10.1038/s44264-023-00002-0

Wei, X. Schnell, U. Hein, K.R.G. (2005) Behaviour of gaseous chlorine and alkali metals during biomass thermal utilisation. *Fuel* 84, 841–8. https://doi.org/10.1016/j.fuel.2004.11.022

Więckol-Ryk, A. Białecka, B. Cempa, M. Adamczyk, Z. (2020) Optimization of chicken manure combustion parameters in the aspect of phosphorus recovery. *International Journal of Recycling of Organic Waste in Agriculture* 9, 273-285. DOI: 10.30486/IJROWA.2020.1899148.1070

Xu, X. Zou, Z. Guo, X. Liang, S. Yang, F. Chen, S. Yu, W. Duan, H. Yuan, S. Yang, J. (2024) Comprehensive evaluation of bioavailable phosphorus in biochar synthesized by co-pyrolysis of sewage sludge and straw ash. *Science of The Total Environment* 954, 176679. https://doi.org/10.1016/j.scitotenv.2024.176679

Xu, Y. Zhang, L. Chen, J. Liu, T. Li, N. Xu, J. Zhou, X. (2023) Phosphorus recovery from sewage sludge ash (SSA): an integrated technical, environmental and economic assessment of wet-chemical and thermochemical methods. *Journal of Environmental Management* 344, 118691. https://doi.org/10.1016/j.jenvman.2023.118691.

Yang, Z.H., Du, C.M. Lu, Z.C. Wang, J.G. (2025) A novel process for extraction of phosphorus from the incinerated sewage sludge ash by modification and leaching. *Separation and Purification Technology* 369, 133077. https://doi.org/10.1016/j.seppur.2025.133077

Zhu, Y. Zhai, Y. Li, S. Liu, X. Wang, B. Liu, X. Fan, Y. Shi, H. Li, C. Zhu, Y. (2022) Thermal treatment of sewage sludge: A comparative review of the conversion principle, recovery methods and bioavailability-predicting of phosphorus, *Chemosphere* 291, 133053. https://doi.org/10.1016/j.chemosphere.2021.133053

# CHAPTER 19

# INVESTIGATION OF COMPOSITE MATERIALS AND ELECTRONIC SYSTEMS SUITABLE FOR UNMANNED AERIAL VEHICLE DESIGN

Samir HAJIYEV[1],  Assoc. Prof. Dr. Mehmet Turan DEMİRCİ[2]

[1]Selçuk University, Faculty of Technology, PhD Student in Metallurgy and Materials Engineering..
ORCID: 0009-0006-9452-1545 email:  haciyevs780@gmail.com
[1]Selcuk University, Technology Faculty, Metallurgical and Materials Engineering Department, Konya, Turkiye
ORCID: 0000-0003-1941-9277, e-mail: turandemirci@selcuk.edu.tr

## 1. INTRODUCTION

The aerospace industry has undergone significant changes in recent years. The use of composite materials has accelerated these changes due to their superior strength-to-weight ratio, durability, and other advantages. Composites have recently become increasingly used in aerospace because they offer a wider range of capabilities than other materials. Composites are not only lighter than metals but also significantly stronger. This property allows aircraft to be lighter and improve their performance. Lighter aircraft are in high demand because they offer advantages such as longer range, higher speed, and improved maneuverability. Lightweight composite materials help aircraft burn less fuel and be more environmentally friendly. Lighter aircraft require less drag, resulting in lower fuel consumption.

This is a key factor in reducing the carbon footprint of the civil industry. The use of composite materials in the modern aerospace industry has exceeded 50%. Composite materials are widely used in many structural components, including rocket motor housings, antenna shrouds, antenna housings, engine nacelles, horizontal and vertical stabilizers, wing boxes, airfoils, pressure bulkheads, landing gear covers, floor sleepers, longitudinal cones, and vertical stabilizer panels. Figure 1 shows the increasing use of composite materials in commercial aircraft.
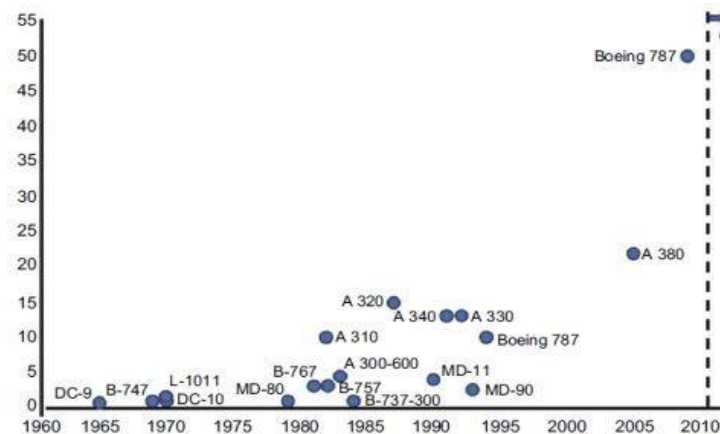


**Figure 1.** Growth of composite material utilization in aircraft over time ( Öztürk AM, 2019)

Good fatigue resistance is another important requirement for composites used in

aerospace engineering. The service life of aerospace structures depends heavily on fatigue resistance. Good fatigue resistance properties extend the service life of aerospace structures, reduce maintenance frequency and costs, and increase safety. Composites for aerospace engineering must also have high fracture toughness and damage tolerance. Cracks and defects in structures must not propagate rapidly and lead to sudden failure. High impact fracture is an important requirement for composites to withstand sudden impacts such as bird strikes and foreign object impacts. In addition, their properties must provide protection against electromagnetic waves. Multifunctionality has become a key performance criterion for composite properties in modern detailing applications. These properties require high bending stability in harsh environments such as freezing, high temperatures, lightning strikes, hail, and corrosive environments. They can also offer improved combustion, smoke and durability (FST) performance, as well as resistance to chemicals such as jet fuel, lubricants and paint strippers.

## 2. LITERATURE REVIEW

Ayesha Kausar and colleagues have highlighted the use of various core materials in sandwich composite structures, including cellular polymer foams, metal foams, honeycomb structures, balsa wood, and tubular core geometries. Among these materials, honeycomb core sandwich composites in particular have found widespread application in the aerospace, marine, and construction sectors. A variety of methods are used to manufacture sandwich composite structures, including hand assembly, pressing, pre-hardening, vacuum bagging/autoclaving, vacuum-assisted resin infusion, resin transfer molding, compression molding, pultrusion, three- dimensional (3D) printing, and four-dimensional (4D) printing. Autoclaving has become a preferred manufacturing technique in the aerospace industry, particularly in advanced composites, due to its ability to reduce interlayer delamination and provide more precise thickness control.

Hang Zhang and colleagues investigated delamination in glass fiber-reinforced composite honeycomb-core sandwich structures using low-velocity impact tests. A three-dimensional analysis model was developed, and the properties of the delamination fence of the honeycomb- core sandwich structures were experimentally evaluated under different impact energies. Furthermore, the methods and relevant parameters used in delamination

repair were determined. The results showed that the area of the sandwich panels expanded with increasing impact energy, with delamination spreading from the impact center to the surrounding areas, and this fence was accompanied by fiber fracture and matrix cracking. The strength recovery rates of the sandwich panels after repair at 5 J, 15 J, and 25 J impact energies were determined as 71.90%, 65.89%, and 67.10%, respectively, demonstrating the significant effectiveness of the applied repair methods.

Al Ali and colleagues conducted a comprehensive analysis of the interlayer properties of physical panels. Three samples, each consisting of four different decorative panels, were prepared. The panels' outer surfaces were made of woven carbon fiber reinforced with fabric and epoxy resin, while their cellular structures were made of Nomex, a two-dimensional honeycomb material. The panels were subjected to transverse impact loading. Honeycomb-reinforced sandwich panel models using this material were examined to determine the most efficient calculation method. Finally, the calculated energy absorption properties based on experimental and numerical studies were examined, and these properties were used to evaluate the performance of the multilayer sandwich composite and provide design recommendations. Alptekin and colleagues prepared hybrid composites in different configurations using glass, aramid, and carbon fibers. TiO2 nanoparticles were added to the resulting hybrid composites. To understand the differences in mechanical properties between pure hybrid composites and nanoparticle hybrid composites, experiments were conducted with pure and doped hybrid composites in different configurations. In this study, the flexural properties, tensile strength, and quasi-static penetration capabilities of the hybrid composites were investigated. 2% TiO2 by weight was used in the additive composites. Hybrid composites were produced in CAG, AGC, and GCA configurations. After examining the mechanical properties of the resulting hybrid composites, the effects of fiber configuration and nanoparticle addition on mechanical properties were investigated. This study demonstrated that fiber configuration and nanoparticle addition have a positive effect on mechanical properties.

Ahsun et al. presented a control fusion scheme to improve the safety of manual UAV control by combining external pilot manual control signals with autopilot commands. UAV flight dynamics were modeled using a standard six-degree-of-freedom nonlinear system and a hardware-based computational fluid dynamics (CFD) model. Several CFD

tests were conducted, with the airframe model being manually controlled using an onboard computer. The results demonstrated the effectiveness of the control fusion scheme in ensuring UAV flight safety.

Altyn and colleagues demonstrated that an unmanned aerial vehicle (UAV) controlled by muscle and brainwave energy via wearable signal receivers could successfully maneuver on a predetermined trajectory without remote control. Using 3D virtual reality software they developed, they simultaneously transmitted EEG and EMG signals from different users to a MATLAB environment. They classified these signals and sent them as commands to a virtual game, enabling remote control of the UAV. To test the system's effectiveness, they used various routes created in different locations to analyze its performance. In this study, human-generated signals were integrated into a virtual reality environment independently of the hardware, and experiments demonstrated the system's functionality.

In a study by Ambroziak and Gosiewski et al., a commercial autopilot was installed on a small fixed-wing aircraft, enabling both manual and autonomous flight. While the autopilot performed navigation and trajectory tracking tasks, PID (proportional-integral-derivative) controllers were tuned. Tuning the PID controllers was noted to be complex, time-consuming, and required careful attention. Anderson, Hagenauer, Erickson, and Bhandari (2008) conducted a study on a Piccolo II autopilot and an autonomous UAV. In this study, a Sig Cadet Senior aircraft was used to develop the flight dynamics. Using this aircraft model, a hardware-in-the- loop simulation environment (HILS) was used to determine the feedback required for autonomous flight. The autopilot was integrated into the aircraft, enabling autonomous

**Fundamentals of Sandwich Structures Applied to Unmanned Aerial Vehicles**

A multilayered shell structure consisting of one or more low-temperature inner layers (cores) is used. This definition, which Hoff and Mautner recommended in 1944 for synthetic structures, is still used today and is discussed in various ways in the relevant literature. Although numerous materials and architectural extensions have been developed for both core and shell structures, the specifications and certification requirements for aerospace applications are significantly broader. In current applications, only honeycomb cores made of Nomex and aluminum alloys and certain types of technical foams can be

used. Similarly, outer shells are most commonly constructed using layers of carbon, aramid fiber, and fiberglass fabric.
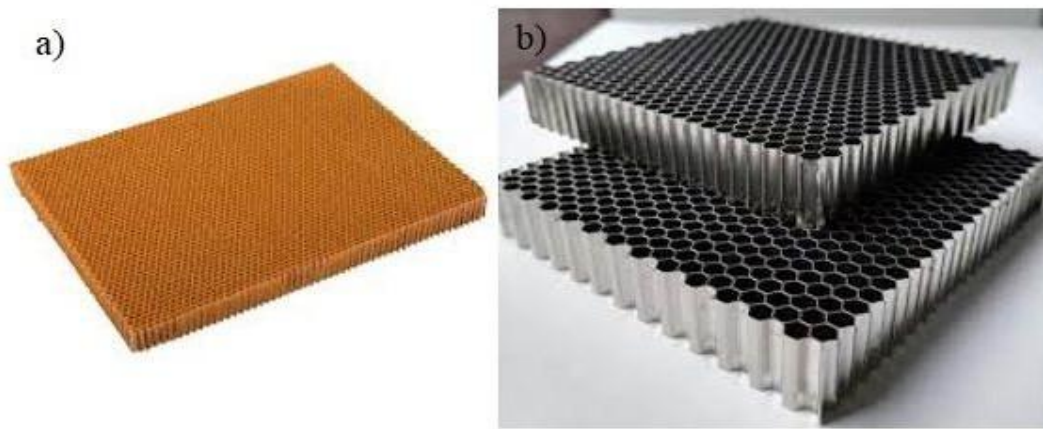


**Figure 2.** (a) Nomex honeycomb core; (b) Aluminum honeycomb core ( Ünlüsoy L, 2010)

Sandwich structures are generally divided into two categories. The symmetrical sandwiches shown in Figure 3 are preferred because they provide particularly high buckling and bending resistance. This type of structure is highly suitable for structures operating under pressure or subject to aerodynamics and is the most commonly used configuration in the literature.
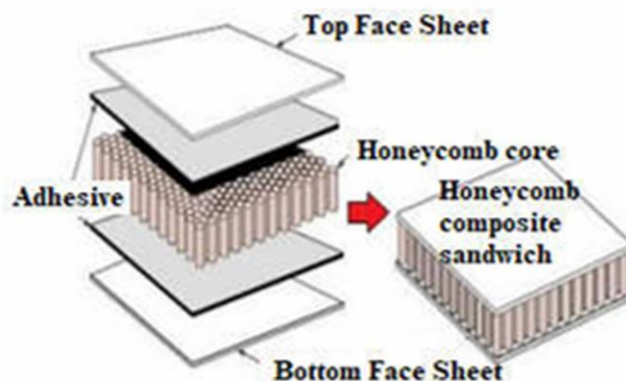


**Figure 3.** Schematic view of honeycomb sandwich (Demirci, 2018; Subaşı, 2017).

Approximately half of the wing surface—including the trailing edges—was made of fiberglass, while the main fuselage skin was constructed with Nomex honeycomb structural elements. While the majority of the winglets had the same economical panel structure, some composites were also made with aluminum honeycomb oils and coatings. However, the

wingbox, vertical tailbox, and fuselage structures were still manufactured from aluminum stiffened panels. The use of composites increased significantly in the following years; this increase was particularly accelerated by the ATR 72, the first civil aircraft to have its carbon fiber structure (wingbox) certified. This aircraft also utilized numerous flexible composite panels for the structures, and the skins were available in various forms, including fiberglass, Kevlar, and carbon.
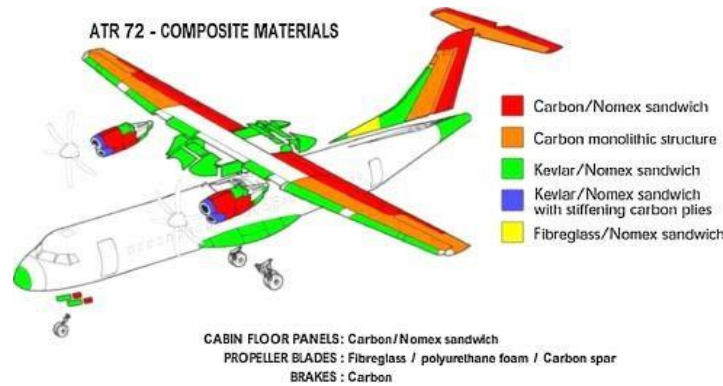


**Figure 4.** Composite materials used in the Boeing 747 aircraft.( İnsuyu ET, 2010.)

Although composite materials are generally used in UAV chassis design due to their light weight, the use of lightweight metals, particularly magnesium and aluminum alloys, is also increasing. In fact, when functionality is more important than weight, UAV chassis components can also be manufactured from materials such as steel, superalloys, etc. The most significant advantages of using aluminum are its strength and flight stability. To minimize vibration in the vehicle's body, which houses its electronic components, the primary material for this area is desired to be relatively heavier than materials such as carbon fiber, plastic, etc. UAVs designed from metal materials can produce UAVs with high flight stability and relatively light weight. This allows UAVs to find applications in a wide range of fields, particularly military and civilian. They can be used in a variety of missions, including minesweeping, firefighting, transporting objects from one location to another, and even being armed and deployed on the battlefield.

**Figure 5.** (a) Carbon fabric, (b) Aramid fabric, (c) Fiberglass fabric.( Soutis C, 2005.)

The most widely known type of polymer matrix composites (PMCs) is carbon fiber-reinforced polymer (CFRP). However, numerous alternative reinforcement fibers are also used, offering different advantages depending on the application. Besides carbon fibers, the most frequently preferred reinforcements are aramid, glass, quartz, and various thermoplastic fibers. Carbon fibers are produced from petroleum-derived pitch or, more commonly, polyacrylonitrile (PAN) polymer. PAN fibers undergo oxidation and carbonization processes, respectively, to remove other elements they contain and achieve the desired carbon structure. If necessary, additional heat treatment steps can be applied to increase the material's strength and stiffness. Aramid fibers are a class of aromatic polyamide-based materials known by trade names such as Nomex (meta-aramid) and Kevlar (para-aramid). Meta-aramids are particularly noted for their resistance to high temperatures, while para-aramids offer high mechanical performance with low weight. While glass fibers don't offer as high a strength-to-weight ratio as carbon fibers, they are more economical and more ductile. Quartz fibers, on the other hand, are preferred in structures requiring electromagnetic permeability, such as radomes, due to their transparency to high-frequency radio waves. Reinforcement fibers are often bonded to an epoxy-based polymer matrix. The fibers are used pre-impregnated with resin (prepreg) in the form of woven fabric or unidirectional tape. These resins contain latent hardeners that are activated by high temperatures, and the final composite structure is formed by cross-linking the molecules during curing. Because the curing reaction can be exothermic, temperature control is critical, especially for thick-section parts. Prepreg materials should be stored in cold storage to prevent undesirable curing at room temperature.

The first phase of an unmanned aerial vehicle is the design phase. Figure 4 shows the UAV's body design.



**Figure 6.** UAV Design.( Sakarya A, 2011.)

Figure 7 presents the visual representation of the T-Motor MT2814 model used  in the unmanned aerial vehicle system. This motor is classified among high- performance brushless DC motors, notable for its low internal resistance and high power output. The figure illustrates the motor's physical structure and connection interfaces in detail. (Chao, H., Cao, Y., & Chen, Y. 2007).



**Figure 7.** Image of T-Motor MT2814 (Bodson,  M. 2003).

**Table 1.** Technical Specifications of T-Motor MT2814 (Bodson, M. 2003).

| Specification | Value |
|---|---|
| KV | 770 |
| Stator Diameter | 28 mm |
| Stator Length | 14 mm |
| Shaft Diameter | 4 mm |
| Weight | 120 g |
| Cells | 3S, 4S |
| Max Current | 29 A |
| Max Power | 500 W |
| Internal Resistance | 100 mΩ |

DJI's 30A Opto 4S-6S was used in the UAV, and 30-amp ESCs were selected because the motors' maximum amp draw is 21.01 amps. These ESCs have a signal frequency between 30 Hz and 450 Hz and a continuous current of 30 A. The battery type used is 3S–4S LiPo.

**Figure 8.** Technical Description of Sunnysky X2814-11000KV
Brushless RC Aircraft Motor (Fnaiech, F. 2017).

**Table 2.** The technical specifications of the Sunnysky X2814-11000KV brushless motor are
as follows

| | |
|---|---|
| • Maximum thrust: | 2330 grams |
| • Operating voltage: | 3S–4S range |
| • Maximum continuous current: | 40 A (30 seconds) |
| • Minimum current: | 1.5 A |
| • Maximum power: | 600 W (180 seconds) |
| Internal resistance: | 32 mΩ |
| • Recommended ESC rating: | 50 A or higher |
| • Motor weight: | 84 grams |

Electronic Speed Control System (ESC) Operating Principle. The battery powering the motor is connected to the ESC. The ESC's control cable is connected to the remote control receiver. Many ESCs feature a feature called a BEC. The BEC (Battery Eliminator Circuit) reduces the voltage from the battery to match the remote control receiver.

Generally, the voltage of the batteries used for the motor is higher than the operating voltage of the remote control receiver. Therefore, to prevent damage to the receiver, this voltage is reduced by the BEC and transmitted to the receiver.

Some ESC models do not include a BEC. In this case, it is necessary to use an external battery with the appropriate voltage to power the receiver.

UAV systems often use ESCs without a BEC. In such systems, the ESC is connected not directly to the receiver, but to the flight control board. The receiver is similarly connected to this board. The ESC connection is made differently for RC airplanes, helicopters, cars, and boats.
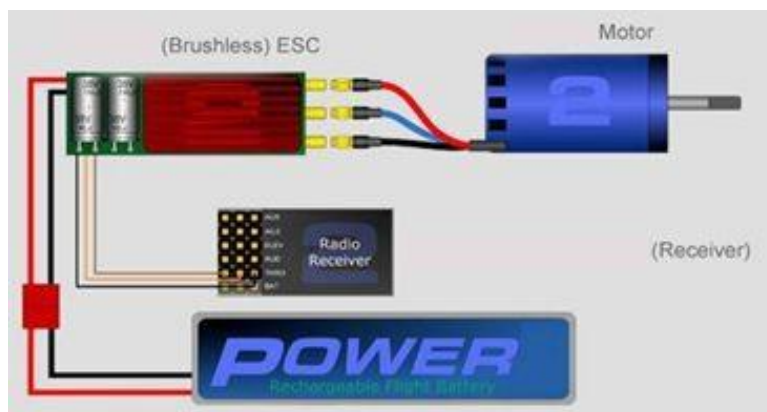


**Figure 9.** ESC Connection of Brushless Electric (Motor Vasiliev VV, Morozov EV, 2001.)

Electronic Speed Control System Selection Criteria

The first step in selecting an ESC is determining the system to be used. This system could be a car, boat, airplane, helicopter, or UAV. The second step is to determine the motor type— brushed or brushless. The third step is to select the ESC based on the motor's voltage and amperage. The amperage rating of the ESC to be purchased is determined by the motor's maximum current draw. For example, if the motor draws 40 amps, an ESC with at least 45-50 amps should be selected for a suitable ESC. This is because the motor will draw higher current than normal when requiring additional power. Therefore, a safety margin is necessary to prevent

damage to the ESC in the short term. Furthermore, the voltage rating of the ESC should be compatible with the motor's operating voltage and the voltage of the battery to be used.

For example, an ESC with at least 7.2 volts is sufficient for a 7.2-volt motor. However, the voltage of the motor or battery should not exceed the maximum voltage rating of the ESC. Electronic Speed Control System Selection Result The primary criteria for ESC selection are the motor, propeller, and battery. The electronic speed control system must be able to provide the 11.1 Volts required by the Sunnysky X2814-1100KV motor. Therefore, the first criterion is to select an ESC compatible with at least a 3S battery. The selected motor does not always draw constant current. To meet the required peak current, especially during takeoff, an ESC with a peak current rating of 50 amps should be selected. If necessary, various servo motor connections can be made to the ESC via the BEC circuit; in this case, the current draw could exceed 50 amps. Therefore, the ESC used in the system must be able to withstand currents exceeding 50 amps. The Hobbywing Skywalker 2-4S 50A UBEC Brushless ESC (5V / 5A BEC) was selected to meet these requirements.

**Table 3.** Technical specifications of ESC Units (Patterson and Grenestedt, 2018)

| Specification | 30A ESC Control Unit | 40A ESC Control Unit |
|---|---|---|
| Continuous Current | 30 A | 50 A |
| Burst Current | 40 A (10 seconds) | — |
| Input Voltage | 2–3S LiPo or 5–9S NiCd/NiMH | 3.7 V – 14.8 V DC |
| BEC | 2A / 5V (linear mode) | 3A / 5V (switching type) |
| Max RPM | 2 poles: 210,000 rpm<br>6 poles: 70,000 rpm<br>12 poles: 35,000 rpm | — |
| Dimensions | 45 × 24 × 11 mm | 45 × 26 × 10 mm |
| Weight | 25 g | 28 g / 31 g |
| PWM Frequency | — | 8K |
| Li-Po Compatibility | — | 2–3 cells |

**Figure 10.** *APC SlowFly SF 12 × 3.8 propeller. (*Sakarya E, 2010.)

**Table 4.** Technical specifications of APC 12 x 3,8 propeller (Ovalı and Esen, 2017)

| Pitch | Diameter (mm) | Hub Diameter | Hub Thickness | Shaft Diameter | Weight |
|-------|---------------|--------------|---------------|----------------|--------|
| 96.52 mm | 304.8 mm | 12.7 mm | 7.62 mm | 6.35 mm | 17.86 g |

Battery: A Gens Ace 7000mAh 4S1P battery was used. The main reason for choosing this battery is its continuous discharge rating of 350 A and its ability to provide 7000 mA of power per hour, allowing the UAV to have a flight endurance of approximately 10-12 minutes. Table 5 shows the specifications of the battery used in the UAV. Figure 8 shows a picture of the battery we used.



Figure 11. **Gens Ace 7000mAh 14.8V Battery (Soutis C, 2005)**

**Table 5**. Specifications of the battery used in the UAV (Soutis, 2005)

| Product Type | Capacity | Voltage | Continuous "C" Rating | Burst "C" Rating | Dimensions (mm) |
|---|---|---|---|---|---|
| LiPo | 7000 mAh | 14.8 V | 50C | 100C | 138.84 × 46.54 × 49.95 |

## REFERENCES

Ahsun, U., Badar, T., Tahir, S., & Aldosari, S. (2014). Autopilot fusion with external pilot inputs for enhancing flight safety of UAVs. *53rd IEEE Conference on Decision and Control*, (s. 236-241).

ALTIN, C., & ER, O. (2018). İnsansız Hava Araçlarının (İHA) Sanal Gerçeklik Yazılımı ile Modellenmesi ve Farklı Kullanıcılar için Performans Analizleri. *Sakarya Unıversıty Journal of Computer And Informatıon Scıences* , 1-13.

Ambroziak, L., & Gosiewski, Z. (2013). Preliminary UAV Autopilot Integration and In-Flight Testing. *Solid State Phenomena,* 198 , 232-237.

Anderson, N., Hagenauer, B., Erickson, R., & Bhandari, S. (2008). Flight-Testing of a UAV Aircraft for Autonomous Operation using Piccolo II Autopilot. *AIAA Atmospheric Flight Mechanics Conference and Exhibit*, (Paper: 2008-6568).

Andrievsky, B., & Fradkov, A. (2002). Combined adaptive autopilot for an UAV flight control. *Proceedings of the International Conference on Control Applications*, (s. 290-291).

Baomar, H., & Bentley, P. J. (2016). An Intelligent Autopilot System that Learns Piloting Skills from Human Pilots by Imıtations. *Unmanned Aircraft Systems*(ICUAS), (s. 1023-1031).

Bhar, A., Sayadi, M., & Fnaiech, F. (2017). Improved modular UAV autopilot simulator for Pinguin BE aircraft. *2017 International Conference on Control, Automation and Diagnosis* (ICCAD), (s. 125-129).

Bodson, M. (2003). Reconfigurable Nonlinear Autopilot. JOURNAL OF GUIDANCE, CONTROL, AND DYNAMICS 26(5) , 719-727. Borys, D. N., & Colgren, R. (2005). Advances in Intelligent Autopilot Systems for Unmanned Aerial Vehicles. *AIAA Guidance, Navigation, and Control Conference and Exhibit*, (Paper: 2005-6482).

Capello, E., Guglieri, G., & Ristorto, G. (2017). Guidance and control algorithms for mini UAV autopilots. *Aircraft Engineering and Aerospace Technology*, Vol. 89 No. 1 , 133-144.

Chao, H., Cao, Y., & Chen, Y. (2007). Autopilots for Small Fixed-Wing Unmanned Air Vehicles: A Survey. *International Conference on Mechatronics and Automation*, (s. 3144-3149).

Çallı, A., Tunçkan, O. 2023. Investigation of glass fiber reinforced aluminum honeycomb panel repair performance according to aviation standards. *Journal of Scientific Reports-A*, 059: 70-86.

Griffin CF, Fogg LD, *Dunning EG, 1981. Advanced composite aileron for L-1011 transport aircraft: Design and analysis*. NASA, Technical Report; NASA-CR-165635, NAS 1.26:165635, LR-29635

İnsuyu ET, 2010. *Aero-Structural Design and Analysis of an Unmanned Aerial Vehicle and its Mission Adaptive Wing*. Middle East Technical University Graduate School of Natural and Applied Sciences, Master Thesis (Printed).

Demirci, M. T. (2022). Investigation of low-velocity impact behavior of aluminum honeycomb composite sandwiches with GNPs doped BFR laminated face-sheets and interfacial adhesive for aircraft structures. *Polymer Composites*, *43*(8), 5675-5689.

Ovalı İ, Esen C, 2017. ANSYS® Workbench. Kodlab Yayın Dağıtım Yazılım ve Eğitim Hizmetleri San. ve Tic. Ltd. Şti., s. 21-26, İstanbul-Türkiye.

Öztürk AM, 2019. *Kompozit Malzemeden Mamul İnsansız Hava Aracı Parçalarının Yapısal Analizi*. Atatürk Üniversitesi Fen Bilimleri Enstitüsü, Yüksek Lisans Tezi (Basılmış).

Patterson JB, Grenestedt JL, 2018. Manufacturing of a composite wing with internal structure in one cure cycle. *Composite Structures*, 206: 601-609.

Romano F, Fiori J, Mercurio, U, 2009. Structural design and test capability of a CFRP aileron. *Composite Structures*, 88 (3): 333–341.

Sakarya A, 2011. *Multidisciplinary Design of An Unmanned Aerial Vehicle Wing. Middle East Technical University Graduate School of Natural and Applied Sciences*, Master Thesis (Printed).

Sakarya E, 2010. *Structural Design and Evaluation of an Adaptive Camber Wing*. Middle East Technical University Graduate School of Natural and Applied Sciences, Master Thesis (Printed).

Sepe R, Citarella R, De Luca A, Armentani E, 2017. Numerical and Experimental Investigation on the Structural Behaviour of a Horizontal Stabilizer under Critical Aerodynamic Loading Conditions. *Advances in Materials Science and Engineering*, ID 1092701.

Soutis C, 2005. Carbon fiber reinforced plastics in aircraft construction. *Materials Science and Engineering:A*, 412 (1-2): 171–176.

Starke Jr EA, Staley JT, 1996. Application of modern aluminum alloys to aircraft. *Progress in erospace Sciences*, 32 (2-3): 131–172.

Starnes Jr JH, Haftka RT, 1979. Preliminary Design of Composite Wings for Buckling, Strength, and Displacement Constraints. *Journal of Aircraft*, 16 (8): 564-570.

Ünlüsoy L, 2010. *Structural Design and Analysis of The Mission Adaptive Wings of An Unmanned Aerial Vehicle*. Middle East Technical University Graduate School of Natural and Applied Sciences, Master Thesis (Printed).

Vasiliev VV, Morozov EV, 2001. Mechanics and Analysis of Composite Materials. *Elsevier Science* Ltd., pp. 271-283, The Boulevard Langford Lane Kidlington Oxford-UK.

# CHAPTER 20

# COMPARISON OF OPEN SOURCE RTEMS AND RTLINUX REAL- TIME OPERATING SYSTEMS

Talha ÇELİK[1], Prof. Dr. Fatih BAŞÇİFTÇİ[2]

[1] Phd. Student, Computer Engineering Department, Faculty of Technology, Selçuk University, Türkiye,
ORCID: 0002-0916-0065, e-mail: tlhcelik81@gmail.com
[2] Prof. Dr. Computer Engineering Department, Faculty of Technology, Selçuk University, Türkiye
ORCID: 0000-0003-1679-7416, e-mail: basciftci@selcuk.edu.tr

# 1. INTRODUCTION

Real-time operating systems (RTOS) are widely used in every field today. These systems have a wide range of applications, from the fuel balancing system of a space rocket to the control systems that operate coffee machines (Pamuk, 2007). Some problems arise from the widespread use of real-time operating systems. These generally differ in terms of hardware compatibility, memory requirements, sustainability of input/output devices, network support, file system, dynamic object loading, memory protection, and target central processing unit (CPU). In the simplest terms, a real-time operating system is fixed software that runs on specialized hardware with an infinite loop and is solely responsible for performing the tasks assigned to it. This software essentially communicates with input/output devices to perform fixed tasks. For example, a system that controls a fan based on room temperature is real-time due to the software it contains and performs its operations on specially designed hardware. In such scenarios, issues like network communication, memory usage, and timing are generally not addressed, but as system complexity increases, these problems also arise. The development of real-time operating system software, which can be considered complex for specialized hardware such as memory management, job scheduling, and network communication, aims to eliminate these issues. (Stankovic, 1996). Although real-time operating systems that provide standard features are commonly available, in specialized applications, the real-time operating system is expected to support the entire hardware structure. Additionally, it should be inexpensive and provide a quick solution for the developer (Çotuk et al., 2008; Kutlu and Gençtürk, 2021).

This study examines two open-source real-time operating systems that are not subject to any licensing fees within a general framework. Both operating systems were run on specific hardware and performance tests were conducted using fixed algorithms. Section 2 provides a detailed explanation of the Real Time Linux (RTLinux) and Real-Time Executive for Multiprocessor System (RTEMS) real-time operating systems. Subsequently, the algorithm used to test response times was examined, and experiments were conducted. Based on the results obtained from the experiments, both operating systems were compared in terms of response time. The final section presents the results obtained.

## 2. RTLINUX REAL TIME OPERATING SYSTEM (REAL TIME LINUX)

RTLinux, a real-time operating system, was first developed by the New Mexico Institute of Mining and Technology. The RTLinux project was then taken over by FSM Labs and continued to be developed as open source. The entire project is licensed under the General Public License (GPL). Technologies covered by this license may be distributed and used commercially, provided the developer is credited. The basic idea behind RTLinux is quite fundamental. It operates as an easily understandable software

257

layer dependent on interrupt handlers and is enabled and disabled by standard Linux operating system interrupt operations. It effectively takes over all the hardware it is embedded in and is managed by a dedicated real- time timer (Slanina and Srovnal, 2007).

The real-time Linux kernel handles all hardware interrupts and forwards them appropriately to the Linux operating system or to the software layer that manages real-time threads. The interrupt manager does not directly allow the Linux operating system to disable interruptions. Instead, when disabling an interrupt request (IRQ), Linux calls an RTLinux flagger that actually marks the target interrupt as disabled (Ji et al., 2008). When the interrupt manager finds an IRQ request marked in this way, it waits for the associated interrupt request to stop before sending it to the Linux operating system to reactivate the IRQ. This behavior is one of the fundamental structures found in the Linux operating system kernel.

Since the Linux operating system is a low-priority task that does not have direct access to interrupt hardware and does not have direct access to interrupt hardware, this means that real- time threads added to the system can only interact very weakly with Linux special communication channels and synchronization-based primitives (Slanina and Srovnal, 2007). This way, the hardware and software layers are isolated from each other, enhancing the system's security. Interrupt requests can only interact with RTLinux kernel services and can execute operations with the timer hardware. The biggest disadvantage of this situation is that the C programming language, which is a low-level language, does not provide standard Linux system services such as mathematical libraries, network, file systems, and drivers developed for input/output.

Therefore, proficiency in the C programming language is required for applications to be developed on RTLinux. Communication with user-space processes is performed not only through hardware and internal system communications, but also via a dedicated real-time first- in-first-out (FIFO) device (Andris and Dobrovodský, 2014). This can be achieved by fully utilizing the capabilities of the C programming language.

Following the RTL philosophy, applications should be integrated as ordinary Linux programs in most user areas. Only real-time critical tasks enter a special module and are loaded into kernel memory using the Linux operating system's standard kernel module loader (Andris and Dobrovodský, 2014).

With version 3.1 of RTLinux (1003.13), features such as pthreads, semaphores, state variables, and a dedicated application software interface for the interrupt subsystem have been made available (BloomandSherrill, 2014). Therefore, the interface provider does not provide the library itself that can be used ready-made with the C programming language.

Among RTLinux's special features are high time resolution and periodic timing (Ji

et al., 2008). High temporal resolution is one of the important features that real-time operating systems must have, but its usefulness is somewhat balanced by relatively high latency. Due to the multi-layered system architecture of Linux on the RTLinux kernel, the RTLinux application must be carefully divided into real-time critical and non-real-time critical parts. For example, critical tasks should not write to files or access non-real-time drivers; instead, they should delegate this task to non-real-time code.

RTLinux supports a subset of CPUs and platforms supported by Linux. This enables the RTLinux real-time operating system to run on a wide range of hardware. X86, PowerPC, Alpha, and MIPS are currently supported by RTLinux. RTLinux development is typically carried out using the well-known GNU toolchain, which is ported to various host platforms. The RTLinux kernel comes with an application software interface that also provides debugging support for real-time modules.
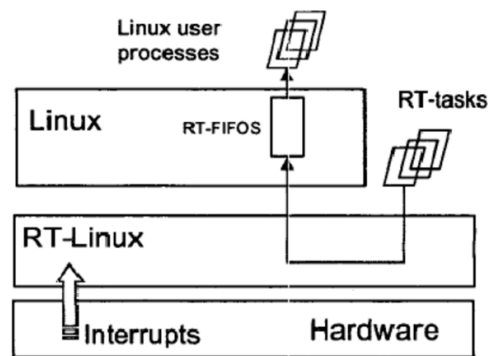


**Figure 1** RTLinux System Architecture (Manivannan M. et. al., 2010)

## 3. RTEMS (REAL-TIME EXECUTIVE FOR MULTIPROCESSOR SYSTEM)

RTEMS stands for Real-Time Execution in Multi-Processor Systems. Developed by OaR Corporation for the U.S. Department of Defense, RTEMS is based on and licensed under a variant of the GPL. OaR coordinates development and provides commercial support for RTEMS and other related services. RTEMS was developed for military purposes, but is used not only in military but also in industrial and scientific projects.

EPICS, a control system software widely used in the Accelerator Control (AC) community, has been ported to RTEMS for use and development starting with the new EPICS version 3.1, and development has continued based on the EPICS 3.1 version.

RTEMS, designed from scratch to be a true RTOS, can be used in embedded systems with low memory. In terms of its working structure, system components are referred to as managers in RTEMS terminology and are isolated into separate modules.

It connects the managers to applications as needed (Norum, 2002). By selecting the appropriate configuration parameters, the necessary system settings are made according to the requirements of the application being developed. This allows the application running on the entire real-time operating system to be fully utilized, ensuring it runs in the fastest and most effective manner. A typical RTEMS application compiles itself by providing the necessary configuration parameters, links to the desired RTEMS manager, and runs on the target system that is downloaded or written to ROM (Bloom et al., 2020; Pizlo et al., 2010). Unlike RTLinux, RTEMS allows all system services and libraries to be used directly for any application task.

RTEMS has a classic/native API for POSIX (1003.1b), ITRON, C, and ADA language bindings. RTEMS includes components such as multitasking, threads, synchronization-based tasks, mutexes, semaphores, message queues, timers, FIFO and Round Robin schedulers, and monotonic speed by default (Barbosa et al., 2003; BloomandSherrill, 2014). This is a significant advantage in general-purpose systems. RTEMS has made a port of the BSD TCP/IP network stack available to support multiple CPUs. This makes the network infrastructure easy to use and integrate (Colin and Puaut, 2001). As with VxWorks, there is no memory protection. The system and application software share the same storage space. RTEMS itself does not provide a shell or dynamic loader as powerful as VxWorks, but it leaves it up to the developer to create the necessary infrastructure to build application programs that provide the relevant functionality. Designed for easy portability, RTEMS supports many CPU architectures, including m68k, ColdFire, Hitachi SH, Intel i386, Intel i960, MIPS, PowerPC, SPARC, AMD A29k, and HP PA- RISC (Pizlo et al., 2010). In a study conducted by Moreaes et al. in 2008, the results obtained from measuring the error conditions created by RTEMS and RTLinux real-time operating systems under certain conditions and similar execution codes showed that the RTEMS real-time operating system is more reliable than the RTLinux real-time operating system in terms of error generation and error behavior rates (Moraes et al., 2008). From this result, it was concluded that the RTEMS real-time operating system should be used in mission-critical tasks, as it surpasses the RTLinux real-time operating system in terms of speed and reliability.

**Table 1.** The Risk Evaluation and Failure Mode (Moraes et al., 2008).

| Component | prob(f) | Crash | | Wrong | | Hang | | Incorrect Behavior | |
|---|---|---|---|---|---|---|---|---|---|
| | | cost(f) | risk | cost(f) | risk | cost(f) | risk | cost(f) | risk |
| **RTEMS** | 0.0749 | 0.09 | 0.67 | % 0.05 | 0.37% | 0.12 | 0.89% | 0.26 | 1.94% |
| **RTLinux** | 0.0650 | 0.25 | 1.62% | 0.01 | 0.06% | 0.24 | 1.56% | 0.50 | 3.25% |

## 4. METOD

In this study, fundamental parameters such as interrupt latency, processing time, and task completion time were considered in the performance analysis of real-time operating systems. In this context, the comparison of RTLinux and RTEMS operating systems allows for an objective evaluation of the systems' deterministic timing capabilities. The study created an experimental environment isolated from physical effects using the PowerPC SAM460ex architecture on the QEMU hardware virtualizer. QEMU aims to provide a controlled test infrastructure by eliminating the need for real hardware to measure low-level timing behavior.

In the comparison method, the ping command, which is a program that can be run on the system, was chosen as the measurement tool. However, in this context, the response times of the ICMP packets generated by ping over the network or data related to packet transmission were not taken into account. Instead, only the time it takes for the ping executable program to reach the processor, the execution time with interrupt triggering, and the total processing time until termination were calculated. The data obtained is shown in Table 2. This approach allows the ping application to be treated as a task at the system call level, enabling measurement in terms of interrupting latency and task completion performance. Furthermore, examination of the ping program's source code revealed that it contained identical source code for both systems. The middleware developed to obtain data in this experiment is software developed using the C programming language that listens to and reports system responses and calls through the API provided by real-time operating systems.

In the experimental design, the ping program is called at specific intervals, the start and end times are recorded for each call, and average processing times and variance values are obtained from this data. The results obtained using this method comparatively demonstrate the timing performance of RTLinux's process scheduling features and the lightweight, embedded- focused kernel architecture of the RTEMS real-time operating system.

### 4.1. Comparison of Board Support Package (BSP) Utilities

Today, there are many different and specialized hardware architectures being produced and developed. The most well-known of these are the Intel and AMD processor architectures that specify x86 and x64 package sizes. However, these central processing units have been developed to be multi-purpose. In addition to these, there are many microprocessors developed for specific purposes. The PowerPC SAM460ex model, a special-purpose hardware used in this research, was run on the QEMU hardware virtualizer to conduct experiments and obtain results.

RTEMS and RTLinux real-time operating systems support the specialized hardware shown in Table 1. As can be seen from Table 1, the RTEMS real-time

operating system offers developers a very extensive BSP infrastructure.

**Table 2** Comparison of RTEMS and RTLinux real-time operating systems with BSD

| Hardware Systems | RTEMS | RTLinux |
|---|---|---|
| m68k | ✓ | × |
| ColdFire | ✓ | × |
| Hitachi SH | ✓ | × |
| Intel i386 | ✓ | ✓ |
| Intel i960 | ✓ | ✓ |
| MIPS | × | - |
| AMD A29k | ✓ | × |
| HP PA-RISC | ✓ | × |
| Alpha | × | ✓ |
| ARM | ✓ | ✓ |
| PowerPC | ✓ | ✓ |

## 4.2. Response Time Test

One of the most important features of real-time systems is the response time, which is the time required for the system to respond to an external event under the worst-case conditions (Duman, 2008). Here, appropriate experiments were conducted by considering two important terms: switching delay and context switching delay.

## 4.3. Interrupt Delay and Context Delay

The time between the device that activates the interruption line and the system that sends the appropriate interrupt service routine (ISR) is called interrupt latency. Context switch latency refers to the time it takes to schedule a task. When performing this operation, the timer decides which task to queue, saves the current task content, and restores the new task content (Coutinho et al., 2005). There are so many possible combinations of conditions within a computer system that it is nearly impossible to find the worst-case scenario. Therefore, a statistical approach is chosen to create the worst-case scenario (ColinandPuaut, 2001). The main idea here is to run the system under heavy load for a period of time while measuring latency. Additionally, it is assumed that the maximum latency recorded during the test reflects the worst-case scenario. In the worst-case scenario, the system's cut-off latency times are recorded for comparison. Figure 2 shows an example of a semaphore transition in the RTEMS real-time operating system (ColinandPuaut, 2001). The diagram indicates that one operation occurs between the times marked 2 and 4. At time 1, the process is acquired; at time 2, the process is transferred to the relevant hardware to be executed; at time 3, a termination request is generated; and at time 4, the process is completely terminated.
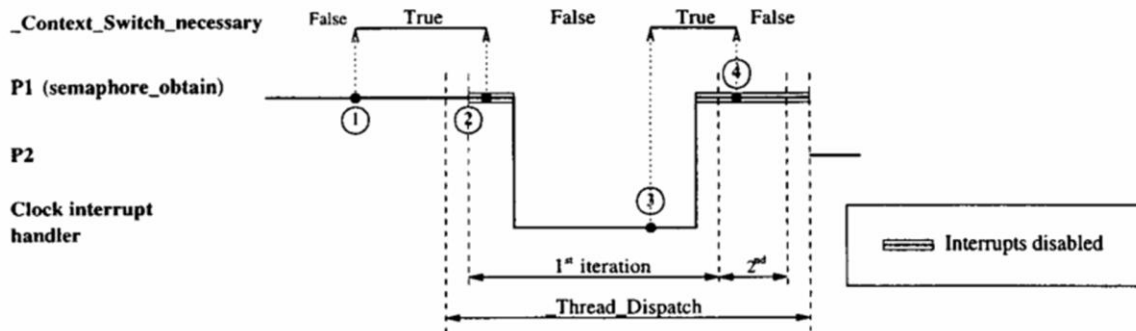
**Figure 2.** Ilustration of function _thread_dispatch (Colinand Puaut, 2001)

### 4.4. Testing Algorithm

To perform the measurements, Motorola's PREP-compliant MVME2306 card and PowerPC SAM460ex cards are equipped with the drivers and periodic interruptions of the QEMU virtualization system and the appropriate infrastructure. This system was obtained by virtualizing the PowerPC-based system on the Windows 10 operating system using QEMU, a hardware virtualization software. This allows both real-time operating systems to be tested on this virtual hardware.

The SAM460ex hardware features a high-resolution timer hardware that can be configured to generate periodic interruptions. Running timers can be read instantly, which facilitates accurate measurement of delays. The test software package consists of a startup routine, an ISR, and a simple measurement procedure. The startup code initializes the timer hardware, connects the ISRs to the appropriate interruptions, and creates a task (MT) to perform the measurement operation with the highest priority available in the system under test. The ISR reads the timer to determine the interrupted delay and releases the semaphore to notify the MT that it is blocked. This allows the system timing MT, as the highest-priority executable task running the timer, to read the timer and determine how long it will take for the ISR to release the semaphore before the MT actually takes over the CPU. After recording the delay, the MT blocks the semaphore again. A schematic representation of the algorithm is shown in Figure 1. The content of the operation to be performed in this algorithm is not considered. The algorithm has been developed taking into account the start, processing, execution, and completion of the operation in order to obtain stable results in both real-time operating systems. The measurement method used in the operations performed is the capture of ISR requests, interrupt requests, and interrupt task termination requests.

The requests published by the real-time operating system were repeated at 1000, 10000, and 100000 time steps of the same test algorithm, and the obtained data were reported. This allowed the response time of the real-time operating system for an average operation to be recorded. The QEMU hardware virtualizer was used in the experiment. This isolated the system from physical factors such as hardware voltage and temperature. This simple test was run on a system loaded with low-priority tasks, network, and serial I/O traffic, and a series of errors were obtained. By definition, a fixed real-time system must ensure that the delay experienced by high-priority ISRs and MTs remains below a certain fixed limit, regardless of the amount of low-priority load, and that a lower-priority interrupt does not interrupt a higher-priority task. Therefore, the maximum delay recorded during testing was evaluated as a measure of a particular system's operational and processing quality.
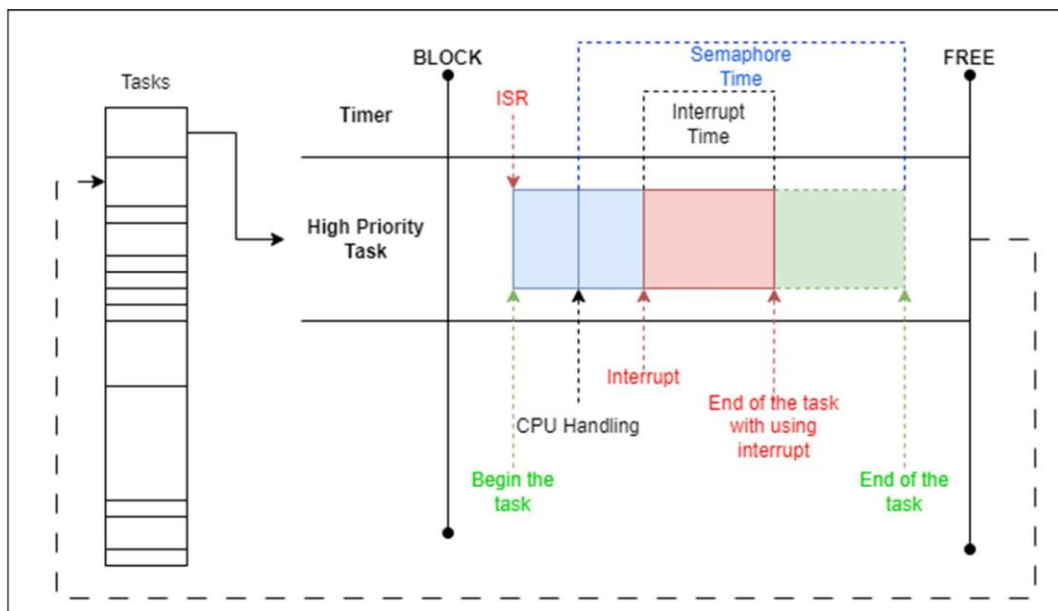


**Figure 3**. Scheme of test algorithm

## 5. EXPERIMENTAL RESULTS

The tests and experiments conducted involved adding PowerPC SAM460ex hardware to the QEMU hardware virtualizer and running RTLinux and RTEMS systems on the same hardware. The added hardware generated timer interrupts with virtual hardware set to a full capacity processor speed of 1,500,000 kHz. Maximum and average delays were reported in repeated time steps. Measurements were performed under both idle and loaded conditions. The processor utilization rate was determined to be approximately 0% in the idle system and approximately 100% in the loaded system. The main point to be emphasized in the tested system is that a low-priority thread is

represented by receiving a TCP path during the loop feedback from host to host. Fully loaded system timing, synchronization principles, and a large amount of interrupt and kernel activity, including some network and driver code, were involved. Table 2 shows that both real-time operating systems exhibit equivalent values in the unloaded system. However, it is observed that the results change significantly under load.

The RTLinux real-time operating system has significantly higher latency in loaded systems. Considering that managing and emulating Linux interrupts requires more complex interrupt distribution, it is expected that the RTLinux real-time operating system will experience latency in a fully loaded system. This situation indicates that RTLinux is not suitable for hard real-time requirements. Considering RTEMS's performance, it can be assumed that improvements would be relatively easy. As Table 2 shows, average latencies are approximately 45% lower than their respective maximums. Statistical tests establish a lower bound for maximum latency, but no clear conclusion can be drawn about the actual worst-case value.

In the broadest sense, the system's interrupting processing component is largely dependent on the hardware architecture. Therefore, the interrupt latency figures cited here represent the PowerPC SAM460ex, but because interrupt latency is hardware-based and calculated independently of CPU architectures, it cannot be easily converted to other CPU architectures.

**Table 3.** Delay time based on interrupts for RTEMS and RTLinux.

|  | Longest Interrupt Time (µs) | Average Delay Time (µs) | Context Switching Time (µs) | Average Change Time (µs) |
|---|---|---|---|---|
|  | Processor Utilization ~%0 (IDLE) | | | |
| RTLinux | 12.9 | 1.9 (± 0.5) | 43.2 | 9.8 (± 0.5) |
| RTEMS | 15.2 | 1.2 (± 0.5) | 16.9 | 3.3 (± 0.5) |
|  | Processor Utilization ~%100 | | | |
| RTLinux | 211.4 | 2.0 (± 4.0) | 186.8 | 10.1 (± 4.0) |
| RTEMS | 20.5 | 2.9 (± 4.0) | 50.1 | 4.5 (± 4.0) |

## 6. CONCLUSION and DISCUSSION

RTEMS and RTLinux are two very different open-source real-time operating system solutions. Both real-time systems have been tested on specific hardware architectures in terms of latency.

In light of the results obtained, it is clear that the RTEMS real-time operating system surpasses the RTLinux real-time operating system in terms of both basic functionality and performance. Furthermore, considering the difficulties arising from the lack of built-in C programming language and libraries required during the development phase of RTLinux, RTEMS stands out as a system that can be used for real-time processing in many respects. RTLinux can be used in situations where maximum performance of a desktop system is required and can extend such systems with real-time capabilities. However, this may result in higher latency and may limit the available system services for real-time tasks. On the other hand, the comparisons made within the scope of this study do not lead to the conclusion that RTLinux should be avoided in situations requiring multimedia use, graphics calculations, and other similar multi-purpose tasks. Real-time operating systems are critical in many conditions, both because of the nature of the tasks they perform and because they must operate within specific time intervals. Considering the tasks performed by real-time operating systems used in vehicle recognition and radar systems, telecommunications systems, satellite systems, and many other areas, the ability of these systems to perform their required tasks within the expected time frame is crucial for their sustainability and security. In light of the data obtained in this study, the BSD infrastructures supported by the real-time operating system planned for use were examined. Experiments were conducted on the hardware architecture supported by both systems.

Based on the data obtained, it was concluded that the RTEMS real-time operating system demonstrated significantly better performance than the RTLinux real-time operating system in terms of task initiation, execution, interrupt handling, and termination. However, since this situation is directly related to the importance of the task to be performed, it has also been concluded that the use of the RTLinux real-time operating system may be preferable in terms of reducing the complexity of the developed system and increasing hardware support.

## REFERENCES

Andris, P., & Dobrovodský, K. 2014. Developing an embedded system based on a real-time version of Linux. *2014 23rd International Conference on Robotics in Alpe-Adria-Danube Region (RAAD)*, 1-7.

Barbosa, R., Maia, R., Esteves, J., Henriques, L., & Costa, D. 2003. RTEMS 4.5.0 Evaluation Report, RAMSCall-offOrder 2, *Portugal,* 10-44.

Bloom, G., & Sherrill, J. 2014. Scheduling and thread management with RTEMS. *ACM Sigbed Review*, *11*(1), 20-25.

Bloom, G., Sherrill, J., Hu, T., & Bertolotti, I. C. 2020. Real-Time Systems Development with RTEMS and Multicore Processors, *CRC Press,* Oxfordshire*,* 103-157.

Colin, A., & Puaut, I. 2001. Worst-case execution time analysis of the RTEMS real-time operating system. *Proceedings 13th Euromicro Conference on Real-Time Systems*, 191-198.

Çotuk, H., Erbaş, C., & Erten, Y. M. 2008. PIC mikrodenetleyiciler için gerçek zamanlı işletim sistemi, Yüksek Lisans, *Fen Bilimleri Enstitüsü*, TOBB Ekonomi ve Teknoloji Üniversitesi, 53-98.

Coutinho, M., Rufino, J., & Almeida, C. 2005. Control of Event Handling Timeliness in RTEMS. *Proceedings of the 17th IAESTED International Conference Parallel and Distributed Computing Systems*, 277-282.

Duman, O. F. 2008. *Gerçek zamanli bilgisayar kontrol sistemlerinde işlem süreci organizasyonu* Ankara Universitesi (Turkey)].

Ji, H., Li, Y., & Wang, J. 2008. A software-oriented CNC system based on Linux/RTLinux. *The international journal of advanced manufacturing technology*, *39*(1), 291-301.

Kutlu, E., & Gençtürk, C. 2021. Uydu Uçuş Yazılımında Gerçek Zamanlı İşletim Sistemleri Zamanlama Algoritmaları. *Türkiye Bilişim Vakfı Bilgisayar Bilimleri ve Mühendisliği Dergisi*, *14*(1), 1-14.

Manivannan, M., & Kumaresan, N. (2010). Embedded web server & GPRS based advanced industrial automation using Linux RTOS. International Journal of Engineering Science and Technology, 2(11), 6074-6081.

Moraes, R., Duraes, J., Barbosa, R., Martins, E., & Madeira, H. (2007, June). Experimental risk assessment and comparison using software fault injection. In 37th Annual IEEE/IFIP International Conference on Dependable Systems and Networks (DSN'07) (pp. 512-521). IEEE.

Norum, W. E. 2002. EPICS on the RTEMS real-time executive for multiprocessor systems. *Review of scientific instruments*, *73*(3), 1560-1562.

Pamuk, E. 2007. Gömülü sistemler için gerçek zamanlı işletim sistemleri ile kontrol, Yüksek Lisans, *Fen Bilimleri Enstitüsü*, Yıldız Teknik Üniversitesi, 25-43.

Pizlo, F., Ziarek, L., Blanton, E., Maj, P., & Vitek, J. 2010. High-level programming of embedded hard real-time devices. *Proceedings of the 5th European conference on Computer systems*, 69–82.

Slanina, Z., & Srovnal, V. 2007. Embedded Linux scheduler monitoring. *IEEE Conference on Emerging Technologies and Factory Automation (EFTA 2007)*, 760-763.

Stankovic, J. A. 1996. Strategic directions in real-time and embedded systems. *ACM Comput. Surv.*, *28*, 751-763.

# CHAPTER 21


# TUBERCULOSIS IN CATTLE; EPIDEMIOLOGY, DIAGNOSTICS, AND GLOBAL CONTROL PERSPECTIVES

Dr. Fatma ATLI[1]

[1] Ege University Faculty of Agriculture, Department of Animal Science, Bornova-İzmir,
ORCID: 0000-0001-6536-5594, e-mail: atli.fatma@ege.edu.tr

## 1. INTRODUCTION

Bovine tuberculosis (bTB) is a chronic infectious disease of cattle caused by Mycobacterium bovis, a member of the Mycobacterium tuberculosis complex (Avele et al., 2004). The disease has been recognized since antiquity, with skeletal remains and historical accounts providing evidence of tuberculosis-like lesions in cattle and humans (Chambers et al., 2011). It is considered one of the most important zoonotic infections due to its dual impact: it compromises livestock productivity and threatens human health through zoonotic transmission (Michel et al., 2010).

From a global perspective, bovine tuberculosis has been eradicated or effectively controlled in many developed nations, primarily due to rigorous test-and-slaughter programs, compulsory pasteurization of milk, and strict surveillance systems (Lange et al., 2022). For example, the United States, Australia, and several European countries report very low prevalence rates, with eradication being nearly achieved. In contrast, in low- and middle-income countries, eradication remains elusive. Limited veterinary infrastructure, economic constraints, reliance on unpasteurized dairy products, and close human–animal interactions facilitate the persistence and spread of M. bovis (Ayele et al., 2004).

The One Health significance of bTB lies in its zoonotic potential. Humans acquire M. bovis primarily by consuming contaminated milk or dairy products, inhaling infectious aerosols, or through direct occupational exposure (farmers, abattoir workers, veterinarians) (Taye et al., 2021). Although the global burden of zoonotic tuberculosis is smaller than that of human tuberculosis caused by M. tuberculosis, the public health implications are serious, especially in areas with high HIV prevalence where coinfection increases susceptibility (Michel et al., 2010).

Economically, bovine tuberculosis causes direct losses due to reduced milk yield, poor weight gain, infertility, and carcass condemnation, as well as indirect losses through trade restrictions and the costs of diagnostic testing and eradication measures (Corner, 2006). In endemic regions, the disease significantly undermines agricultural development and food security, exacerbating poverty cycles.

Scientific advances in immunology and molecular biology have expanded our understanding of M. bovis pathogenesis and host–pathogen interactions. Nevertheless, major challenges remain. Current diagnostic tests are imperfect, subclinical infections are common, and the presence of wildlife reservoirs complicates eradication (Corner, 2006). Moreover, the absence of an effective and widely deployable vaccine that does not interfere with diagnostic tools is a critical limitation (Collins et al., 2022).

In summary, bovine tuberculosis is not merely a veterinary concern but a multifaceted problem at the interface of animal health, public health, and socio-economic development. Addressing it requires an integrated One Health approach combining improved diagnostics, vaccination strategies, wildlife management, and public health interventions tailored to local contexts.

## 2. ETIOLOGY

The causative agent of bovine tuberculosis is *Mycobacterium bovis*, a slow-growing, aerobic, acid-fast bacillus that belongs to the *Mycobacterium tuberculosis* complex (MTBC) (Akurut et al., 2025). The MTBC also includes *M. tuberculosis*, *M. africanum*, *M. microti*, and others, but *M. bovis* is the predominant species affecting cattle and a wide range of domestic and wild mammals (Lange et al., 2022).

- Cell wall structure: The organism possesses a lipid-rich cell wall composed of mycolic acids, glycolipids, and lipoarabinomannan, which confer resistance to desiccation, many disinfectants, and host immune defenses (Riopel et al., 2024).

- Growth characteristics: *M. bovis* grows slowly in culture, typically requiring 4–12 weeks to produce visible colonies on Löwenstein–Jensen medium or Middlebrook agar (Philips et al., 2003). This slow growth contributes to diagnostic delays.

- Host range: Unlike *M. tuberculosis*, which is primarily a human pathogen, *M. bovis* has a remarkably broad host range, infecting cattle, buffalo, goats, pigs, deer, badgers, possums, lions, and even humans (Michel et al., 2010). This host diversity complicates eradication efforts.

## 2. PATHOGENESIS

The pathogenesis of bovine tuberculosis involves a complex interaction between the pathogen and the host immune system.

1. Entry into the host: Infection most commonly occurs via inhalation of aerosolized bacilli from coughing or sneezing animals (Phillips et al., 2003). Alternatively, ingestion of contaminated milk or feed can initiate infection, particularly in calves (Ayele et al., 2004).

2. Initial infection and macrophage invasion: Once inhaled or ingested, *M. bovis* is phagocytosed by alveolar macrophages. Instead of being destroyed, the bacilli survive and replicate by preventing phagosome–lysosome fusion and resisting reactive oxygen and nitrogen intermediates (Thacker et al., 2006).

3. **Innate and adaptive immune response**

- Innate immunity: Infected macrophages release cytokines (IL-12, TNF-α, IFN-γ), recruiting T lymphocytes and other immune cells to the site of infection (Pollock and Neill, 2002).
- Adaptive immunity: A cell-mediated immune response develops, characterized by activation of CD4+ T cells, which are crucial in containing infection. However, the pathogen's ability to persist within macrophages leads to a chronic infection.

4. **Granuloma formation**: The hallmark lesion of bovine tuberculosis is the granuloma, also known as a tubercle. Granulomas consist of a central area of infected macrophages and necrosis, surrounded by lymphocytes, multinucleated giant cells (Langhans cells), and a fibrous capsule (Waters et al., 2012).

- Protective role: Granulomas serve to wall off the infection and limit bacterial spread.

270

- Pathological role: Over time, granulomas undergo caseous necrosis, calcification, and liquefaction, which may lead to bacillary dissemination.

5. **Dissemination**: Although primary lesions occur in the lungs and associated lymph nodes, bacilli can spread via the lymphatic and hematogenous routes to the liver, kidneys, spleen, intestines, and mammary glands (Pollock and Neill, 2002). Dissemination is often associated with advanced disease and increased zoonotic risk, particularly via excretion in milk.

6. **Latent versus active disease**
- Latent infection: Many infected cattle remain asymptomatic for long periods, harboring viable bacilli in granulomas. Stress, co-infections, or immunosuppression can reactivate the disease (Pollock and Neill, 2002).
- Active infection: Progressive breakdown of granulomas leads to extensive tissue damage, clinical signs, and shedding of bacilli.

7. **Comparative Aspects**
- Similarity to human TB: The pathogenic mechanisms of *M. bovis* in cattle are strikingly similar to *M. tuberculosis* in humans, making cattle a useful model for studying tuberculosis immunopathology (Pereira et al., 2024).
- Wildlife reservoirs: In wildlife hosts, granuloma formation and progression follow similar patterns, reinforcing their role as long-term reservoirs (Corner, 2006).

## 3. TRANSMISSION

The transmission of *Mycobacterium bovis* among cattle and between cattle and other species is a complex process influenced by environmental, host, and management factors. The primary routes are aerosol inhalation, ingestion, and less commonly direct contact or environmental contamination (Phillips et al., 2003).

### 3.1. Aerosol Transmission
- Dominant pathway in cattle herds: Aerosol spread is the most common and epidemiologically significant route of infection. Infected animals excrete bacilli in respiratory droplets when coughing, sneezing, or even breathing. Close contact in enclosed housing facilitates airborne transmission (Phillips et al., 2003).
- Influencing factors: Stocking density, ventilation quality, and duration of contact strongly affect transmission efficiency (Waters et al., 2012). Poor ventilation in barns and intensive farming systems increase the risk.

### 3.2. Ingestion
- Milk and colostrum: Calves can become infected by ingesting milk or colostrum from cows with tuberculous mastitis. This was historically a major route of zoonotic infection in humans before the widespread adoption of milk pasteurization (Ayele et al., 2004).
- Feed and water contamination: Bacilli may survive in the environment for extended periods, particularly in moist and shaded conditions. Contaminated feed, pastures, or communal water sources may facilitate ingestion-based transmission (Hildebrond et al., 2022).

### 3.3. Vertical and Direct Contact

• In utero transmission: Though relatively rare, infection can be transmitted across the placenta to the fetus, particularly in cows with generalized disease (Pollock and Neill, 2002).

• Contact with secretions: Direct exposure to excretions such as urine, feces, or nasal discharge containing bacilli may lead to infection, but this is considered a minor route compared to aerosols and ingestion (Riopel et al., 2024).

### 3.4. Wildlife Reservoirs

The role of wildlife reservoirs is one of the greatest obstacles to eradication efforts. Many wild species act as maintenance hosts, sustaining *M. bovis* transmission independently of cattle.

• Badgers (UK, Ireland): Badgers are a major reservoir and source of reinfection for cattle, with complex social behaviors and burrow systems that facilitate persistence (Corner, 2006).

• White-tailed deer (USA): Wild deer populations in Michigan have maintained endemic infection, posing a significant risk to cattle herds (Pereira et al., 2024).

• Possums (New Zealand): The brush-tailed possum is considered the main wildlife reservoir in New Zealand, and controlling their populations has been essential for reducing bTB prevalence in cattle (Corner, 2006).

• Other wildlife species: Wild boar, lions, and elephants have also been reported as hosts, particularly in Africa and Asia, adding to the ecological complexity (Michel et al., 2010).

### 3.5. Environmental Persistence

*M. bovis* can persist for weeks to months in the environment, depending on temperature, humidity, and exposure to sunlight.

• It survives longer in cool, moist, and shaded conditions, especially in organic matter such as feces or slurry (Ayele et al., 2004).

• Although environmental persistence alone may not sustain outbreaks, it contributes to indirect transmission, particularly in extensive grazing systems.

### 3.6. Human–Animal Interface

Transmission is not restricted to cattle and wildlife; humans may also serve as incidental hosts and, rarely, sources of reverse zoonosis.

• Occupational exposure is common among farmers, veterinarians, and abattoir workers (Akurut et al., 2025).

• Human-to-cattle transmission is unusual but has been documented in rare cases, particularly in immunocompromised individuals shedding bacilli (Michel et al., 2010).

### 4. CLINICAL SIGNS

Bovine tuberculosis (bTB) is typically a chronic and slowly progressive disease, and clinical signs are often absent until advanced stages. Many infected cattle remain asymptomatic for months or years, which complicates early detection and control efforts (Pollock and Neill, 2002). The spectrum of clinical presentation depends on the route of infection, infectious dose, host immunity, and stage of disease progression.

**4.1. Subclinical Stage**

• Most infected animals show no outward signs during early infection.

• The only evidence of infection may be immunological responses detectable through diagnostic tests (Taye et al., 2021).

• These "silent carriers" play an important role in disease transmission within herds.

**4.2. Respiratory Signs**

Since inhalation is the predominant route of infection, the lungs and associated lymph nodes are most commonly affected.

• Chronic cough: A dry, intermittent cough that gradually worsens over time.

• Dyspnea and tachypnea: Difficulty breathing and increased respiratory rate in advanced cases due to extensive pulmonary lesions.

• Nasal discharge: May be mucoid or purulent, sometimes containing blood (Taye et al., 2021).

• Exercise intolerance: Affected animals tire easily due to reduced lung function.

**4.3. Generalized Clinical Signs**

As the disease progresses beyond the lungs, systemic signs of debilitation appear:

• Progressive weight loss despite normal or increased appetite (Hadi, 2022).

• Weakness and lethargy due to chronic inflammation.

• Decreased milk production in dairy cattle, often one of the earliest economic indicators of disease (Pollock and Neill, 2002).

• Anorexia and emaciation in terminal stages.

**4.4. Lymph Node Involvement**

• Enlargement of superficial lymph nodes, especially the retropharyngeal and bronchial nodes, may occur.

• Palpation may reveal firm, enlarged nodes, sometimes associated with abscessation or caseous necrosis (Waters et al., 2012).

**4.5. Extrapulmonary Manifestations**

While pulmonary disease predominates, *M. bovis* can spread hematogenously or via lymphatics to multiple organs:

• Gastrointestinal form: Occurs after ingestion of contaminated milk/feed; signs include chronic diarrhea, ruminal stasis, and abdominal pain (Ayele et al., 2004).

• Mammary gland infection: Tuberculous mastitis leads to hard, swollen udders and bacillary shedding in milk, posing a significant zoonotic risk (Collins et al., 2022).

• Renal involvement: Pyuria and bacilluria may occur, though rarely diagnosed in live cattle.

• Reproductive tract involvement: Infertility or abortion may be seen in advanced disseminated cases (Pollock and Neill, 2002).

**4.6. Terminal Stage**

• Advanced cases are marked by severe emaciation, labored breathing, chronic pneumonia, and persistent cough.

• The disease often leads to death if left unmanaged, but in most intensive farming systems, affected animals are detected and removed before reaching this stage.

**Diagnostic Relevance of Clinical Signs**

• Clinical signs alone are not reliable indicators of bTB, as they overlap with other chronic diseases such as bovine respiratory disease, parasitism, and chronic mastitis (O'Brien et al., 2006).

• Most infected cattle are identified through tuberculin testing or abattoir surveillance, not through visible symptoms.

• Nevertheless, recognition of advanced clinical signs is crucial for differential diagnosis and for raising suspicion in endemic regions.

## 5. DIAGNOSIS

The diagnosis of bovine tuberculosis (bTB) is challenging due to its chronic, insidious progression and the high proportion of subclinical infections. Most infected animals do not display overt clinical signs until advanced disease, making laboratory and field-based diagnostic methods essential for early detection and control (Chambers et al., 2011).

### 5.1. Clinical Suspicion

• Based on history (e.g., herd prevalence, wildlife contact, previous outbreaks) and clinical signs (chronic cough, weight loss, decreased milk yield).

• However, clinical presentation is nonspecific and often indistinguishable from other chronic respiratory or wasting diseases (Lange et al., 2022).

• Therefore, clinical suspicion serves primarily as a trigger for confirmatory testing.

### 5.2. Immunological Tests

### a. Tuberculin Skin Tests

The tuberculin skin test remains the cornerstone of bTB diagnosis and eradication programs worldwide.

• Single Intradermal Test (SIT): Uses bovine purified protein derivative (PPD) injected intradermally, with skin thickness measured after 72 hours (Collins et al., 2022).

• Comparative Intradermal Test (CIT): Employs both bovine and avian PPD to differentiate *M. bovis* from environmental mycobacteria exposure (DEFRA, 2019).

• Advantages: Widely available, inexpensive, suitable for field use.

• Limitations: Sensitivity varies (70–90%), influenced by host immune status, co-infections, and stage of disease. False negatives may occur in anergic or advanced cases (Pollock and Neill, 2002).

**b. Interferon-Gamma Release Assays (IGRAs)**

• Measure cell-mediated immune responses by quantifying interferon-gamma (IFN-γ) released from sensitized lymphocytes after exposure to mycobacterial antigens (Wood and Jones, 2001).

• Commercial tests such as Bovigam® are used as ancillary diagnostics.

• Advantages: Higher sensitivity than tuberculin test, detects infection earlier.

- Limitations: Higher cost, laboratory infrastructure required, risk of false positives from non-tuberculous mycobacteria (Waters et al., 2012).

**5.3. Bacteriological Diagnosis**

**a. Culture**

- Gold standard for confirmation of *M. bovis* infection.
- Samples: lymph nodes (retropharyngeal, bronchial), lung tissue, milk, or nasal swabs.
- Advantages: Definitive diagnosis, enables strain typing and epidemiological tracing.
- Limitations: Slow growth (6–12 weeks), requires biosafety level 3 laboratory (Hadi, 2022).

**b. Molecular Methods**

- PCR (Polymerase Chain Reaction): Rapid detection of *M. bovis* DNA from tissue, milk, or clinical specimens (Taye et al., 2021).
- Advantages: Faster than culture, high specificity.
- Limitations: Lower sensitivity in paucibacillary samples, cannot distinguish live from dead bacilli.

**5.4. Postmortem Examination**

- Lesions are typically found in lungs, lymph nodes, and thoracic organs.
- Gross pathology: Caseous necrosis, calcification, and granuloma formation are characteristic (Chambers et al., 2011).
- Histopathology: Granulomas with central necrosis surrounded by epithelioid macrophages, Langhans giant cells, and fibrous capsules (Waters et al., 2012).
- Postmortem detection remains important in abattoir surveillance programs.

5.5. Imaging and Novel Diagnostics

- Ultrasound and radiography: Useful in research or high-value animals, but impractical for routine herd diagnosis.
- Next-generation approaches: Genomic sequencing and advanced antigen-based assays are being developed to improve sensitivity and specificity (Thacker et al., 2006).

**6.  CONTROL AND PREVENTION**

The control and prevention of bovine tuberculosis (bTB) remain a major challenge due to its chronic nature, wide host range, and the presence of wildlife reservoirs. Eradication efforts must combine surveillance, testing, culling, biosecurity, and wildlife management (Tsogtbayar et al., 2025).

**6.1. Test-and-Slaughter Policy**

- The most widely adopted strategy in industrialized countries.
- Regular tuberculin testing of herds is conducted, and all positive animals are culled (Riopel et al., 2024).
- Has been successful in many countries, including the USA, parts of Europe, and Australia.
- Advantages: Reduces prevalence over time, prevents silent carriers.

- Limitations: Expensive for farmers and governments; less effective in regions with uncontrolled wildlife reservoirs or poor compliance (Collins et al., 2022).

## 6.2. Movement Control and Quarantine

- Restrictions on the movement of cattle from infected or high-risk herds are essential (OIE, 2018).
- **Quarantine measures** prevent spread to new regions.
- Pre-movement testing is often mandated in eradication programs (Corner, 2006).

## 6.3. Abattoir Surveillance

- Routine inspection of carcasses at slaughterhouses plays a key role in identifying infected cattle not detected on farms.
- Provides important epidemiological data for mapping disease prevalence (Akurut et al., 2025).
- Detects both subclinical and advanced cases through lesion examination and culture confirmation.

## 6.4. Wildlife Management

- Wildlife reservoirs pose one of the greatest obstacles to eradication.
- Strategies vary by region:
- Badger culling or vaccination in the UK and Ireland (Corner, 2006).
- Deer population control in the USA (O'Brien et al., 2006).
- Possum eradication programs in New Zealand, which have been crucial to reducing bTB (Corner, 2006).
- Wildlife vaccination research (e.g., oral BCG for badgers) shows promise but faces logistical challenges (Chambers et al., 2011).

## 6.5. Vaccination

- BCG (Bacille Calmette-Guérin): Currently the only available vaccine.
- Reduces severity of disease but does not provide complete protection, nor does it prevent infection (Waters et al., 2012).
- **Challenges:**
- Vaccinated cattle may react to tuberculin tests, complicating diagnosis (Pollock and Neill, 2002).
- Differentiating Infected from Vaccinated Animals (DIVA) tests are under development to overcome this limitation (Thacker et al., 2006).
- Widely used in humans, but its role in cattle remains limited to research and pilot programs in endemic regions.

## 6.6. Farm-Level Biosecurity

- Segregation of calves from adult cattle to reduce risk from milk-borne transmission.
- Pasteurization of milk to prevent both zoonotic spread and calf infection (Ayele et al., 2004).
- Improved ventilation in housing to minimize aerosol transmission (Phillips et al., 2003).

• Proper disposal of manure and carcasses to reduce environmental persistence of bacilli.

### 6.7. Zoonotic Risk Reduction

• Public health measures are essential, as *M. bovis* can infect humans.

• Key strategies include:

• Pasteurization of milk.

• Use of protective equipment for veterinarians, farmers, and abattoir workers (Akurut et al., 2025).

• Public awareness campaigns in endemic regions.

### 6.8. Integrated One Health Approach

• Effective control requires coordination between veterinary, environmental, and public health sectors (Michel et al., 2010).

• Surveillance of cattle, wildlife, and humans is necessary to understand transmission dynamics.

• Adoption of One Health frameworks is increasingly recognized as essential for long-term eradication.

## 7. ECONOMIC IMPACT

Bovine tuberculosis (bTB) has significant **economic consequences** worldwide, not only due to direct effects on cattle health and productivity but also through trade restrictions, eradication costs, and zoonotic implications. The impact varies between developed and developing regions, depending on the stage of eradication programs, presence of wildlife reservoirs, and national disease control policies (Phillips et al., 2003).

### 7.1. Direct Economic Losses

#### a. Reduced Productivity

• Milk yield: Infected dairy cows often experience a decline in milk production, even in subclinical stages (Pollock and Neill, 2002).

• Weight gain: Chronic infection leads to reduced growth rates, lowering beef production efficiency (Ayele et al., 2004).

• Reproductive performance: bTB can cause infertility, increased calving intervals, and occasional abortions, further diminishing herd productivity (Hadi, 2022).

#### b. Mortality and Morbidity

• Although bTB is typically chronic rather than acutely fatal, advanced cases may lead to **premature culling or death**, resulting in financial losses to farmers (Taye et al., 2022).

### 7.2. Indirect Economic Losses

#### a. Test-and-Slaughter Programs

• The requirement to cull positive animals imposes direct losses for farmers, especially in valuable dairy or pedigree herds (Hildebrond et al., 2022).

• Compensation schemes vary by country but often fail to cover the full economic value of culled animals (Phillips et al., 2003).

**b. Trade Restrictions**

• bTB-free certification is essential for the export of live animals, meat, and dairy products.

• Countries with endemic bTB face international trade barriers, limiting market opportunities (Riopel et al., 2024).

c. Surveillance and Control Costs

• Governments invest heavily in diagnostic testing, compensation, veterinary services, and wildlife management.

• For example, the UK spends over £100 million annually on bTB eradication efforts (DEFRA, 2019).

• Developing countries often lack the resources for sustained programs, leading to persistent economic burden (Pereira et al., 2024).

**7.3. Public Health Costs**

• Zoonotic transmission to humans through raw milk or occupational exposure increases healthcare costs, particularly in regions without pasteurization (Ayele et al., 2004).

• Human infections can result in long-term treatment, loss of productivity, and increased burden on healthcare systems (Thacker et al., 2006).

7.4. Wildlife Reservoir Management

• Controlling bTB in wildlife adds further expenses:

• Badger culling/vaccination in the UK (Corner, 2006).

• Possum control in New Zealand.

• Deer management in the USA.

• These programs are controversial, logistically difficult, and costly, yet necessary to reduce reinfection risk.

**7.5. Broader Socioeconomic Impact**

• Farmer livelihood: Loss of animals and trade opportunities undermines farmer income, particularly in smallholder systems.

• Food security: Lower productivity in endemic regions reduces availability of milk and meat for human consumption.

• Rural economy: Ongoing bTB outbreaks discourage investment in the cattle industry, affecting rural development (Michel et al., 2010).


**8.CONCLUSION**

Bovine tuberculosis (*Mycobacterium bovis*) continues to pose a major challenge to global cattle health, agricultural economies, and public health. Despite significant progress in eradication programs across developed countries, the persistence of wildlife reservoirs, environmental contamination, and asymptomatic carriers complicates control efforts.

The disease is characterized by its chronic and insidious progression, with most cattle remaining subclinical for long periods, thereby facilitating unnoticed transmission. Diagnosis relies on a combination of immunological tests, bacteriological culture, molecular methods, and abattoir surveillance, though each has inherent limitations. Control strategies,

particularly the test-and-slaughter approach, strict movement restrictions, and abattoir inspection, have proven effective in many regions but require sustained financial and logistical investment.
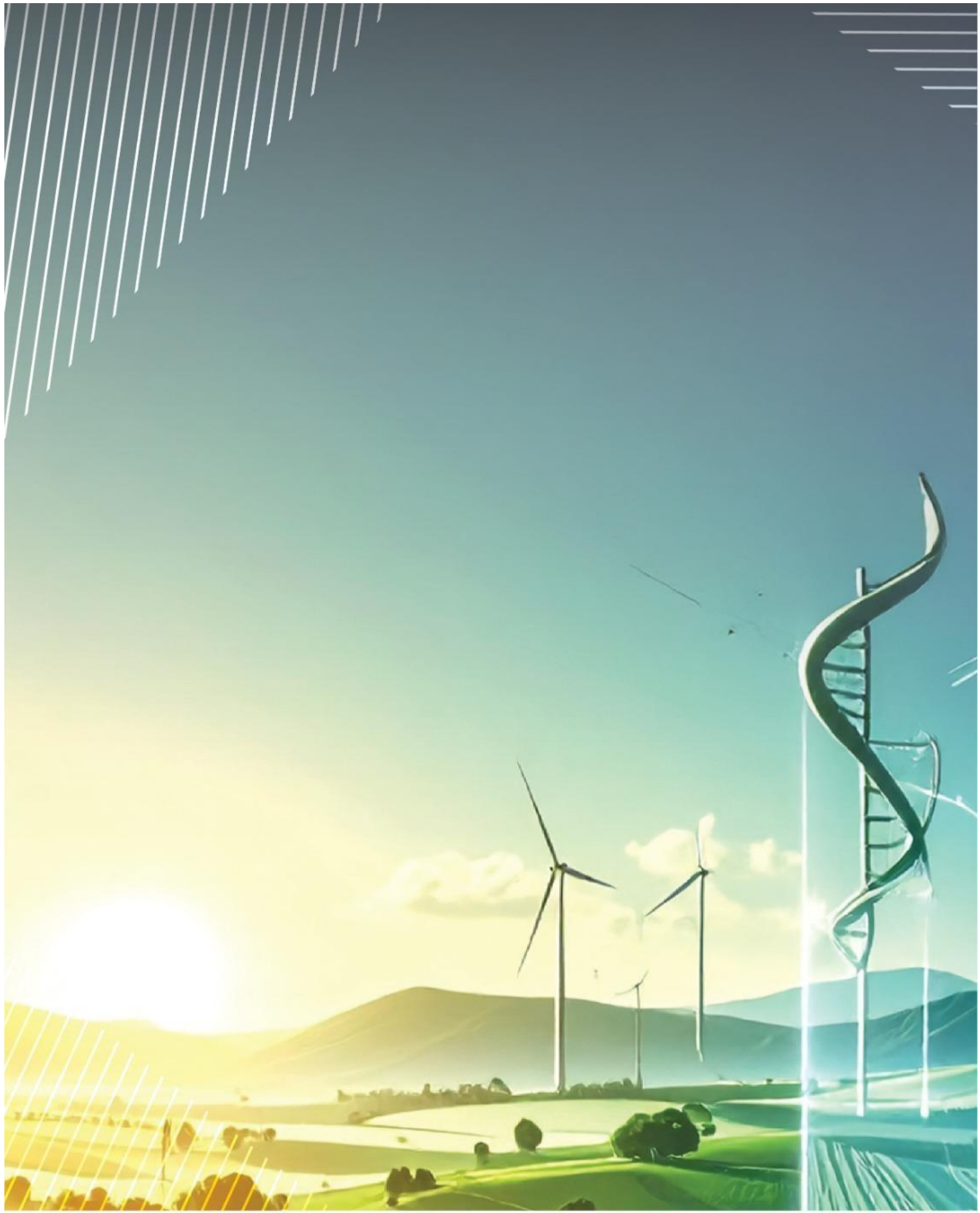
The economic burden of bTB is substantial, encompassing reduced productivity, trade limitations, costs of eradication programs, and zoonotic health risks. In resource-limited settings, where eradication programs are often not feasible, vaccination and improved farm-level biosecurity represent practical interim measures.

Looking forward, the adoption of One Health approaches, integrating veterinary, human, and environmental health perspectives, is essential for long-term control. The development of effective cattle vaccines compatible with DIVA diagnostics, along with sustainable wildlife management strategies, will play a pivotal role in achieving global reduction of bovine tuberculosis.

## REFERENCES

Akurut, E., Gavamukulya, Y., Mulindwa, J., Isiagi, M., Galiwango, R., Bbuye, M., ... & Mboowa, G. (2025). Design of a multi-epitope vaccine against drug-resistant mycobacterium tuberculosis and *mycobacterium bovis* using reverse vaccinology. Scientific reports, 15(1), 27298.

Ayele, W. Y., Neill, S. D., Zinsstag, J., Weiss, M. G., & Pavlik, I. (2004). Bovine tuberculosis: An old disease but a new threat to Africa. *The International Journal of Tuberculosis and Lung Disease, 8*(8), 924–937.

Chambers, M. A., Carter, S. P., Wilson, G. J., Jones, G., Brown, E., Hewinson, R. G., & Vordermeier, H. M. (2011). Vaccination against tuberculosis in badgers and cattle: An overview of the challenges, developments and current research priorities in Great Britain. *Veterinary Record, 169*(2), 45–51.

Collins, Á. B., Floyd, S., Gordon, S. V., & More, S. J. (2022). Prevalence of Mycobacterium bovis in milk on dairy cattle farms: An international systematic literature review and meta-analysis. Tuberculosis, 132, 102166.

Corner, L. A. (2006). The role of wild animal populations in the epidemiology of tuberculosis in domestic animals: How to assess the risk. *Veterinary Microbiology, 112*(2–4), 303–312.

DEFRA. (2019). *Bovine TB strategy review*. Department for Environment, Food and Rural Affairs. https://www.gov.uk/government/publications/a-strategy-for-achieving-bovine-tb-free-status-for-england-2019-review

Hadi, S. A. (2022). Epidemiology, Evolution, and Diagnostics of Tuberculosis in Humans and Animals. Michigan State University.

Hildebrand, R. E., Chandrasekar, S. S., Riel, M., Touray, B. J., Aschenbroich, S. A., & Talaat, A. M. (2022). Superinfection with SARS-CoV-2 has deleterious effects on *Mycobacterium bovis* BCG immunity and promotes dissemination of *Mycobacterium tuberculosis*. Microbiology spectrum, 10(5), e03075-22.

Lange, C., Aaby, P., Behr, M. A., Donald, P. R., Kaufmann, S. H., Netea, M. G., & Mandalakas, A. M. (2022). 100 years of *Mycobacterium bovis bacille* Calmette-Guérin. The Lancet Infectious Diseases, 22(1), e2-e12.

Michel, A. L., Müller, B., & van Helden, P. D. (2010). Mycobacterium bovis at the animal–human interface: A problem, or not? *Veterinary Microbiology, 140*(3–4), 371–381.

O'Brien, D. J., Schmitt, S. M., Fitzgerald, S. D., Berry, D. E., & Hickling, G. J. (2006). Managing the wildlife reservoir of *Mycobacterium bovis*: the Michigan, USA, experience. Veterinary microbiology, 112(2-4), 313-323.

Pereira, A. C., Pinto, D., & Cunha, M. V. (2024). First time whole genome sequencing of *Mycobacterium bovis* from the environment supports transmission at the animal-environment interface. Journal of Hazardous Materials, 472, 134473.

Phillips, C. J. C., Foster, C. R. W., Morris, P. A., & Teverson, R. (2003). The transmission of *Mycobacterium bovis* infection to cattle. *Research in Veterinary Science, 74*(1), 1–15.

Pollock, J. M., & Neill, S. D. (2002). *Mycobacterium bovis* infection and tuberculosis in cattle. *Veterinary Journal, 163*(2), 115–127.

Riopel, N. D., Long, R., Heffernan, C., Tyrrell, G. J., Shandro, C., Li, V., ... & Cooper, R. (2024). Characterization of Mycobacterium orygis, *Mycobacterium bovis*, and *Mycobacterium caprae* infections in humans in Western Canada. The Journal of Infectious Diseases, 230(4), e789-e797.

Taye, H., Alemu, K., Mihret, A., Wood, J. L., Shkedy, Z., Berg, S., & Aseffa, A. (2021). Global prevalence of *Mycobacterium bovis* infections among human tuberculosis cases: Systematic review and meta-analysis. Zoonoses and public health, 68(7), 704-718.

Thacker, T. C., Palmer, M. V., & Waters, W. R. (2006). Correlation of cytokine gene expression with pathology in white-tailed deer (*Odocoileus virginianus*) infected with Mycobacterium bovis. Clinical and Vaccine Immunology, 13(6), 640-647.

Tsogtbayar, O., Munkhbayarlakh, B., Dorjsurenkhor, N., & Gray, G. C. (2025). Major Livestock-associated Zoonoses in Mongolia: An Overview. Zoonoses, 5(1), 977.

Waters, W. R., Palmer, M. V., Buddle, B. M., & Vordermeier, H. M. (2012). Bovine tuberculosis vaccine research: Historical perspectives and recent advances. *Vaccine, 30*(16), 2611–2622.

Wood, P. R., & Jones, S. L. (2001). BOVIGAM™: An in vitro cellular diagnostic test for bovine tuberculosis. *Tuberculosis, 81*(1–2), 147–155.